

VARIATIONAL METHODS IN THE MATHEMATICS OF LIQUID
CRYSTALS

Michael R. Novack

Submitted to the faculty of the University Graduate School
in partial fulfillment of the requirements
for the degree
Doctor of Philosophy
in the Department of Mathematics,
Indiana University

June 2019

ProQuest Number: 13900243

All rights reserved

INFORMATION TO ALL USERS

The quality of this reproduction is dependent upon the quality of the copy submitted.

In the unlikely event that the author did not send a complete manuscript and there are missing pages, these will be noted. Also, if material had to be removed, a note will indicate the deletion.



ProQuest 13900243

Published by ProQuest LLC (2019). Copyright of the Dissertation is held by the Author.

All rights reserved.

This work is protected against unauthorized copying under Title 17, United States Code
Microform Edition © ProQuest LLC.

ProQuest LLC.
789 East Eisenhower Parkway
P.O. Box 1346
Ann Arbor, MI 48106 – 1346

Accepted by the Graduate Faculty, Indiana University, in partial fulfillment of the requirements
for the degree of Doctor of Philosophy.

Doctoral Committee

Dmitry Golovaty, Ph.D.

Peter Sternberg, Ph.D.

Nam Le, Ph.D.

Norm Levenberg, Ph.D.

Kevin Zumbrun, Ph.D.

April 29, 2019.

Acknowledgements

It is only with the generous support of many people that this dissertation is complete. I am truly grateful to my advisors, Professor Peter Sternberg and Professor Dmitry Golovaty, for their constant guidance throughout the process. Each of them has patiently listened to countless explanations and carefully read draft after draft, never failing to point me in the correct direction. I am also indebted to my committee members Professor Nam Le, Professor Norm Levenberg, and Professor Kevin Zumbrun.

The research leading to this thesis was made infinitely more enjoyable by the presence of my collaborators and friends in Bloomington. The innumerable hours spent on the third chapter were tolerable in no small part due to Raghav Venkatraman.

Finally, I would like to thank Grace Adduci, my parents, and my siblings Matt and Annemarie for their love and encouragement. Their unwavering support during graduate school was an inspiration.

Michael R. Novack

VARIATIONAL METHODS IN THE MATHEMATICS OF LIQUID CRYSTALS

In this thesis, we investigate several variational problems in the mathematical theory of liquid crystals. First, we analyze nematic liquid crystalline films within the framework of the Landau-de Gennes theory in a certain distinguished limit involving the film thickness and the nematic correlation length. We address several issues: Γ -convergence of a 3D sequence of energies F_ε to a 2D limiting energy F_0 , compactness for an energy-bounded sequence, the existence of local minimizers for F_ε , and an asymptotic energy expansion for the minimizers of F_ε subject to a strong-anchoring (Dirichlet) condition on the lateral boundary of the film.

Next, motivated by the need to explain the existence of singularities that form on interfaces during the nematic-to-isotropic phase transition, we study a version of the Chern-Simons-Higgs energy. The crucial feature of the corresponding variational problem is that the square of the divergence is penalized more heavily than other elastic energy terms. We analyze this energy, conjecture the form of the Γ -limit, and produce several examples that exhibit “tactoids” with corners or cusps along the phase boundary. We also prove a Γ -convergence theorem for energies with vanishing elastic constants that in effect demonstrates that a non-vanishing coefficient for the square of the divergence is necessary in order to observe this behavior in the limit.

In the third part of the thesis, we propose a Landau-de Gennes model with quartic elastic terms coming from the generalized Landau-de Gennes theory. We prove that the Oseen-Frank model can be realized as an asymptotic limit of our model, and we show that our model is well-posed. To demonstrate the appropriateness of our model, we consider nematic-isotropic phase transitions in the thin film setting. By choosing an appropriate combination of highly disparate elastic constants, we use numerical simulations to qualitatively reproduce experimentally observed interfaces and topological defects.

Dmitry Golovaty, Ph.D.

Peter Sternberg, Ph.D.

Nam Le, Ph.D.

Norm Levenberg, Ph.D.

Kevin Zumbrun, Ph.D.

Table of Contents

1	Introduction	1
1.1	Liquid Crystals: A Primer	2
1.2	Dimension Reduction for the Landau-de Gennes Model	10
1.3	A Model Problem for Nematic-Isotropic Transitions with Highly Disparate Elastic Constants	17
1.4	A Novel Landau-de Gennes Model with Higher Order Elastic Terms	25
2	Dimension Reduction for the Landau-de Gennes Model	30
2.1	Notation and Preliminaries	30
2.2	Proof of Γ -convergence	34
2.3	Local Minimizers of F_ε	49
2.4	Isolated Local Minimizers for F_0	54
2.5	Asymptotic Energy of Minimizers of F_ε for Boundary Data with Degree	68
2.6	Appendix to Chapter 2: Characterization of Minimal States for Limiting Potential	88
3	A Model Problem for Nematic-Isotropic Transitions with Highly Disparate Elastic Constants	93
3.1	First Try: A Model Whose Elastic Disparity Is Weak	93
3.2	A Model with Large Elastic Disparity and Singular Phase Boundaries	104
3.2.1	A Conjecture for the Γ -Limit of E_ε	106

3.2.2	Compactness	113
3.2.3	The Γ -Limit of E_ε Among 1D Competitors	119
3.2.4	Criticality Conditions for E_0	122
3.3	Examples: Analytical Constructions for Large L and Some Numerics	134
3.3.1	Critical Points of E_0 in a Rectangle.	136
3.3.2	Degrees Other than 0 or 1 Are Too Costly	138
3.3.3	Critical Points of E_0 and E_0^∞ in a Disk.	143
3.3.4	Examples for Degree Zero Boundary Data	151
3.4	Appendix to Chapter 3: Proof of the Junction Condition	161
4	A Novel Landau-de Gennes Model with Higher Order Elastic Terms	168
4.1	A Well-Posed Landau-de Gennes Model that Converges to Oseen-Frank	168
4.1.1	Alternative Forms for the Oseen-Frank Elastic Terms	168
4.1.2	Landau-de Gennes Energy	173
4.1.3	Non-dimensionalization and Analysis of the 3D Model	176
4.2	A Landau-de Gennes Model for Thin Film Nematic-Isotropic Transitions with Highly Disparate Elastic Constants	183
4.2.1	Experimental Results	183
4.2.2	Model Development	184
4.2.3	Simulations vs Experiment	192
Bibliography		204
Curriculum Vitae		

Chapter 1

Introduction

In this thesis, we investigate several variational problems in the mathematical theory of liquid crystals. Our analysis of these models is informed by applications as well as by theoretical concepts. We are particularly interested in understanding singular structures which arise mathematically and correspond to experimentally observed phenomena. There are three main topics that we consider in this study.

- (i) Dimension reduction for the Landau-de Gennes model: We analyze nematic liquid crystalline films within the framework of the Landau-de Gennes theory in a certain distinguished limit involving the film thickness and the nematic correlation length. We address several issues: Γ -convergence of a 3D sequence of energies F_ε to a 2D limiting energy F_0 , compactness for an energy-bounded sequence, the existence of local minimizers for F_ε , and an asymptotic energy expansion for the minimizers of F_ε subject to a strong–anchoring (Dirichlet) condition on the lateral boundary of the film. This project resulted in publication [84].
- (ii) A model problem for nematic isotropic phase transitions with highly disparate elastic constants: Motivated by the desire to capture nematic–isotropic phase transitions in liquid crystals, in particular to explain the existence of defects along the phase boundaries [59], we study a variation of the Chern-Simons-Higgs energy that penalizes the square of the divergence more than other elastic energy terms. We analyze this sequence of energies in the limit where the thickness of the isotropic-nematic transition region is vanishingly small com-

pared to size of the domain, and we conjecture the form of the Γ -limit. We produce several examples that exhibit “tactoids” with corners or cusps along the phase boundary. We also prove a Γ -convergence theorem for energies with elastic constants vanishing at potentially different rates that in effect demonstrates that a non-vanishing coefficient for the square of the divergence is necessary in order to observe this behavior in the limit. This project was carried out jointly with Dmitry Golovaty, Peter Sternberg, and Raghavendra Venkatraman and resulted in the article [49].

- (iii) A novel Landau-de Gennes model with higher order elastic terms: We propose a Landau-de Gennes model with quartic elastic terms that originate from the generalized Landau-de Gennes theory [68]. We prove that the Oseen-Frank model can be realized as an asymptotic limit of our model, and we show that our model is well-posed. As an application, we study nematic-isotropic phase transitions in the thin film setting. By choosing an appropriate combination of highly disparate elastic constants, we obtain a model for which numerical simulations qualitatively reproduce experimentally observed interfaces and topological defects. This project involved a collaboration with Dmitry Golovaty and Peter Sternberg as well as the physicists Oleg Lavrentovich and Young-Ki Kim and resulted in the article [46].

The remainder of the introduction is devoted to a review of the requisite background material regarding liquid crystals followed by separate discussions of each of the results pertaining to topics (i)-(iii), corresponding to Chapters 2-4.

1.1 Liquid Crystals: A Primer

Liquid crystals are intermediate states of matter which flow like fluids but also retain several characteristics of crystalline solids. The liquid crystal phase is usually induced in suitable substances either by changing the concentration of the substance in a solvent or varying the temperature. We describe the liquid crystal as lyotropic in the former case and thermotropic in the latter. Liquid

crystals are further subdivided into three broad categories: nematic, cholesteric, also known as chiral nematic, and smectic. In this thesis, we are solely concerned with nematic liquid crystals and the mathematical theory associated with them.

Nematic liquid crystals are composed of rod-like molecules which prefer to align along the same direction as the neighboring molecules. This partial orientational ordering leads to the crystalline features of nematics. In contrast, the absence of a positional ordering of the molecules allows the nematic to flow like a liquid. The nematic molecules also possess a reflection symmetry in which the head and tail of a molecule are indistinguishable. This symmetry will have important mathematical consequences which we will illuminate shortly. Both thermotropic and lyotropic liquid crystals may exhibit the nematic phase. When orientational order of the nematic phase disappears, the substance becomes isotropic, either due to a change in concentration (lyotropics) or an increase in temperature (thermotropics). It should be noted that in some sense, the properties we have ascribed to the molecules in a nematic liquid crystal are applicable only to ideal molecules. However, these properties do apply to real molecules in an average sense, so that the viewpoint of the preceding discussion is reasonable.

There are many mathematical theories for liquid crystals, ranging from the molecular dynamics based Onsager model [72] to the mean field Maier-Saupe model [23] to the continuum Ericksen-Leslie description [34, 35, 65]. We will restrict our attention to the continuum models for liquid crystals, some of which we propose and others which come from the literature. Additionally, the bulk of our analysis concerns static models, although we will occasionally consider dynamics, mostly in the context of numerical simulations. To familiarize the reader with the language of continuum theories for liquid crystals, we will provide a brief overview of three liquid crystal models: the Oseen-Frank, Ericksen, and Landau-de Gennes models.

The Oseen-Frank model [42, 85, 108] represents the behavior of the nematic molecules by a director - a unit vector $n(x) \in \mathbb{S}^2$ in the direction preferred by the rod-like molecules at a given

point x . The classical bulk free energy is given by the functional

$$F_{OF}(n) := \int_{\Omega} \sigma(n, \nabla n) dx,$$

where $\Omega \subset \mathbb{R}^3$ is the region occupied by the liquid crystal. The function σ is required to satisfy frame indifference, material symmetry, evenness, and positive-definiteness conditions due to the physical features of the system. As a result of the first three conditions, it can be shown as in [42, 104] that σ must be of the form

$$\begin{aligned} \sigma(n, \nabla n) = & K_1(\operatorname{div} n)^2 + K_2((\operatorname{curl} n) \cdot n)^2 + K_3|(\operatorname{curl} n) \times n|^2 \\ & + (K_2 + K_4)(\operatorname{tr}(\nabla n)^2 - (\operatorname{div} n)^2), \end{aligned}$$

so that

$$\begin{aligned} F_{OF}(n) = & \int_{\Omega} (K_1(\operatorname{div} n)^2 + K_2((\operatorname{curl} n) \cdot n)^2 + K_3|(\operatorname{curl} n) \times n|^2 \\ & + (K_2 + K_4)(\operatorname{tr}(\nabla n)^2 - (\operatorname{div} n)^2)) dx. \end{aligned} \quad (1.1)$$

In order to ensure the positive-definiteness of σ , Ericksen established that the constants K_i , known as the Frank constants, should satisfy

$$2K_1 \geq K_2 + K_4, \quad K_2 \geq |K_4|, \quad K_3 \geq 0. \quad (\text{Ericksen's inequalities})$$

Values of the Frank constants have been determined experimentally for a variety of liquid crystals. We remark that the term $(K_2 + K_4)(\operatorname{tr}(\nabla n)^2 - (\operatorname{div} n)^2)$ is a null Lagrangian in that its integral over the bulk depends only on boundary values, since

$$(\operatorname{tr}(\nabla n)^2 - (\operatorname{div} n)^2) = \operatorname{div}(\nabla n \cdot n - (\operatorname{div} n)n). \quad (1.2)$$

In fact, the integral of this term only depends on the values of n and its tangential derivatives along $\partial\Omega$.

The Oseen-Frank model has proven effective for modeling many problems in liquid crystals and has also been well studied in the mathematical literature. We will not discuss further the various

applications of the model, but for the purpose of this thesis it is worthwhile to recall the important mathematical results. The existence and partial regularity of solutions is established in [51]. The same authors strengthen the partial regularity in [50], showing that away from a singular set of Hausdorff dimension less than 1, minimizers are analytic. In the case when $K_1 = K_2 = K_3$ and $K_4 = 0$, one can apply the identity

$$((\operatorname{curl} n) \cdot n)^2 + |(\operatorname{curl} n) \times n|^2 + \operatorname{tr} (\nabla n)^2 = |\nabla n|^2 \quad (1.3)$$

to reduce the Oseen-Frank model to the harmonic map problem for maps into \mathbb{S}^2 . In this so-called equal constants case, it is shown in [20, 96] that any minimizer of F_{OF} is smooth away from finitely many points, around which it looks locally like $(x - x_0)/|x - x_0|$, up to a rotation. Finally, for the equal constants case, the authors in [20] and later in [66] show that the map $x/|x|$ is the minimizer on the unit ball among competitors subject to its own boundary conditions.

A significant drawback of the Oseen-Frank theory is the fact that line defects, known as disclinations, have infinite F_{OF} energy. This essentially follows from the fact that $x/|x|$ is not an H^1 function in a neighborhood of the origin in 2 dimensions. To address this deficiency, Ericksen [36] introduced a scalar order parameter s that reflects the degree of local orientational order. In the equal constant case, the energy of a configuration (s, n) is given by

$$F_E(s, n) = \int_{\Omega} (k_E(k|\nabla s|^2 + s^2|\nabla n|^2) + \sigma_0(s)) \, dx,$$

where k_E and k are positive constants and σ_0 is a quartic polynomial with coefficients dependent on temperature. The scalar s is allowed to vanish at defects so that the energy remains finite for disclinations. The model we propose with highly disparate elastic constants in Chapter 3 resembles somewhat the energy above. However, the Ericksen model is not one of our main objects of study. We refer the reader to [36, 104] for further development of the Ericksen theory.

The previous models fail to satisfactorily describe two important features of liquid crystals. First, as explained earlier, the liquid crystal molecules possess a reflectional symmetry that ren-

ders the head and tail of a molecule indistinguishable. However, in both the Oseen-Frank and Ericksen theories, the vector n and $-n$ are distinct. In addition to not respecting the head/tail symmetry, these theories presume a single direction of orientation preferred by the director in a small neighborhood of any point in space. This is called the uniaxial state of a liquid crystal. However, it is possible that the liquid crystal is in a biaxial state, in which there is no axis of rotational symmetry as in the uniaxial state but rather three orthogonal reflectional symmetries. A biaxial state has been conjectured to exist at the core of a nematic defect [62], and a stable biaxial thermotropic nematic liquid crystal has also been announced in [2, 71, 73]. To address these issues, a more comprehensive treatment is needed. Both of these issues can be circumvented within the Landau-de Gennes theory, which will be a principal focus throughout this thesis.

The Landau-de Gennes theory is based on the Q -tensor order parameter, which is related to the second moment of local orientational probability distribution. Following the exposition in [104], for a fixed point p and a small neighborhood B of p , let

$$f : \mathbb{S}^2 \rightarrow \mathbb{R}_+$$

be the probability density function representing the distribution of the orientations of the molecules in B . We assume that f is an even function, that is

$$f(\rho) = f(-\rho) \tag{1.4}$$

for all $\rho \in \mathbb{S}^2$. This condition encodes the head-tail symmetry mentioned earlier. The first moments of f , given by

$$\int_{\mathbb{S}^2} \rho f(\rho) d\mathcal{H}^2(\rho),$$

vanish due to (1.4). Thus the first non-trivial information regarding the probability distribution is given by the second moments tensor

$$M := \int_{\mathbb{S}^2} (\rho \otimes \rho) f(\rho) d\mathcal{H}^2(\rho).$$

Now from the facts that $|\rho|^2 = 1$ and $\int_{\mathbb{S}^2} f = 1$, it follows that

$$\mathrm{tr} M = \int_{\mathbb{S}^2} \mathrm{tr}(\rho \otimes \rho) f(\rho) d\mathcal{H}^2(\rho) = \int_{\mathbb{S}^2} 1 f(\rho) d\mathcal{H}^2(\rho) = 1. \quad (1.5)$$

Also, M is symmetric since

$$M^T = \int_{\mathbb{S}^2} (\rho \otimes \rho)^T f(\rho) d\mathcal{H}^2(\rho) = \int_{\mathbb{S}^2} (\rho \otimes \rho) f(\rho) d\mathcal{H}^2(\rho) = M. \quad (1.6)$$

When the orientation of the molecules is completely random, so that there is no orientational order, the liquid crystal is in the isotropic state. In this case, $f \equiv (4\pi)^{-1}$ and elementary symmetry considerations imply that $M = \frac{1}{3}\mathbf{I}$, where \mathbf{I} is the identity matrix.

For an arbitrary second moments tensor M , the matrix

$$Q = M - \frac{1}{3}\mathbf{I}, \quad (1.7)$$

is thus symmetric and traceless by (1.6) and (1.5). In the isotropic state, $Q = 0$, so one can interpret (1.7) as a measure of the deviation of the second moments tensor from the isotropic value. A word of caution regarding this interpretation: Q may equal 0 for distributions other than the uniform distribution, such as any distribution with one axis of rotational symmetry. We finally define the Landau-de Gennes order parameter Q to be an element of

$$\mathcal{S} := \{Q \in \mathbb{R}^{3 \times 3} : \mathrm{tr} Q = 0, Q = Q^T\},$$

the space of traceless, symmetric matrices. By the spectral theorem, Q has an orthonormal basis of eigenvectors v_i for $i = 1, 2, 3$ and corresponding real eigenvalues λ_i . When two of the eigenvalues of Q are equal, for example $\lambda_1 = \lambda_2$, then the nematic liquid crystal is in the uniaxial state and the Q -tensor can be written as

$$Q = S \left(v_3 \otimes v_3 - \frac{1}{3}\mathbf{I} \right), \quad (1.8)$$

where $S = 3\lambda_3/2$. If no two eigenvalues of Q are equal, then the liquid crystal is in the biaxial state, and

$$Q = S_1 \left(v_1 \otimes v_1 - \frac{1}{3}\mathbf{I} \right) + S_2 \left(v_3 \otimes v_3 - \frac{1}{3}\mathbf{I} \right), \quad (1.9)$$

where $S_1 = 2\lambda_1 + \lambda_3$ and $S_2 = \lambda_1 + 2\lambda_3$. In (1.8) and (1.9), the eigenvectors v_1 and v_3 can be understood as representing the preferred direction(s) of molecular alignment. When all three eigenvalues are equal, they are all zero, and the Q -tensor is in the isotropic state. It should be noted that in this formulation, there are no bounds imposed on the eigenvalues of Q . Strict adherence to the statistical mechanics principles underlying the derivation of the renormalized second moments tensor $M - \frac{1}{3}\mathbf{I}$ would entail that the eigenvalues of Q fall in the interval $[-1/3, 2/3]$. This approach is taken in the mean-field Maier-Saupe theory. Several issues related to eigenvalue bounds, or the lack thereof, on the order parameter Q within the Landau-de Gennes theory are addressed in [15, 74].

The variational theory for the Landau-de Gennes model involves minimization of elastic, bulk, and surface terms. The most commonly used elastic energy [79] for (achiral) nematics is

$$f_E(Q) := \frac{L_1}{2}Q_{ij,k}Q_{ij,k} + \frac{L_2}{2}Q_{ij,j}Q_{ik,k} + \frac{L_3}{2}Q_{ik,j}Q_{ij,k} + \frac{L_6}{2}Q_{lk}Q_{ij,l}Q_{ij,k}, \quad (1.10)$$

where here and throughout the thesis we assume the summation convention on repeated indices. Each term in f_E respects the frame indifference and material symmetry of the liquid crystal. There are many more possible elastic terms that also satisfy these criteria, and these terms have been calculated up to quartic terms in Q and its derivatives [68]. However, this particular combination of terms reduces to the Oseen-Frank energy when Q is uniaxial with fixed degree of orientation S [33, 78]. This fact, combined with the desire to avoid higher order terms, motivates the choice of f_E . We will explore an alternate elastic energy involving quartic terms in Q and its derivatives in depth in Chapter 4.

The bulk energy comes from a thermotropic potential function f_B that determines which state - uniaxial, biaxial, or isotropic - the liquid crystal prefers. Due to the frame indifference and material symmetry, the function f_B must depend only on the principal invariants of Q , which for symmetric, traceless matrices are $\text{tr}(Q^2)$ and $\det Q$. Considering a truncated Taylor expansion

around the isotropic state $Q = 0$ yields the following form of the potential [79]:

$$a \text{tr}(Q^2) + \frac{2b}{3} \text{tr}(Q^3) + \frac{c}{2} (\text{tr}(Q^2))^2, \quad (1.11)$$

generally referred to as the Landau-de Gennes potential. It is clear from this equation that the potential depends only on the eigenvalues λ_i of Q . The coefficient a is temperature dependent and $c > 0$. For $a > \frac{b^2}{27c}$, the high temperature regime, the isotropic state is the global minimizer, and for $a < \frac{b^2}{27c}$, the low-temperature regime, the uniaxial nematic state with degree of orientation $s_* := \frac{1}{4c} \left(-b + \sqrt{b^2 - 24ac} \right)$ is the global minimizer [79].

In the absence of a Dirichlet boundary condition (strong anchoring) on admissible Q -tensor fields, a surface energy penalizes deviations from some preferred alignment. This is known as weak anchoring. We will only use a weak anchoring term in Chapter 2 for the dimension reduction problem, so let us postpone the discussion of possible surface energies until a more in-depth discussion of that problem. Anchoring conditions are often used to enforce that the director is parallel or perpendicular to the substrate, situations known as parallel or homeotropic anchoring, respectively.

The existence of a minimizer for a Landau-de Gennes energy with the elastic and bulk terms mentioned above is delicate. In the case where $L_6 = 0$ and L_1-L_3 satisfy certain inequalities, it is shown in [28] that a minimizer exists and is smooth by elliptic regularity. When $L_6 \neq 0$, the energy is in fact unbounded from below for any choice of boundary conditions [15]. The difficulty occurs when the eigenvalues of Q leave the “physical regime” $(-1/3, 2/3)$. To address the fact that the energy is unbounded from below, the authors in [15] modify the bulk potential (1.11) so that it blows up when Q approaches the bounds of the physical regime. In Chapter 4, we propose a novel Landau-de Gennes energy involving quartic elastic terms rather than the cubic L_6 term for which the energy is bounded from below.

We briefly mention the relationship between the Landau-de Gennes order parameter Q and the Oseen-Frank director n . It is clear from equations (1.8) and (1.9) that Q is invariant under reflections $v_i \rightarrow -v_i$, so that Q respects the head-tail symmetry of the liquid crystal molecules. In

particular, when Q is uniaxial, the local orientational order of the liquid crystal is described by a line field, rather than a vector field, as in the Oseen-Frank model. The question of when these two notions coincide leads to the following definition. A uniaxial tensor field

$$Q = S \left(n \otimes n - \frac{1}{3} I \right) \in W^{1,p}(\Omega; \mathcal{S})$$

is orientable [16] if there exists a lifting $\varphi(Q) \in W^{1,p}(\Omega; \mathbb{S}^2)$ such that

$$Q = S \left(\varphi(Q) \otimes \varphi(Q) - \frac{1}{3} I \right).$$

In [16], it is shown that when Ω is simply connected and $p \geq 2$, Q is orientable. In this case, there is no difference between considering the Oseen-Frank director n and the uniaxial Landau-de Gennes order parameter $S(n \otimes n - \frac{1}{3}I)$. In contrast, when Ω is not simply connected or $p < 2$, there may not be a one-to-one correspondence between uniaxial tensor fields and director fields; see [16] for a more detailed development.

1.2 Dimension Reduction for the Landau-de Gennes Model

In this first project, we study thin nematic liquid crystalline films. We analyze the Landau-de Gennes Q -tensor variational model in the thin film limit by carrying out a dimension reduction from three dimensions to two. This model exhibits features similar to two-dimensional Allen-Cahn and Ginzburg-Landau theories. We also generalize the local minimizer existence result of [61] to functionals with potentials vanishing on high dimensional sets and limiting energy which incorporates interior interfacial cost and cost associated to a Dirichlet condition on the boundary of the domain.

To arrive at the two-dimensional models, we use the theory of Γ -convergence. Originally introduced by de Giorgi, Γ -convergence is a notion of convergence for functionals that guarantees that any limit point of a sequence of minimizers is also a minimizer. The precise definition can be found in the statements of Theorem 2.1 and Theorem 4.2. We refer the reader to the book [27] for

a thorough treatment of the topic and its many applications in the calculus of variations.

Dimension reduction for planar nematic thin films via Γ -convergence has also been studied in [48]. In that paper, the authors derive a two dimensional model in the asymptotic limit of vanishing aspect ratio. For the limiting model, they provide heuristics regarding the behavior of minimizers in different parameter regimes. Depending on the boundary conditions, the problem takes on the flavor of an Allen-Cahn or Ginzburg-Landau type minimization with the non-dimensional nematic correlation length as the small parameter. In order to obtain rigorous results which expand upon their work, we use a similar model as in [48] but scale the functional differently by assuming that the non-dimensional nematic correlation length vanishes along with the aspect ratio of the film. This distinguished limit is the framework for our study.

We fix a bounded, C^2 domain $\Omega \subset \mathbb{R}^2$ and work on the cylinder $\Omega \times (0, h)$, where $0 < h \ll 1$. We require admissible Q -tensors to satisfy a uniaxial Dirichlet condition g on the lateral boundary $\partial\Omega \times (0, h)$ of the cylinder. In addition to being uniaxial, g is chosen such that the normal to the top and bottom of the cylinder, in this case the vector $\hat{z} = (0, 0, 1)$, is an eigenvector. This requirement is motivated by the desire to model both homeotropic and parallel anchoring, in which the majority of the nematic molecules are oriented either perpendicular or parallel to the surface of the film, respectively [104]. Reduced Q -tensor models for thin films such as [18, 97] have incorporated this condition based on experiments in [25].

Our starting point is the non-dimensional energy functional

$$E_\varepsilon(Q) = \int_{\Omega' \times (0,1)} \left(|\nabla_x Q|^2 + \frac{1}{\varepsilon^2} |\nabla_z Q|^2 + \frac{1}{\delta^2} f_{LdG}(Q) \right) dx dz + \frac{1}{\varepsilon} \int_{\Omega' \times \{0,1\}} f_s(Q) dx,$$

derived in [48, Eq. 25]. The spatial coordinates $(x, z) = (x_1, x_2, z)$ have been rescaled using the change of variables $(x_1, x_2, z) \rightarrow (x_1/R, x_2/R, z/h)$, where $R := \text{diam}(\Omega)$, and $\Omega' = \Omega/R$. From now on we will refer to the rescaled domain simply as Ω . Here $\varepsilon := h/R$, and $\delta := \xi_{NI}/R$ with ξ_{NI} being the nematic correlation length [43]. The non-dimensional elastic energy density $|\nabla_x Q|^2 + \frac{1}{\varepsilon^2} |\nabla_z Q|^2$ corresponds to case where L_1 is a non-negative constant and the other L_i

are 0 in the general Landau–de Gennes elastic energy density (1.10). The f_{LdG} term is the non-dimensional Landau–de Gennes bulk energy density (1.11).

The surface term f_s from [48] is given by

$$f_s(Q) = \gamma |(\mathbf{I} - \hat{z} \otimes \hat{z})Q\hat{z}|^2 + \alpha(Q\hat{z} \cdot \hat{z} - \beta)^2,$$

where $\alpha, \gamma > 0$, β is real, and \mathbf{I} is the 3×3 identity matrix. It is evident from this expression that the minimizers of f_s are precisely those Q -tensors which have \hat{z} as an eigenvector with eigenvalue β . This surface energy is a specific example of the “bare” surface energy

$$f_s(Q) = c_1(Q\hat{z} \cdot \hat{z}) + c_2|Q|^2 + c_3(Q\hat{z} \cdot \hat{z})^2 + c_4|Q\hat{z}|^2,$$

for a planar film, where $\alpha = c_3 + c_4 > 0$, $\beta = -\frac{c_1}{2(c_3 + c_4)}$, $c_2 = 0$, and $\gamma = c_4 > 0$. Choosing the constants c_i to satisfy these constraints ensures that the energies F_ε are bounded from below and also allows for nontrivial behavior in the limit due to the degeneracy of the set of minimizers for f_s .

Next, we wish to choose a suitable scaling for δ in terms of ε and carry out the one-parameter dimension reduction for the distinguished limit. In order for both the Landau–de Gennes and surface terms to play a role in the asymptotic regime, a natural scaling to consider is $\delta \sim \sqrt{\varepsilon}$ when the core radius of nematic defects, although small, is still much larger than the thickness of the film. Then the energy E_ε can be expressed in the form

$$E_\varepsilon(Q) = \int_{\Omega \times (0,1)} \left(|\nabla_x Q|^2 + \frac{|\nabla_z Q|^2}{\varepsilon^2} + \frac{1}{\varepsilon} f_{LdG}(Q) \right) dx dz + \frac{1}{\varepsilon} \int_{\Omega \times \{0,1\}} f_s(Q) dx.$$

With this scaling in place, we consider an asymptotic limit of the functionals E_ε as $\varepsilon \rightarrow 0$. This is in contrast to [48], where the aspect ratio is first sent to 0 to obtain a two-dimensional model and then the small δ regime is discussed.

For convenience, we replace ε by ε^2 and multiply the modified functionals by ε . This results in functionals for which the minimum energy will be $O(1)$ to leading order:

$$F_\varepsilon(Q) = \int_{\Omega \times (0,1)} \left(\varepsilon |\nabla_x Q|^2 + \frac{|\nabla_z Q|^2}{\varepsilon^3} + \frac{1}{\varepsilon} f_{LdG}(Q) \right) dx dz + \frac{1}{\varepsilon} \int_{\Omega \times \{0,1\}} f_s(Q) dx. \quad (1.12)$$

Heuristically, due to the high cost associated with z -dependence, reasonable competitors for F_ε should be essentially independent of z . This observation allows us to rewrite the integral of f_s over $\Omega \times \{0, 1\}$ as twice the integral of f_s over $\Omega \times (0, 1)$. With the equal scaling of the Landau–de Gennes and the surface terms then, we obtain a potential which is f_{LdG} perturbed by $2f_s$. Due to the growth of f_{LdG} and f_s at infinity, the minimum value of $f_{LdG} + 2f_s$ is achieved and then, without loss of generality, we can subtract an appropriate constant and set the minimum to be zero. Denoting the zero set of $f_{LdG} + 2f_s$ by P , we see that the bulk and surface terms penalize those Q which take values away from P .

Let us denote by P_i a connected component of P and define the function

$$\varphi_i(Q) := d_{\sqrt{W}}(Q, P_i), \quad (1.13)$$

where $d_{\sqrt{W}}$ is the degenerate Riemannian metric with the conformal factor $\sqrt{f_{LdG} + 2f_s}$. Also, we will frequently identify maps on Ω as maps defined on $\Omega \times (0, 1)$ by the trivial z -independent extension. Our first main theorem is:

Theorem 1.1. *The F_ε Γ -converge in the L^1 topology to the functional F_0 , defined by*

$$F_0(Q) = \sum_{i,j=1}^n \varphi_i(P_j) \mathcal{H}^1(\partial^* A_i \cap \partial^* A_j) + 2 \sum_{i=1}^n \int_{\partial A_i \cap \partial \Omega} \varphi_i(g(x)) d\mathcal{H}^1(x),$$

where $A_i := \{x \in \Omega : Q(x) \in P_i\}$, the set $\partial^* A_i$ is the reduced boundary of A_i , cf. [44], and \mathcal{H}^1 denotes the one-dimensional Hausdorff measure.

The Γ -convergence of Allen–Cahn type functionals is well-studied in the literature; see for example [14, 41, 61, 77, 99, 100]. In each of these examples, the zero set of the potential function is a finite number of points. In our case, however, the minimal set of the potential is the zero set of a quartic polynomial in five variables, and we do not have a full description of its structure. Generally, the wells are high-dimensional and perhaps contain singularities. The Γ -convergence of Allen–Cahn type functionals possessing a general potential function with a zero set of arbitrary

dimension and smoothness has been established in [6]. The model we consider is distinct from [6] in that it combines a high-dimensional potential well with a Dirichlet condition. We also point out that it has been more common in the study of such problems to impose a volume constraint on the space of admissible functions, as in [14, 41, 99], rather than a Dirichlet condition, as considered here.

For the case admissible competitors are scalar functions, Γ -convergence of Allen–Cahn functionals with competitors satisfying a Dirichlet condition is proved in [86]. The asymptotics of vector-valued minimizers of Allen–Cahn functionals, rather than full Γ -convergence, in the presence of a suitable Dirichlet condition is addressed in [67]. To the best of our knowledge, these appear to be a few of the rare instances of a discussion of Γ -convergence for singular perturbations of multi-well potentials among maps subject to a Dirichlet condition. This may be due to the inherent difficulty in building a boundary layer consisting of a smoothly varying family of geodesics bridging the Dirichlet condition lying off the potential wells to values in the wells.

One of the main contributions of the present work is obtaining full Γ -convergence for Allen–Cahn type functionals with higher-dimensional wells among competitors that satisfy a Dirichlet condition. The invariance of the Landau–de Gennes potential f_{LdG} and the surface term f_s under rotations which fix the \hat{z} direction is crucial to the proof of Γ -convergence, in particular, to the construction of a recovery sequence. This symmetry is also utilized by the authors in [3] in the context of studying a nematic liquid crystal outside a spherical particle under an external field. Away from the boundary, we are able to apply the techniques from [6]. We point out that the techniques in the Γ -convergence proof would apply equally well to similar functionals with a potential vanishing on a higher-dimensional set, as long as the potential has some symmetry respected by the Dirichlet boundary data; see the discussion at the end of Section 2.3. It is also possible to prove Γ -convergence in the interior without appealing to the theory of metric space valued BV functions developed in [6]. In fact, our original proof combined an approximation

argument with the techniques from [14], and it was only upon receiving the referee report that we modified the proof to incorporate [6].

A natural question regarding Allen–Cahn type functionals such as F_ε is the possibility of finding local minimizers for the functionals F_ε . In cases such as the one discussed here, where the zero set of the potential consists of curves or even surfaces as opposed to isolated points, this has not been addressed in the literature. When the zero set consists of two points, an answer is provided by the authors in [61]. Crucial to their proof is the L^1 –compactness of a bounded energy sequence, which cannot be expected in general when the zero set is higher–dimensional. We resolve this question for very general functionals by working with a distance which is weaker than the usual L^1 metric.

For two tensors Q_1 and Q_2 , we define

$$\Lambda(Q_1, Q_2) = \sum_i \|\varphi_i(Q_1) - \varphi_i(Q_2)\|_{L^1(\Omega)},$$

where $\varphi_i(Q)$ is given by (1.13). For Q_1 and Q_2 whose range is contained in the zero set $P = \cup_i P_i$, the distance $\Lambda(Q_1, Q_2)$ is zero precisely when the sets where Q_1 and Q_2 lie in P_i coincide for each i . It can be quickly shown (see Section 2.3) that a sequence $\{Q_\varepsilon\}$ with bounded energy is Λ –compact. A similar pseudo–metric is proposed in [6], under which bounded energy sequences enjoy compactness. This also allows us to prove theorems showing the existence of local minimizers of F_ε and F_0 in Sections 2.3 and 2.4 similar to those in [61] and [101] for potentials that vanish on sets more complicated than a finite collection of points. The theorems apply to our particular liquid crystal models as well as a wide range of other functionals. Phrasing the rather general result in terms of our specific liquid crystal problem, we prove

Theorem 1.2. *Let Q_0 be an isolated Λ –local minimizer of F_0 . Then there exists $\varepsilon_0 > 0$ and a family $\{Q_\varepsilon\}_{\varepsilon < \varepsilon_0}$ such that*

$$Q_\varepsilon \text{ is a } \Lambda\text{–local minimizer of } F_\varepsilon \tag{1.14}$$

and

$$\Lambda(Q_0, Q_\varepsilon) \rightarrow 0. \tag{1.15}$$

It can be easily shown (see Remark 2.1) that the Q_ε are in fact H^1 -local minimizers, and therefore are classical solutions, by elliptic regularity, to the Euler-Lagrange system corresponding to F_ε .

In order to apply Theorem 1.2, we must obtain a Λ -isolated local minimizer for F_0 , an energy which has interior interfacial cost as well as cost associated to the boundary of Ω . We prove the existence of such a local minimizer in certain domains by using a calibration argument. The interface of the locally minimizing partition is contained in a “neck” of such a domain. However, unlike for example the situation in [61], the optimal interface is a straight line which does *not* meet the boundary of Ω at the narrowest part of the neck. Rather, the interface satisfies a contact angle condition, given by (2.58), in which the boundary energy is balanced by the interfacial energy.

We also wish to study the formation of defects for equilibrium configurations of liquid crystalline films. Such defects often take the form of disclination lines, which arise due to the degree of the Dirichlet boundary data g . Within the closely related Ginzburg-Landau context, these types of questions have been thoroughly explored; see [19]. More recently, for liquid crystalline films, the authors in [18] consider such defects for a two-dimensional Landau-de Gennes model. The study of defects, or vortices, in the presence of boundary layers for Ginzburg-Landau type energies is analyzed in [8–10]. In our scaling, the energy associated to these types of defects should be on the order of $\varepsilon |\log \varepsilon|$. This is lower order than the $O(1)$ cost associated to any boundary layers for finite energy Q_ε . Although the maps under consideration here are \mathbb{R}^5 -valued, as opposed to \mathbb{R}^2 -valued, the main techniques of these papers are applicable to our problem after some adjustments. In the following theorem, we use the techniques from [10] to obtain an asymptotic expansion for the energy of a minimizer Q_ε of F_ε , given in (1.12), for a specific choice of the surface energy density f_s .

Theorem 1.3. *Let Ω be a simply-connected domain and g have degree k . Assume that*

$$f_s = \gamma |(\mathbf{I} - \hat{\mathbf{z}} \otimes \hat{\mathbf{z}}) Q \hat{\mathbf{z}}|^2.$$

Then the minimizers Q_ε of F_ε satisfy the asymptotic development

$$F_\varepsilon(Q_\varepsilon) = 2 \int_{\partial\Omega} \varphi_1(g(x)) d\mathcal{H}^1(x) + s_*^2 \pi k \varepsilon \log \frac{1}{\varepsilon} + O(\varepsilon)$$

as $\varepsilon \rightarrow 0$. The constant s_* is explicit and depends on the bulk term f_{LdG} .

We also briefly discuss the convergence of Q_ε to a limiting map resembling the canonical harmonic map from [19], as is done in [18], and the location of the defects governed by a certain “renormalized energy.”

Our work on dimension reduction in thin nematic films is discussed in Chapter 2 of the present thesis. This chapter is organized as follows. In Section 2.1 we introduce the problem in full detail. We also present some preliminaries which will be necessary in the proofs of our results. In Section 2.2 we state the exact version of the Γ -convergence result, Theorem 1.1, and give its proof. In Sections 2.3 and 2.4 we prove the existence of local minimizers of F_ε and F_0 , respectively. In Section 2.5 we analyze the issue of defects. Rather than giving full proofs for every result in that section, we outline the ideas and refer the reader to [10, 18] for the specific calculations. Finally, in the appendix, we give a partial characterization of the zero set of the modified potential by establishing conditions under which \hat{z} is an eigenvector of any minimizer of $f_{LdG} + 2f_s$.

1.3 A Model Problem for Nematic-Isotropic Transitions with Highly Disparate Elastic Constants

Our second project aims to propose and analyze a family of models inspired by phase transitions in liquid crystals. We have in mind tactoids, or islands of the isotropic phase incorporated in the bulk of the nematic phase (or vice versa). Here phase boundaries separate a locally well-ordered state of nematic liquid crystals from a disordered isotropic state. Our models might be relevant more generally to other phase transition problems for which large disparity in the elastic constants

is a salient feature. Our analysis is mainly rigorous, but also includes formal calculations as well as computational experiments.

Many models, of course, exist for nematic liquid crystals, including the Oseen-Frank energy, based on the elastic deformations of an \mathbb{S}^1 - or \mathbb{S}^2 -valued director n , and the Q -tensor based Landau-de Gennes model, whose energy density consists of a bulk potential favoring either a uniaxial nematic state, an isotropic state, or both, depending on temperature. What distinguishes our effort here is the attempt to capture the singularities of nematic/isotropic phase boundaries using a model that has a structure similar to that of the Landau-de Gennes model but is simpler to handle.

The modeling of phase transitions in thin liquid crystalline films has attracted the attention of materials scientists and physicists for some time, [38, 59, 94, 103]. In experiments, one observes thin liquid crystal samples separated into nematic and isotropic phases. The islands of phase, i.e. the “tactoids,” appear as planar regions, with boundaries consisting of two or more smooth curves. Depending on temperature and on the type of liquid crystals, these smooth boundary curves may meet each other at singular points, known as “boojums,” forming angles or perhaps even cusps.

Regarding the significance of tactoids as an object of study, we quote from the recent computational study of tactoids [31], “Tactoid structures have been shown to act as sensors via chirality amplification and can be used to guide motile bacteria. They are also valuable architectural elements of self assembly, for example providing nucleation sites for growth of the smectic phase.”

In modeling these regions, the typical approach found in the materials science literature is to use a director theory and to postulate a surface energy that depends on the angle the director n makes with the normal ν to the phase boundary. Calling the region occupied by the phase of uniaxial nematic say Ω_N , and writing $n = (\cos \theta, \sin \theta)$ and $\nu = (\cos \phi, \sin \phi)$, this leads to minimization of a surface energy of the form

$$F_s(n) := \int_{\partial\Omega_N} \sigma(\theta - \phi) ds \quad (1.16)$$

where a typical choice for the function $\sigma : \mathbb{R} \rightarrow \mathbb{R}$, based on symmetries (and simplicity), is given by

$$\sigma(\theta - \phi) = c_1 + c_2 \cos 2(\theta - \phi),$$

a form referred to as a Rapini-Papoulier type surface density, (see e.g. [79], section 3.4). In some studies within the physics literature the phase domain Ω_N is taken as a given region having a simple geometry such as a disk and then the minimization, taken over director fields $n : \Omega_N \rightarrow \mathbb{S}^1$, may involve coupling the surface term above to an elastic term such as $\int_{\Omega_N} |\nabla n|^2 dx$, corresponding to the so-called ‘equal constants’ form of elastic energy, see e.g. [103]. In other studies, the shape itself is an unknown, but then, due to the difficulty of the analysis, the director field is often ‘frozen,’ that is, taken to be a constant so that there is no elastic energy contribution and one minimizes (1.16) alone. Then the problem resembles somewhat the Wulff shape problem arising in the classical study of crystal morphology, see e.g. [39, 94].

Rather than postulating a specific surface energy, here we seek a model based on an order parameter, $u : \Omega \rightarrow \mathbb{R}^2$ defined on a planar domain Ω in which the singularities of the phase boundary emerge as a result of large disparity between the values of the elastic constants. We are not alone in taking this viewpoint; see for example, [31], where the authors write “It is clear that significant shape deformation is only achieved with the introduction of elastic anisotropy.”

In [45], my co-authors propose a model problem coupling the Ginzburg-Landau potential to an elastic energy density with large elastic disparity, namely

$$\inf_{u \in H^1(\Omega; \mathbb{R}^2)} \frac{1}{2} \int_{\Omega} \left(\frac{1}{\varepsilon} (1 - |u|^2)^2 + \varepsilon |\nabla u|^2 + L (\operatorname{div} u)^2 \right) dx. \quad (1.17)$$

The minimization is taken over competitors satisfying an \mathbb{S}^1 -valued Dirichlet condition on $\partial\Omega$ so as to avoid a trivial minimizer. Here one might view the positive constant $\varepsilon \ll 1$ as being comparable in size to the elastic constant L_1 in say a Landau-de Gennes elastic energy density while the positive constant L , independent of ε , is playing the role of L_2 , the coefficient of squared divergence in more standard elastic energy densities.

This choice of potential clearly favors \mathbb{S}^1 -valued states, which are a stand-in in our models for uniaxial nematic states. As such, the model (1.17) precludes any phase transitions between \mathbb{S}^1 -valued states and the isotropic state $u = 0$, and corresponds to the situation where the temperature—and therefore the potential—favor only the nematic state. Analysis of (1.17) in the $\varepsilon \rightarrow 0$ limit involves a ‘wall energy’ along a jump set J_u penalizing jumps of any \mathbb{S}^1 -valued competitor u , and bulk elastic energy favoring low divergence. The conjectured Γ -limit of (1.17) is

$$\frac{L}{2} \int_{\Omega} (\operatorname{div} u)^2 dx + \frac{1}{6} \int_{J_u \cap \Omega} |u_+ - u_-|^3 d\mathcal{H}^1, \quad (1.18)$$

where u_+ and u_- are the one-sided traces of u along J_u . The natural space for competitors for this limit should be some subset of $H_{\operatorname{div}}(\Omega; \mathbb{S}^1)$, the Hilbert space of L^2 vector fields having L^2 divergence. In order to make sense of the jump set we make the additional assumption in [45] that $u \in BV(\Omega; \mathbb{S}^1)$, though this is surely not optimal. As a simple consequence of the Divergence Theorem, it follows that allowable jumps for an H_{div} vector field must satisfy continuity of the normal component

$$u_+ \cdot \nu = u_- \cdot \nu \quad \text{along } J_u, \quad (1.19)$$

where ν denotes the normal to J_u . Hence the cubic jump cost is penalizing the jump in the tangential component only.

In the present work, we allow for co-existence of both nematic and isotropic phases by replacing the Ginzburg-Landau potential in (1.17) with a potential $W : \mathbb{R}^2 \rightarrow [0, \infty)$ that still depends on the magnitude of u but that instead vanishes on $\mathbb{S}^1 \cup \{0\}$. This is reminiscent of the zero set of the Landau-de Gennes potential in the critical temperature regime within the thin film context, see e.g. [18]. A prototype for what we have in mind is a potential of the form $W(u) = W_{CSH}(u) := |u|^2 (|u|^2 - 1)^2$, or what is known in other physical contexts as the Chern-Simons-Higgs potential, see e.g. [63].

We thus arrive at two models based on this potential. In the first model, analyzed in Section

2, we examine the asymptotic limit in ε of the energy

$$G_\varepsilon(u) := \frac{1}{2} \int_{\Omega} \left(\frac{1}{\varepsilon} W(u) + \varepsilon |\nabla u|^2 + L_\varepsilon(\operatorname{div} u)^2 \right) dx,$$

where we assume $\varepsilon \ll L_\varepsilon \rightarrow 0$. Our main result for this model is Theorem 3.1.1, which states that in the L^1 -topology, this sequence of energies Γ -converges to a perimeter functional, measuring the arclength of the phase boundary between the \mathbb{S}^1 -valued phase and the zero phase. In short, despite the much stronger penalty on divergence—think of say $L_\varepsilon = \frac{1}{|\log \varepsilon|}$ —this amount of ‘elastic disparity’ is too weak to be felt in the limit. In particular, minimizers of the limiting energy, even under an area constraint to induce co-existence of \mathbb{S}^1 -valued and $\{u = 0\}$ phases, will have smooth phase boundaries. Thus, in this scaling, our model cannot capture the singular phase boundaries observed in experiments. We mention that in [63], the authors study the Γ -convergence of $\frac{1}{\varepsilon} G_\varepsilon$ for $L_\varepsilon = 0$. In that scaling, vortices rather than perimeter contributes at leading order.

Our second model, and the main focus of our project, involves the same type of potential W as in G_ε , but now we ‘ramp up’ the cost of divergence still further, leading us to the energy

$$E_\varepsilon(u) := \frac{1}{2} \int_{\Omega} \left(\frac{1}{\varepsilon} W(u) + \varepsilon |\nabla u|^2 + L(\operatorname{div} u)^2 \right) dx, \quad (1.20)$$

where L is a positive constant *independent of ε* . As $\varepsilon \rightarrow 0$ in this model, the jump set J_u features two distinct types of discontinuities: as in (1.18), there are what we will call ‘walls’ involving a jump discontinuity between two \mathbb{S}^1 -valued states that respect (1.19), and there are what we will call ‘interfaces’ involving a jump between an \mathbb{S}^1 -valued state and the isotropic $\{u = 0\}$ phase.

We mention that one can consider minimization of E_ε subject to a Dirichlet condition $g : \partial\Omega \rightarrow \mathbb{R}^2$, or a constraint such as $\int_{\Omega} |u|^2 = \text{const}$, or both in order to induce the co-existence of phases. The weak H_{div} convergence of energy bounded sequences, however, implies that the appropriate condition for the limiting functional E_0 is that it inherits only the condition

$$u \cdot n_{\partial\Omega} = g \cdot n_{\partial\Omega} \quad \text{along } \partial\Omega, \quad (1.21)$$

or simply $\operatorname{meas}(\{u = 0\}) = \text{const}$ in the case of the constraint.

In any event, it is the interfaces that represent the nematic/isotropic phase boundary and in light of the requirement (1.19), one sees that whatever form the Γ -limit takes, the competitors, being in H_{div} , must have \mathbb{S}^1 -valued traces *that are tangent to the phase boundaries*. As we will demonstrate through examples and numerics in Section 4, it is this tangency requirement that may induce singularities in the phase boundary. On this point, we mention that in this work we chose to penalize divergence more than other elastic energy terms, but had we replaced the term $L \int (\text{div } u)^2$ in (1.20) by $L \int (\text{div } R_\theta u)^2$ where R_θ is any rotation matrix, we would arrive at a limiting requirement on the nematic/isotropic interface in which tangency is replaced by u making some non-zero angle with the tangent to the phase boundary. In particular, for $\theta = \pi/2$ one penalizes the curl rather than the divergence and the resulting interface requirement is that the trace is orthogonal to the boundary.

In Fig. 1.1, we present an example of experimental nematic/isotropic configuration obtained in the laboratory of Oleg Lavrentovich along with a figure showing a numerically generated phase boundary based on gradient flow for E_ε . Both figures represent transient states but we point out the similar nature of the singular phase boundaries. Note that in the experimental picture, the phase boundary is singular only for the isotropic island whose surrounding nematic phase has degree 0 on the boundary of the isotropic tactoid, not for the island where the degree is 1. This distinction will come up frequently in our analysis.

Regarding a rigorous identification of the Γ -limit of E_ε , we only have partial results at this point. We present rigorous compactness results in $L^2(\Omega; \mathbb{R}^2)$ in Theorem 3.2.4 based on an adaptation of [32], but roughly put, it is easy to verify that any limit u of an energy bounded sequence, i.e. $\{u_\varepsilon\}$ such that $E_\varepsilon(u_\varepsilon) < C$, is a vector field $u \in H_{\text{div}}(\Omega; \mathbb{S}^1 \cup \{0\})$ such that the isotropic phase $\{x : u(x) = 0\}$ is a set of finite perimeter. Then making the extra assumption that u is of bounded variation in the nematic phase where $u(x) \in \mathbb{S}^1$, one can invoke a combination of known

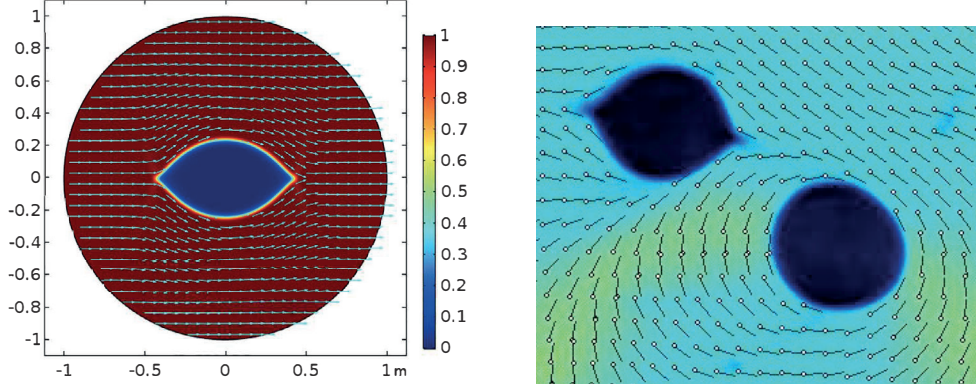


Figure 1.1: Tactoids observed in simulations (left) and the experiments (right). The figure on the right is courtesy of O. D. Lavrentovich.

techniques [45, 88] to establish a lower bound on the limit of the form

$$E_0(u) = \frac{L}{2} \int_{\Omega} (\operatorname{div} u)^2 dx + c_0 \operatorname{Per}_{\Omega}(\{|u| = 0\}) + \int_{J_u \cap \{|u|=1\}} K(u \cdot \nu) d\mathcal{H}^1, \quad (1.22)$$

where c_0 is the standard Modica-Mortola cost of an interface, cf. (3.3), and $K : \mathbb{R} \rightarrow [0, \infty)$ is a wall cost, arising through an abstractly defined solution to a certain cell problem. We wish to emphasize that, unlike for example (1.16), the limiting problem that arises involves both interfacial energy terms and a bulk term.

We strongly suspect that this wall cost K is in fact the cost associated with the heteroclinic connection between the states $(-u \cdot \tau, u \cdot \nu)$ and $(u \cdot \tau, u \cdot \nu)$ where τ is the approximate tangent to the jump set, see (3.21) and (3.22). The upper bound based on a recovery sequence for such a “one-dimensional” wall where only the tangential component varies across the boundary layer is the content of Theorem 3.2.1.

The optimality of one-dimensional walls is a delicate point that turns out to hold in the analysis of (1.17)-(1.18), cf. [45], as well as in the analysis of the divergence-free, or equivalently $L = \infty$, versions of these problems known as the Aviles-Giga problem, see e.g. [7, 12, 26, 32, 52, 69, 70, 87, 88]. However, for Aviles-Giga and in [45], the matching of lower bound to upper bound is achieved

through the somewhat miraculous Jin-Kohn entropy, cf. [55] and (3.26). The divergence of this vector field on the one hand bounds the Aviles-Giga energy from below but at the same time yields a value for the cost of a wall that coincides with the one-dimensional upper bound construction described above. As far as we can tell, there is no analogous entropy that works similarly for (1.20).

In Section 3.2.3, in contrast to the partial results from Section 3.2.1, we establish a complete Γ -convergence analysis along with optimal compactness, in the case where Ω is an interval.

In Section 3.2.4, we turn to the derivation of criticality conditions for the proposed Γ -limit, E_0 . As in [45], we find that in the \mathbb{S}^1 -valued phase, away from walls, we can phrase criticality in terms of a system of conservation laws sharing characteristics, cf. Corollary 3.2.10. Characteristics turn out to be circular arcs along which divergence is constant with the curvature of the arc being given by the value of the divergence. We also explore criticality conditions for the wall and interface in Theorems 3.2.8 and 3.2.11, as well as for possible junctions between walls and interfaces in Theorem 3.2.12, whose somewhat technical proof we delay until the appendix.

Section 3.3 is crucial to the work in that we explore the possible morphology of vortices, interfaces and walls through a series of examples. We focus on constructing critical points to the formal $L \rightarrow \infty$ limit of E_0 which one might describe as the Aviles-Giga Γ -limit augmented by isotropic regions, see (3.88). These constructions are in particular divergence-free competitors for E_0 for L finite that should be close to optimal for L large. One might expect that when no area constraint on the size of the isotropic phase is imposed and \mathbb{S}^1 -valued Dirichlet data g is specified in (1.21) for E_0 , then only critical points that are nematic—i.e. \mathbb{S}^1 -valued—would emerge, with perhaps a certain number of defects in order to accommodate the degree of g , as in [19]. However, in Example 3.3.3, we take Ω to be the unit disk and g to have negative degree, and we show that, somewhat surprisingly, an $O(1)$ isotropic region opens up. We provide a possible explanation for this phenomenon in Theorem 3.3.1.

In Section 3.3.4, we construct a divergence-free example in all of \mathbb{R}^2 in which a singular phase

boundary encloses an isotropic island and in which the infinite nematic complement of this island obeys a trivial degree zero condition at infinity, i.e. $u \rightarrow \vec{e}_1$ as $|x| \rightarrow \infty$. Unlike in the first example, this island is induced through an area constraint. This somewhat delicate calculation involves construction of both interfaces and walls with proper junction conditions holding at their intersection.

In this section we also comment on the following crucial feature of the model observed in several of our examples. At defects on the phase boundary, the director u often switches the sense of tangency. If a defect is a corner in the interior of the domain and a change in tangency occurs, then walls necessarily emanate from the defect in order to avoid infinite energy from the bulk divergence term; see Fig. 3.6 and the discussions at the end of Section 3.3.2 and preceding Example 3.3.4.

1.4 A Novel Landau-de Gennes Model with Higher Order Elastic Terms

In the final chapter, we combine the ideas from the previous chapters by studying the effect of elastic disparity within the Landau-de Gennes Q -tensor theory. First, we propose a three dimensional Landau-de Gennes model which contains elastic terms coming from the generalized theory [68]. Our motivation for proposing this model is mainly mathematical, in that we hope to address issues such as the lack of lower bounds in related models and the relationship between the Landau-de Gennes and Oseen-Frank descriptions. Then, we analyze a special two-dimensional example of this model for thin nematic films with highly disparate elastic constants. Our goal in this section is to successfully describe the interesting morphologies arising in nematic-isotropic phase transitions within the Landau-de Gennes theory.

We begin by analyzing a Landau-de Gennes energy of the form

$$F_\gamma(Q) = \int_{\Omega} f_\gamma(Q, \nabla Q) dx \quad (1.23)$$

in the temperature regime where the uniaxial nematic state is energetically preferable. We pay

special attention to the choice of elastic terms. In choosing an appropriate model, we have two main goals:

- (i) the minimization problem for F_γ should be well-posed, and
- (ii) in the asymptotic limit $\gamma \rightarrow 0$, the minimization problem for F_γ among orientable fields should yield similar results to the minimization of the director-based Oseen-Frank model F_{OF} , given in (1.1).

In other words, we are interested in obtaining the Oseen-Frank model as the asymptotic limit of a sequence of well-posed Landau-de Gennes models.

This natural question has been partially addressed in the literature. For the equal elastic constants case, in [75], it is shown that minimizers of

$$F_\gamma(Q) := \int_{\Omega} \left(\frac{\gamma}{2} |\nabla Q|^2 + f_{LdG}(Q) \right) dx$$

converge strongly in H^1 and uniformly away from singularities to a uniaxial limiting map as $\gamma \rightarrow 0$.

See also [83] for refined convergence results. It is quickly seen that minimizers of F_γ exist by using the direct method in the calculus of variations. To our knowledge, it has not yet been shown that the Oseen-Frank model in the case of unequal elastic constants, cf. (1.1), can be obtained as an asymptotic limit of the Landau-de Gennes model. In [78], following the approach of [33], the authors formally derive the Oseen-Frank energy density as a certain combination of Landau-de Gennes elastic terms for Q of the form

$$Q = s_* \left(n \otimes n - \frac{1}{3} I \right),$$

where s_* is a constant chosen so that Q minimizes the Landau-de Gennes bulk energy density. In particular, the calculation does not work for any uniaxial or biaxial Q which does not take the form above. Furthermore, the elastic terms proposed in [78] for Q yield an energy which is unbounded from below; see [15]. In [15], the authors circumvent this issue by introducing a potential which blows up when the eigenvalues of Q reach certain bounds.

In constructing an appropriate Landau-de Gennes model, we choose four elastic terms which are quartic in Q and ∇Q . The advantage of quartic terms as opposed to cubic terms is that the former yield a well posed variational problem. In particular, it is bounded from below. The functional F_γ we propose is

$$F_\gamma(Q) = \int_{\Omega} \left(\frac{L_1}{2} |\nabla Q|^2 + \frac{L_2}{2} |(\mathbf{I} - Q)\operatorname{div}(Q)|^2 + \frac{L_3}{2} |(\mathbf{I} - Q)\operatorname{curl}(Q)|^2 \right. \quad (1.24)$$

$$\left. + \frac{L_4}{2} |(2\mathbf{I} + Q)\operatorname{div}(Q)|^2 + \frac{L_5}{2} |(2I + Q)\operatorname{curl}(Q)|^2 + \frac{1}{4\gamma} f_{LdG}(Q) \right) dx. \quad (1.25)$$

The calculations

$$\begin{aligned} (\operatorname{div} n)^2 &= \frac{1}{81} |(\mathbf{I} - Q)\operatorname{div}(Q)|^2, \\ ((\operatorname{curl} n) \cdot n)^2 &= \frac{1}{81} |(\mathbf{I} - Q)\operatorname{curl}(Q)|^2, \\ |(\operatorname{curl} n) \times n|^2 &= \frac{1}{81} |(2\mathbf{I} + Q)\operatorname{div}(Q)|^2, \end{aligned}$$

and

$$|\nabla n|^2 = \frac{1}{81} |(2I + Q)\operatorname{curl}(Q)|^2$$

for (non-dimensionalized) uniaxial Q that minimize f_{LdG} imply that in the $\gamma \rightarrow 0$ limit, the limiting energy F_0 coincides with the Oseen-Frank energy for orientable fields. Our main theorem is

Theorem 1.4. *For boundary data g satisfying mild regularity conditions (cf. Theorem 4.2), the sequence $\{F_\gamma\}$ Γ -converges in the weak topology of $H_g^1(\Omega; \mathcal{S})$ to F_0 . That is,*

(i) *for any $Q \in H_g^1(\Omega; \mathcal{S})$ and for any sequence $\{Q_\gamma\}$ in $H_g^1(\Omega; \mathcal{S})$,*

$$Q_\gamma \rightharpoonup Q \text{ in } H_g^1(\Omega; \mathcal{S}) \text{ implies } \liminf_{\gamma \rightarrow 0} F_\gamma(Q_\gamma) \geq F_0(Q),$$

and

(ii) *for each $Q \in H_g^1(\Omega; \mathcal{S})$ there exists a recovery sequence $\{Q_\gamma\}$ in $H_g^1(\Omega; \mathcal{S})$ satisfying*

$$Q_\gamma \rightharpoonup Q_0 \text{ in } H_g^1(\Omega; \mathcal{S}), \quad (1.26)$$

$$\lim_{\gamma \rightarrow 0} F_\gamma(Q_\gamma) = F_0(Q_0). \quad (1.27)$$

The lower semi-continuity of these elastic terms follows from a short functional analytic argument. This section is the result of ongoing work with my advisors, Peter Sternberg and Dmitry Golovaty.

In the second section, we investigate nematic-isotropic phase transitions using a specific case of the model (1.24) in which L_3 - L_5 are zero. Phase transitions between ordered and isotropic states in nematic liquid crystals are of interest both for technological reasons as well as because nematics offer one of the simplest experimental systems where interfaces and topological defects may coexist. Two different types of topological defects can be present in a nematic in three dimensions: 0-dimensional point defects also known as vortices or nematic hedgehogs and 1-dimensional disclinations. Point defects may also be present on the surface of a nematic; such defects are known as boojums. There is a large body of literature devoted to the study of nematic defects, and we refer the reader to [60] for a comprehensive exposition on the topic. Our principal interest in this work is to examine the interaction between the nematic defects and isotropic-to-nematic interfaces.

The interfaces form in the process of the first order isotropic-to-nematic phase transition. Typically, nuclei of the nematic phase form within the isotropic phase upon lowering the temperature. The nematic nuclei are separated from the isotropic regions by phase boundaries or interfaces. The interfaces subsequently propagate converting the isotropic phase to the nematic phase in the process. In addition to motion of interfaces, the resulting dynamics of the system involves formation, annihilation and propagation of various types of defects.

In a recent work [59], the authors examine the interplay between the interfaces and defects that are present during phase transitions in lyotropic chromonic liquid crystals (LCLC). The principal feature of the isotropic-to-nematic phase transition in LCLC is that the interface provides an “easy direction” for nematic anchoring on the interface which in this case forces the director field to be tangent to this phase boundary. When combined with the anchoring (boundary) conditions on the walls of the container, the topology of the nematic configuration leads to formation of structural

defects. This is precisely the feature we sought in our “toy model” from Chapter 3.

Our goal in this section is to demonstrate that the zoo of singularities observed in [59] can be described within the framework of the Landau-de Gennes model for Q -tensors related to the projection matrix descriptor of the nematic phase. Critical to our modeling will be an assumption of large disparity between the values of the elastic constants appearing in the energy. In Section 4.2.1 we briefly describe the experimental observations that expand on some of the results presented in [59] by incorporating scenarios of the phase transition in which the isotropic phase regions, often called “negative tactoids” [82], [59], or simply “tactoids”, shrink into a uniform nematic state or a state with a topological defect, depending on the winding number of the tactoid. Note here that positive tactoids, i.e., regions of a nematic surrounded by an isotropic melt, have been previously theoretically treated in [56, 57, 89–91, 106].

In Section 4.1.2 we review the basics of the Landau-de Gennes theory and then develop our model in Section 4.2.2. In Section 4.2.3 we describe our numerical results and compare them with experimental observations.

Chapter 2

Dimension Reduction for the Landau-de Gennes Model

2.1 Notation and Preliminaries

In this chapter, we consider thin nematic liquid crystalline films. For the Landau-de Gennes Q -tensor model, we perform a dimension reduction in the distinguished limit in which both the aspect ratio of the film and the non-dimensional nematic correlation length vanish. After non-dimensionalizing, the film thickness and diameter are both 1, and the rescaled energy functionals are given by

$$\int_{\Omega \times (0,1)} \left(\varepsilon |\nabla_x Q|^2 + \frac{|\nabla_z Q|^2}{\varepsilon^3} + \frac{1}{\varepsilon} f_{LdG}(Q) \right) dx dz + \frac{1}{\varepsilon} \int_{\Omega \times \{0,1\}} f_s(Q) dx$$

for every $\varepsilon > 0$. Thus, our energy functional consists of elastic– and bulk–volume terms as well as a weak anchoring surface term. The most general elastic term one might use includes quadratic and even cubic terms in Q and its derivatives [79]. Throughout this chapter, however, we will work in the so-called equal elastic constants regime which corresponds to the usual Dirichlet energy. For the bulk energy density, we will use the Landau–de Gennes bulk energy density given by

$$f_{LdG}(Q) := a \text{tr}(Q)^2 + \frac{2b}{3} \text{tr}(Q^3) + \frac{c}{2} (\text{tr}(Q^2))^2. \quad (2.1)$$

The coefficient a depends on temperature and is negative for sufficiently low temperatures, while $c > 0$. One quickly sees that f_{LdG} only depends on the eigenvalues of Q . It can be shown that for high temperatures, the global minimum of f_{LdG} is attained by the isotropic state, whereas for low

temperatures, the global minimum is achieved by the uniaxial state

$$s_\star \left(m \otimes m - \frac{1}{3} \mathbf{I} \right), \quad (2.2)$$

where $m \in \mathbb{S}^2$ and s_\star is a real number given explicitly in terms of a , b , and c [79]. Throughout most of this chapter, we do not impose any assumptions on the temperature. Note however that since $c > 0$, f_{LdG} is bounded from below, and moreover, it grows quartically at infinity. We refer the reader to [43] for a thorough overview of the proper non-dimensionalization procedure for (2.1).

Recall from the introduction that the weak anchoring surface term is given by:

$$f_s(Q) = \gamma |(\mathbf{I} - \hat{z} \otimes \hat{z})Q\hat{z}|^2 + \alpha(Q\hat{z} \cdot \hat{z} - \beta)^2. \quad (2.3)$$

From the perspective of modeling nematics, the constant β satisfies $-1/3 < \beta < 2/3$; see [104, p. 24]. However, our arguments hold for any real β . Models with weak anchoring surface terms have been a source of much recent research, for example in [4, 15, 22, 47, 75, 98].

Next, let us introduce in full detail the problem under consideration, including boundary conditions and the limiting functional. Let \mathcal{S} be the set of real, symmetric, traceless, 3×3 matrices. We assume Ω is a bounded domain in \mathbb{R}^2 with C^2 boundary. For $(x, z) \in \partial\Omega \times (0, 1)$, let g be a Lipschitz function given by

$$g(x, z) = \frac{3\beta}{2} \left(\hat{z} \otimes \hat{z} - \frac{1}{3} \mathbf{I} \right) \quad (2.4)$$

or

$$g(x, z) = -3\beta \left(n(x) \otimes n(x) - \frac{1}{3} \mathbf{I} \right), \quad (2.5)$$

where n is $\mathbb{S}^1 \times \{0\}$ -valued vector field and does not depend on z . We remark that in both cases, g does not depend on z , so we will refer to g as a function of x only from now on. Since minimizers of f_s must have \hat{z} as an eigenvector with eigenvalue β , we see that these are the only uniaxial minimizers of f_s . Let

$$\mathcal{A}_g = \{Q \in H^1(\Omega \times (0, 1); \mathcal{S}) : Q|_{\partial\Omega \times (0, 1)} = g\}.$$

Define $W : \mathcal{S} \rightarrow \mathbb{R}$ by

$$W(Q) = f_{LdG}(Q) + 2f_s(Q), \quad (2.6)$$

and let us suppose that $W(g)$ is never 0; if it were, the problem would be trivial to zero order.

By the growth of f_{LdG} at infinity, we know that W achieves a global minimum value. Adding a constant to W , we can assume without loss of generality the minimum of W is 0.

We define

$$F_\varepsilon(Q) = \begin{cases} \int_{\Omega \times (0,1)} \left(\varepsilon |\nabla_x Q|^2 + \frac{|\nabla_z Q|^2}{\varepsilon^3} + \frac{1}{\varepsilon} f_{LdG}(Q) \right) dx dz \\ \quad + \frac{1}{\varepsilon} \int_{\Omega \times \{0,1\}} f_s(Q) dx, & Q \in \mathcal{A}_g, \\ \infty, & \text{otherwise,} \end{cases}$$

for every $\varepsilon > 0$. Let $P = \{Q \in \mathcal{S} : W(Q) = 0\}$; then we will write $P = \cup_{i=1}^n P_i$, where the P_i 's are the connected components of P . It is known that n is finite by a theorem of Whitney [105]. In the appendix to this chapter we prove a result showing when \hat{z} is an eigenvector for any element of P . Note that the growth of W at infinity implies that each P_i is compact.

We now introduce the proposed limiting functional F_0 for the sequence of functionals $\{F_\varepsilon\}$.

First, define for any two subsets U, V of \mathcal{S}

$$\begin{aligned} d_{\sqrt{W}}(U, V) := \\ \inf \left\{ \int_a^b \sqrt{W(\gamma(t))} |\gamma'(t)| dt \text{ s.t. } \gamma : [a, b] \rightarrow \mathcal{S} \text{ is Lipschitz, } \gamma(a) \in U, \gamma(b) \in V \right\}. \end{aligned} \quad (2.7)$$

Note that the above integral is independent of parametrization. For any $Q : \Omega \rightarrow P$, we set $A_i = \{x : Q(x) \in P_i\}$ and

$$\varphi_i(Q) := d_{\sqrt{W}}(P_i, Q). \quad (2.8)$$

Define

$$\mathcal{A}_0 = \{Q \in L^1(\Omega; \mathcal{S}) : W(Q(x)) = 0 \text{ a.e., and } \mathbb{1}_{A_i} \in BV(\Omega)\}. \quad (2.9)$$

For maps in \mathcal{A}_0 , we will view them as maps defined on the cylinder $\Omega \times (0, 1)$ via the trivial extension to three dimensions. We will similarly view maps defined on the cylinder as defined on

Ω if they do not depend on z . We then define our candidate for the Γ -limit F_0 by

$$F_0(Q) := \begin{cases} \sum_{i,j=1}^n \varphi_i(P_j) \mathcal{H}^1(\partial^* A_i \cap \partial^* A_j) & Q \in \mathcal{A}_0, \\ +2 \sum_{i=1}^n \int_{\partial A_i \cap \partial \Omega} \varphi_i(g(x)) d\mathcal{H}^1(x) \\ \infty & \text{otherwise.} \end{cases} \quad (2.10)$$

Finally, we present some preliminaries necessary for the proof of Theorem 1.1. Following [6], we recall the definition of a BV function taking values in a locally compact metric space E . For an arbitrary open set $D \subset \mathbb{R}^3$, the space $BV(D, E)$ is the class of Borel functions $v : D \rightarrow E$ such that for any Lipschitz $\psi : E \rightarrow \mathbb{R}$,

$$\psi(v) \in BV(D; \mathbb{R})$$

and there exists a finite measure m satisfying

$$|\nabla(\psi \circ v)|(B) \leq \text{Lip}(\psi)m(B) \text{ for all Borel sets } B \subset D. \quad (2.11)$$

Here $|\nabla(\psi \circ v)|$ is the usual total variation measure for real-valued BV functions. The total variation measure $|\nabla v|$ of v is the least such measure satisfying (2.11). For our purposes, E will be the canonical quotient space of $(\mathbb{R}^5, d_{\sqrt{W}})$, with distance function in E also denoted by $d_{\sqrt{W}}$. In this space, each P_i is identified with a single point. We will need the following form of lower-semicontinuity in $BV(D, E)$: if $d_{\sqrt{W}}(v_\varepsilon, v) \rightarrow 0$ in L^1 and $v_\varepsilon \in BV(D, E)$, then $v \in BV(D, E)$ and

$$|\nabla v|(D) \leq \liminf_{\varepsilon \rightarrow 0} |\nabla v_\varepsilon|(D). \quad (2.12)$$

The last preliminary result is a lemma from [14] regarding approximating a partition of Ω by polygonal domains and will be used in our construction of a recovery sequence.

Lemma 2.1. (cf. [14, Lemma 3.1]). *Let A_i , $1 \leq i \leq n$, be a partition of Ω by sets of finite perimeter. There exists a sequence $\{A_1^h, \dots, A_n^h\}_{h \in \mathbb{N}}$ of collections of polygons such that*

- (i) $\Omega \subset \cup_i A_i^h$ and the A_i^h are pairwise disjoint up to sets of measure zero;
- (ii) $\mathcal{H}^1(\partial A_i^h \cap \partial\Omega) = 0$;
- (iii) $|A_i^h \Delta A_i| \rightarrow 0$ as $h \rightarrow \infty$;
- (iv) $\sum_{i,j=1}^n \varphi_i(P_j) \mathcal{H}^1(\partial^* A_i^h \cap \partial^* A_j^h \cap \Omega) \rightarrow \sum_{i,j=1}^n \varphi_i(P_j) \mathcal{H}^1(\partial^* A_i \cap \partial^* A_j \cap \Omega)$ as $h \rightarrow \infty$.

2.2 Proof of Γ -convergence

In this section, we prove

Theorem 2.1. *For either choice (2.4) or (2.5) of boundary data g , the sequence $\{F_\varepsilon\}$ Γ -converges in the topology of $L^1(\Omega \times (0, 1); \mathcal{S})$ to F_0 . That is,*

- (i) *for any $Q \in L^1(\Omega \times (0, 1); \mathcal{S})$ and for any sequence $\{Q_\varepsilon\}$ in $L^1(\Omega \times (0, 1); \mathcal{S})$,*

$$Q_\varepsilon \rightarrow Q \text{ in } L^1(\Omega \times (0, 1); \mathcal{S}) \text{ implies } \liminf_{\varepsilon \rightarrow 0} F_\varepsilon(Q_\varepsilon) \geq F_0(Q), \quad (2.13)$$

and

- (ii) *for each $Q \in L^1(\Omega \times (0, 1); \mathcal{S})$ there exists a recovery sequence $\{Q_\varepsilon\}$ in $L^1(\Omega \times (0, 1); \mathcal{S})$ satisfying*

$$Q_\varepsilon \rightarrow Q_0 \text{ in } L^1(\Omega \times (0, 1); \mathcal{S}), \quad (2.14)$$

$$\lim_{\varepsilon \rightarrow 0} F_\varepsilon(Q_\varepsilon) = F_0(Q_0). \quad (2.15)$$

For the rest of this section, we fix g as specified in (2.5) and proceed with the proof for this choice of g . The proof for g given by (2.4) is omitted since it is similar but simpler due to the constancy of g . Throughout the proofs, we will make use of the following symmetry of W and its zero set P . Fix any $\theta \in [0, 2\pi)$ and consider the rotation matrix

$$r_\theta = \begin{bmatrix} \cos(\theta) & -\sin(\theta) & 0 \\ \sin(\theta) & \cos(\theta) & 0 \\ 0 & 0 & 1 \end{bmatrix}.$$

For any Q -tensor, which we can write as $Q = \sum_{i=1}^3 \lambda_i v_i \otimes v_i$ in some orthonormal frame $\{v_i\}$, we have

$$r_\theta Q r_\theta^T = \sum_{i=1}^3 \lambda_i r_\theta v_i \otimes r_\theta v_i.$$

Recall that f_{LdG} only depends on the eigenvalues λ_i of Q , and so the preceding equality implies that $f_{LdG}(Q) = f_{LdG}(r_\theta Q r_\theta^T)$. Also, for $f_s(Q)$, using the facts $\hat{z} = r_\theta \hat{z} = r_\theta^T \hat{z}$, $(I - \hat{z} \otimes \hat{z}) r_\theta = r_\theta (I - \hat{z} \otimes \hat{z})$, and $|r_\theta v| = |v|$ for any $v \in \mathbb{R}^3$, we can calculate

$$f_s(r_\theta Q r_\theta^T) = f_s(Q).$$

It follows that $W(Q) = f_{LdG}(Q) + 2f_s(Q)$ remains unchanged after conjugating Q by r_θ . From this we deduce that for any connected component P_i of P , conjugating P_i by r_θ fixes P_i , i.e.,

$$r_\theta P_i r_\theta^T = P_i. \quad (2.16)$$

We remark that this equation implies that any well P_i of W will in general be at least 1-dimensional. Finally, note that conjugation by r_θ preserves the quantity $|Q|^2 := \text{tr}(QQ^T)$, the sum of the squares of the entries of Q . Using this observation and the preceding comments regarding W , we deduce that for any piecewise C^1 path $\gamma : [a, b] \rightarrow \mathcal{S}$,

$$\int_a^b \sqrt{W(\gamma(t))} |\gamma'(t)| dt = \int_a^b \sqrt{W(r_\theta \gamma(t) r_\theta^T)} |(r_\theta \gamma r_\theta^T)'(t)| dt. \quad (2.17)$$

We can use (2.17) to show that for any g satisfying (2.5) and any $1 \leq i \leq n$, the distance $d_{\sqrt{W}}(P_i, g(x))$ defined in (2.7) does not depend on the choice of (x, z) in $\partial\Omega \times (0, 1)$. The previous equality implies that for any $(x, z) \in \partial\Omega \times (0, 1)$ and $\theta \in [0, 2\pi)$,

$$d_{\sqrt{W}}(P_i, g(x)) = d_{\sqrt{W}}(r_\theta P_i r_\theta^T, r_\theta g(x) r_\theta^T).$$

But since $r_\theta P_i r_\theta^T = P_i$, we conclude that

$$d_{\sqrt{W}}(P_i, g(x)) = d_{\sqrt{W}}(P_i, r_\theta g(x) r_\theta^T) \quad (2.18)$$

For any fixed (x, z) in $\partial\Omega \times (0, 1)$, the set $P_0 = g(\partial\Omega \times (0, 1))$, is contained in $\{r_\theta g(x)r_\theta^T : 0 \leq \theta \leq 2\pi\}$, so in fact (2.18) yields

$$d_{\sqrt{W}}(P_i, P_0) = d_{\sqrt{W}}(P_i, g(x)). \quad (2.19)$$

Let us now proceed with the proof of Theorem 2.1. Throughout the estimates, whenever appropriate, the generic constant C varies from line to line.

Proof of lower semicontinuity (2.13). Let Q_ε converge to Q in $L^1(\Omega \times (0, 1); \mathcal{S})$, and fix a subsequence ε_m such that $\lim_{\varepsilon_m \rightarrow 0} F_{\varepsilon_m}(Q_{\varepsilon_m}) = \liminf_{\varepsilon \rightarrow 0} F_\varepsilon(Q_\varepsilon)$. We may without loss of generality assume that the limit $F_{\varepsilon_m}(Q_{\varepsilon_m})$ is finite and that the energies $F_{\varepsilon_m}(Q_{\varepsilon_m})$ are uniformly bounded by some C . Using this assumption we can make a calculation which will simplify the proof of lower semicontinuity by replacing integrals of f_s over the top and bottom of the cylinder by the integral of $2f_s$ over the whole cylinder $\Omega \times (0, 1)$. For the matrix Q_{ε_m} , we denote the entry in the i -th row and j -th column by $q_{ij}^{\varepsilon_m}$. In the following calculation, it is helpful to rewrite $f_s(Q)$ as $f_s(Q) = \gamma(q_{13}^2 + q_{23}^2) + \alpha(q_{33} - \beta)^2$. Now, the uniform energy bound implies that

$$\int_{\Omega \times (0, 1)} |\nabla_z Q_{\varepsilon_m}|^2 dx dz \leq C \varepsilon_m^3 \quad (2.20)$$

and

$$\int_{\Omega \times \{0, 1\}} (\gamma(q_{13}^2 + q_{23}^2) + \alpha(q_{33} - \beta)^2) dx dz \leq C \varepsilon_m. \quad (2.21)$$

Using these two estimates it follows that

$$\begin{aligned}
& \frac{1}{\varepsilon_m} \left| \int_{\Omega \times (0,1)} f_s(Q_{\varepsilon_m}) dx dz - \int_{\Omega \times \{0\}} f_s(Q_{\varepsilon_m}) dx \right| \\
&= \frac{1}{\varepsilon_m} \left| \int_{(0,1)} \int_{\Omega} (f_s(Q_{\varepsilon_m}) - f_s(Q_{\varepsilon_m}(x,0))) dx dz \right| \\
&= \frac{1}{\varepsilon_m} \left| \int_{(0,1)} \int_{\Omega} \int_0^z \frac{\partial}{\partial z} f_s(Q_{\varepsilon_m}(x,t)) dt dx dz \right| \\
&\leq \frac{C}{\varepsilon_m} \int_{\Omega} \int_0^1 \left| 2q_{13}^{\varepsilon_m} \frac{\partial}{\partial z} q_{13}^{\varepsilon_m} \right| + \left| 2q_{23}^{\varepsilon_m} \frac{\partial}{\partial z} q_{23}^{\varepsilon_m} \right| + \left| 2(q_{33}^{\varepsilon_m} - \beta) \frac{\partial}{\partial z} q_{33}^{\varepsilon_m} \right| dt dx \\
&\leq \frac{C}{\varepsilon_m} \|q_{13}^{\varepsilon_m}\|_{L^2} \left\| \frac{\partial}{\partial z} q_{13}^{\varepsilon_m} \right\|_{L^2} + \frac{C}{\varepsilon_m} \|q_{23}^{\varepsilon_m}\|_{L^2} \left\| \frac{\partial}{\partial z} q_{23}^{\varepsilon_m} \right\|_{L^2} \\
&\quad + \frac{C}{\varepsilon_m} \|q_{33}^{\varepsilon_m} - \beta\|_{L^2} \left\| \frac{\partial}{\partial z} q_{33}^{\varepsilon_m} \right\|_{L^2} \\
&\leq C\varepsilon_m. \tag{2.22}
\end{aligned}$$

$$A similar estimate holds for the other surface term: \tag{2.23}$$

$$\frac{1}{\varepsilon_m} \left| \int_{\Omega \times (0,1)} f_s(Q_{\varepsilon_m}) dx dz - \int_{\Omega \times \{1\}} f_s(Q_{\varepsilon_m}) dx \right| \leq C\varepsilon_m. \tag{2.24}$$

Together these estimates imply that in order to prove lower semicontinuity for the sequence Q_{ε_m} , we can replace $F_{\varepsilon_m}(Q_{\varepsilon_m})$ by

$$\tilde{F}_{\varepsilon_m}(Q_{\varepsilon_m}) := \int_{\Omega \times (0,1)} \left(\varepsilon_m |\nabla_x Q_{\varepsilon_m}|^2 + \frac{|\nabla_z Q_{\varepsilon_m}|^2}{\varepsilon_m^3} + \frac{1}{\varepsilon_m} W(Q_{\varepsilon_m}) \right) dx dz \tag{2.25}$$

where, as usual, W is given by (2.6), and prove the lower semicontinuity inequality for these energies.

Next, in order to capture the cost associated with $\partial\Omega \times (0,1)$ coming from the transition layer from the boundary data g , we will need to consider a smooth domain $\tilde{\Omega}$ containing Ω and extend the domain of definition of each Q_{ε_m} to $\tilde{\Omega} \times (0,1)$. We do this by setting each Q_{ε_m} equal to $g(x,z)$ on the segment normal to $\partial\Omega \times (0,1)$ at (x,z) . Note this extension preserves the H^1 regularity possessed by Q_{ε_m} . We also perform the same extension on Q . Restricting to a further subsequence (still denoted Q_{ε_m}) which converges pointwise to Q , we use Fatou's Lemma and the preceding

remark to obtain:

$$\int_{\Omega \times (0,1)} W(Q) dx dz \leq \liminf_{m \rightarrow \infty} \int_{\Omega \times (0,1)} W(Q_{\varepsilon_m}) dx dz \leq \liminf_{m \rightarrow \infty} \varepsilon_m \tilde{F}_{\varepsilon_m}(Q_{\varepsilon_m}) = 0;$$

hence $W(Q) = 0$ a.e. in $\Omega \times (0,1)$. Finally, we claim that we can truncate Q_{ε_m} , in the sense of truncating each component at a certain size, and reduce all of the energies $\tilde{F}_{\varepsilon_m}(Q_{\varepsilon_m})$ as well as preserve the L^1 convergence of Q_{ε_m} . The energies decrease if we truncate far enough from 0 because of the quartic growth at infinity of W . The L^1 convergence is preserved because Q must be bounded, given that the zero set of W is compact.

Now, utilizing [6, Proposition 4.3], we find that $\pi \circ Q_{\varepsilon_m} \in BV(\tilde{\Omega} \times (0,1), E)$, where E is the quotient of $(\mathbb{R}^5, d_{\sqrt{W}})$ and π is the projection from \mathbb{R}^5 onto E . Furthermore, according to [6, Equation 4.6], $\pi \circ Q_{\varepsilon_m}$ satisfies the bound

$$|\nabla(\pi \circ Q_{\varepsilon_m})|(\tilde{\Omega} \times (0,1)) \leq \int_{\tilde{\Omega} \times (0,1)} \sqrt{W(Q_{\varepsilon_m})} |\nabla Q_{\varepsilon_m}| dx dz.$$

Splitting the right hand side into two integrals and multiplying by 2, we estimate

$$\begin{aligned} & 2|\nabla(\pi \circ Q_{\varepsilon_m})|(\tilde{\Omega} \times (0,1)) \\ & \leq 2 \int_{\Omega \times (0,1)} \sqrt{W(Q_{\varepsilon_m})} |\nabla Q_{\varepsilon_m}| dx dz + 2 \int_{(\tilde{\Omega} \setminus \Omega) \times (0,1)} \sqrt{W(Q_{\varepsilon_m})} |\nabla Q_{\varepsilon_m}| dx dz \\ & \leq \tilde{F}_{\varepsilon_m}(Q_{\varepsilon_m}) + 2 \int_{(\tilde{\Omega} \setminus \Omega) \times (0,1)} \sqrt{W(Q_{\varepsilon_m})} |\nabla Q_{\varepsilon_m}| dx dz \end{aligned} \quad (2.26)$$

We observe that by the definition of the extension of Q_{ε_m} to $\tilde{\Omega} \times (0,1)$, the integrand of second integral is bounded by constant $C(g)$ depending only the boundary data g .

Next, since $d_{\sqrt{W}}$ is bounded above by the Euclidean distance on compact sets and the Q_{ε_m} are bounded, we have that $d_{\sqrt{W}}(\pi \circ Q_{\varepsilon_m}, \pi \circ Q) \rightarrow 0$ in L^1 . Then the lower–semicontinuity property (2.12) in $BV(\tilde{\Omega} \times (0,1), E)$ yields

$$2|\nabla(\pi \circ Q)|(\tilde{\Omega} \times (0,1)) \leq \liminf_{m \rightarrow \infty} 2|\nabla(\pi \circ Q_{\varepsilon_m})|(\tilde{\Omega} \times (0,1)).$$

By throwing away the absolutely continuous and Cantor parts of $|\nabla(\pi \circ Q)|$, cf. [6, Equation 2.11], we can estimate the left hand side of the previous inequality to get

$$2 \int_{J_Q} d_{\sqrt{W}}(Q^+(x), Q^-(x)) d\mathcal{H}^2(x) \leq \liminf_{m \rightarrow \infty} 2|\nabla(\pi \circ Q_{\varepsilon_m})|(\tilde{\Omega} \times (0, 1)).$$

Here $J_Q \subset \tilde{\Omega} \times (0, 1)$ is the jump set of Q and Q^+, Q^- are the trace values from opposite sides of J_Q , cf. [6, Definition 1.3]. Note that (2.20) implies that the L^1 limit Q of Q_{ε_m} cannot depend on z , so we may identify Q with its canonical restriction to $\tilde{\Omega}$ and write

$$2 \int_{J_Q} d_{\sqrt{W}}(Q^+(x), Q^-(x)) d\mathcal{H}^1(x) \leq \liminf_{m \rightarrow \infty} 2|\nabla(\pi \circ Q_{\varepsilon_m})|(\tilde{\Omega} \times (0, 1)). \quad (2.27)$$

Then $Q \in \mathcal{A}_0$ since $W(Q) = 0$ a.e. and Q is independent of z , hence

$$F_0(Q) = \sum_{i,j=1}^n d_{\sqrt{W}}(P_i, P_j) \mathcal{H}^1(\partial^* A_i \cap \partial^* A_j) + 2 \sum_{i=1}^n \int_{\partial A_i \cap \partial \Omega} d_{\sqrt{W}}(P_i, g(x)) d\mathcal{H}^1(x),$$

which is easily seen to be equal to

$$2 \int_{J_Q} d_{\sqrt{W}}(Q^+(x), Q^-(x)) d\mathcal{H}^1(x).$$

Combining this with (2.27) and (2.26) yields

$$F_0(Q) = 2 \int_{J_Q} d_{\sqrt{W}}(Q^+(x), Q^-(x)) d\mathcal{H}^1(x) \leq \liminf_{m \rightarrow \infty} \tilde{F}_{\varepsilon_m}(Q_{\varepsilon_m}) + C(g) \text{meas}(\tilde{\Omega} \setminus \Omega).$$

By choosing $\tilde{\Omega}$ so that $\tilde{\Omega} \setminus \Omega$ has small measure, we can make $C(g) \text{meas}(\tilde{\Omega} \setminus \Omega)$ arbitrarily small. The lower semicontinuity property (2.13) follows. The proof is now complete in the case where g is as in (2.5); the proof for g as in (2.4) is similar. \square

Proof of the existence of a recovery sequence satisfying (2.14), (2.15). Fix any $Q_0 \in L^1$. If $F_0(Q_0) = \infty$, then the constant sequence $Q_\varepsilon = Q_0$ satisfies (2.14) and (2.15). Therefore we may assume $F_0(Q_0) \neq \infty$, and thus $Q_0 \in \mathcal{A}_0$. In particular, Q_0 does not depend on z . Our recovery sequence will also be independent of z ; therefore in the rest of the proof, we will work

on Ω rather than $\Omega \times (0, 1)$. To obtain a recovery sequence for Q_0 , we will approximate Q_0 by a sequence of functions $\{Q_h\}_{h \in \mathbb{N}}$ and furnish recovery sequences $\{Q_\varepsilon^h\}_{\varepsilon > 0}$ for each $h \in \mathbb{N}$.

Before proceeding with the details, we summarize the main ingredients. In the construction of the recovery sequence for each Q_h , we will use the rotational symmetry of W described at the beginning of this section. This symmetry allows us to create a family of geodesics under the degenerate metric $d_{\sqrt{W}}$ indexed by $x \in \partial\Omega$ which are Lipschitz in x . These curves form the boundary layer near $\partial\Omega$ which contributes the cost associated with the transition from the boundary data g to the values of Q_h . After some modifications due to the fact that the boundary data g is non-constant, we can utilize similar estimates as in [14] to provide an upper bound for the F_ε energy of Q_ε^h coming from this boundary layer. Away from $\partial\Omega$, we will use the construction from [6, Section 4]. A diagonal argument will then yield the desired result. The proof is divided into several steps.

Step 1. In this step, we construct the sequence $\{Q_h\}_{h \in \mathbb{N}}$. Applying Lemma 2.1 to the sets

$$A_i := \{x \in \Omega : Q_0(x) \in P_i\},$$

we obtain a sequence $\{\tilde{A}_1^h, \dots, \tilde{A}_n^h\}_{h \in \mathbb{N}}$ of collections of polygons which satisfy the conditions of Lemma 2.1. We claim that we can modify the polygons \tilde{A}_i^h and obtain polygonal partitions $\{A_1^h, \dots, A_n^h\}$ for each h such that for each A_i^h , in a neighborhood of $\partial\Omega$,

$$\partial A_i^h \text{ is a union of line segments, each intersecting } \partial\Omega \text{ at a } 90^\circ \text{ angle;} \quad (2.28)$$

and the $\{A_1^h, \dots, A_n^h\}$ still satisfy the conditions of the lemma; see Fig. 2.1. Indeed, for each h , this can be done by making the neighborhood of $\partial\Omega$ on which we modify the polygons sufficiently small. By restricting to a further subsequence of the A_i^h , we can assume that

$$\mathbb{1}_{A_i^h} \rightarrow \mathbb{1}_{A_i} \text{ a.e. as } h \rightarrow \infty. \quad (2.29)$$

Define

$$Q_h = \begin{cases} Q_0(x) & \text{if } x \in A_i^h \cap A_i \text{ and } \text{dist}(x, \partial\Omega) \geq 1/h \\ \alpha_i & \text{if } x \in A_i^h \setminus A_i \text{ or } \text{dist}(x, \partial\Omega) < 1/h, \end{cases}$$

where α_i is any fixed element of P_i chosen independently of h . We have defined Q_h to be locally constant near $\partial\Omega$ to simplify the boundary layer construction there. Then (2.29) implies that $Q_h \rightarrow Q_0$ a.e. on Ω since for almost every fixed $x \in \Omega$, $\mathbb{1}_{A_i^h}(x) = \mathbb{1}_{A_i}(x)$ for large enough h depending on x . Applying the dominated convergence theorem yields

$$Q_h \rightarrow Q_0 \text{ in } L^1(\Omega; \mathcal{S}). \quad (2.30)$$

In addition, due to Lemma 2.1

$$F_0(Q_h) \rightarrow F_0(Q_0). \quad (2.31)$$

Properties (2.30) and (2.31) will allow us to diagonalize recovery sequences for Q_h to obtain a recovery sequence for Q_0 .

Step 2. We fix $h \in \mathbb{N}$ and present some preliminaries necessary for construction of the boundary layer near $\partial\Omega$ for the recovery sequence of Q_h . First, in order to construct the boundary layer near $\partial\Omega$ which bridges a constant matrix α_i to the boundary data g , we need to construct a family of paths indexed by $x \in \partial\Omega$ connecting α_i to $g(x)$ which have sufficient smoothness in x and are geodesics in the degenerate metric $d_{\sqrt{W}}$. In general, this might be quite difficult, but in our particular case, the choice of boundary data g and the symmetry of W will facilitate the process. We recall by (2.19) that $d_{\sqrt{W}}(g(x), \alpha_i)$ does not depend on the choice of $x \in \partial\Omega$. Therefore, for each connected component of $\partial\Omega$, we fix a point x_l , $1 \leq l \leq L$, find geodesics connecting α_i to $g(x_l)$, and then suitably modify them to obtain geodesics connecting α_i to other $g(x)$.

For any $x_l \in \partial\Omega$, and let $\gamma_{i,x_l} : [0, 1/2] \rightarrow \mathcal{S}$ satisfy $\gamma_{i,x_l}(0) = g(x_l)$, $\gamma_{i,x_l}(1/2) = \alpha_i$ and

$$\int_0^{1/2} \sqrt{W(\gamma_{i,x_l}(t))} |\gamma'_{i,x_l}(t)| dt = d_{\sqrt{W}}(\alpha_i, g(x_l)). \quad (2.32)$$

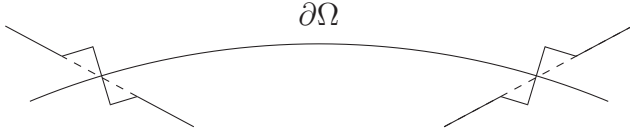


Figure 2.1: The dashed lines represent the portions of $\partial\tilde{A}_i^h$ which are modified to obtain ∂A_i^h . The A_i^h can be constructed so that the perimeter of A_i^h is arbitrarily close to the perimeter of \tilde{A}_i^h .

The existence of such a geodesic follows from [109]. We can without loss of generality assume that $|\gamma'_{i,x_l}|$ is constant. For each x in the connected component of $\partial\Omega$ containing x_l , we have $g(x) = r_{\theta(x)}g(x_l)r_{\theta(x)}^T$ for some $\theta(x)$ and $1 \leq l \leq L$, and we can choose the function $\theta : \partial\Omega \rightarrow \mathbb{R}$ to be continuous on $\partial\Omega \setminus x_l$. Near x_l , the value of $\theta(x)$ approaches 0 coming from one side and a possibly non-zero multiple of 2π from the other side. We rotate γ_{i,x_l} so it connects $g(x)$ to $r_{\theta(x)}\alpha_i r_{\theta(x)}^T$ and then connect that point to α_i by letting $\theta(x)$ go to 0. We define

$$\gamma_{i,x}(t) = \begin{cases} r_{\theta(x)}\gamma_{i,x_l}(t)r_{\theta(x)}^T & \text{if } 0 \leq t \leq 1/2 \\ r_{\theta(x)(-2t+2)}\alpha_i r_{\theta(x)(-2t+2)}^T & \text{if } 1/2 < t \leq 1. \end{cases} \quad (2.33)$$

It is straightforward to see that away from x_l , $\gamma_{i,x}(t)$ is locally Lipschitz in x and t . In fact, viewing $\gamma_{i,x}(t)$ as a function of t indexed by x , it can be quickly seen that the Lipschitz constants for each $\gamma_{i,x}(\cdot)$ are uniformly bounded in x . Note that for $t \geq 1/2$, $W(\gamma_{i,x}(t)) = 0$. We can use this fact and (2.17) to calculate

$$\begin{aligned} \int_0^1 \sqrt{W(\gamma_{i,x}(t))} |\gamma'_{i,x}(t)| dt &= \int_0^{1/2} \sqrt{W(\gamma_{i,x_l}(t))} |\gamma'_{i,x_l}(t)| dt \\ &= d_{\sqrt{W}}(\alpha_i, g(x_l)) \\ &= d_{\sqrt{W}}(\alpha_i, g(x)). \end{aligned}$$

We recall the following facts from [14, Lemma 3.2] which are useful in the construction. Consider the family of ordinary differential equations indexed by $x \in \partial\Omega$ and $i = 1, \dots, n$:

$$\left(\frac{\partial}{\partial t} y_{\varepsilon,\delta}^{i,x}(t) \right)^2 = \frac{\delta + W(\gamma_{i,x}(y_{\varepsilon,\delta}^{i,x}(t)))}{\varepsilon^2 |\gamma'_{i,x}(y_{\varepsilon,\delta}^{i,x}(t))|^2}, \quad (2.34)$$

where $0 < \delta l_1$ is a fixed constant. We have for every $\varepsilon > 0$, constants $C_{1,\delta}$, $C_{2,\delta}$, and $C_{3,\delta}$ independent of ε and x , and strictly increasing solutions $y_{\varepsilon,\delta}^{i,x} : [0, C_{i,x}] \rightarrow [0, 1]$ to (2.34) such that

$$C_{i,x} < C_{1,\delta}\varepsilon, \quad (2.35)$$

$$y_{\varepsilon,\delta}^{i,x}(0) = 0 \text{ and } y_{\varepsilon,\delta}^{i,x}(C_{i,x}) = 1, \quad (2.36)$$

$$\|(y_{\varepsilon,\delta}^{i,x})^{-1}\|_{L^\infty} \leq C_{2,\delta}\varepsilon, \quad (2.37)$$

$$\text{for fixed } t, y_{\varepsilon,\delta}^{i,x} \text{ is Lipschitz in } x \text{ away from } x_0 \text{ with} \quad (2.38)$$

Lipschitz constant $C_{3,\delta}$ independent of t as well.

The first three properties, (2.35)–(2.38), are all established in or follow quickly from [14, Lemma 3.2] along with the uniform Lipschitz bounds on $\gamma_{i,x}(\cdot)$. We remark that the fourth item, (2.38), follows from applying Gronwall’s inequality. It is convenient to have the $y_{\varepsilon,\delta}^{i,x}$ defined on one common interval, so let us extend each $y_{\varepsilon,\delta}^{i,x}$ to $[0, C_{1,\delta}\varepsilon]$ by setting $y_{\varepsilon,\delta}^{i,x} = 1$ for $t > C_{i,x}$.

Step 3. We will now present the construction of the recovery sequence $\{Q_\varepsilon^h\}_{\varepsilon>0}$ for Q_h for fixed h . We recall from the first step that Q_h is one of the approximations of the original element Q_0 of \mathcal{A}_0 . We will in fact construct sequences $\{Q_\varepsilon^{h,\delta}\}$ for $0 < \delta l_1$, prove that

$$\lim_{\delta \rightarrow 0} \limsup_{\varepsilon \rightarrow 0} F_\varepsilon(Q_\varepsilon^{h,\delta}) = F_0(Q_h), \quad (2.39)$$

and then diagonalize over δ and ε . Let us fix $0 < \delta \ll 1$. By utilizing the result from [6, Section 4], we obtain a sequence $\{\hat{Q}_\varepsilon^h\}$ such that

$$\hat{Q}_\varepsilon^h \rightarrow Q_h \text{ in } L^1(\Omega; \mathcal{S}) \text{ as } \varepsilon \rightarrow 0 \quad (2.40)$$

and

$$\limsup_{\varepsilon \rightarrow 0} F_\varepsilon(\hat{Q}_\varepsilon^h) \leq \sum_{i,j=1}^n d_{\sqrt{W}}(P_i, P_j) \mathcal{H}^1(\partial^* A_i^h \cap \partial^* A_j^h) \quad (2.41)$$

For now, we assume that there exists C_4 such that

$$\text{if } x \in A_i^h \text{ with } \text{dist}(x, \partial A_i^h) \geq C_4\varepsilon \text{ and } \text{dist}(x, \partial\Omega) \leq C_4, \text{ then } \hat{Q}_\varepsilon^h(x) = \alpha_i. \quad (2.42)$$

This assumption simplifies the calculations to follow, and we will see at the end of the proof that this assumption is not restrictive.

The \hat{Q}_ε^h do not assume the boundary values g , and the right hand side of (2.41) does not account for cost associated to the boundary of Ω . To address these issues, we will modify \hat{Q}_ε^h near $\partial\Omega$; away from $\partial\Omega$, the \hat{Q}_ε^h will be unchanged. Briefly, we will set $Q_\varepsilon^{h,\delta}$ to be \hat{Q}_ε^h on $\Omega_{C_{1,\delta}\varepsilon} := \{x \in \Omega : \text{dist}(x, \partial\Omega) > C_{1,\delta}\varepsilon\}$ and then, using the curves $\gamma_{m,x}$, define a boundary layer which bridges the values of $\hat{Q}_\varepsilon^{h,\delta}$ to the boundary data $g(x)$ along segments normal to $\partial\Omega$. Recall from (2.28) that each ∂A_i^h intersects $\partial\Omega$ at a 90° angle; this fact allows us to avoid technicalities which would arise from a point $x \in A_i^h \cap \partial\Omega_{C_{1,\delta}\varepsilon}$ whose projection $\sigma(x)$ onto $\partial\Omega$ is in A_j^h for $j \neq i$. We will need a different strategy near $x \in \partial\Omega \cap \partial A_i^h \cap \partial A_j^h$ for $i \neq j$, due to the obvious fact that $\gamma_{i,x}$ do not vary smoothly in i . In addition, each $\gamma_{i,x}$ was not continuous at $x_l \in \partial\Omega$, so we will need to cut out a small set near each x_l and modify our analysis there as well.

For each $x \in \Omega \setminus \Omega_{C_{1,\delta}\varepsilon}$, consider its projection $\sigma(x)$ onto $\partial\Omega$ and the inward pointing unit normal vector $\nu(\sigma(x))$ to $\partial\Omega$ at $\sigma(x)$. By the condition (2.28) on A_i^h , we see that $\{\partial A_i^h \cap \partial A_j^h \cap \partial\Omega : i \neq j\}$ is finite; we enumerate this set as $\{x_l\}_{l=L+1}^{\tilde{L}}$. Let $\mathcal{C}_\varepsilon \subset \partial\Omega$ be a finite union of curves $\mathcal{C}_\varepsilon^l$ contained in $\partial\Omega$ for $1 \leq l \leq \tilde{L}$, each of length $2C_4\varepsilon$ and centered around an x_l , so that x_l divides $\mathcal{C}_\varepsilon^l$ into two pieces of length $C_4\varepsilon$. We define

$$\Omega_0^\varepsilon = \{x \in \Omega \setminus \Omega_{C_{1,\delta}\varepsilon} : \sigma(x) \in \mathcal{C}_\varepsilon\}.$$

Let us denote by $d(x)$ the distance from x to $\partial\Omega$ for $x \in \Omega$. We now define

$$Q_\varepsilon^{h,\delta}(x) = \begin{cases} \hat{Q}_\varepsilon^h(x), & \text{if } x \in \Omega_{C_{1,\delta}\varepsilon}, \\ \gamma_{i,\sigma(x)}(y_{\varepsilon,\delta}^{i,\sigma(x)}(d(x))), & \text{if } x \in (\Omega \setminus (\Omega_{C_{1,\delta}\varepsilon} \cup \Omega_0^\varepsilon)). \end{cases}$$

We note that for $x \in \partial\Omega_{C_{1,\delta}}$ such that $x \in A_i^h$ but $\sigma(x) \in A_j^h$ for $i \neq j$, defining $Q_\varepsilon^{h,\delta}$ using $\gamma_{i,\sigma(x)}$ will result in a jump discontinuity. However, since ∂A_j^h is normal to $\partial\Omega$ in a neighborhood of $\partial\Omega$ by (2.28) and $\hat{Q}_\varepsilon^h(x) = \alpha_i$ if $\text{dist}(x, \partial A_i^h) \geq C_{4,\delta}\varepsilon$, for small enough ε , any such x must be in Ω_0^ε .

Hence for small ε , $Q_\varepsilon^{h,\delta}$ as defined thus far is Lipschitz. We have not yet defined $Q_\varepsilon^{h,\delta}$ on Ω_0^ε , but we will do so at the end of the proof.

First, we remark that $Q_\varepsilon^{h,\delta} \rightarrow Q_h$ in L^1 as $\varepsilon \rightarrow 0$ due to (2.40) and the fact that $Q_\varepsilon^{h,\delta}$ is bounded on $\Omega \setminus \Omega_{C_1, \delta\varepsilon}$ independently of ε . Next, we estimate $F_\varepsilon(Q_\varepsilon^{h,\delta})$. Let us denote for any $U \subset \Omega$ and tensor Q

$$F_\varepsilon(Q, U) = \int_U \left(\varepsilon |\nabla Q|^2 + \frac{1}{\varepsilon} W(Q) \right) dx.$$

Using (2.41) yields

$$\begin{aligned} \limsup_{\varepsilon \rightarrow 0} F_\varepsilon(Q_\varepsilon^{h,\delta}, \Omega_{C_1, \delta\varepsilon}) &= \limsup_{\varepsilon \rightarrow 0} F_\varepsilon(\hat{Q}_\varepsilon^{h,\delta}, \Omega_{C_1, \delta\varepsilon}) \\ &\leq \sum_{i,j=1}^n d_{\sqrt{W}}(P_i, P_j) \mathcal{H}^1(\partial A_i^h \cap \partial A_j^h \cap \Omega). \end{aligned} \quad (2.43)$$

Let us denote by Ω_i^ε the set $\{x \in \Omega \setminus (\Omega_{C_1, \delta\varepsilon} \cup \Omega_0^\varepsilon) : x \in A_i^h\}$. We now examine $F_\varepsilon(Q_\varepsilon^{h,\delta}, \Omega_i^\varepsilon)$. We will make use of the map

$$P_t : \partial\Omega \rightarrow \{x \in \Omega : d(x) = t\}$$

which sends $x \in \partial\Omega$ to $x + t\nu(x)$, where $\nu(x)$ is the inward pointing normal to $\partial\Omega$ at x . Because of the C^2 assumption on $\partial\Omega$, P_t is a C^1 -diffeomorphism with Jacobian J satisfying

$$|J(P_t)(x) - 1| \leq Ct \quad (2.44)$$

for some $C > 0$ independent of x and t .

For each $x \in \Omega_i^\varepsilon$, let $\tau = \tau(x)$ be a unit vector tangent to the level set of d at x and $\eta = \eta(x)$ be a unit vector perpendicular to τ . We write

$$\begin{aligned} F_\varepsilon(Q_\varepsilon^{h,\delta}, \Omega_i^\varepsilon) &= \int_{\Omega_i^\varepsilon} \left(\varepsilon |\nabla Q_\varepsilon^{h,\delta}|^2 + \frac{1}{\varepsilon} W(Q_\varepsilon^{h,\delta}) \right) dx \\ &= \int_{\Omega_i^\varepsilon} \left(\varepsilon \left| \frac{\partial}{\partial \tau} Q_\varepsilon^{h,\delta} \right|^2 + \varepsilon \left| \frac{\partial}{\partial \eta} Q_\varepsilon^{h,\delta} \right|^2 + \frac{1}{\varepsilon} W(Q_\varepsilon^{h,\delta}) \right) dx. \end{aligned}$$

Now from (2.38), it follows that

$$\frac{\partial}{\partial \tau}(Q_\varepsilon^{h,\delta}) = \frac{\partial}{\partial \tau}(\gamma_{i,\sigma(x)} \circ y_{\varepsilon,\delta}^{i,\sigma(x)} \circ d)(x)$$

is bounded independently of ε and x . Since $|\Omega_i^\varepsilon| \leq C\varepsilon$, where C is independent of ε , we have

$$\int_{\Omega_i^\varepsilon} \varepsilon \left| \frac{\partial}{\partial \tau} Q_\varepsilon^{h,\delta} \right|^2 dx \leq \int_{\Omega_i^\varepsilon} C\varepsilon dx \leq C\varepsilon^2.$$

Using now the coarea formula and the fact that $|\nabla d| = 1$, we write

$$\begin{aligned} F_\varepsilon(Q_\varepsilon^{h,\delta}, \Omega_i^\varepsilon) &\leq \int_{\Omega_i^\varepsilon} \left(\varepsilon \left| \frac{\partial}{\partial \eta} Q_\varepsilon^{h,\delta} \right|^2 + \frac{1}{\varepsilon} W(Q_\varepsilon^{h,\delta}) \right) dx + C\varepsilon^2 \\ &\leq \int_{\Omega_i^\varepsilon} \left(\varepsilon \left| \frac{\partial}{\partial \eta} (\gamma_{i,\sigma(x)} \circ y_{\varepsilon,\delta}^{i,\sigma(x)} \circ d)(x) \right|^2 + \frac{1}{\varepsilon} W(\gamma_{i,\sigma(x)} \circ y_{\varepsilon,\delta}^{i,\sigma(x)} \circ d)(x) \right) |\nabla d(x)| dx \\ &\quad + C\varepsilon^2 \\ &= \int_0^{C_{1,\delta}\varepsilon} \int_{\{d=t\} \cap \Omega_i^\varepsilon} \left(\varepsilon (\gamma'_{i,\sigma(x)}(y_{\varepsilon,\delta}^{i,\sigma(x)}(t)))^2 ((y_{\varepsilon,\delta}^{i,\sigma(x)})')^2 + \frac{1}{\varepsilon} W(\gamma_{i,\sigma(x)} \circ y_{\varepsilon,\delta}^{i,\sigma(x)})(t) \right) d\mathcal{H}^1(x) dt \\ &\quad + C\varepsilon^2. \end{aligned}$$

Then, recalling (2.34) and using the map P_t , we have:

$$\begin{aligned} F_\varepsilon(Q_\varepsilon^{h,\delta}, \Omega_i^\varepsilon) &\leq \int_0^{C_{1,\delta}\varepsilon} \int_{\{d=t\} \cap \Omega_i^\varepsilon} 2|\gamma'_{i,\sigma(x)}(y_{\varepsilon,\delta}^{i,\sigma(x)}(t))||\delta + W(\gamma_{i,\sigma(x)} \circ y_{\varepsilon,\delta}^{i,\sigma(x)})(t)|^{1/2} d\mathcal{H}^1(x) dt \\ &\quad + C\varepsilon^2 \\ &= \int_0^{C_{1,\delta}\varepsilon} \int_{\partial\Omega \cap \Omega_i^\varepsilon} 2|\gamma'_{i,x}(y_{\varepsilon,\delta}^{i,x}(t))||\delta + W(\gamma_{i,x} \circ y_{\varepsilon,\delta}^{i,x})(t)|^{1/2} |J(P_t(x))| d\mathcal{H}^1(x) dt \\ &\quad + C\varepsilon^2 \\ &= \int_{\partial\Omega \cap \Omega_i^\varepsilon} \int_0^{C_{1,\delta}\varepsilon} 2|\gamma'_{i,x}(y_{\varepsilon,\delta}^{i,x}(t))||\delta + W(\gamma_{i,x} \circ y_{\varepsilon,\delta}^{i,x})(t)|^{1/2} |J(P_t(x))| dt d\mathcal{H}^1(x) \\ &\quad + C\varepsilon^2. \end{aligned}$$

Making the change of variables $s = y_{\varepsilon,\delta}^{i,x}(t)$ and recalling from the definition of Ω_i^ε that $\partial\Omega \cap \Omega_i^\varepsilon \subset A_i$,

we have

$$\begin{aligned} F_\varepsilon(Q_\varepsilon^{h,\delta}, \Omega_i^\varepsilon) &\leq \int_{\partial\Omega \cap A_i} \int_0^1 2|\gamma'_{i,x}(s)||\delta + W(\gamma_{i,x}(s))|^{1/2} |J(P_{(y_{\varepsilon,\delta}^{i,x})^{-1}(s)}(x))| ds d\mathcal{H}^1(x) + C\varepsilon^2. \end{aligned}$$

By using (2.44) and the bound $\|(y_{\varepsilon,\delta}^{i,x})^{-1}\|_{L^\infty} \leq C_{2,\delta}\varepsilon$ from (2.37), we estimate $|J(P_{(y_{\varepsilon,\delta}^{i,x})^{-1}(s)})| \leq 1 + C\varepsilon$. Taking the limsup on both sides as $\varepsilon \rightarrow 0$ gives

$$\begin{aligned} \limsup_{\varepsilon \rightarrow 0} F_\varepsilon(Q_\varepsilon^{h,\delta}, \Omega_i^\varepsilon) &\leq \limsup_{\varepsilon \rightarrow 0} \int_{\partial\Omega \cap B_i} \int_0^1 2|\gamma'_{i,x}(s)| |\delta + W(\gamma_{i,x}(s))|^{1/2} ds d\mathcal{H}^1(x) \\ &\quad + C\varepsilon + C\varepsilon^2 \\ &\leq 2 \int_{\partial\Omega \cap A_i^h} \int_0^1 |\gamma'_{i,x}(s)| |\delta + W(\gamma_{i,x}(s))|^{1/2} ds d\mathcal{H}^1(x). \end{aligned} \quad (2.45)$$

Using the right hand side of the previous inequality as our estimate for $\limsup_{\varepsilon \rightarrow 0} F_\varepsilon(Q_\varepsilon^{h,\delta}, \Omega_i^\varepsilon)$

yields, upon summing,

$$\begin{aligned} \limsup_{\varepsilon \rightarrow 0} \sum_{i=1}^n F_\varepsilon(Q_\varepsilon^{h,\delta}, \Omega_i^\varepsilon) &\leq 2 \sum_{i=1}^n \int_{\partial\Omega \cap A_i^h} \int_0^1 |\gamma'_{i,x}(s)| |\delta + W(\gamma_{i,x}(s))|^{1/2} ds d\mathcal{H}^1(x) \\ &= 2 \sum_{i=1}^n \int_{\partial\Omega \cap A_i^h} d_{\sqrt{W}}(g(x), \alpha_i) d\mathcal{H}^1(x) + C\sqrt{\delta} \\ &= 2 \sum_{i=1}^n \int_{\partial\Omega \cap A_i^h} d_{\sqrt{W}}(g(x), P_i) d\mathcal{H}^1(x) + C\sqrt{\delta}, \end{aligned} \quad (2.46)$$

where C only depends on the lengths of the $\gamma_{i,x}$, which in turn depend on h . Combining (2.43) and (2.46) yields

$$\limsup_{\varepsilon \rightarrow 0} F_\varepsilon(Q_\varepsilon^{h,\delta}, \cup_{i=1}^n \Omega_i^\varepsilon \cup \Omega_{C_1, \delta\varepsilon}) \leq F_0(Q_h) + C_h \sqrt{\delta}, \quad (2.47)$$

We will take the infimum over δ at the end of the proof, so as not to confuse the order in which δ and ε are sent to zero in the remaining estimates.

To finish proving the estimate

$$\limsup_{\varepsilon \rightarrow 0} F_\varepsilon(Q_\varepsilon^{h,\delta}, \Omega) \leq F_0(Q_h) + C_h \sqrt{\delta},$$

it suffices to define $Q_\varepsilon^{h,\delta}$ on Ω_0^ε and show that

$$F_\varepsilon(Q_\varepsilon^{h,\delta}, \Omega_0^\varepsilon) \rightarrow 0$$

as $\varepsilon \rightarrow 0$ for any fixed $\delta > 0$. We will define $Q_\varepsilon^{h,\delta}$ on this set so that the integrand $\varepsilon|\nabla Q_\varepsilon^{h,\delta}|^2 + \frac{1}{\varepsilon}W(Q_\varepsilon^{h,\delta})$ is $O(1/\varepsilon)$ there, and then show that the measure of this set is $O(\varepsilon^2)$. Since δ is fixed

in this argument, we will suppress its appearance in the constants for the following estimates. We assume that $Q_\varepsilon^{h,\delta}$ restricted $\overline{\Omega} \setminus (\Omega_{C_4} \cup \Omega_0^\varepsilon)$ satisfies:

$$\begin{cases} \|Q_\varepsilon^{h,\delta}\|_{L^\infty(\overline{\Omega} \setminus (\Omega_{C_4} \cup \Omega_0^\varepsilon))} \leq C \\ \|\nabla Q_\varepsilon^{h,\delta}\|_{L^\infty(\overline{\Omega} \setminus (\Omega_{C_4} \cup \Omega_0^\varepsilon))} \leq \frac{C}{\varepsilon}, \end{cases}$$

where C is independent of ε . If $Q_\varepsilon^{h,\delta}$ did not satisfy these estimates, then $Q_\varepsilon^{h,\delta}$ can be modified inside Ω_{C_4} near $\partial\Omega_{C_4}$ and extended to $\Omega \setminus \Omega_{C_4}$ using level sets of the distance function so as to meet these requirements. This can be done by utilizing the techniques of [17, Lemma 3.2], in which it is shown that the boundary values of a sequence such as $Q_\varepsilon^{h,\delta}$ can be changed without increasing the total energy in the limit. The application of [17, Lemma 3.2] also allows us to assume that (2.42) holds as well.

Let us consider $\{x \in \Omega_0^\varepsilon : \sigma(x) \in \mathcal{C}_\varepsilon^l\} \subset \Omega_0^\varepsilon$. Since $\{x \in \Omega_0^\varepsilon : \sigma(x) \in \mathcal{C}_\varepsilon^l\}$ is a “strip” of length $2C_{4,\delta}\varepsilon$ and width $C_{1,\delta}\varepsilon$, it is easy to see from the coarea formula that for fixed δ ,

$$|\Omega_0^\varepsilon| = O(\varepsilon^2).$$

Now, since on the boundary of this strip, $\|\nabla Q_\varepsilon^{h,\delta}\| \leq \frac{C}{\varepsilon}$, it can be quickly seen that $Q_\varepsilon^{h,\delta}$ can be extended to a Lipschitz function satisfying

$$\begin{cases} \|Q_\varepsilon^{h,\delta}\|_{L^\infty(\{x \in \Omega_0^\varepsilon : \sigma(x) \in \mathcal{C}_\varepsilon^l\})} \leq C \\ \|\nabla Q_\varepsilon^{h,\delta}\|_{L^\infty(\{x \in \Omega_0^\varepsilon : \sigma(x) \in \mathcal{C}_\varepsilon^l\})} \leq \frac{C_\kappa}{\varepsilon}, \end{cases}$$

where $C_\kappa \geq C$ is a constant depending on the curvature κ of $\partial\Omega$. If $\partial\Omega$ is flat, so that Ω_0^ε is a rectangle, then linearly interpolating the values of $Q_\varepsilon^{h,\delta}$ from the boundary of the rectangle along diagonal segments across the rectangle works and gives $C_\kappa = C$. We estimate

$$\int_{\{x \in \Omega_0^\varepsilon : \sigma(x) \in \mathcal{C}_\varepsilon^l\}} \left(\varepsilon |\nabla Q_\varepsilon^{h,\delta}|^2 + \frac{W(Q_\varepsilon^{h,\delta})}{\varepsilon} \right) dx \leq \frac{C_\kappa}{\varepsilon} |\Omega_0^\varepsilon| = O(\varepsilon). \quad (2.48)$$

Since Ω_0^ε is the union of the sets $\{x \in \Omega_0^\varepsilon : \sigma(x) \in \mathcal{C}_\varepsilon^l\}$, we have

$$\int_{\Omega_0^\varepsilon} \left(\varepsilon |\nabla Q_\varepsilon^{h,\delta}|^2 + \frac{W(Q_\varepsilon^{h,\delta})}{\varepsilon} \right) dx = O(\varepsilon). \quad (2.49)$$

Summing the estimates (2.46), (2.48), and (2.49) gives

$$\limsup_{\varepsilon \rightarrow 0} F_\varepsilon(Q_\varepsilon^{h,\delta}) \leq F_0(Q_h) + C_h \sqrt{\delta},$$

so that

$$\lim_{\delta \rightarrow 0} \limsup_{\varepsilon \rightarrow 0} F_\varepsilon(Q_\varepsilon^{h,\delta}) \leq F_0(Q_h). \quad (2.50)$$

Now diagonalizing over δ and ε , we obtain a recovery sequence $\{Q_\varepsilon^h\}_{\varepsilon > 0}$ for Q_h .

Conclusion of proof: Combining (2.31) and (2.50), we have

$$\lim_{h \rightarrow \infty} \lim_{\delta \rightarrow 0} \limsup_{\varepsilon \rightarrow 0} F_\varepsilon(Q_\varepsilon^{h,\delta}) \leq \lim_{h \rightarrow \infty} F_0(Q_h) = F_0(Q_0).$$

Having already diagonalized $\{Q_\varepsilon^{h,\delta}\}_{\varepsilon > 0}$ over δ and ε to obtain a recovery sequence $\{Q_\varepsilon^h\}_{\varepsilon > 0}$ for Q_h , we diagonalize the recovery sequences $\{Q_\varepsilon^h\}_{\varepsilon > 0}$ over ε and h and obtain a recovery sequence $\{Q_\varepsilon\}_{\varepsilon > 0}$ for Q_0 . The case for constant boundary data g is simpler and follows from the above calculations. \square

2.3 Local Minimizers of F_ε

Now that we have proven Γ -convergence, we aim to prove the existence of local minimizers of F_ε . A similar theorem was proved for the Allen-Cahn functionals in [61] by minimizing the functionals in an L^1 -ball around an isolated L^1 -local minimizer of the Γ -limit. The proof required the existence of such an isolated local minimizer in addition to L^1 -compactness for any sequence of functions with bounded energies. Neither of these conditions holds in the problem we are considering. Indeed, for any local minimizer Q_0 of F_0 , we have that $F_0(r_\theta^T Q_0 r_\theta) = F_0(Q_0)$. This follows from the rotational symmetry of W described in the beginning of Section 2.2. Also, since the zero set P of W is higher-dimensional, as opposed to a finite collection of points, we cannot obtain L^1 -compactness of a sequence of minimizers Q_ε . To account for both of these issues, we introduce the distance

$$\Lambda(Q_1, Q_2) = \sum_i \|\varphi_i(Q_1) - \varphi_i(Q_2)\|_{L^1(\Omega)}$$

for any Q_1 and Q_2 in \mathcal{A}_0 , cf. (2.8) and (2.9), respectively. We observe that $\Lambda(Q_1, Q_2) = 0$ if and only if for each i , $\{x : Q_1(x) \in P_i\} = \{x : Q_2(x) \in P_i\}$ up to a set of measure zero.

Proposition 2.3.1. *Let Q_ε be a sequence of maps from $\Omega \times (0, 1)$ to \mathcal{S} and assume that the sequence of energies $F_\varepsilon(Q_\varepsilon)$ is uniformly bounded. Then there exists a subsequence $\{Q_{\varepsilon_j}\}$ and $Q \in L^1(\Omega \times (0, 1); P)$ such that $\Lambda(Q_{\varepsilon_j}, Q) \rightarrow 0$.*

Proof. By similar arguments as in the proof of lower–semicontinuity in Section 2.2, we can truncate the Q_ε to obtain \tilde{Q}_ε such that $\Lambda(Q_\varepsilon, \tilde{Q}_\varepsilon) \rightarrow 0$ and \tilde{Q}_ε are uniformly bounded in L^∞ . Hence if we obtain Q such that $\Lambda(\tilde{Q}_{\varepsilon_m}, Q) \rightarrow 0$, then $\Lambda(Q_{\varepsilon_m}, Q) \rightarrow 0$ as well. Suppressing the tildes, from the L^∞ bound we see that

$$\|\varphi_i \circ Q_\varepsilon\|_{L^1(\Omega)} \leq C < \infty.$$

Next, using the calculations preceding (2.25), which replaced the surface integrals of f_s by volume integrals, we have

$$\begin{aligned} 2 \int_{\Omega \times (0, 1)} \sqrt{W(Q_\varepsilon)} |\nabla Q_\varepsilon| dx dz &\leq \int_{\Omega \times (0, 1)} \left(\varepsilon |\nabla Q_\varepsilon|^2 + \frac{W(Q_\varepsilon)}{\varepsilon} \right) dx dz \\ &\leq F_\varepsilon(Q_\varepsilon) + O(\varepsilon) \\ &\leq C < \infty. \end{aligned}$$

It is straightforward then to see that

$$2 \int_{\Omega \times (0, 1)} |\nabla(\varphi_i \circ Q_\varepsilon)| dx dz \leq 2 \int_{\Omega \times (0, 1)} \sqrt{W(Q_\varepsilon)} |\nabla Q_\varepsilon| dx dz \leq C < \infty.$$

Thus $\{\varphi_i \circ Q_\varepsilon\}$ are uniformly bounded in BV .

It remains to construct a limiting element Q . For each i , up to a subsequence,

$$\varphi_i(Q_{\varepsilon_j}) \rightarrow \omega_i \text{ as } j \rightarrow \infty$$

in $L^1(\Omega \times (0, 1))$ for some function ω_i . We claim that the sets $E_i := \{(x, z) \in \Omega \times (0, 1) : \omega_i(x, z) = 0\}$ partition $\Omega \times (0, 1)$ up to sets of measure zero. To see this, first suppose by way of contradiction

that there exists a set $A \subset \Omega \times (0, 1)$ of positive measure such that none of the ω_i 's are zero on A . By restricting to a further subsequence, we can assume for each i that $\varphi_i(Q_{\varepsilon_j})$ converges almost everywhere and hence, by Egoroff's Theorem, almost uniformly on A . Since $\omega_i > 0$ on A for each i , we can obtain a set $B \subset A$ of positive measure and an $\eta > 0$ such that on B ,

$$\varphi_i(Q_{\varepsilon_j}) > \eta > 0$$

for each i and for j sufficiently large. But if the distance φ_i to P_i is greater than η on B for each i , it follows that for j sufficiently large, $W(Q_{\varepsilon_j}) > \tilde{\eta}$ on B for some $\tilde{\eta} > 0$. We also recall from (2.25) that for a sequence such as $\{Q_\varepsilon\}$ with bounded energies we can replace $F_\varepsilon(Q_\varepsilon)$ by $\tilde{F}_\varepsilon(Q_\varepsilon)$ up to an error of order $O(\varepsilon)$. Combining these observations we deduce that

$$\frac{|B|\tilde{\eta}}{\varepsilon_j} \leq \int_B \frac{W(Q_{\varepsilon_j})}{\varepsilon_j} dx dz \leq \tilde{F}_{\varepsilon_j}(Q_{\varepsilon_j}) \leq C < \infty,$$

which is a contradiction for j sufficiently large. We conclude that the union of the E_i 's contains Ω up to a set of measure zero. To see that the E_i are disjoint, note that if $\varphi_i(Q_{\varepsilon_j})$ is very close to zero, then for $k \neq i$, $\varphi_k(Q_{\varepsilon_j})$ must be away from zero. Therefore, the sets $\{E_i\}$ have empty intersection, so they partition Ω up to a set of measure zero.

We see that each ω_i has finite range, since it can only take the values $d_{\sqrt{W}}(P_i, P_k)$. Using the partition $\{E_i\}$, we can take any $Q \in L^1(\Omega \times (0, 1); \mathcal{S})$ such that $\{(x, z) \in \Omega \times (0, 1) : Q(x, z) \in P_i\} = E_i$ as our limiting element. As a specific example of such a Q , define $Q \equiv \alpha_i \in P_i$ on each E_i , where α_i is any constant in P_i . □

We now prove the existence of local minimizer for F_ε if there exists a Λ -isolated local minimizer of F_0 .

Theorem 2.2. *Let Q_0 be an isolated Λ -local minimizer in the sense that there exists $\delta > 0$ such that*

$$F_0(Q_0) < F_0(Q)$$

if $0 < \Lambda(Q, Q_0) \leq \delta$. Then there exists $\varepsilon_0 > 0$ and a family $\{Q_\varepsilon\}_{\varepsilon < \varepsilon_0}$ such that

$$Q_\varepsilon \text{ is a } \Lambda\text{-local minimizer of } F_\varepsilon \quad (2.51)$$

and

$$\Lambda(Q_0, Q_\varepsilon) \rightarrow 0. \quad (2.52)$$

Remark 2.1. We note that Q_ε are in fact H^1 -local minimizers of F_ε . This is because the distance Λ is weaker than the H^1 metric.

Proof. The direct method in the calculus of variations yields for each $\varepsilon > 0$ a Q_ε which minimizes F_ε on the ball $\{Q : \Lambda(Q, Q_0) \leq \delta\}$. By the existence of recovery sequences for F_ε established in Theorem 2.1, we know that for ε sufficiently small, the recovery sequence $\{Q_\varepsilon^0\}$ for Q_0 is contained in B . We then have

$$\liminf_{\varepsilon \rightarrow 0} F_\varepsilon(Q_\varepsilon) \leq \liminf_{\varepsilon \rightarrow 0} F_\varepsilon(Q_\varepsilon^0) = F_0(Q_0). \quad (2.53)$$

We will now show that for sufficiently small ε , $\Lambda(Q_\varepsilon, Q_0) < \delta$, thus establishing that the Q_ε are local minimizers of F_ε . Suppose this does not hold, so that there exists a subsequence $\{\varepsilon_j\}$ such that $\Lambda(Q_{\varepsilon_j}, Q_0) = \delta$. By Proposition 2.3.1, we obtain $Q \in L^1(\Omega \times (0, 1); P)$ such that up to a further subsequence, still denoted by Q_{ε_j} ,

$$\Lambda(Q_{\varepsilon_j}, Q) \rightarrow 0.$$

We will show that $F_0(Q) \leq F_0(Q_0)$ and $Q \in \{Q : \Lambda(Q, Q_0) \leq \delta\}$. This will contradict that Q_0 is a Λ -isolated local minimizer of F_0 .

We observe $\|d_{\sqrt{W}}(Q_{\varepsilon_j}, Q)\|_{L^1} \leq \|\varphi_i \circ Q_{\varepsilon_j}\|_{L^1} + \|\varphi_i \circ Q\|_{L^1}$, so that $\|d_{\sqrt{W}}(Q_{\varepsilon_j}, Q)\| \rightarrow 0$. Next, examining the proof of the lower semicontinuity condition (2.13), we see that the L^1 convergence of $d_{\sqrt{W}}(Q_{\varepsilon_j}, Q)$ to 0 along with the fact that Q takes values in P are in fact sufficient conditions to conclude that

$$F_0(Q) \leq \liminf_{j \rightarrow \infty} F_{\varepsilon_j}(Q_{\varepsilon_j}).$$

But we also have from (2.53) that

$$\liminf_{j \rightarrow \infty} F_{\varepsilon_j}(Q_{\varepsilon_j}) \leq F_0(Q_0).$$

It follows that $F_0(Q) \leq F_0(Q_0)$. Combining this with our assumption that $\Lambda(Q_0, Q) = \delta$ we obtain a contradiction to the fact that Q_0 is an isolated Λ -local minimizer of F_0 . We have thus shown that $\Lambda(Q_0, Q_\varepsilon) < \delta$ for sufficiently small ε . The proof that $\Lambda(Q_\varepsilon, Q_0) \rightarrow 0$ proceeds using similar reasoning. \square

We point out that the arguments in the preceding theorem apply in more general scenarios. Below, we formulate one such generalization.

Let $\mathcal{N} \subset \mathbb{R}^l$ be an open, bounded domain with smooth boundary. Also, we fix a smooth, disconnected, and bounded set $\mathcal{M} \in \mathbb{R}^k$ with components $\mathcal{M}_1, \dots, \mathcal{M}_n$. Let $W : \mathbb{R}^k \rightarrow [0, \infty)$ satisfy $W^{-1}(0) = \mathcal{M}$ and $W(v) \rightarrow \infty$ as $|v| \rightarrow \infty$. Consider the functionals

$$H_\varepsilon(u) = \int_{\mathcal{N}} \left(\varepsilon |\nabla u|^2 + \frac{1}{\varepsilon} W(u) \right) dx,$$

for maps u satisfying either a prescribed volume constraint or a Dirichlet boundary condition g . Let φ_i be the distance to \mathcal{M}_i under the degenerate Riemannian metric with the conformal factor \sqrt{W} . If we define the distance

$$\Lambda_{\mathcal{M}, \mathcal{N}}(u_1, u_2) = \sum_{i=1}^n \|\varphi_i(u_1) - \varphi_i(u_2)\|_{L^1(\mathcal{N})}, \quad (2.54)$$

then any sequence $\{u_\varepsilon\}$ with bounded energy is $\Lambda_{\mathcal{M}, \mathcal{N}}$ -compact. Suppose that in the $L^1(\mathcal{N}; \mathcal{M})$ topology, the H_ε Γ -converge to a functional H_0 as $\varepsilon \rightarrow 0$. Then we have the following theorem.

Theorem 2.3. *Let u_0 be an isolated $\Lambda_{\mathcal{M}, \mathcal{N}}$ -local minimizer in the sense that there exists $\delta > 0$ such that*

$$H_0(u_0) < H_0(u)$$

if $0 < \Lambda_{\mathcal{M}, \mathcal{N}}(u, u_0) \leq \delta$. Then there exists $\varepsilon_0 > 0$ and a family $\{u_\varepsilon\}_{\varepsilon < \varepsilon_0}$ such that

$$u_\varepsilon \text{ is a } \Lambda_{\mathcal{M}, \mathcal{N}}\text{-local minimizer of } H_\varepsilon \quad (2.55)$$

and

$$\Lambda_{\mathcal{M}, \mathcal{N}}(u_0, u_\varepsilon) \rightarrow 0. \quad (2.56)$$

Remark 2.2. *Using the techniques from the proof of Theorem 2.1, the Γ -convergence of H_ε could be established in the case of a volume constraint. In the case of a Dirichlet boundary condition, one would need to be able to construct a smoothly varying family of paths connecting the boundary data g to any element in the domain of a map in the admissible set for H_0 . Provided this is possible, the Γ -convergence could be proved using our techniques.*

2.4 Isolated Local Minimizers for F_0

In this section, we will prove the existence of an isolated local minimizer to a partitioning problem on certain two-dimensional domains. For a domain Ω , we will refer to a partition of Ω as an ordered pair (C, D) of subsets of Ω with finite perimeter and disjoint measure theoretic interiors such that

$$|\Omega - (C \cup D)| = 0.$$

The notation $|\cdot|$ refers to the Lebesgue measure. We introduce the notation

$$\theta(C, x) = \lim_{r \rightarrow 0} \frac{|C \cap B(x, r)|}{|B(x, r)|}$$

to refer to the density of a set C at a point x . If the above limit does not exist, we will use $\underline{\theta}(C, x)$ and $\bar{\theta}(C, x)$ to refer to the corresponding \liminf and \limsup , respectively. We define the measure theoretic interior of a set C as the set of points x where $\theta(C, x) = 1$ and denote it by C^i . The measure theoretic boundary of a finite perimeter set C is defined as the set

$$\partial_M C = \{x : 0 < \bar{\theta}(C, x)\} \cap \{x : \underline{\theta}(C, x) < 1\}.$$

Note that finite perimeter sets are only defined up to sets of Lebesgue measure zero. Throughout, in order to avoid ambiguity, we will always use the measure-theoretic closure of a set C , the set of

points where $\bar{\theta}(C, x) > 0$, as its representative, and we will denote the measure-theoretic boundary of C by ∂C rather than $\partial_M C$.

The functional F_0 is defined on partitions (C, D) of Ω by the formula

$$F_0(C, D) = c_1 \mathcal{H}^1(\partial C \cap \partial\Omega) + c_2 \mathcal{H}^1(\partial D \cap \partial\Omega) + c_3 \mathcal{H}^1(\partial C \cap \partial D). \quad (2.57)$$

We reuse the notation F_0 since F_0 as in (2.57) is a special case of the F_0 defined in (2.10) when there are only two connected components of the zero set P of W .

Let us assume the following inequalities for the constants c_i :

$$0 < c_1 < c_2$$

and

$$c_2 < c_1 + c_3.$$

The first inequality is natural, since in the case that $c_1 = c_2$, the cost on $\partial\Omega$ is the same for every competitor and hence minimizing F_0 reduces to minimizing the interfacial length of any partition. In this case, the problem is the same as that studied in [61]. Phrased in the language of an Allen–Cahn type problems with a potential W , the second inequality is an assumption that the triangle inequality is strict for the degenerate Riemannian metric with conformal factor \sqrt{W} .

We now describe the type of domains for which we will be able to construct a local minimizer to F_0 ; see Fig. 2.2. Let $\Omega \subset \mathbb{R}^2$ be a simply connected C^2 domain, and denote the outward unit normal vector to Ω by ν_Ω . Assume that Ω contains a line segment \overline{PQ} such that $P, Q \in \partial\Omega$ and there exists a unit vector v perpendicular to $P - Q$ satisfying the following conditions:

$$v \cdot \nu_\Omega = \frac{c_1 - c_2}{c_3} < 0 \text{ at } P \text{ and } Q, \quad (2.58)$$

and in neighborhoods N_1, N_2 of P and Q , respectively,

$$\partial\Omega \cap N_i \text{ is the graph of a strictly convex function over an interval of length } l. \quad (2.59)$$

The first condition is the contact angle condition which arises as a necessary condition for criticality.

It represents a local balance between interfacial and boundary energy.

Define Γ_1 to be $\partial\Omega \cap N_1$ and similarly $\Gamma_2 = \partial\Omega \cap N_2$. Note that under our assumptions, $v \cdot \nu_\Omega$ is a monotone function of the arc-length variable along Γ_1 and Γ_2 . We can now define the candidate (A, B) for the isolated local minimizer of F_0 . Let $\partial A \cap \partial B = \overline{PQ}$ and choose A such that for each i , $v \cdot \nu_\Omega$ is strictly larger on $\Gamma_i \cap \partial A$ than on $\Gamma_i \cap \partial B$; see Fig. 2.2. The inequality $c_1 < c_2$ forces us to specify A and B in this manner, since F_0 is not symmetric regarding the boundary costs. Consider the following variational problem:

$$\text{minimize } F_0(C, D) \text{ over partitions } (C, D) \text{ satisfying } |A \Delta C| + |B \Delta D| \leq \delta. \quad (2.60)$$

We will prove the following theorem:

Theorem 2.4. *There exists $\delta = \delta(\Omega, \{c_i\})$ such that (A, B) is the unique solution to the problem (2.60).*

Note that the direct method and compactness in BV yield that a minimizer exists for the variational problem (2.60). To prove Theorem 2.4, we will first show in Lemma 2.4 that the boundary $\partial A' \cap \partial B' \cap \Omega$ of any solution (A', B') to (2.60) must be “uniformly close” to \overline{PQ} . Then, using a calibration argument, we will show that (A, B) is an isolated local minimizer.

We make a few remarks about Ω which will be used throughout the proof of Theorem 2.4. Denote the set $\{x \in \Omega : d(x, \partial\Omega) < \eta\}$ by Ω_η . Let $\gamma : [0, L) \rightarrow \partial\Omega$ parametrize $\partial\Omega$ by arclength. The assumption that $\partial\Omega$ is C^2 implies that for some small η_0 , the map

$$T : [0, L) \times [0, \eta_0] \rightarrow \overline{\Omega}_{\eta_0}$$

defined by

$$T(s, y) := \gamma(s) - y\nu_\Omega(\gamma(s))$$

is a local C^1 -diffeomorphism. Under this map, the distance from a point $T(s, y) \in \Omega$ to $\partial\Omega$ is y .

We will refer to the nearest point projection of a point $x \in \Omega$ onto $\partial\Omega$ by $\sigma(x)$ and the projection

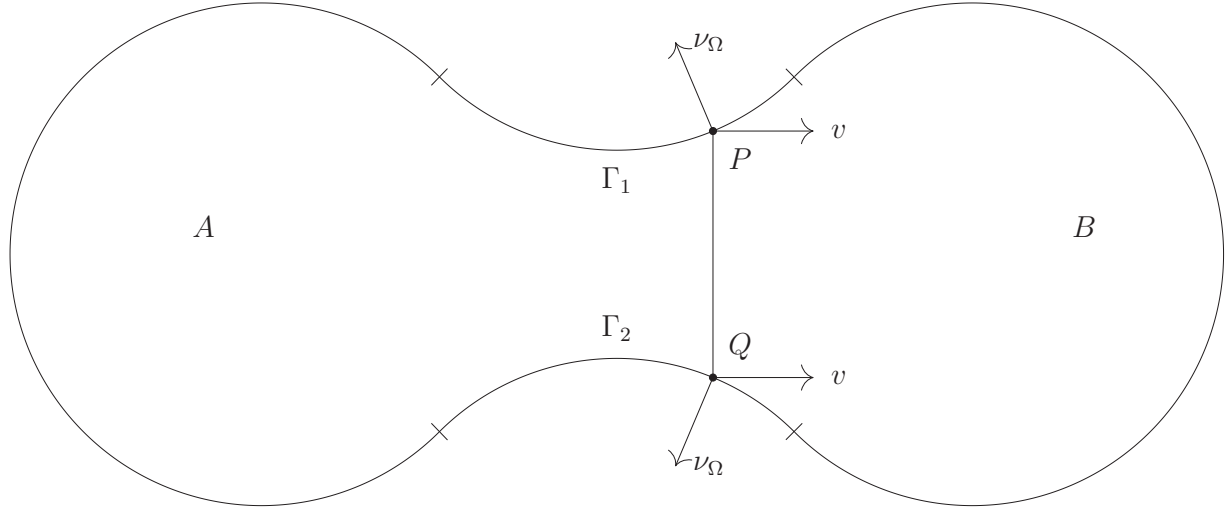


Figure 2.2: A dumbbell domain with an isolated local minimizer (A, B) of F_0 .

$(s, y) \rightarrow (s, 0)$ onto the s -axis in \mathbb{R}^2 by π . Note that with these conventions,

$$T \circ \pi = \sigma \circ T.$$

The following lemma provides a lower bound on the interior perimeter of a finite perimeter set $V \subset \Omega_\eta$ in terms of the length of its projection $\sigma(V)$ onto $\partial\Omega$ and will be needed in the proof of Lemma 2.4.

Lemma 2.2. *Let V be a set of finite perimeter such that $V \subset T([a, b] \times [0, \eta])$ for some $\eta < \eta_0$.*

Then if we set $\kappa_\infty := \max\{|\gamma_{ss}|\}$ (the maximum of the curvature of $\partial\Omega$) we have the estimates

$$(1 - \eta\kappa_\infty)\mathcal{H}^1(\sigma(V)) \leq \mathcal{H}^1(\partial V \cap T((a, b) \times (0, \eta))) \quad (2.61)$$

and

$$\mathcal{H}^1(\partial V \cap \partial\Omega) \leq \mathcal{H}^1(\sigma(V)). \quad (2.62)$$

Remark 2.3. *Regarding Lemma 2.2, we remark that sets of finite perimeter which differ by a set of Lebesgue measure zero (and are thus equivalent) could have projections onto $\partial\Omega$ which differ by a set of possibly large \mathcal{H}^1 measure. This would invalidate (2.61). Recall however that we employ the*

convention for a set V of finite perimeter, $x \in V$ if and only if $\bar{\theta}(V, x) > 0$. It is this representative of V for which the lemma holds.

Proof. Let us first consider the case where $\partial V \cap T((a, b) \times (0, \eta))$ is a single smooth curve. Let $(s(t), y(t)) : (c, d) \rightarrow (a, b) \times (0, \eta)$ be a smooth curve parametrized by arc-length such that $T \circ (s, y) : (c, d) \rightarrow \Omega$ parametrizes $\partial V \cap T((a, b) \times (0, \eta))$. Using the chain rule on $T \circ (s, y)$ and the identities $\langle \gamma_s, \nu_\Omega \rangle = 0$, $\langle \nu_\Omega, (\nu_\Omega)_s \rangle = 0$, and $1 = |\gamma_s|^2 = |\nu_\Omega|^2$, we write

$$\begin{aligned} \mathcal{H}^1(\partial V \cap T((a, b) \times (0, \eta))) &= \int_c^d \langle (T \circ (x, y))', (T \circ (x, y))' \rangle^{1/2} dt \\ &= \int_c^d \langle \gamma_s s' + y' \nu_\Omega + y(\nu_\Omega)_s s', \gamma_s s' + y' \nu_\Omega + y(\nu_\Omega)_s s' \rangle^{1/2} dt \\ &= \int_c^d (s'^2 + 2s'^2 y \langle \gamma_s, (\nu_\Omega)_s \rangle + y'^2 + y^2 s'^2 |(\nu_\Omega)_s|^2)^{1/2} dt. \end{aligned}$$

Recall that by construction, $s'^2 + y'^2 = 1$, which also implies $s'^2 \geq s'^4$. Also note that $|\langle \gamma_s, (\nu_\Omega)_s \rangle| = |(\nu_\Omega)_s|, |(\nu_\Omega)_s| \leq \kappa_\infty$, and $|y| \leq \eta$. Continuing the previous line using these observations yields the estimate

$$\begin{aligned} \mathcal{H}^1(\partial V \cap T((a, b) \times (0, \eta))) &\geq \int_c^d (1 - 2|s'^2 y| |(\nu_\Omega)_s| + s'^4 y^2 |(\nu_\Omega)_s|^2)^{1/2} dt \\ &= \int_c^d (1 - |s'^2 y| |(\nu_\Omega)_s|) dt \\ &\geq \int_c^d 1 - \eta \kappa_\infty dt \\ &\geq (1 - \eta \kappa_\infty) \mathcal{H}^1(\pi(T^{-1}(V))). \end{aligned} \tag{2.63}$$

Next, since γ parametrizes the boundary $\partial\Omega$ by arc-length, we see that $T^{-1}|_{\partial\Omega}$ preserves \mathcal{H}^1 measure. In addition, $T^{-1} \circ \sigma = \pi \circ T^{-1}$. These two facts imply that

$$\mathcal{H}^1(\pi(T^{-1}(V))) = \mathcal{H}^1(T^{-1}(\sigma(V))) = \mathcal{H}^1(\sigma(V)).$$

This equality in conjunction with (2.63) yields (2.61), namely

$$(1 - \eta \kappa_\infty) \mathcal{H}^1(\sigma(V)) \leq \mathcal{H}^1(\partial V \cap T((a, b) \times (0, \eta)))$$

for the case where $\partial V \cap T((a, b) \times (0, \eta_0))$ is a single smooth curve. For $\partial V \cap T((a, b) \times (0, \eta))$ still smooth but with more than one component, we apply the above calculation to each component and sum the results to obtain (2.61). Finally, for such V , (2.62) is immediate.

Now, for arbitrary V with finite perimeter, by mollifying V and using super-level sets of the mollifications as in Chapter 1 of [44], we obtain a sequence of smooth sets V_n approximating V and take limits in (2.61) for V_n . \square

We conclude the preliminaries with a standard result which we will need in proof of Theorem 2.4. The proof is found in [101, p. 1065].

Lemma 2.3. *Let $E \subset \mathbb{R}$ be a set of finite perimeter. Suppose there exists a point x_0 in ∂E with the property that for some closed cube Q_0 centered at x_0 , $\nu_E(x)$ is a constant v for all $x \in Q_0 \cap \partial E$. Then $Q_0 \cap \partial E = Q_0 \cap P$, where P is the hyperplane containing x_0 with normal v .*

Lemma 2.4. *Let $\Omega \subset \mathbb{R}^2$ be a domain satisfying the conditions (2.58) and (2.59). Then there exists $\delta = \delta(\Omega) > 0$ such that*

$$\partial A' \cap \partial B' \subset \{x : d(x, \overline{PQ}) < 10\sqrt{\delta}\} \cup (\sigma^{-1}(\Gamma_1 \cup \Gamma_2) \cap \Omega_{10\sqrt{\delta}})$$

for any solution (A', B') of (2.60).

Proof of Lemma 2.4. For the convenience of the reader, we first summarize the main arguments.

Let (A', B') be a solution of (2.60). The proof is divided into two steps.

In the first step, we argue that $\partial A' \cap \partial B'$ must be contained in a neighborhood of ∂B . The proof of this step follows closely the proof in [101]. The main idea is that since (A', B') is close to (A, B) in L^1 , it will incur significant cost $c_3(\partial A' \cap \partial B')$ if it protrudes too far from ∂B . Next, using the result of the first step, we are able to further restrict $\partial A' \cap \partial B'$ to a neighborhood of $\overline{PQ} \cup \Gamma_1 \cup \Gamma_2$. Since $\partial A' \cap \partial B'$ is contained in a neighborhood of ∂B , the result of Lemma 2.2 implies that near $\partial \Omega \cap \partial B$, the interior perimeter $\mathcal{H}^1(\partial A' \cap \partial B')$ is bounded below by the boundary

perimeter $\mathcal{H}^1(\partial A' \cap \partial \Omega)$. Together with the inequality $c_1 + c_3 > c_2$, this will allow us to enlarge B' into B'' near $\partial \Omega$ and exchange greater cost associated with

$$c_1 \mathcal{H}^1(\partial A' \cap \partial \Omega) + c_3 \mathcal{H}^1(\partial A' \cap \partial B')$$

for lesser cost associated with

$$c_2 \mathcal{H}^1(\partial B'' \cap \partial \Omega).$$

We begin with some preliminaries regarding the parameters in the proof. The parameter δ in the statement of the lemma depends on the constants $\{c_i\}$ and the domain Ω . Let $\gamma : [p, q] \rightarrow \partial \Omega$ parametrize $\partial B \cap \partial \Omega$ with $\gamma(p) = P$ and $\gamma(q) = Q$, and choose $p < b_1 < b_2 < q$ such that $\gamma([p, b_1]) \subset \Gamma_1$ and $\gamma([b_2, q]) \subset \Gamma_2$. Fix any $a_1 \in (p, b_1)$ and then choose $a_2 \in (b_2, q)$ such that $b_1 - a_1 = a_2 - b_2$ (this is merely for convenience later). We choose δ small enough to satisfy two conditions:

$$T([a_1, a_2] \times \{10\sqrt{\delta}\}) \subset \{x : d(x, \partial B) = 10\sqrt{\delta}\} \quad (2.64)$$

and

$$0 < \frac{20\sqrt{\delta}}{c_1 + c_3(1 - 10\sqrt{\delta}\kappa_\infty) - c_2} < b_1 - a_1. \quad (2.65)$$

Recall our assumption that $c_1 + c_3 > c_2$, which implies that any sufficiently small δ satisfies (2.65). Also, the first condition might not hold for δ too large because a point in B at distance $10\sqrt{\delta}$ from $\partial \Omega$ might be within $10\sqrt{\delta}$ of \overline{PQ} and hence not in $\{x : d(x, \partial B) = 10\sqrt{\delta}\}$; see Fig. 2.3. We now proceed with the proof.

Step 1. We argue that

$$\partial A' \cap \partial B' \subset \{x \in \Omega : \text{dist}(x, \partial B) < 10\sqrt{\delta}\}; \quad (2.66)$$

see Fig. 2.4. To prove this, one follows closely the method of proof of [101, Lemma 3.1] with minor changes. For convenience, we summarize the argument here. First, we argue that $\{x \in A : \text{dist}(x, \partial B) \geq 10\sqrt{\delta}\} \cap B' = \emptyset$. Consider slices $S_t = \{x \in A : \text{dist}(x, \partial B) = t\}$. If there exists a

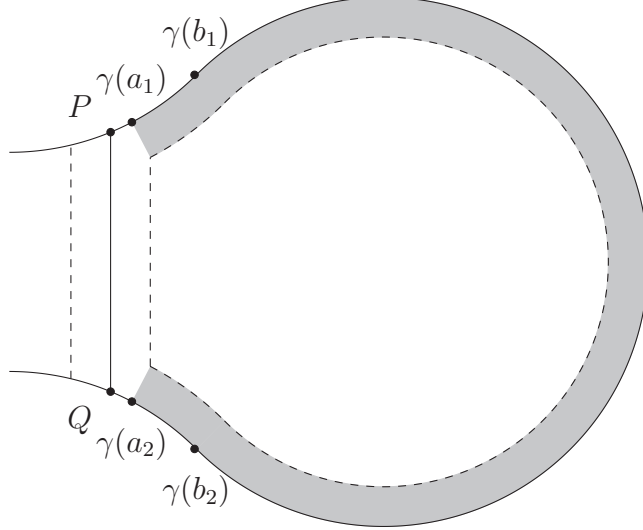


Figure 2.3: The shaded region is $T([a_1, a_2] \times [0, 10\sqrt{\delta}])$. The dashed curves comprise $\{x \in \Omega : d(x, \partial B) = 10\sqrt{\delta}\}$. Note that $T([a_1, a_2] \times \{10\sqrt{\delta}\})$ is entirely contained in this level set.

$t_0 < 10\sqrt{\delta}$ such that $\mathcal{H}^1(S_{t_0} \cap B') = 0$, then setting

$$A'' = A' \cup \{x \in A : \text{dist}(x, \partial B) \geq t_0\}$$

yields a modified partition (A'', B'') which still satisfies the L^1 constraint in (2.60). Assume for contradiction $\{x \in A : \text{dist}(x, \partial B) > t_0\} \cap B' \neq \emptyset$. Then, by following the calculations from [101, p. 1067], we see that (A'', B'') satisfies

$$c_3 \mathcal{H}^1(\partial A'' \cap \partial B'') < c_3 \mathcal{H}^1(\partial A' \cap \partial B').$$

Note that since $A' \subset A''$, $B'' \subset B'$, and $c_1 < c_2$,

$$c_1 \mathcal{H}^1(\partial A'' \cap \partial \Omega) + c_2 \mathcal{H}^1(\partial B'' \cap \partial \Omega) \leq c_1 \mathcal{H}^1(\partial A' \cap \partial \Omega) + c_2 \mathcal{H}^1(\partial B' \cap \partial \Omega),$$

so in fact $F_0(A'', B'') < F_0(A', B')$, which contradicts the fact that (A', B') is a minimizer of (2.60). We conclude that $\{x \in A : \text{dist}(x, \partial B) > t_0\} \cap B' = \emptyset$, which together with the definition of t_0 yields the desired result. On the other hand, suppose there does not exist $t_0 < 10\sqrt{\delta}$ such that $\mathcal{H}^1(S_{t_0} \cap B') = 0$. The L^1 constraint from (2.60) and the mean value theorem yield $T_0 \in (\sqrt{\delta}, 2\sqrt{\delta})$

such that $\mathcal{H}^1(S_{T_0} \cap B) < \sqrt{\delta}$. It can then be shown (using the calculations from [101, p. 1068]) that setting

$$A'' = A' \cup \{x \in A : \text{dist}(x, \partial B) \geq T_0\}$$

results in a partition (A'', B'') such that $F_0(A'', B'') < F_0(A', B')$, which again contradicts the minimality of (A', B') . This is due to the fact that T_0 was chosen so that the interior perimeter gain of at most $\sqrt{\delta}$ from $c_3 \mathcal{H}^1(\partial A'' \cap S_{T_0})$ is offset by the loss of perimeter of $c_3 \mathcal{H}^1(\partial A' \cap \{x \in A : 2\sqrt{\delta} < \text{dist}(x, \partial B)\})$. In either case, we obtain that $\{x \in A : \text{dist}(x, \partial B) \geq 10\sqrt{\delta}\} \cap B' = \emptyset$. The corresponding result, that $\{x \in B : \text{dist}(x, \partial B) \geq 10\sqrt{\delta}\} \cap A' = \emptyset$, is proved similarly, by setting

$$B'' = B' \cap \{x \in B : \text{dist}(x, \partial B) \geq t\}$$

for some carefully chosen t . These two results then yield (2.66), since we see that

$$\begin{aligned} \partial A' \cap \partial B' &\subset \Omega \setminus \left(\{x \in A : \text{dist}(x, \partial B) \geq 10\sqrt{\delta}\} \cup \{x \in B : \text{dist}(x, \partial B) \geq 10\sqrt{\delta}\} \right) \\ &= \{x \in \Omega : \text{dist}(x, \partial B) < 10\sqrt{\delta}\}. \end{aligned}$$

Observe that in Step 1, we have avoided modifying (A', B') by enlarging B' near $\partial\Omega$. The reason for this is that a priori, the loss of interior perimeter resulting from such a modification might be offset by an increase in the cost on $\partial\Omega$ due to the inequality $c_1 < c_2$. This difficulty will be addressed in the subsequent step.

Step 2. The second step, similar to the first, has two main parts. First, we eliminate “islands” of A' in $T((a_1, a_2) \times (0, 10\sqrt{\delta}))$ separated from the main portion of A' by slices of the form $T(\{d\} \times (0, 10\sqrt{\delta}))$. Consider the set $\{d \in (a_1, a_2) : \mathcal{H}^1(T(\{d\} \times (0, 10\sqrt{\delta})) \cap A') = 0\}$, and suppose it is non-empty. We choose d_1 and d_2 from this set with $d_1 \leq d_2$; if possible we choose d_i such that $\gamma(d_i) \subset \Gamma_i$. See Fig. 4 for an example of the case where d_1 can be chosen so that $\gamma(d_1) \in \Gamma_1$ but d_2 cannot be chosen so that $\gamma(d_2) \in \Gamma_2$. Now define

$$B'' = B' \cup T([d_1, d_2] \times [0, 10\sqrt{\delta}])$$

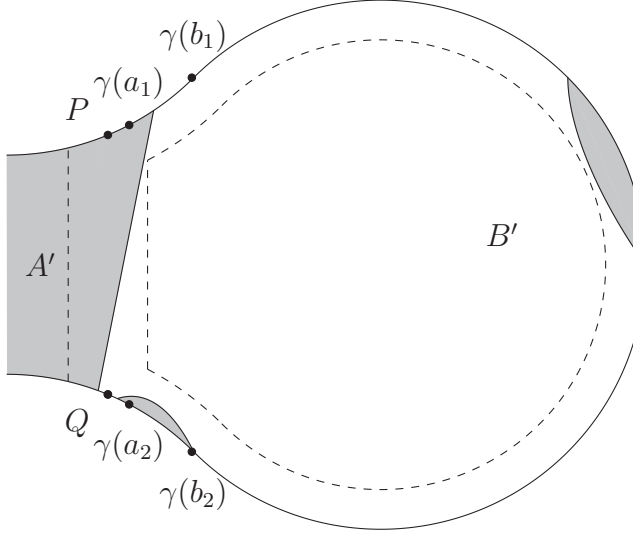


Figure 2.4: The shaded set is A' and the unshaded set is B' . The boundary $\partial A' \cap \partial B'$ is contained in a $10\sqrt{\delta}$ neighborhood of ∂B due to Step 1.

and A'' as the measure-theoretic closure of $\Omega \setminus B''$. Note that (A'', B'') still satisfies the L^1 constraint from (2.60). We claim that

$$B'' \triangle B', A'' \triangle A' \subset T([d_1, d_2] \times [0, 10\sqrt{\delta}]).$$

This will simplify the calculation below of $F_0(A', B') - F_0(A'', B'')$ since it will allow us to only examine $T([d_1, d_2] \times [0, 10\sqrt{\delta}])$. It is straightforward to see that $B'' \triangle B'$ and $A'' \triangle A'$ are contained in $T([d_1, d_2] \times [0, 10\sqrt{\delta}])$, so to prove the claim it remains to show that $B'' \triangle B'$ and $A'' \triangle A'$ have empty intersection with $T([d_1, d_2] \times \{10\sqrt{\delta}\})$. This holds because of the choice of δ in (2.64). By the result of Step 1 and the inclusion (2.64), $T([d_1, d_2] \times \{10\sqrt{\delta}\}) \subset (B')^i$, which implies it has empty intersection with $B'' \triangle B'$ and $A'' \triangle A'$. Therefore, we can calculate the difference in energies $F_0(A', B') - F_0(A'', B'')$ as

$$\begin{aligned} F_0(A', B') - F_0(A'', B'') &= c_1 \mathcal{H}^1(\gamma(d_1, d_2) \cap \partial A') + c_2 \mathcal{H}^1(\gamma(d_1, d_2) \cap \partial B') \\ &\quad + c_3 \mathcal{H}^1(T([d_1, d_2] \times (0, 10\sqrt{\delta})) \cap \partial A') - c_2 \mathcal{H}^1(\gamma(d_1, d_2)). \end{aligned} \tag{2.67}$$

Assuming that $|A' \cap T([d_1, d_2] \times [0, 10\sqrt{\delta}])| > 0$, we will show that $F_0(A', B') - F_0(A'', B'') > 0$,

which contradicts the minimality of (A', B') . First, we bound the first three terms on the right hand side of (2.67) from below. As a preliminary estimate, note that Lemma 2.2 with $V = T((d_1, d_2) \times (0, 10\sqrt{\delta})) \cap A'$ implies that

$$\mathcal{H}^1(\gamma(d_1, d_2) \cap \partial A') \leq \mathcal{H}^1(\gamma(d_1, d_2) \cap \sigma(A')).$$

Using this in conjunction with the inequality $c_1 - c_2 < 0$ we write for the first two terms of (2.67)

$$\begin{aligned} c_1 \mathcal{H}^1(\gamma(d_1, d_2) \cap \partial A') + c_2 \mathcal{H}^1(\gamma(d_1, d_2) \cap \partial B') \\ = (c_1 - c_2) \mathcal{H}^1(\gamma(d_1, d_2) \cap \partial A') + c_2 \mathcal{H}^1(\gamma(d_1, d_2)) \\ \geq (c_1 - c_2) \mathcal{H}^1(\gamma(d_1, d_2) \cap \sigma(A')) + c_2 \mathcal{H}^1(\gamma(d_1, d_2)) \\ = c_1 \mathcal{H}^1(\gamma(d_1, d_2) \cap \sigma(A')) + c_2 \mathcal{H}^1(\gamma(d_1, d_2) \setminus \sigma(A')). \end{aligned} \quad (2.68)$$

For the third term of (2.67), also apply Lemma 2.2 to obtain

$$c_3 \mathcal{H}^1(T([d_1, d_2] \times (0, 10\sqrt{\delta})) \cap \partial A') \geq c_3(1 - 10\sqrt{\delta}\kappa_\infty) \mathcal{H}^1(\gamma(d_1, d_2) \cap \sigma(A')). \quad (2.69)$$

Then adding (2.68) and (2.69) yields

$$\begin{aligned} c_1 \mathcal{H}^1(\gamma(d_1, d_2) \cap \partial A') + c_2 \mathcal{H}^1(\gamma(d_1, d_2) \cap \partial B') + c_3 \mathcal{H}^1(T([d_1, d_2] \times (0, 10\sqrt{\delta})) \cap \partial A') \\ \geq c_1 \mathcal{H}^1(\gamma(d_1, d_2) \cap \sigma(A')) + c_2 \mathcal{H}^1(\gamma(d_1, d_2) \setminus \sigma(A')) \\ + c_3(1 - 10\sqrt{\delta}\kappa_\infty) \mathcal{H}^1(\gamma(d_1, d_2) \cap \sigma(A')). \end{aligned} \quad (2.70)$$

Now observe that (2.65) implies that $c_1 + c_3(1 - 10\sqrt{\delta}\kappa_\infty) > c_2$ and that the assumption $|A' \cap T([d_1, d_2] \times [0, 10\sqrt{\delta}])| > 0$ implies $\mathcal{H}^1(\gamma(d_1, d_2) \cap \sigma(A')) > 0$. Together these observations imply that

$$c_1 \mathcal{H}^1(\gamma(d_1, d_2) \cap \sigma(A')) + c_3(1 - 10\sqrt{\delta}\kappa_\infty) \mathcal{H}^1(\gamma(d_1, d_2) \cap \sigma(A')) > c_2 \mathcal{H}^1(\gamma(d_1, d_2) \cap \sigma(A')).$$

Using this inequality for the first and third terms on the right hand side of (2.70), we obtain our

estimate for the first three terms of (2.67):

$$\begin{aligned}
& c_1 \mathcal{H}^1(\gamma(d_1, d_2) \cap \partial A') + c_2 \mathcal{H}^1(\gamma(d_1, d_2) \cap \partial B') + c_3 \mathcal{H}^1(T([d_1, d_2] \times (0, 10\sqrt{\delta})) \cap \partial A') \\
& > c_2 \mathcal{H}^1(\gamma(d_1, d_2) \cap \sigma(A')) + c_2 \mathcal{H}^1(\gamma(d_1, d_2) \setminus \sigma(A')) \\
& = c_2 \mathcal{H}^1(\gamma(d_1, d_2)). \tag{2.71}
\end{aligned}$$

Combining (2.67) and (2.71) yields

$$F_0(A', B') - F_0(A'', B'') > c_2 \mathcal{H}^1(\gamma(d_1, d_2)) - c_2 \mathcal{H}^1(\gamma(d_1, d_2)) = 0.$$

But this contradicts the fact that (A', B') is a solution to (2.60), so it must be the case that $|A' \cap T([d_1, d_2] \times [0, 10\sqrt{\delta}])| = 0$. It follows that $\partial A' \cap T((d_1, d_2) \times [0, 10\sqrt{\delta}]) = \emptyset$, which together with the result of Step 1 gives

$$\partial A' \cap \partial B' \subset \{x \in \Omega : \text{dist}(x, \partial B) < 10\sqrt{\delta}\} \setminus T((d_1, d_2) \times [0, 10\sqrt{\delta}])$$

If it was possible to choose $\gamma_i(d_i) \in \Gamma_i$ for $i = 1, 2$, the lemma is proved, since

$$\begin{aligned}
& \{x \in \Omega : \text{dist}(x, \partial B) < 10\sqrt{\delta}\} \setminus T((d_1, d_2) \times [0, 10\sqrt{\delta}]) \tag{2.72} \\
& \subset \{x : \text{dist}(x, \overline{PQ}) < 10\sqrt{\delta}\} \cup (\sigma^{-1}(\Gamma_1 \cup \Gamma_2) \cap \Omega_{10\sqrt{\delta}}).
\end{aligned}$$

Then it remains consider the scenario in which $\{d \in (a_1, a_2) : \mathcal{H}^1(T(\{d\} \times (0, 10\sqrt{\delta})) \cap A') = 0\} = \emptyset$ or d_i cannot be chosen such that $\gamma(d_i) \in \Gamma_i$. Fix $i = 1$; $i = 2$ is handled similarly. Define

$$B'' = B' \cup T([a_1, b_1] \times [0, 10\sqrt{\delta}])$$

and A'' as the measure theoretic closure of $\Omega \setminus B''$. Note that (A'', B'') still satisfies the L^1 constraint.

As in the previous part of Step 2, we can calculate

$$\begin{aligned}
F_0(A', B') - F_0(A'', B'') &= c_1 \mathcal{H}^1(\gamma(a_1, b_1) \cap \partial A') + c_2 \mathcal{H}^1(\gamma(a_1, b_1) \cap \partial B') \\
&\quad + c_3 \mathcal{H}^1(T([a_1, b_1] \times (0, 10\sqrt{\delta})) \cap \partial A') - c_2 \mathcal{H}^1(\gamma(a_1, b_1)) \\
&\quad - c_3 \mathcal{H}^1(T(\{a_1, b_1\} \times (0, 10\sqrt{\delta})) \cap \partial A'). \tag{2.73}
\end{aligned}$$

First, we estimate the fifth term from below:

$$-c_3\mathcal{H}^1(T(\{a_1, b_1\} \times (0, 10\sqrt{\delta})) \cap \partial A') \geq -20\sqrt{\delta}. \quad (2.74)$$

Using the same reasoning as preceding (2.70), we can estimate the first three terms of (2.73):

$$\begin{aligned} & c_1\mathcal{H}^1(\gamma(a_1, b_1) \cap \partial A') + c_2\mathcal{H}^1(\gamma(a_1, b_1) \cap \partial B') + c_3\mathcal{H}^1(T([a_1, b_1] \times (0, 10\sqrt{\delta})) \cap \partial A') \\ & \geq c_1\mathcal{H}^1(\gamma(a_1, b_1) \cap \sigma(A')) + c_2\mathcal{H}^1(\gamma(a_1, b_1) \setminus \sigma(A')) \\ & \quad + c_3(1 - 10\sqrt{\delta}\kappa_\infty)\mathcal{H}^1(\gamma(a_1, b_1) \cap \sigma(A')). \end{aligned}$$

The assumption that d_1 either doesn't exist or can't be chosen such that $\gamma(d_1) \subset \Gamma_1$ implies that $\gamma(a_1, b_1) \cap \sigma(A') = \gamma(a_1, b_1)$. After using this in the previous inequality and combining with (2.74), we obtain

$$\begin{aligned} F_0(A', B') - F_0(A'', B'') & \geq c_1\mathcal{H}^1(\gamma(a_1, b_1)) + c_3(1 - 10\sqrt{\delta}\kappa_\infty)\mathcal{H}^1(\gamma(a_1, b_1)) - 20\sqrt{\delta} \\ & = c_1(b_1 - a_1) + c_3(1 - 10\sqrt{\delta}\kappa_\infty)(b_1 - a_1) - 20\sqrt{\delta}. \end{aligned} \quad (2.75)$$

Recalling (2.65), we rearrange it as

$$c_1(b_1 - a_1) + c_3(1 - 10\sqrt{\delta}\kappa_\infty)(b_1 - a_1) - 20\sqrt{\delta} > 0.$$

But it immediately follows from this inequality and (2.75) that $F_0(A', B') - F_0(A'', B'') > 0$, which contradicts the minimality of (A', B') . It must then be the case that $\{d \in (a_1, a_2) : \mathcal{H}^1(T(\{d\} \times (0, 10\sqrt{\delta})) \cap A') = 0\} \neq \emptyset$ and $\gamma(d_1) \in \Gamma_1$. It can be argued similarly that $\gamma(d_2) \in \Gamma_2$. In view of (2.72), the lemma is proven. \square

Finally we can prove Theorem 2.4.

Proof of Theorem 2.4. Fix δ small enough to satisfy the assumptions of Lemma 2.4. Then the direct method yields the existence of a solution (A', B') to (2.60). By Lemma 2.4, we have that

$$\partial A' \cap \partial B' \subset \{x : \text{dist}(x, \overline{PQ}) < 10\sqrt{\delta}\} \cup (\sigma^{-1}(\Gamma_1 \cup \Gamma_2) \cap \Omega_{10\sqrt{\delta}}).$$

In particular, this implies that (A', B') satisfies

$$\partial A' \cap \partial \Omega \subset \Gamma_1 \cup \Gamma_2 \cup (\partial \Omega \cap \partial A), \text{ and } \partial B' \cap \partial \Omega \subset \Gamma_1 \cup \Gamma_2 \cup (\partial \Omega \cap \partial B). \quad (2.76)$$

We can now use a calibration argument to show that (A, B) is the only minimal partition satisfying (2.76) and hence the unique minimizer of (2.60). Denote by ν_Ω the measure theoretic exterior normal to Ω . Let (C, D) be an admissible partition. By Cauchy–Schwarz and the Gauss–Green theorem, we have

$$\begin{aligned} F_0(C, D) &= c_1 \mathcal{H}^1(\partial C \cap \partial \Omega) + c_2 \mathcal{H}^1(\partial D \cap \partial \Omega) + c_3 \mathcal{H}^1(\partial C \cap \partial D) \\ &\geq c_1 \mathcal{H}^1(\partial C \cap \partial \Omega) + c_2 \mathcal{H}^1(\partial D \cap \partial \Omega) + c_3 \int_{\partial C \cap \partial D} (v \cdot \nu_C) d\mathcal{H}^1 \\ &= c_1 \mathcal{H}^1(\partial C \cap \partial \Omega) + c_2 \mathcal{H}^1(\partial D \cap \partial \Omega) - c_3 \int_{\partial C \cap \partial \Omega} (v \cdot \nu_\Omega) d\mathcal{H}^1 \\ &= \int_{\partial C \cap (\Gamma_1 \cup \Gamma_2)} (c_1 - c_3 v \cdot \nu_\Omega) d\mathcal{H}^1 + \int_{(\partial C \cap \partial \Omega) \setminus (\Gamma_1 \cup \Gamma_2)} (c_1 - c_3 v \cdot \nu_\Omega) d\mathcal{H}^1 \\ &\quad + \int_{\partial D \cap (\Gamma_1 \cup \Gamma_2)} c_2 d\mathcal{H}^1 + \int_{(\partial D \cap \partial \Omega) \setminus (\Gamma_1 \cup \Gamma_2)} c_2 d\mathcal{H}^1. \end{aligned} \quad (2.77)$$

Note that because of the restrictions in (2.76) on the admissible partitions, the second and fourth integrals in the previous lines do not depend on (C, D) . In fact, $(\partial C \cap \partial \Omega) \setminus (\Gamma_1 \cup \Gamma_2) = (\partial A \cap \partial \Omega) \setminus (\Gamma_1 \cup \Gamma_2)$ and $(\partial D \cap \partial \Omega) \setminus (\Gamma_1 \cup \Gamma_2) = (\partial B \cap \partial \Omega) \setminus (\Gamma_1 \cup \Gamma_2)$. Thus if we set

$$I := \int_{(\partial C \cap \partial \Omega) \setminus (\Gamma_1 \cup \Gamma_2)} (c_1 - c_3 v \cdot \nu_\Omega) d\mathcal{H}^1 + \int_{(\partial D \cap \partial \Omega) \setminus (\Gamma_1 \cup \Gamma_2)} c_2 d\mathcal{H}^1,$$

the above inequality becomes

$$F_0(C, D) \geq I + \int_{\partial C \cap (\Gamma_1 \cup \Gamma_2)} (c_1 - c_3 v \cdot \nu_\Omega) d\mathcal{H}^1 + \int_{\partial D \cap (\Gamma_1 \cup \Gamma_2)} c_2 d\mathcal{H}^1, \quad (2.78)$$

where I does not depend on the choice of partition. Now, due to the strict convexity of Γ_1 and Γ_2 and the assumption that $c_1 - c_3 v \cdot \nu_\Omega = c_2$ at P and Q , the following inequalities hold:

$$c_1 - c_3 v \cdot \nu_\Omega < c_2 \text{ on } \partial A \cap \Omega$$

and

$$c_1 - c_3 v \cdot \nu_\Omega > c_2 \text{ on } \partial B \cap \Omega.$$

Consequently, the only partitions which minimize the right hand side of (2.78) are those satisfying

$$\partial C \cap \partial \Omega = \partial A \cap \partial \Omega \text{ and } \partial D \cap \partial \Omega = \partial B \cap \partial \Omega. \quad (2.79)$$

In addition, the inequality in (2.77) is sharp unless

$$v = \nu_C \quad \mathcal{H}^1 \text{ a.e. on } \partial C \cap \Omega. \quad (2.80)$$

Thus by applying (2.3), it follows that if (2.77) is an equality, then $\partial C \cap \partial D$ is a line segment. We have shown that (A, B) is the only partition satisfying (2.79) and (2.80) and therefore the unique minimizer of F_0 over all partitions satisfying (2.76), and so the theorem follows. \square

2.5 Asymptotic Energy of Minimizers of F_ε for Boundary Data with Degree

In this section we consider the behavior of minimizers of F_ε with the surface term

$$f_s = \gamma |(\mathbf{I} - \hat{z} \otimes \hat{z}) Q \hat{z}|^2 \quad (2.81)$$

and also subject to the boundary condition given by (2.5), $g(x) = -3\beta \left(n(x) \otimes n(x) - \frac{1}{3}\mathbf{I} \right)$. The invariance of Q -tensors under reflection through the origin implies that

$$\text{the degree of } g \text{ is an integer multiple of one-half;} \quad (2.82)$$

see [18, Definition 2]. We will denote this integer by k . Throughout this section, we will assume that the temperature is low enough so that the uniaxial nematic state with nematic order parameter s_* is the minimizer of f_{LdG} . From the description (2.2) of the zero set of f_{LdG} , we see that the only effect of perturbing f_{LdG} by $2f_s$ as in (2.81) is to require now that \hat{z} be an eigenvector of any minimizer of $f_{LdG} + 2f_s$. Hence the zero set P of $W = f_{LdG} + 2f_s$ is the union of the circle $P_1 := \left\{ s_* \left(m \otimes m - \frac{1}{3}\mathbf{I} \right) : m \in \mathbb{S}^1 \times \{0\} \right\}$ and the point $P_2 := s_* \left(\hat{z} \otimes \hat{z} - \frac{1}{3}\mathbf{I} \right)$. Let us assume β is such that

$$\varphi_1(g) < \varphi_2(g), \quad (2.83)$$

i.e., the boundary data g is closer to the circle P_1 than to the point P_2 in the degenerate metric $d_{\sqrt{W}}$.

We recall the notation P_0 for the image of g . In the following theorem regarding the energy of the minimizers Q_ε of F_ε , we capture both the leading order boundary layer contribution reminiscent of vector Allen–Cahn and the lower order vortex contribution reminiscent of Ginzburg–Landau.

Theorem 2.5. *Let Ω be a simply-connected domain and g have degree k . Assume that f_s is given by $\gamma|(\mathbf{I} - \hat{z} \otimes \hat{z})Q\hat{z}|^2$. Then the minimizers Q_ε of F_ε satisfy the asymptotic development*

$$F_\varepsilon(Q_\varepsilon) = 2 \int_{\partial\Omega} \varphi_1(g(x)) d\mathcal{H}^1(x) + s_*^2 \pi k \varepsilon \log \frac{1}{\varepsilon} + O(\varepsilon) \quad (2.84)$$

as $\varepsilon \rightarrow 0$.

The proof of the theorem will consist of showing that the right hand side of (2.84) bounds $F_\varepsilon(Q_\varepsilon)$ from above and from below.

Proof of the upper bound. We will first prove the upper bound by constructing a sequence of functions R_ε which satisfy

$$F_\varepsilon(R_\varepsilon) \leq 2 \int_{\partial\Omega} \varphi_1(g(x)) d\mathcal{H}^1(x) + s_*^2 \pi k \varepsilon \log \frac{1}{\varepsilon} + O(\varepsilon). \quad (2.85)$$

The R_ε will be independent of z , so we will refer to them as functions of $x \in \Omega$ and treat the surface term as a bulk term, since for $R_\varepsilon = R_\varepsilon(x)$ only we have

$$\begin{aligned} F_\varepsilon(R_\varepsilon) &= \int_{\Omega \times (0,1)} \left(\varepsilon |\nabla_x R_\varepsilon|^2 + \frac{f_{LdG}(R_\varepsilon)}{\varepsilon} \right) dx dz + \frac{1}{\varepsilon} \int_{\Omega \times \{0,1\}} f_s(R_\varepsilon) dx \\ &= \int_{\Omega} \left(\varepsilon |\nabla_x R_\varepsilon|^2 + \frac{W(R_\varepsilon)}{\varepsilon} \right) dx. \end{aligned} \quad (2.86)$$

Our strategy will be to combine the construction of [18] away from $\partial\Omega$ with a boundary layer near $\partial\Omega$. The interior construction will contribute the $\varepsilon \log \frac{1}{\varepsilon}$ term and the boundary layer will contribute the order 1 term in (2.84). Throughout the estimates, the generic constant C varies from line to line but does not depend on ε .

We first present some preliminaries regarding W and $d_{\sqrt{W}}(\cdot, P)$. Let us denote the uniaxial well of f_{LdG} by

$$Z := \left\{ s_\star \left(m \otimes m - \frac{1}{3} \mathbf{I} \right) : m \in \mathbb{S}^2 \right\}.$$

First, as observed in [18, Equation 1.14], we have the following inequality regarding f_{LdG} and $\text{dist}(\cdot, Z)$, the Euclidean distance to Z : there exists $\delta > 0$ and $C > 0$ such that

$$\frac{1}{C} \text{dist}(Q, Z)^2 \leq f_{LdG}(Q) \leq C \text{dist}(Q, Z)^2$$

for any Q such that $\text{dist}(Q, Z) < \delta$. We will say $f_{LdG} \sim \text{dist}(\cdot, Z)^2$ in a δ -neighborhood of Z . It is quickly seen that after adding $2f_s = 2\gamma|(\mathbf{I} - \hat{z} \otimes \hat{z})Q\hat{z}|^2$ to f_{LdG} , we have $W \sim \text{dist}(\cdot, P)^2$ in some δ' -neighborhood of P . Since W and $\text{dist}(\cdot, P)$ both vanish exactly on P , it follows that for any compact set $B \subset \mathcal{S}$, there exists $C > 0$, depending on B , such that

$$W \sim \text{dist}(\cdot, P)^2 \tag{2.87}$$

on B . It is straightforward to see using (2.87) and the definition of $d_{\sqrt{W}}$ that $d_{\sqrt{W}}(\cdot, P)$ satisfies the same property, namely that on any compact set $B \subset \mathcal{S}$,

$$d_{\sqrt{W}}(\cdot, P) \sim \text{dist}(\cdot, P)^2. \tag{2.88}$$

We will also need, similar to Section 2.2, geodesics under the degenerate metric $d_{\sqrt{W}}$ along with the solutions of an ODE to construct the boundary layer. We aim to bridge the boundary data

$$g(x) = -3\beta \left(n(x) \otimes n(x) - \frac{1}{3} \mathbf{I} \right)$$

to the well P_1 . The details are different than those in Section 2.2 due to the need for precise estimates of the error involved in the construction. First, fix $x_0 \in \partial\Omega$ and obtain a curve γ_{x_0} which is a geodesic for $d_{\sqrt{W}}(g(x_0), P_1)$. We assume $\gamma_{x_0} : [0, b] \rightarrow \mathcal{S}$ which is parametrized with respect to arc length, so that b is the Euclidean length of γ , and satisfies $\gamma_{x_0}(0) = g(x_0)$, $\gamma_{x_0}(b) \in P_1$, and

$$\int_0^b \sqrt{W(\gamma_{x_0}(t))} |\gamma'_{x_0}(t)| dt = \varphi_1(g(x_0)).$$

By the assumption (2.83) that $\varphi_1(g) < \varphi_2(g)$, we have $\varphi_1(g(x_0)) = d_{\sqrt{W}}(P, g(x_0))$. We note also that (2.83) allows us to require without loss of generality that

$$W(\gamma_{x_0}(t)) \text{ vanishes only for } t = b. \quad (2.89)$$

For $x \in \partial\Omega$ with $x \neq x_0$, we define $\gamma_x = r_{\theta_x} \gamma_{x_0} r_{\theta_x}^T$, where θ_x is chosen so that $r_{\theta_x} g(x_0) r_{\theta_x}^T = g(x)$.

We see that due to the rotational symmetry described at the beginning of Section 2.2, $\gamma_x(0) = g(x)$, $\gamma_x(b) \in P_1$, and

$$\int_0^b \sqrt{W(\gamma_x(t))} |\gamma'_x(t)| dt = \varphi_1(g(x)) = d_{\sqrt{W}}(P, g(x)) = d_{\sqrt{W}}(P, P_0). \quad (2.90)$$

In addition, we remark that unlike in Section 2.2, the γ_x vary smoothly in x over all of $\partial\Omega$, even near x_0 .

Next, we consider the following ODE:

$$\begin{cases} \frac{\partial}{\partial s} h(s) = \sqrt{W(\gamma_{x_0}(h(s)))}, \\ h(0) = 0. \end{cases} \quad (2.91)$$

Using the fact that $W(\gamma_{x_0}(t)) \geq C(t-b)^2$ for some $C > 0$, which follows from (2.87) and (2.89), one can argue as in [99, Equations (1.17)-(1.21)] and conclude that the solution h to (2.91) is defined on $[0, \infty)$, increasing, and approaches b exponentially as $s \rightarrow \infty$. We observe that h also solves the same ODE with γ_{x_0} replaced by γ_x for any $x \in \partial\Omega$ because of the rotational symmetry of W .

Let us now define the R_ε near $\partial\Omega$. We recall from Section 2.2 the notation $\sigma(x)$ for the projection of x onto $\partial\Omega$, $d(x)$ for the distance to $\partial\Omega$, and Ω_ζ for the set $\{x \in \Omega : d(x) \geq \zeta\}$. We fix $\zeta > 0$ such that d, σ are C^1 on $\Omega \setminus \Omega_\zeta$ and define for small ε

$$R_\varepsilon(x) = \begin{cases} \gamma_{\sigma(x)}(b), & 2\sqrt{\varepsilon} \leq d(x) \leq \zeta, \\ \gamma_{\sigma(x)} \left(h \left(\frac{d(x)}{\varepsilon} \right) \right), & d(x) \leq \sqrt{\varepsilon}. \end{cases}$$

For x such that $\sqrt{\varepsilon} < d(x) < 2\sqrt{\varepsilon}$, we define R_ε separately on each segment normal to $\{x : d(x) = \sqrt{\varepsilon}\}$ by linearly interpolating between the values of R_ε at the intersections of the segment with $\{x : d(x) = \sqrt{\varepsilon}\}$ and $\{x : d(x) = 2\sqrt{\varepsilon}\}$. We will define R_ε on Ω_ζ at the end.

We will now estimate the energy of R_ε on $\Omega \setminus \Omega_\zeta$ and prove that it contributes the leading order term in (2.84) up to an error of $O(\varepsilon)$. For each $x \in \Omega \setminus \Omega_\zeta$, let $\tau = \tau(x)$ be a unit vector tangent to the level set of d at x and $\eta = \eta(x)$ be the unit vector $\nabla d(x)$ perpendicular to τ . We write

$$\int_{\Omega \setminus \Omega_\zeta} \left(\varepsilon |\nabla R_\varepsilon|^2 + \frac{1}{\varepsilon} W(R_\varepsilon) \right) dx = \int_{\Omega \setminus \Omega_\zeta} \left(\varepsilon \left| \frac{\partial}{\partial \tau} R_\varepsilon \right|^2 + \varepsilon \left| \frac{\partial}{\partial \eta} R_\varepsilon \right|^2 + \frac{1}{\varepsilon} W(R_\varepsilon) \right) dx.$$

First, we have that $\left| \frac{\partial}{\partial \tau} R_\varepsilon \right|$ is bounded by some constant C depending on the Lipschitz constant of g and independent of ε on $\Omega \setminus \Omega_\zeta$, so that

$$\int_{\Omega \setminus \Omega_\zeta} \varepsilon \left| \frac{\partial}{\partial \tau} R_\varepsilon \right|^2 dx \leq O(\varepsilon).$$

Since $\varepsilon \left| \frac{\partial}{\partial \tau} R_\varepsilon \right|^2$ is the only non-zero term in the integrand when $2\sqrt{\varepsilon} \leq d(x) \leq \zeta$, we have

$$\int_{\Omega \setminus \Omega_\zeta} \left(\varepsilon |\nabla R_\varepsilon|^2 + \frac{1}{\varepsilon} W(R_\varepsilon) \right) dx = \int_{\{x: d(x) < 2\sqrt{\varepsilon}\}} \left(\varepsilon \left| \frac{\partial}{\partial \eta} R_\varepsilon \right|^2 + \frac{1}{\varepsilon} W(R_\varepsilon) \right) dx + O(\varepsilon).$$

Next, using the fact that $h(s)$ approaches b exponentially as $s \rightarrow \infty$, one can easily conclude as in [99, Equation (2.26)] that

$$\int_{\{x: \sqrt{\varepsilon} < d(x) < 2\sqrt{\varepsilon}\}} \left(\varepsilon \left| \frac{\partial}{\partial \eta} R_\varepsilon \right|^2 + \frac{1}{\varepsilon} W(R_\varepsilon) \right) dx \leq O(\varepsilon), \quad (2.92)$$

so that in order to capture the leading order term in (2.84), it remains to estimate

$$I := \int_{\{x: d(x) < \sqrt{\varepsilon}\}} \left(\varepsilon \left| \frac{\partial}{\partial \eta} R_\varepsilon \right|^2 + \frac{1}{\varepsilon} W(R_\varepsilon) \right) dx. \quad (2.93)$$

Our estimates for I utilize a similar strategy as in [10, Proposition 2.1]. In particular, the remarks (2.87), (2.88) along with the ODE (2.91) will be crucial in obtaining a precise form of the error. We note that (2.87) and (2.88) imply that $W \sim d_{\sqrt{W}}(\cdot, P)$ on any compact set B . With $B = \{R_\varepsilon(x) : x \in \Omega \setminus \Omega_\zeta\}$, we can write

$$W(R_\varepsilon) \sim d_{\sqrt{W}}(R_\varepsilon, P) = \varphi_1(R_\varepsilon) \quad (2.94)$$

on $\Omega \setminus \Omega_\zeta$. We will also use the identity

$$\sqrt{\varepsilon} \frac{\partial}{\partial \eta} R_\varepsilon(x) = \frac{1}{\sqrt{\varepsilon}} \sqrt{W(R_\varepsilon(x))} \gamma'_{\sigma(x)} \left(h \left(\frac{d(x)}{\varepsilon} \right) \right) = -\frac{1}{\sqrt{\varepsilon}} (\nabla \varphi_1)(R_\varepsilon(x)),$$

for x such that $d(x) < \sqrt{\varepsilon}$, which follows from (2.91) and the fact that as the gradient of a distance function, $(\nabla \varphi_1)(\gamma_{\sigma(x)})$ is parallel to the geodesic direction $\gamma'_{\sigma(x)}$. From this identity and the fact that $|\gamma'_{\sigma(x)}| = 1$ we conclude that

$$\varepsilon \left| \frac{\partial}{\partial \eta} R_\varepsilon \right|^2 = \sqrt{\varepsilon} \frac{\partial}{\partial \eta} R_\varepsilon \cdot -\frac{1}{\sqrt{\varepsilon}} (\nabla \varphi_1)(R_\varepsilon) = \frac{1}{\varepsilon} W(R_\varepsilon). \quad (2.95)$$

Now applying the coarea formula and (2.95), we write

$$\begin{aligned} I &= 2 \int_0^{\sqrt{\varepsilon}} \int_{\{x: d(x)=s\}} \frac{\partial}{\partial \eta} R_\varepsilon \cdot (-\nabla \varphi_1)(R_\varepsilon) d\mathcal{H}^1(x) ds \\ &= 2 \int_0^{\sqrt{\varepsilon}} \int_{\{x: d(x)=s\}} -\frac{\partial}{\partial \eta} (\varphi_1 \circ R_\varepsilon) d\mathcal{H}^1(x) ds \\ &= 2 \int_0^{\sqrt{\varepsilon}} \int_{\{x: d(x)=s\}} -\frac{\partial}{\partial s} \left(\varphi_1 \left(\gamma_{\sigma(x)} \left(h \left(\frac{s}{\varepsilon} \right) \right) \right) \right) d\mathcal{H}^1(x) ds \\ &= 2 \int_0^{\sqrt{\varepsilon}} \int_{\partial \Omega} -\frac{\partial}{\partial s} \left(\varphi_1 \left(\gamma_x \left(h \left(\frac{s}{\varepsilon} \right) \right) \right) \right) |J(P_t)(x)| d\mathcal{H}^1(x) ds, \end{aligned}$$

where $J(P_t)(x)$ is the Jacobian of the map $P_t : \partial \Omega \rightarrow \{x \in \Omega : d(x) = t\}$. For ease of notation let us refer to $\varphi_1(\gamma_x(h(s\varepsilon^{-1})))$ as $(\varphi_1 \circ R_\varepsilon)(x, s)$ for $x \in \partial \Omega$ and $0 \leq s \leq \sqrt{\varepsilon}$. Recalling the estimate $|J(P_t)(x) - 1| \leq Ct$ from (2.44), we can write

$$\begin{aligned} I &\leq 2 \int_0^{\sqrt{\varepsilon}} \int_{\partial \Omega} -\left(\frac{\partial}{\partial s} (\varphi_1 \circ R_\varepsilon)(x, s) \right) (1 + Cs) d\mathcal{H}^1(x) ds \\ &= 2 \int_{\partial \Omega} \int_0^{\sqrt{\varepsilon}} -\left(\frac{\partial}{\partial s} (\varphi_1 \circ R_\varepsilon)(x, s) \right) (1 + Cs) ds d\mathcal{H}^1(x). \end{aligned} \quad (2.96)$$

We estimate the inner integral with the goal of improving our estimate of $\int_{\Omega \setminus \Omega_\zeta} W(R_\varepsilon) dx$. For each $x \in \partial \Omega$, we have

$$\begin{aligned} &\int_0^{\sqrt{\varepsilon}} -\left(\frac{\partial}{\partial s} (\varphi_1 \circ R_\varepsilon)(x, s) \right) (1 + Cs) ds \\ &= (\varphi_1 \circ R_\varepsilon)(x, 0) - (\varphi_1 \circ R_\varepsilon)(x, \sqrt{\varepsilon}) (1 + C\sqrt{\varepsilon}) + \int_0^{\sqrt{\varepsilon}} (\varphi_1 \circ R_\varepsilon)(x, s) C ds \\ &\leq (\varphi_1 \circ R_\varepsilon)(x, 0) + \int_0^{\sqrt{\varepsilon}} (\varphi_1 \circ R_\varepsilon)(x, s) C ds \\ &\leq C \end{aligned} \quad (2.97)$$

for some constant C independent of x and ε . This estimate on the inner integral then yields $I \leq C$ after substituting into (2.96), which implies

$$\int_{\{x:d(x)<\sqrt{\varepsilon}\}} W(R_\varepsilon) dx \leq C\varepsilon. \quad (2.98)$$

But since $W(R_\varepsilon) \sim \varphi_1(R_\varepsilon)$ by (2.94), we see from (2.98) that

$$\int_{\{x:d(x)<\sqrt{\varepsilon}\}} \varphi_1(R_\varepsilon) dx \leq C\varepsilon. \quad (2.99)$$

Finally, integrating (2.97) over $x \in \partial\Omega$ and using (2.99), we have

$$\begin{aligned} I_1 &\leq 2 \int_{\partial\Omega} (\varphi_1 \circ R_\varepsilon)(x, 0) d\mathcal{H}^1(x) + 2C \int_{\{x:d(x)<\sqrt{\varepsilon}\}} \varphi_1(R_\varepsilon) dx \\ &= 2 \int_{\partial\Omega} \varphi_1(g(x)) d\mathcal{H}^1(x) + O(\varepsilon). \end{aligned} \quad (2.100)$$

From (2.93) and (2.100), we conclude

$$\int_{\Omega \setminus \Omega_\zeta} \left(\varepsilon |\nabla R_\varepsilon|^2 + \frac{1}{\varepsilon} W(R_\varepsilon) \right) dx \leq 2 \int_{\partial\Omega} \varphi_1(g(x)) d\mathcal{H}^1(x) + O(\varepsilon). \quad (2.101)$$

Next, we define the R_ε 's on Ω_ζ . We will use a construction from [18], in which the authors examine the functionals

$$\int_A (f_e(Q) + \varepsilon^{-2} f_b(Q)) dx$$

among Q -tensors which have \hat{z} as an eigenvector and P_1 -valued boundary data \tilde{g} with degree \tilde{k} .

Here $A \subset \mathbb{R}^2$, f_e is the general Landau-de Gennes elastic energy density, and f_b is a general bulk energy density which includes f_{LdG} as a specific example. In the proof of [18, Lemma 3.6], a sequence of Q -tensors is constructed with energies bounded by $s_*^2 \pi \tilde{k} \log \frac{1}{\varepsilon} + O(1)$. The interested reader can find the sequence, denoted by (\mathbf{w}', r') , in the proof in [18, p. 810]. Since we defined R_ε on $\Omega \setminus \Omega_\zeta$ so that $R_\varepsilon(\partial\Omega_\zeta) = \{\gamma_{\sigma(x)}(b) : x \in \partial\Omega_\zeta\} \subset P_1$ and R_ε restricted to $\partial\Omega_\zeta$ has degree k in the sense of (2.82), we can apply the result of [18, Lemma 3.6]. We obtain $R_\varepsilon : \Omega_\zeta \rightarrow \mathcal{S}$ such that

\hat{z} is an eigenvector for each $R_\varepsilon(x)$ and

$$\begin{aligned} \int_{\Omega_\zeta} \left(\varepsilon |\nabla R_\varepsilon|^2 + \frac{W(R_\varepsilon)}{\varepsilon} \right) dx &= \int_{\Omega_\zeta} \left(\varepsilon |\nabla R_\varepsilon|^2 + \frac{f_{LdG}(R_\varepsilon)}{\varepsilon} \right) dx \\ &\leq s_*^2 \pi k \varepsilon \log \frac{1}{\varepsilon} + O(\varepsilon). \end{aligned} \quad (2.102)$$

Adding the estimates (2.101) and (2.102) gives

$$F_\varepsilon(R_\varepsilon) \leq 2 \int_{\partial\Omega} \varphi_1(g(x)) d\mathcal{H}^1(x) + s_*^2 \pi k \varepsilon \log \frac{1}{\varepsilon} + O(\varepsilon),$$

and the upper bound is proved. \square

Proof of the lower bound. We turn now to the proof of the lower bound

$$F_\varepsilon(Q_\varepsilon) \geq 2 \int_{\partial\Omega} \varphi_1(g(x)) d\mathcal{H}^1(x) + s_*^2 \pi k \varepsilon \log \frac{1}{\varepsilon} + O(\varepsilon). \quad (2.103)$$

Similar to the proof of the lower semicontinuity condition (2.13) in Section 2.2, we want to replace the integrals of f_s over the top and bottom of the cylinder by the integral of $2f_s$ over $\Omega \times (0, 1)$.

By the calculations (2.23) and (2.24), we have

$$F_\varepsilon(Q_\varepsilon) = \int_{\Omega \times (0, 1)} \left(\varepsilon |\nabla_x Q_\varepsilon|^2 + \frac{|\nabla_z Q_\varepsilon|^2}{\varepsilon^3} + \frac{1}{\varepsilon} W(Q_\varepsilon) \right) dx dz + O(\varepsilon).$$

Next, using the fact that the boundary data g is independent of z , we further estimate the energy

$F_\varepsilon(Q_\varepsilon)$ from below. We write

$$\begin{aligned} F_\varepsilon(Q_\varepsilon) &\geq \int_{\Omega \times (0, 1)} \left(\varepsilon |\nabla_x Q_\varepsilon|^2 + \frac{1}{\varepsilon} W(Q_\varepsilon) \right) dx dz + O(\varepsilon) \\ &= \int_0^1 \int_{\Omega} \left(\varepsilon |\nabla_x Q_\varepsilon|^2 + \frac{1}{\varepsilon} W(Q_\varepsilon) \right) dx dz + O(\varepsilon) \\ &\geq \int_0^1 \min_{Q \in H_g^1(\Omega; \mathcal{S})} \left\{ \int_{\Omega} \left(\varepsilon |\nabla_x Q|^2 + \frac{1}{\varepsilon} W(Q) \right) dx \right\} dz + O(\varepsilon) \\ &= \min_{Q \in H_g^1(\Omega; \mathcal{S})} \left\{ \int_{\Omega} \left(\varepsilon |\nabla_x Q|^2 + \frac{1}{\varepsilon} W(Q) \right) dx \right\} + O(\varepsilon). \end{aligned}$$

Let G_ε be the functional

$$G_\varepsilon(Q) := \int_{\Omega} \left(\varepsilon |\nabla_x Q|^2 + \frac{1}{\varepsilon} W(Q) \right) dx$$

defined on $H_g^1(\Omega; \mathcal{S})$ and denote its minimizer by \tilde{Q}_ε . We have now that

$$F_\varepsilon(Q_\varepsilon) \geq G_\varepsilon(\tilde{Q}_\varepsilon) + O(\varepsilon).$$

It then suffices to show that

$$G_\varepsilon(\tilde{Q}_\varepsilon) \geq 2 \int_{\partial\Omega} \varphi_1(g(x)) d\mathcal{H}^1(x) + s_\star^2 \pi k \varepsilon \log \frac{1}{\varepsilon} + O(\varepsilon). \quad (2.104)$$

Proposition 2.5.1. *The minimizers \tilde{Q}_ε of G_ε with the boundary data and surface term as in the above discussion satisfy*

$$\frac{1}{\varepsilon} G_\varepsilon(\tilde{Q}_\varepsilon) \geq \frac{2}{\varepsilon} \int_{\partial\Omega} \Psi(g(\sigma)) d\sigma + s_\star^2 k \pi \log \frac{1}{\varepsilon} + O(1). \quad (2.105)$$

The proof of Proposition 2.5.1 is broken up into several lemmas and propositions which follow very closely the argument in [10, Proposition 3.1]. Indeed, although the unknown \tilde{Q}_ε is an element of \mathbb{R}^5 rather than \mathbb{R}^2 , as in [10], the proof from [10] goes through with minor modifications and was not included in [84]. The functional has been rescaled by $\frac{1}{\varepsilon}$ so that it coincides with the scaling in [10].

Lemma 2.5. *(cf. [10, Lemma 3.1]) There exist positive constants \tilde{C}_1, \tilde{C}_2 such that for all $\varepsilon > 0$ we have*

$$|\tilde{Q}_\varepsilon| \leq \tilde{C}_1 \text{ in } \Omega \quad (2.106)$$

and

$$\|\nabla \tilde{Q}_\varepsilon\|_{L^\infty(\Omega)} \leq \frac{\tilde{C}_2}{\varepsilon}. \quad (2.107)$$

Proof. (2.106) follows from the facts that both f_{LdG} and f_s grow at infinity, so truncating \tilde{Q}_ε far enough from zero decreases the energy. (2.107) follows from rescaling and following a similar argument as in [18, Lemma 3.1]. \square

Lemma 2.6. *(cf. [10, Lemma 3.2]) Let I be a compact subinterval of $(1/2, 1)$. Then, there exist constants $a = a(I) \in (0, 1)$, and $\mu = \mu(I)$, $C = C(I) > 0$ and, for any $\alpha \in I$ and $\varepsilon \in (0, 1)$, a set*

$J = J(\alpha, \varepsilon) \subset (0, C(I))$ satisfying $\text{meas}(J) \geq \mu$, such that

$$\int_{\Omega \setminus \Omega_{c_0 \varepsilon^\alpha}} |\nabla \tilde{Q}_\varepsilon|^2 + \frac{W(\tilde{Q}_\varepsilon)}{\varepsilon^2} \geq \frac{2}{\varepsilon} \int_{\partial\Omega} \Psi(g(\sigma)) d\sigma - C \quad (2.108)$$

and if $\Sigma_c := \{x \in \Omega : \text{dist}(x, \partial\Omega) = c\}$

$$\int_{\Sigma_{c_0 \varepsilon^\alpha}} \Psi(\tilde{Q}_\varepsilon(\sigma)) \leq C\varepsilon^{1+a} \text{ for all } c_0 \in J. \quad (2.109)$$

Proof. The Cauchy-Schwarz inequality allows us to conclude that for $\alpha \in I$ and any $c > 0$

$$\begin{aligned} \int_{\Omega \setminus \Omega_{c\varepsilon^\alpha}} |\nabla \tilde{Q}_\varepsilon|^2 + \frac{W(\tilde{Q}_\varepsilon)}{\varepsilon^2} &\geq \frac{2}{\varepsilon} \int_{\Omega \setminus \Omega_{c\varepsilon^\alpha}} |\nabla \tilde{Q}_\varepsilon| \sqrt{W(\tilde{Q}_\varepsilon)} \\ &\geq \frac{2}{\varepsilon} \int_{\Omega \setminus \Omega_{c\varepsilon^\alpha}} |\nabla(\Psi(\tilde{Q}_\varepsilon))| \\ &\geq \frac{2}{\varepsilon} \int_{\Omega \setminus \Omega_{c\varepsilon^\alpha}} \nabla(\Psi(\tilde{Q}_\varepsilon)) \cdot V \end{aligned}$$

for every $V \in C^1(\Omega \setminus \Omega_{c\varepsilon^\alpha}; B(0, 1))$. If we set $V = -\nabla\delta$, where δ is the (Euclidean) distance to $\partial\Omega$, we have

$$\begin{aligned} \int_{\Omega \setminus \Omega_{c\varepsilon^\alpha}} |\nabla \tilde{Q}_\varepsilon|^2 + \frac{W(\tilde{Q}_\varepsilon)}{\varepsilon^2} &\geq \frac{2}{\varepsilon} \int_{\partial\Omega} \Psi(g(\sigma)) d\sigma - \frac{2}{\varepsilon} \int_{\Sigma_{c\varepsilon^\alpha}} \Psi(\tilde{Q}_\varepsilon(\sigma)) d\sigma - \frac{2}{\varepsilon} \int_{\Omega \setminus \Omega_{c\varepsilon^\alpha}} \Psi(\tilde{Q}_\varepsilon) \operatorname{div}(V) dV \\ &:= I_1 + I_2 + I_3 \end{aligned} \quad (2.110)$$

Utilizing (2.85), it follows that $\int_\Omega W(\tilde{Q}_\varepsilon) dV \leq C\varepsilon$. Therefore, since $\Psi \leq CW$ on \mathbb{R}^5 (by the growth of W at ∞ and the positive-definiteness at the wells), I_3 is uniformly bounded uniformly for all ε .

By the inequality $\int_\Omega W(\tilde{Q}_\varepsilon) \leq C\varepsilon$, we see that $\int_\Omega \Psi(\tilde{Q}_\varepsilon) \leq C\varepsilon$, and co-area formula implies that there exists $c_1 \in (0, 1)$ such that

$$\int_{\Sigma_{c_1 \varepsilon^\alpha}} \Psi(\tilde{Q}_\varepsilon(\sigma)) d\sigma \leq C\varepsilon^{1-\alpha}.$$

When $c = c_1$, $I_2 \leq C\varepsilon^{-\alpha}$, so that (2.110) becomes

$$\int_{\Omega \setminus \Omega_{c_1\varepsilon^\alpha}} |\nabla \tilde{Q}_\varepsilon|^2 + \frac{W(\tilde{Q}_\varepsilon)}{\varepsilon^2} \geq \frac{2}{\varepsilon} \int_{\partial\Omega} \Psi(g(\sigma)) d\sigma - C\varepsilon^{-\alpha}.$$

Together with the upper bound

$$G_\varepsilon(\tilde{Q}_\varepsilon) \leq \frac{2}{\varepsilon} \int_{\partial\Omega} \Psi(g(\sigma)) + s_*^2 k \pi \log \frac{1}{\varepsilon} + C,$$

this implies that

$$\int_{\Omega_{c_1\varepsilon^\alpha}} |\nabla \tilde{Q}_\varepsilon|^2 + \frac{W(\tilde{Q}_\varepsilon)}{\varepsilon^2} \leq C\varepsilon^{-\alpha}.$$

Rearranging the inequality for the potential term yields

$$\int_{\Omega_{c_1\varepsilon^\alpha}} W(\tilde{Q}_\varepsilon) \leq C\varepsilon^{2-\alpha}.$$

Then we obtain the existence of $c_2 \in (1, 2)$ such that

$$\int_{\Sigma_{c_2\varepsilon^\alpha}} W(\tilde{Q}_\varepsilon(\sigma)) d\sigma \leq C\varepsilon^{2-2\alpha},$$

from which it follows that

$$\int_{\Sigma_{c_2\varepsilon^\alpha}} \Psi(\tilde{Q}_\varepsilon(\sigma)) d\sigma \leq C\varepsilon^{2-2\alpha}.$$

These steps are then repeated with the previous estimate starting from (2.110).

Choose $n = n(\alpha)$ so that

$$\frac{n-1}{n} \leq \alpha < \frac{n}{n+1}. \quad (2.111)$$

It is easily seen that $\sup\{n(\alpha) \text{ satisfying (2.111)} : \alpha \in I\} < \infty$. By repeating this argument n times, we find that there exists some $c_n \in (n-1, n)$ such that

$$\int_{\Omega \setminus \Omega_{c_n\varepsilon^\alpha}} |\nabla \tilde{Q}_\varepsilon|^2 + \frac{W(\tilde{Q}_\varepsilon)}{\varepsilon^2} \geq \frac{2}{\varepsilon} \int_{\partial\Omega} \Psi(g(\sigma)) d\sigma - C\varepsilon^{n-1-n\alpha}.$$

Once more utilizing the upper bound yields

$$\int_{\Omega_{c_n\varepsilon^\alpha}} |\nabla \tilde{Q}_\varepsilon|^2 + \frac{W(\tilde{Q}_\varepsilon)}{\varepsilon^2} \leq C\varepsilon^{n-1-n\alpha} + C \log \frac{1}{\varepsilon},$$

which in turn implies that

$$\int_{\Omega_{c_n \varepsilon^\alpha}} \Psi(\tilde{Q}_\varepsilon) \leq C \varepsilon^2 \left(\varepsilon^{n-1-n\alpha} + \log \frac{1}{\varepsilon} \right)$$

and there exists $c_0 \in (n, n+1)$ such that

$$\int_{\Sigma_{c_0 \varepsilon^\alpha}} \Psi(\tilde{Q}_\varepsilon(\sigma)) d\sigma \leq C \varepsilon^{(n+1)(1-\alpha)} + C \varepsilon^{2-\alpha} \log \frac{1}{\varepsilon}. \quad (2.112)$$

If $0 < a < \min(1 - \alpha, (n+1)(1 - \alpha) - 1)$, then (2.112) can be used to show that

$$\int_{\Sigma_{c_0 \varepsilon^\alpha}} \Psi(\tilde{Q}_\varepsilon(\sigma)) d\sigma \leq C \varepsilon^{1+a}. \quad (2.113)$$

Now it is possible to choose $a(I)$ such that (2.112) holds for all $\alpha \in I$. From the co-area formula and Chebyshev's inequality, the measure of the set of c_0 's in $(n, n+1)$ which obey (2.113) is bounded from below by some μ . Furthermore, the bound is uniform in $\alpha \in I \subset \subset (1/2, 1)$ and $\varepsilon \in (0, 1)$. We have thus shown (2.109), and plugging in (2.113) into (2.110) with $c = c_0$ gives $I_2 \leq C$. Finally, (2.108) follows as well. \square

We now turn to a lower bound for $|\nabla \tilde{Q}_\varepsilon|^2$. First we make some remarks and set some notation. For convenience, we assume that Ψ is C^2 in a neighborhood of the zero set of W . We remark that Ψ is clearly locally Lipschitz, and that higher regularity could be shown using the quadratic growth of W away from its zero set as in [10, Proposition 5.1]. Note also that the nondegeneracy of W at the well and the fact that $|\nabla \Psi|^2 = W$ imply that Ψ is nondegenerate at the well. This allows us to conclude that on any bounded set, such as the union of the ranges of the \tilde{Q}_ε 's, $\Psi \sim W$. Recall that “ \sim ” is used to denote that each quantity is bounded above and below by the other, up to constants.

Next if we define $S_\lambda := \{Q \in \mathcal{S} : \Psi(Q) < \lambda\}$, there exists λ_0 such that Ψ is in $C^2(\overline{S_{\lambda_0}})$. Then we can cover S_{λ_0} by gradient lines of Ψ which intersect only on the zero set of Ψ , which is the zero set of W , too. In particular, for any $Q \in S_{\lambda_0}$, there is a unique gradient line of Ψ though Q which intersects the zero set of Ψ . Denote by $\tilde{s}(Q)$ the intersection of this gradient line with the zero set

of Ψ . Recall the assumption that the boundary data g is in S_{λ_0} is closer to the circle C than the point P under the degenerate metric induced by W . Finally, let us denote by $\theta(Q)$ the function $\phi^{-1}(\tilde{s}(Q))$, where $\phi : [a, b] \rightarrow C$ parametrizes the circle C by arc-length.

Lemma 2.7. (cf. [10, Lemma 3.3]) *We have the estimates*

$$|\nabla_x \tilde{Q}_\varepsilon|^2 \geq \frac{|\nabla_x(\Psi(\tilde{Q}_\varepsilon))|^2}{W(\tilde{Q}_\varepsilon)} \text{ a.e. in } \Omega \quad (2.114)$$

and

$$|\nabla_x \tilde{Q}_\varepsilon|^2 \geq \rho |\nabla_x(\theta(\tilde{Q}_\varepsilon))|^2 + \frac{|\nabla_x(\Psi(\tilde{Q}_\varepsilon))|^2}{W(\tilde{Q}_\varepsilon)} \quad (2.115)$$

in $\Omega_0^\varepsilon := \{x \in \Omega : \tilde{Q}_\varepsilon(x) \in S_{\lambda_0}\}$ for some $\rho > 0$, independent of ε .

Proof. We begin by calculating

$$\begin{aligned} |\nabla_x(\Psi(\tilde{Q}_\varepsilon))|^2 &= |\nabla_Q(\Psi(\tilde{Q}_\varepsilon)) \cdot \nabla_x(\tilde{Q}_\varepsilon)|^2 \\ &\leq |\nabla_Q(\Psi(\tilde{Q}_\varepsilon))|^2 |\nabla_x(\tilde{Q}_\varepsilon)|^2 \\ &= W(\tilde{Q}_\varepsilon) |\nabla_x(\tilde{Q}_\varepsilon)|^2 \end{aligned} \quad (2.116)$$

a.e. in Ω . Now, for each $Q \in S_{\lambda_0}$, let $\nu = \nu(Q)$ be a unit vector parallel to $\nabla_Q \Psi(Q)$ and $\tau = \tau(Q)$ be an orthogonal unit vector in parallel to $\nabla_Q \theta(\tilde{Q}_\varepsilon)$ (the orthogonality follows from the constancy of $\theta(\tilde{Q}_\varepsilon)$ on the gradient lines of Ψ). Then we can write

$$\begin{aligned} |\nabla_x \tilde{Q}_\varepsilon|^2 &= \sum_{i=1}^2 \left| \frac{\partial}{\partial x_i} \tilde{Q}_\varepsilon \right|^2 \\ &\geq \sum_{i=1}^2 \left(\frac{\partial}{\partial x_i} \tilde{Q}_\varepsilon \cdot \tau \right)^2 + \sum_{i=1}^2 \left(\frac{\partial}{\partial x_i} \tilde{Q}_\varepsilon \cdot \nu \right)^2 \\ &= \sum_{i=1}^2 \left(\frac{\partial}{\partial x_i} \tilde{Q}_\varepsilon \cdot \frac{\nabla_Q \theta(\tilde{Q}_\varepsilon)}{|\nabla_Q \theta(\tilde{Q}_\varepsilon)|} \right)^2 + \sum_{i=1}^2 \left(\frac{\partial}{\partial x_i} \tilde{Q}_\varepsilon \cdot \frac{\nabla_Q \Psi(\tilde{Q}_\varepsilon)}{|\nabla_Q \Psi(\tilde{Q}_\varepsilon)|} \right)^2 \\ &= \frac{1}{|\nabla_Q \theta(\tilde{Q}_\varepsilon)|^2} \sum_{i=1}^2 \left(\frac{\partial}{\partial x_i} (\theta(\tilde{Q}_\varepsilon)) \right)^2 + \frac{1}{|\nabla_Q \Psi(\tilde{Q}_\varepsilon)|^2} \sum_{i=1}^2 \left(\frac{\partial}{\partial x_i} (\Psi(\tilde{Q}_\varepsilon)) \right)^2 \\ &= \frac{|\nabla_x(\theta(\tilde{Q}_\varepsilon))|^2}{|\nabla_Q \theta(\tilde{Q}_\varepsilon)|^2} + \frac{|\nabla_x(\Psi(\tilde{Q}_\varepsilon))|^2}{|\nabla_Q \Psi(\tilde{Q}_\varepsilon)|^2}. \end{aligned}$$

Since $|\nabla_Q \theta(\tilde{Q}_\varepsilon)| \leq \frac{1}{\sqrt{\rho}}$ for all \tilde{Q}_ε in S_{λ_0} for some $\rho > 0$ and $|\nabla_Q \Psi(\tilde{Q}_\varepsilon)|^2 = W(\tilde{Q}_\varepsilon)$, we see that Eq. (2.115) holds in Ω_0^ε . \square

In what follows, we will choose an interval $I \subset \subset (1/2, 1)$ and let $\alpha \in I$. We will need the function $\chi_{0\varepsilon}$, which is the minimizer for

$$\int_{\Omega \setminus \Omega_{c_0\varepsilon^\alpha}} \frac{|\nabla \chi|^2}{W(\tilde{Q}_\varepsilon) + \varepsilon^2} \text{ among } \chi \in H^1, \chi = \Psi(\tilde{Q}_\varepsilon) \text{ on } \partial\Omega_{c_0\varepsilon^\alpha}. \quad (2.117)$$

The function $\chi_{0\varepsilon}$ is easily seen to be unique with Euler-Lagrange equation

$$\begin{cases} \operatorname{div} \left(\frac{\nabla \chi_{0\varepsilon}}{W(\tilde{Q}_\varepsilon) + \varepsilon^2} \right) = 0 \text{ in } \Omega \setminus \Omega_{c_0\varepsilon^\alpha} \\ \chi_{0\varepsilon} = \Psi(\tilde{Q}_\varepsilon) \text{ on } \partial\Omega_{c_0\varepsilon^\alpha} \end{cases} \quad (2.118)$$

for any $c_0 \in J$.

Lemma 2.8. (*cf. [10, Lemma 3.4]*) *There exists $\varepsilon_0 > 0$ such that for every $\varepsilon \leq \varepsilon_0$, and $\alpha \in I$ we have*

$$0 \leq \chi_{0\varepsilon} \leq \lambda_1 \text{ in } \Omega \setminus \Omega_{c_0\varepsilon^\alpha} \quad (2.119)$$

where $\lambda_1 = \max_{\sigma \in \partial\Omega} \{\Psi(g(\sigma))\}$.

Proof. With an eye towards applying the maximum principle to (2.118), we aim to show that for small enough ε ,

$$\chi_{0\varepsilon} = \Psi(\tilde{Q}_\varepsilon) \leq \lambda_1 \text{ on } \Omega \setminus \partial\Omega_{c_0\varepsilon^\alpha} = \partial\Omega \cup \Sigma_{c_0\varepsilon^\alpha}. \quad (2.120)$$

Since, $\chi_{0\varepsilon} = \Psi$ on $\partial\Omega$, (2.120) holds on $\partial\Omega$. We turn to proving (2.120) on $\Sigma_{c_0\varepsilon^\alpha}$. For $\Sigma_{c_0\varepsilon^\alpha}$, the estimate is a consequence of (2.109) on Ψ and the gradient bound (2.107) on \tilde{Q}_ε . Let $x_0 \in \Sigma_{c_0\varepsilon^\alpha}$ be the point on $\Sigma_{c_0\varepsilon^\alpha}$ farthest in terms of Euclidean distance $\tilde{\delta}$ from the well of W , so that

$$|\tilde{\delta}(\tilde{Q}_\varepsilon(x_0))| = m := \max_{x \in \Sigma_{c_0\varepsilon^\alpha}} |\tilde{\delta}(\tilde{Q}_\varepsilon(x))|.$$

From the gradient bound (2.107), there exists $c > 0$ such that

$$|\tilde{\delta}(\tilde{Q}_\varepsilon(x))| \geq \frac{m}{2}$$

if $x \in \Sigma_{c_0\varepsilon^\alpha} \cap B(x_0, m\varepsilon/(2c))$. Thus for some $a_0 > 0$, we have

$$\Psi(\tilde{Q}_\varepsilon(x)) \geq a_0 \tilde{\delta}^2(\tilde{Q}_\varepsilon(x)) \geq a_0 \frac{m^2}{4}$$

for $x \in \Sigma_{c_0\varepsilon^\alpha} \cap B(x_0, m\varepsilon/(2c))$, from which it follows that

$$\begin{aligned} a_0 \frac{m^3 \varepsilon}{8c} &= \frac{m\varepsilon}{2c} \cdot \frac{a_0 m^2}{4} \\ &\leq \int_{\Sigma_{c_0\varepsilon^\alpha}} \Psi(\tilde{Q}_\varepsilon) \leq C\varepsilon^{1+\alpha}. \end{aligned}$$

We used here the fact that the \mathcal{H}^1 measure of $\Sigma_{c_0\varepsilon^\alpha}$ in the ball $B(x_0, m\varepsilon/(2c))$ is at least the diameter, since $\Sigma_{c_0\varepsilon^\alpha}$ contains the center x_0 . But $a_0 \frac{m^3 \varepsilon}{8c} \leq C\varepsilon^{1+\alpha}$ implies that $m \leq C\varepsilon^{\alpha/3}$ for small ε . Hence

$$\Psi(\tilde{Q}_\varepsilon) \leq C\varepsilon^{2\alpha/3} < \lambda_1 \text{ on } \Sigma_{c_0\varepsilon^\alpha}$$

if ε is small enough, and we are done. \square

Next, using the definition of $\chi_{0\varepsilon}$, Lemma 2.7, and the upper bound we have

$$\int_{\Omega \setminus \Omega_{c_0\varepsilon^\alpha}} \frac{|\nabla \chi_{0\varepsilon}|^2}{W(\tilde{Q}_\varepsilon) + \varepsilon^2} \leq \int_{\Omega \setminus \Omega_{c_0\varepsilon^\alpha}} \frac{|\nabla(\Psi(\tilde{Q}_\varepsilon))|^2}{W(\tilde{Q}_\varepsilon) + \varepsilon^2} \leq \frac{C}{\varepsilon}. \quad (2.121)$$

Setting $\chi_{1\varepsilon} = \Psi(\tilde{Q}_\varepsilon) - \chi_{0\varepsilon}$, we write

$$\begin{aligned} \int_{\Omega \setminus \Omega_{c_0\varepsilon^\alpha}} \frac{|\nabla(\Psi(\tilde{Q}_\varepsilon))|^2}{W(\tilde{Q}_\varepsilon) + \varepsilon^2} &= \int_{\Omega \setminus \Omega_{c_0\varepsilon^\alpha}} \frac{1}{W(\tilde{Q}_\varepsilon) + \varepsilon^2} (|\nabla \chi_{0\varepsilon}|^2 + 2\nabla \chi_{0\varepsilon} \cdot \nabla \chi_{1\varepsilon} + |\nabla \chi_{1\varepsilon}|^2) \\ &= \int_{\Omega \setminus \Omega_{c_0\varepsilon^\alpha}} \frac{|\nabla \chi_{0\varepsilon}|^2}{W(\tilde{Q}_\varepsilon) + \varepsilon^2} + \frac{|\nabla \chi_{1\varepsilon}|^2}{W(\tilde{Q}_\varepsilon) + \varepsilon^2}, \end{aligned} \quad (2.122)$$

where in the last line we used the weak formulation of (2.118). We proceed by proving a key lower bound for

$$\int_{\Omega \setminus \Omega_{c_0\varepsilon^\alpha}} \frac{|\nabla \chi_{0\varepsilon}|^2}{W(\tilde{Q}_\varepsilon) + \varepsilon^2}.$$

Lemma 2.9. (cf. [10, Lemma 3.5]) *There exists a constant $C_1(I)$ such that*

$$\int_{\Omega \setminus \Omega_{c_0\varepsilon^\alpha}} \frac{|\nabla \chi_{0\varepsilon}|^2}{W(\tilde{Q}_\varepsilon) + \varepsilon^2} + \frac{W(\tilde{Q}_\varepsilon) + \varepsilon^2}{\varepsilon^2} \geq \frac{2}{\varepsilon} \int_{\partial\Omega} \Psi(g(\sigma)) d\sigma - C_1$$

for all $\varepsilon \in (0, 1)$, for all $\alpha \in I$.

Proof. By the same argument as in Lemma 2.6, if $V = -\nabla\delta$, then

$$\begin{aligned} \int_{\Omega \setminus \Omega_{c_0\varepsilon^\alpha}} \frac{|\nabla\chi_{0\varepsilon}|^2}{W(\tilde{Q}_\varepsilon) + \varepsilon^2} + \frac{W(\tilde{Q}_\varepsilon) + \varepsilon^2}{\varepsilon^2} &\geqslant \frac{2}{\varepsilon} \int_{\Omega \setminus \Omega_{c_0\varepsilon^\alpha}} |\nabla\chi_{0\varepsilon}| d\sigma \\ &\geqslant \frac{2}{\varepsilon} \int_{\Omega \setminus \Omega_{c_0\varepsilon^\alpha}} \nabla\chi_{0\varepsilon} \cdot V \\ &= \frac{2}{\varepsilon} \int_{\partial(\Omega \setminus \Omega_{c_0\varepsilon^\alpha})} \Psi(\tilde{Q}_\varepsilon) - \frac{2}{\varepsilon} \int_{\Omega_{c_0\varepsilon^\alpha}} \chi_{0\varepsilon} \operatorname{div} V \\ &\geqslant \frac{2}{\varepsilon} \int_{\partial\Omega} \Psi(g) - \frac{2}{\varepsilon} \int_{\Omega \setminus \Omega_{c_0\varepsilon^\alpha}} \chi_{0\varepsilon} \operatorname{div} V - C \end{aligned}$$

where we used (2.109) on the integral over $\Sigma_{c_0\varepsilon^\alpha}$. So if we show that

$$\int_{\Omega \setminus \Omega_{c_0\varepsilon^\alpha}} \chi_{0\varepsilon} \leqslant C\varepsilon, \quad (2.123)$$

we are done. Consider any $\delta \in (0, c_0\varepsilon^\alpha)$ and let $\delta_0 = \frac{\delta}{5}$. From the upper bound and the co-area formula, we obtain $\delta_1 \in (\delta_0, 2\delta_0)$ such that

$$\int_{\Sigma_{\delta_1}} W(\tilde{Q}_\varepsilon) \leqslant \frac{C\varepsilon}{\delta}.$$

Arguing similarly as in Lemma 2.6 gives

$$\int_{\Omega_{\delta_1}} W(\tilde{Q}_\varepsilon) \leqslant \frac{C\varepsilon^2}{\delta} + C\varepsilon^2 \log \frac{1}{\varepsilon}.$$

Repeating the argument a second time yields $\delta_2 \in (2\delta_0, 3\delta_0)$ such that

$$\int_{\Omega_{\delta_2}} W(\tilde{Q}_\varepsilon) \leqslant \frac{C\varepsilon^3}{\delta^2} + C\varepsilon^2 \log \frac{1}{\varepsilon},$$

and a third time time yields $\delta_3 \in (3\delta_0, 4\delta_0)$ such that

$$\int_{\Omega_{\delta_3}} W(\tilde{Q}_\varepsilon) \leqslant \frac{C\varepsilon^4}{\delta^3} + C\varepsilon^2 \log \frac{1}{\varepsilon}.$$

Thus

$$\int_{\Omega_\delta} W(\tilde{Q}_\varepsilon) \leqslant \frac{C\varepsilon^4}{\delta^3} + C\varepsilon^2 \log \frac{1}{\varepsilon} \quad (2.124)$$

for any $\delta \in (\varepsilon, c_0 \varepsilon^\alpha)$. Changing to local coordinates (σ, δ) in a neighborhood of $\partial\Omega$, where δ is the distance to $\partial\Omega$, we estimate

$$\begin{aligned} \int_{\Omega_\varepsilon \setminus \Omega_{c_0 \varepsilon^\alpha}} \chi_{0\varepsilon} &\leq C \int_\varepsilon^{c_0 \varepsilon^\alpha} \left(\int_{\partial\Omega} \chi_{0\varepsilon}(\sigma, \delta) d\sigma \right) d\delta \\ &\leq C \int_\varepsilon^{c_0 \varepsilon^\alpha} \left(\int_{\partial\Omega} (\chi_{0\varepsilon}(\sigma, c_0 \varepsilon^\alpha) d\sigma + \int_\delta^{c_0 \varepsilon^\alpha} |\nabla \chi_{0\varepsilon}(\sigma, t)| dt) d\sigma \right) d\delta \\ &\leq C \varepsilon^{1+a+\alpha} + C \int_\varepsilon^{c_0 \varepsilon^\alpha} \left(\int_{\Omega_\delta} |\nabla \chi_{0\varepsilon}| dV \right) d\delta \end{aligned} \quad (2.125)$$

From Cauchy-Schwarz, (2.121), and (2.124) we have

$$\begin{aligned} &\int_\varepsilon^{c_0 \varepsilon^\alpha} \left(\int_{\Omega_\delta} |\nabla \chi_{0\varepsilon}| \right) d\delta \\ &\leq \int_\varepsilon^{c_0 \varepsilon^\alpha} \left(\int_{\Omega_\delta} \frac{|\nabla \chi_{0\varepsilon}|^2}{W(\tilde{Q}_\varepsilon) + \varepsilon^2} \right)^{1/2} \left(\int_{\Omega_\delta} W(\tilde{Q}_\varepsilon) + \varepsilon^2 \right)^{1/2} d\delta \\ &\leq \frac{C}{\varepsilon^{1/2}} \int_\varepsilon^{c_0 \varepsilon^\alpha} \left(\int_{\Omega_\delta} W(\tilde{Q}_\varepsilon) + \varepsilon^2 \right)^{1/2} d\delta \\ &\leq \frac{C}{\varepsilon^{1/2}} \int_\varepsilon^{c_0 \varepsilon^\alpha} \left(\frac{\varepsilon^2}{\delta^{3/2}} + \varepsilon \left(\log \frac{1}{\varepsilon} \right)^{1/2} + \varepsilon \right) d\delta \\ &\leq -C \varepsilon^{1/2} \cdot s^{-1/2} \Big|_\varepsilon^{c_0 \varepsilon^\alpha} + c \varepsilon^{\alpha+1/2} + c \varepsilon^{\alpha+1/2} \left(\log \frac{1}{\varepsilon} \right)^{1/2} + C \varepsilon^{1/2+\alpha} \\ &\leq C \varepsilon. \end{aligned} \quad (2.126)$$

Equations (2.125)-(2.126) together give

$$\int_{\Omega_\varepsilon \setminus \Omega_{c_0 \varepsilon^\alpha}} \chi_{0\varepsilon} \leq C \varepsilon.$$

In addition, it is quickly seen that

$$\int_{\Omega \setminus \Omega_\varepsilon} \chi_{0\varepsilon} \leq |\Omega \setminus \Omega_\varepsilon| \lambda_1 \leq C \varepsilon,$$

so that the proof of (2.123) and thus the lemma is done. \square

Proposition 2.5.2. (*cf. [10, Proposition 3.2]*) *There exist positive constants $K = K(I)$ and $C_2 =$*

$C_2(I)$ such that for every $\varepsilon \in (0, 1)$, $\alpha \in I$, and $c_0 \in J_{\alpha, \varepsilon}$,

$$\begin{aligned} & \int_{\Omega_{c_0\varepsilon^\alpha}} |\nabla \tilde{Q}_\varepsilon|^2 + \frac{W(\tilde{Q}_\varepsilon)}{\varepsilon^2} dV \\ & \geq \frac{2}{\varepsilon} \int_{\partial\Omega} \Psi(g(\sigma)) d\sigma + K \int_{\partial\Omega} \frac{|\tilde{Q}_\varepsilon(\sigma, c_0\varepsilon^\alpha) - \tilde{s}(g(\sigma))|^2}{e^\alpha} d\sigma - C_2 \end{aligned} \quad (2.127)$$

Proof. Lemma 2.9 and (2.122) imply

$$\int_{\Omega_{c_0\varepsilon^\alpha}} \frac{|\nabla \Psi(\tilde{Q}_\varepsilon)|^2}{W(\tilde{Q}_\varepsilon)} + \frac{W(\tilde{Q}_\varepsilon)}{\varepsilon^2} \geq \frac{2}{\varepsilon} \int_{\partial\Omega} \Psi(g(\sigma)) d\sigma + \int_{\Omega_{c_0\varepsilon^\alpha}} \frac{|\nabla \chi_{1\varepsilon}|^2}{W(\tilde{Q}_\varepsilon) + \varepsilon^2} - C.$$

Estimating the left hand side of the previous inequality using Eq. (2.114) and Eq. (2.115) gives

$$\begin{aligned} & \int_{\Omega_{c_0\varepsilon^\alpha}} |\nabla \tilde{Q}_\varepsilon|^2 + \frac{W(\tilde{Q}_\varepsilon)}{\varepsilon^2} \\ & \geq \frac{2}{\varepsilon} \int_{\partial\Omega} \Psi(g(\sigma)) d\sigma + \int_{\Omega_{c_0\varepsilon^\alpha}} \frac{|\nabla \chi_{1\varepsilon}|^2}{W(\tilde{Q}_\varepsilon) + \varepsilon^2} + \rho \int_{\Omega_{c_0\varepsilon^\alpha} \cap \Omega_0^\varepsilon} |\nabla(\theta(\tilde{Q}_\varepsilon))|^2 - C. \end{aligned} \quad (2.128)$$

Fix any $\sigma_0 \in \partial\Omega$. We split the argument into cases.

Case 1: For any $\delta \in (0, c_0\varepsilon^\alpha)$

$$\chi_{1\varepsilon}(\sigma_0, \delta) \leq \lambda_0 - \lambda_1,$$

where $\lambda_1 := \max\{\Psi(g)\}$.

Since $\chi_{0\varepsilon} \leq \lambda_1$ by Eq. (2.119), we see that $(\sigma_0, \delta) \in \Omega_0^\varepsilon$ for any $\delta \in (0, c_0\varepsilon^\alpha)$. Using Jensen's inequality and the Fundamental Theorem of Calculus we have

$$\begin{aligned} \frac{C}{\varepsilon^\alpha} |\tilde{s}(g(\sigma_0)) - \tilde{s}(\tilde{Q}_\varepsilon(\sigma_0, c_0\varepsilon^\alpha))|^2 & \leq \frac{C}{\varepsilon^\alpha} |\theta(g(\sigma_0)) - \theta(\tilde{Q}_\varepsilon(\sigma_0, c_0\varepsilon^\alpha))|^2 \\ & \leq \rho \int_0^{\varepsilon^\alpha} |\nabla(\theta(\tilde{Q}_\varepsilon(\sigma_0, \delta)))|^2 d\delta. \end{aligned}$$

Since $\Psi \sim \delta^2 \sim W$, it follows that

$$\begin{aligned} |\tilde{Q}_\varepsilon(\sigma_0, c_0\varepsilon^\alpha) - \tilde{s}(\tilde{Q}_\varepsilon(\sigma_0, c_0\varepsilon^\alpha))|^2 & = O(\Psi(\tilde{Q}_\varepsilon(\sigma_0, c_0\varepsilon^\alpha))) \\ & = O(W(\tilde{Q}_\varepsilon(\sigma_0, c_0\varepsilon^\alpha))). \end{aligned}$$

We deduce that for some $K_0, K_1 > 0$,

$$\rho \int_0^{c_0\varepsilon^\alpha} |\nabla(\theta(\tilde{Q}_\varepsilon(\sigma, \delta)))|^2 d\delta \geq K_0 \frac{|\tilde{Q}_\varepsilon(\sigma_0, c_0\varepsilon^\alpha) - \tilde{s}(g(\sigma_0))|^2}{\varepsilon^\alpha} - K_1 \frac{W(\tilde{Q}_\varepsilon(\sigma_0, c_0\varepsilon^\alpha))}{\varepsilon^\alpha}. \quad (2.129)$$

Case 2: For some $\delta' \in (0, c_0 \varepsilon^\alpha)$, $\chi_{1\varepsilon}(\sigma_0, \delta') > \lambda_0 - \lambda_1$.

Now, using the bound (2.106) on \tilde{Q}_ε , we may write

$$\begin{aligned} \int_0^{c_0 \varepsilon^\alpha} \frac{|\nabla \chi_{1\varepsilon}(\sigma, \delta)|^2 d\delta}{W(\tilde{Q}_\varepsilon(\sigma, \delta)) + \varepsilon^2} &\geq C \int_0^{\delta'} |\nabla \chi_{1\varepsilon}(\sigma_0, \delta)|^2 d\delta \\ &\geq C \frac{\chi_{1\varepsilon}^2(\sigma, \delta')}{\delta'} \\ &\geq C \frac{(\lambda_0 - \lambda_1)^2}{c_0 \varepsilon^\alpha} \\ &\geq K_2 \frac{|\tilde{Q}_\varepsilon(\sigma_0, c_0 \varepsilon^\alpha) - \tilde{s}(g(\sigma))|^2}{\varepsilon^\alpha} \end{aligned} \quad (2.130)$$

for some $K_2 > 0$. If we integrate either (2.129) or (2.130) over $\sigma_0 \in \partial\Omega$, we get for some constants

K, \tilde{K}_1 :

$$\begin{aligned} \int_{\Omega_{c_0 \varepsilon^\alpha}} \frac{|\nabla \chi_{1\varepsilon}|^2}{W(\tilde{Q}_\varepsilon) + \varepsilon^2} + \rho \int_{\Omega_{c_0 \varepsilon^\alpha} \cap \Omega_0^\varepsilon} |\nabla(\theta(\tilde{Q}_\varepsilon))|^2 \\ \geq K \int_{\partial\Omega} \frac{|\tilde{Q}_\varepsilon(\sigma, c_0 \varepsilon^\alpha) - \tilde{s}(g(\sigma))|^2}{\varepsilon^\alpha} d\sigma - \tilde{K}_1 \int_{\partial\Omega} \frac{W(\tilde{Q}_\varepsilon(\sigma, c_0 \varepsilon^\alpha))}{\varepsilon^\alpha} \\ := I_1 - I_2. \end{aligned} \quad (2.131)$$

But I_2 is bounded by Eq. (2.109), so the lemma follows from Eq. (2.128) and Eq. (2.131). \square

Proof of Proposition 2.5.1. Let D be the Euclidean distance to C , which is the “circular” component of the zero set of W . By the gradient bound along with the same argument as in [18, Lemma 3.2], one can show that

$$W(\tilde{Q}_\varepsilon(x)) \geq \kappa D^2(\tilde{Q}_\varepsilon(x)) \text{ except on a set of size } O(\varepsilon^2). \quad (2.132)$$

We will need the following change of variables for \tilde{Q}_ε and the boundary data g :

$$\tilde{Q}_\varepsilon = \begin{bmatrix} \tilde{q}_{11}^\varepsilon & \tilde{q}_{12}^\varepsilon & \tilde{q}_{13}^\varepsilon \\ \tilde{q}_{21}^\varepsilon & \tilde{q}_{22}^\varepsilon & \tilde{q}_{23}^\varepsilon \\ \tilde{q}_{31}^\varepsilon & \tilde{q}_{32}^\varepsilon & \tilde{q}_{33}^\varepsilon \end{bmatrix} =: \begin{bmatrix} p_1^\varepsilon + r_\varepsilon/2 & p_2^\varepsilon & \tilde{q}_{13}^\varepsilon \\ p_2^\varepsilon & r_\varepsilon/2 - p_1^\varepsilon & \tilde{q}_{23}^\varepsilon \\ \tilde{q}_{31}^\varepsilon & \tilde{q}_{32}^\varepsilon & -r_\varepsilon \end{bmatrix}$$

and

$$g = \begin{bmatrix} g_{11} & g_{12} & g_{13} \\ g_{21} & g_{22} & g_{23} \\ g_{31} & g_{32} & g_{33} \end{bmatrix} =: \begin{bmatrix} p'_1 + r'/2 & p'_2 & g_{13} \\ p'_2 & r'/2 - p'_1 & g_{23} \\ g_{31} & g_{32} & -r' \end{bmatrix}.$$

Let us call $p_\varepsilon = (p_\varepsilon^1, p_\varepsilon^2)$ and $p' = (p'_1, p'_2)$. In these variables, the circular component C of the zero set of W corresponds to $|p_\varepsilon| = |s_\star|/2$ and $r = s_\star/3$. Now using Proposition 2.5.2 and these new variables, we obtain for any $\alpha \in I \subset \subset (1/2, 1)$

$$\begin{aligned} G_\varepsilon(\tilde{Q}_\varepsilon) - \frac{2}{\varepsilon} \int_{\partial\Omega} \Psi(g(\sigma)) d\sigma \\ \geq \int_{\Omega \setminus \Omega_{c_0\varepsilon^\alpha}} |\nabla \tilde{Q}_\varepsilon|^2 + \kappa \frac{D^2(\tilde{Q}_\varepsilon)}{\varepsilon^2} + K \int_{\partial\Omega} \frac{|\tilde{Q}_\varepsilon(\sigma, c_0\varepsilon^\alpha) - \tilde{s}(g(\sigma))|^2}{\varepsilon^\alpha} d\sigma - C_2 \\ \geq \int_{\Omega \setminus \Omega_{c_0\varepsilon^\alpha}} |\nabla \tilde{p}_\varepsilon|^2 + \kappa \frac{|p_\varepsilon| - |s_\star|/2|^2}{\varepsilon^2} + K \int_{\partial\Omega} \frac{|p_\varepsilon(\sigma, c_0\varepsilon^\alpha) - \tilde{s}(p'(\sigma))|^2}{\varepsilon^\alpha} d\sigma - C_2. \end{aligned} \quad (2.133)$$

By appealing to [8, Proposition 5.1], which deals with such a lower bound when the potential depends on the distance to a curve, we see that the right hand side of (2.133) is bounded from below by

$$2k \frac{\ell^2(C)}{2\pi} \log \frac{1}{\varepsilon} - C = s_\star^2 \pi k \log \frac{1}{\varepsilon} - C. \quad (2.134)$$

Combining Eq. (2.134) with Eq. (2.133) finishes the proof. □

With the asymptotic development of Theorem 2.5 in hand, a natural question is whether a subsequence of the minimizers Q_ε converges to some Q_0 . Results of this nature have been obtained for the case of Ginzburg–Landau type problems in [8–10, 19] and for a two-dimensional Landau–de Gennes model in [18]. The limiting map for the Ginzburg–Landau type problems is the so-called “canonical harmonic map” identified in [19] and generalized in [8–10]. By utilizing a suitable change of variables, a similar result is proved for the two-dimensional Landau–de Gennes model in [18]. In the latter case, the limiting map is uniaxial and the minimizers along a convergent subsequence have degree 1/2 around the singularities of the limiting map, cf. [18, Corollary A]. We expect a similar result to hold for our problem, but we have not carried out the details. Finally, one could certainly determine the location of the singularities of the limiting map, corresponding to the disclination lines in the nematic film. In all of the above works, the locations of the singularities

are governed by the minimization of a “renormalized energy,” and such a program could be carried out for this problem as well.

2.6 Appendix to Chapter 2: Characterization of Minimal States for Limiting Potential

Lemma 2.10. *The minimum of $W = f_{LdG} + 2f_s$ is achieved and can be characterized as follows:*

- (i) *If β cannot be written as a convex linear combination of λ_i 's, where $\lambda = (\lambda_1, \lambda_2, \lambda_3)$ is a stationary point of f_{LdG} , then \hat{z} is an eigenvector of any minimizer.*
- (ii) *If β can be written as a convex linear combination of λ_i 's, then there are two cases:*
 - (i) *if $\beta = \lambda_i$ for some i , so that the convex linear combination is trivial, then \hat{z} is an eigenvector of any minimizer;*
 - (ii) *if β is not equal to one of the λ_i 's, so the convex linear combination is non-trivial, then \hat{z} is not a eigenvector of any minimizer.*

In either case (1) or (2), minimizers may be isotropic, uniaxial, or biaxial.

Proof. The quartic growth of f_{LdG} at infinity and the fact that f_s is positive immediately yield the existence of a global minimizer for W . Next, we state the equations for stationary points of $f_{LdG}(Q)$, expressed as $f_{LdG}(\lambda)$, subject to the condition $\sum \lambda_i = 0$. We obtain the system

$$\begin{cases} (f_{LdG})_{\lambda_i} + k = 0 \\ \sum \lambda_i = 0, \end{cases}$$

where k is a Lagrange multiplier. We are interested in finding critical points for $W(Q) = f_{LdG}(\lambda) + \alpha(Q\hat{z} \cdot \hat{z} - \beta)^2 + \gamma|(\mathbf{I} - \hat{z} \otimes \hat{z})Q\hat{z}|^2$, where $\lambda = (\lambda_1, \lambda_2, \lambda_3)$ is the set of eigenvalues for Q . Let us write $Q = \lambda_i v_i \otimes v_i$, where $\{v_i\}$ is a mutually orthonormal set of vectors in \mathbb{R}^3 . First, we consider the case where $\gamma = 0$. Rewriting W using the λ_i 's and v_i 's, we obtain

$$W(Q) = f_{LdG}(\lambda) + \alpha(\lambda_i(v_i \cdot \hat{z})^2 - \beta)^2.$$

Note that since $1 = |\hat{z}|^2 = \sum(v_i \cdot \hat{z})^2$, if we let $y_i = (v_i \cdot \hat{z})^2$, then $\sum y_i = 1$ and $y_i \geq 0$ for each i .

Minimizing W subject to the constraint $\sum \lambda_i = 0$ is therefore equivalent to minimizing

$$\tilde{W}(\lambda, y) = f_{LdG}(\lambda) + \alpha(\lambda_i y_i - \beta)^2$$

subject to the constraints $\sum \lambda_i = 0$, $\sum y_i = 1$, and $y_i \geq 0$ for each i . We define the auxiliary function

$$F(\lambda, y) = f_{LdG}(\lambda) + \alpha(\lambda \cdot y - \beta)^2 + h_\lambda \sum \lambda_i + h_y (\sum y_i - 1), \quad (2.135)$$

where h_λ and h_y are Lagrange multipliers. Any minimizer of \tilde{W} must be a stationary point of F .

We calculate

$$\nabla_\lambda F = \nabla_\lambda f_{LdG}(\lambda) + 2\alpha(\lambda \cdot y - \beta)y + h_\lambda(1, 1, 1) = 0 \quad (2.136)$$

and

$$\nabla_y F = 2\alpha(\lambda \cdot y - \beta)\lambda + h_y(1, 1, 1) = 0. \quad (2.137)$$

Adding the components of both sides of (2.137) and using $\sum \lambda_i = 0$, we find that $h_y = 0$. Doing the same for (2.136) gives

$$\sum (f_{LdG})_{\lambda_i}(\lambda) + 2\alpha(\lambda \cdot y - \beta) + 3h_\lambda = 0,$$

so we solve for h_λ and get

$$h_\lambda = -\frac{1}{3} \sum (f_{LdG})_{\lambda_i}(\lambda) - \frac{2}{3}\alpha(\lambda \cdot y - \beta).$$

Using this expression for h_λ in (2.136), we see that we need to solve

$$(f_{LdG})_{\lambda_i}(\lambda) + 2\alpha(\lambda \cdot y - \beta)(y_i - \frac{1}{3}) - \frac{1}{3} \sum (f_{LdG})_{\lambda_i}(\lambda) = 0 \quad (2.138)$$

and

$$2\alpha(\lambda \cdot y - \beta)\lambda_i = 0$$

subject to the constraints $\sum y_i = 1$, $y_i \geq 0$, and $\sum \lambda_i = 0$. If there exists λ and y such that $\lambda \cdot y - \beta = 0$, then the second equation is automatically satisfied and the first equation reduces to

(2.136). Hence any critical point (λ, y) of W which satisfies $\lambda \cdot y - \beta = 0$ must also be a critical point of f_{LdG} . For example, if $\bar{\lambda} = (\bar{\lambda}_1, \bar{\lambda}_2, \bar{\lambda}_3)$ is the minimizer of f_{LdG} and β is equal to $\sum \bar{y}_i \bar{\lambda}_i$ for some $0 \leq \bar{y}_i \leq 1$, then setting $y_i = \bar{y}_i$ and $\lambda = \bar{\lambda}$ yields a minimizer for W , since

$$f_{LdG}(\bar{\lambda}) \leq \min W(\lambda, y) \leq W(\bar{\lambda}, \bar{y}) = f_{LdG}(\bar{\lambda}).$$

If $\beta = \bar{\lambda}_i$, so the convex linear combination is the trivial one with the corresponding $\bar{y}_i = 1$, then we see from the definition of y_i that \hat{z} is an eigenvector for the minimizer. Conversely, if the convex linear combination is non-trivial, so that at least two of the y_i 's are non-zero, we see that it is impossible that \hat{z} is an eigenvector. Note that the minimizer is uniaxial in this case if the minimizer of f_{LdG} is uniaxial.

Suppose now that $\lambda \cdot y - \beta \neq 0$. Then $\lambda_i = 0$ for each i ; since $(f_{LdG})_\lambda(0) = 0$, (2.136) is satisfied by setting $y_i = 1/3$ for each i . Note in this case the minimizer is isotropic and so of course \hat{z} is an eigenvector. Any other stationary points of f_{LdG} , and thus extrema, must occur on the boundary of the admissible set in y , which happens when any one of the y_i is 0 or 1. By symmetry, we only analyze the cases when y_3 is 0 or 1.

Suppose that $y_3 = 0$. We need to find critical points for

$$F(y_1, y_2, \lambda) = f_{LdG}(\lambda) + \alpha(y_1\lambda_1 + y_2\lambda_2 - \beta)^2 + h_y(y_1 + y_2 - 1) + h_\lambda \sum \lambda_i,$$

subject to the constraints $y_1 + y_2 = 1$, $\sum \lambda_i = 0$. Hence, we have

$$\left\{ \begin{array}{l} (f_{LdG})_{\lambda_1} + 2\alpha(y_1\lambda_1 + y_2\lambda_2 - \beta)y_1 + h_\lambda = 0, \\ (f_{LdG})_{\lambda_2} + 2\alpha(y_1\lambda_1 + y_2\lambda_2 - \beta)y_2 + h_\lambda = 0, \\ (f_{LdG})_{\lambda_3} + h_\lambda = 0, \\ 2\alpha(y_1\lambda_1 + y_2\lambda_2 - \beta)\lambda_1 + h_y = 0, \\ 2\alpha(y_1\lambda_1 + y_2\lambda_2 - \beta)\lambda_2 + h_y = 0, \\ y_1 + y_2 = 1, \quad \sum \lambda_i = 0. \end{array} \right.$$

If $\beta = y_1\lambda_1 + y_2\lambda_2$ for a solution, we argue as before and see that such a critical point must be a critical point of f_{LdG} . If not, the fourth and fifth equations show that $\lambda_1 = \lambda_2 := \bar{\lambda}$ and the first and second equations along with the symmetry of f_{LdG} with respect to permutations of the λ_i 's show that $y_1 = y_2 = 1/2$. It follows that $\bar{\lambda}$ must solve

$$(f_{LdG})_{\lambda_1}(\bar{\lambda}, \bar{\lambda}, -2\bar{\lambda}) - (f_{LdG})_{\lambda_3}(\bar{\lambda}, \bar{\lambda}, -2\bar{\lambda}) + \alpha(\lambda - \beta) = 0.$$

Note that the solution is uniaxial. Also note that y_3 must be 0, which implies that v_3 , the eigenvector associated to λ_3 , must be perpendicular to \hat{z} . Hence \hat{z} is in the eigenplane spanned by v_1 and v_2 and is thus an eigenvector.

Now suppose that $y_2 = y_3 = 0$, so that $y_1 = 1$. We are looking for critical points of

$$f_{LdG}(\lambda) + \alpha(\lambda_1 - \beta)^2 + h_\lambda \sum \lambda_i$$

subject to the constraint $\sum \lambda_i = 0$. Suppose that $\lambda_1 \neq \beta$; if it was, we argue as before. We need to solve

$$\left\{ \begin{array}{l} (f_{LdG})_{\lambda_1} + 2\alpha(\lambda_1 - \beta) + h_\lambda = 0, \\ (f_{LdG})_{\lambda_2} + h_\lambda = 0, \\ (f_{LdG})_{\lambda_3} + h_\lambda = 0, \\ \sum \lambda_i = 0. \end{array} \right.$$

It follows that λ_1, λ_2 must solve:

$$\left\{ \begin{array}{l} (f_{LdG})_{\lambda_1}(\lambda_1, \lambda_2, -\lambda_1 - \lambda_2) - (f_{LdG})_{\lambda_3}(\lambda_1, \lambda_2, -\lambda_1 - \lambda_2) + 2\alpha(\lambda_1 - \beta) = 0, \\ (f_{LdG})_{\lambda_2}(\lambda_1, \lambda_2, -\lambda_1 - \lambda_2) = (f_{LdG})_{\lambda_3}(\lambda_1, \lambda_2, -\lambda_1 - \lambda_2). \end{array} \right.$$

Clearly, the second equation is always satisfied when the second and third eigenvalue are the same, so that $\lambda_1 = -2\lambda_2$, and the corresponding critical point is uniaxial. It is also possible that the second equation holds for other, biaxial, choices of λ 's as numerics seems to indicate. Regardless, \hat{z} is an eigenvector of the minimizing Q in this case, since $y_3 = 1$.

We have shown now that \hat{z} is an eigenvector for any minimizer of W when γ is 0 and β is not a convex linear combination of the eigenvalues λ_i of a stationary point of f_{LdG} . This also remains true under the same assumption on β if γ is positive, since any minimizer of W when γ is 0 which has \hat{z} as an eigenvector must also minimize W for any positive γ . In the case where β is such a linear combination, we are able to construct examples in which \hat{z} is and is not an eigenvector for the corresponding minimizers of W with $\gamma = 0$. Such examples should also be possible with positive γ , depending perhaps on the relationship between γ and α . \square

Chapter 3

A Model Problem for Nematic-Isotropic Transitions with Highly Disparate Elastic Constants

3.1 First Try: A Model Whose Elastic Disparity Is Weak

In this section, we begin our examination of the effect of disparity in elastic energy. Throughout this section, we will consider a continuous potential $W : \mathbb{R}^2 \rightarrow [0, \infty)$ which vanishes on $\mathbb{S}^1 \cup \{0\}$. We assume that for some continuous function $V : \mathbb{R} \rightarrow [0, \infty)$, one has $W(u) = V(|u|)$ with then $V(0) = V(1) = 0$ and $V > 0$ elsewhere. The prototype for what we have in mind is the Chern-Simons-Higgs potential

$$W_{CSH}(u) := |u|^2 (|u|^2 - 1)^2. \quad (3.1)$$

Then for a sequence of positive numbers $L_\varepsilon \downarrow 0$, we consider the sequence of functionals

$$G_\varepsilon(u) := \begin{cases} \frac{1}{2} \int_\Omega \left(\frac{1}{\varepsilon} W(u) + \varepsilon |\nabla u|^2 + L_\varepsilon (\operatorname{div} u)^2 \right) dx & \text{if } u \in H^1(\Omega; \mathbb{R}^2), \\ +\infty & \text{otherwise.} \end{cases} \quad (3.2)$$

Though the Γ -convergence result below holds for any sequence $\{L_\varepsilon\}$ approaching zero, we are especially interested in the situation where

$$\frac{L_\varepsilon}{\varepsilon} \rightarrow \infty \text{ as } \varepsilon \rightarrow 0,$$

so that the divergence term in the elastic energy is heavily emphasized. Our goal is to explore whether or not this disparity can produce a Γ -limit whose minimizers possess the types of phase

boundary singularities reminiscent of isotropic-nematic interfaces as described in the introduction. What we shall find is that this level of elastic disparity is in fact *not* sufficiently strong to achieve this goal.

To this end, we define our candidate for the Γ -limit:

$$G_0(u) := \begin{cases} c_0 \text{Per}_\Omega(\{|u| = 0\}) & \text{if } |u| \in BV(\Omega; \{0, 1\}), \\ +\infty & \text{otherwise.} \end{cases}$$

Here,

$$c_0 := \int_0^1 \sqrt{V(s)} ds. \quad (3.3)$$

The reader may well recognize this Γ -limit as precisely the well-known limit of the Modica-Mortola energies, an indication that to leading order in the energy, the divergence term has no effect on the asymptotic behavior of minimizers.

Our main result for this section is:

Theorem 3.1.1. *The sequence $\{G_\varepsilon\}$ Γ -converges to G_0 in the topology induced by the L^1 norm of the modulus $|\cdot|$. That is,*

(i) *for any $u \in L^1(\Omega; \mathbb{R}^2)$ and for any sequence $\{u_\varepsilon\}$ in $L^1(\Omega; \mathbb{R}^2)$,*

$$|u_\varepsilon| \rightarrow |u| \text{ in } L^1(\Omega) \text{ implies } \liminf_{\varepsilon \rightarrow \infty} G_\varepsilon(u_\varepsilon) \geq G_0(u), \quad (3.4)$$

and

(ii) *for each $u \in L^1(\Omega, \mathbb{R}^2)$ there exists a recovery sequence $\{w_\varepsilon\}$ in $L^1(\Omega, \mathbb{R}^2)$ satisfying*

$$|w_\varepsilon| \rightarrow |u| \text{ in } L^1(\Omega; \mathbb{R}^2) \quad \text{and} \quad \limsup_{\varepsilon \rightarrow \infty} G_\varepsilon(w_\varepsilon) \leq G_0(u). \quad (3.5)$$

In fact, we can construct the sequence $\{w_\varepsilon\}$ so that $w_\varepsilon \rightarrow u$ in L^1 .

Remark 3.1.2. *Regarding the asymptotic behavior of global minimizers, this result does not seem to address the possibility of a phase transition since there is no ‘incentive’ for a minimizer of G_ε*

to take on both 0 and \mathbb{S}^1 values. To encourage a phase transition for a minimizer, one could, for example, impose a mass constraint such as

$$\int_{\Omega} |u_{\varepsilon}|^2 dx = m \quad \text{or} \quad \int_{\Omega} |u_{\varepsilon}| dx = m \quad \text{where } m \in (0, |\Omega|) \quad \text{with } |\Omega| = \text{Lebesgue measure of } \Omega.$$

Alternatively, one could impose a Dirichlet condition on $\partial\Omega$ such as $u_{\varepsilon} = g_{\varepsilon}$ where g_{ε} is \mathbb{S}^1 -valued on one portion of the boundary and then transitions smoothly down to 0 on the rest of the boundary. Either of these alterations in the problem can be easily accommodated using what are by now standard techniques in Γ -convergence, see e.g. [76, 86, 99]. However, in order to present the main ideas without excessive technicalities, we formulate and prove a Γ -convergence theorem without either of these conditions, and merely remark that they could be incorporated if desired.

Though as indicated below (3.5), we can in fact establish Γ -convergence in the stronger topology $L^1(\Omega)$, it is not possible to obtain L^1 -compactness for an arbitrary energy bounded sequence due to the degeneracy of the well \mathbb{S}^1 . However, L^1 -compactness of $\{|u_{\varepsilon}|\}$ follows by a standard argument, cf. e.g. [99, Proposition 3].

Proposition 3.1.3. *Let $\{u_{\varepsilon}\}$ be a sequence of maps from Ω to \mathbb{R}^2 and assume that the sequence of energies $G_{\varepsilon}(u_{\varepsilon})$ is uniformly bounded. Then there exists a subsequence $\{u_{\varepsilon_j}\}$ and $u \in L^1(\Omega; \mathbb{S}^1 \cup \{0\})$ such that $|u_{\varepsilon_j}| \rightarrow |u|$ in $L^1(\Omega)$.*

As observed in [84], this rather weak form of compactness is nonetheless sufficient to imply the existence of local minimizers of G_{ε} given a local minimizer of G_0 which is isolated in this weaker topology, by modifying an argument of [61]. For example, on a “dumbbell”-type domain, there always exist local minimizers of G_{ε} for ε sufficiently small, cf. [84, Theorems 4.2, 5.1].

Proof of the lower semi-continuity condition (3.4). Lower semi-continuity follows as in the Modica-Mortola setting since one simply ignores the divergence term. Since the argument is short, however, we present it here. The cases in which $\liminf_{\varepsilon \rightarrow 0} G_{\varepsilon}(u_{\varepsilon}) = \infty$ or $W(u) \neq 0$ on a set of positive measure are trivial. We therefore assume that $\liminf_{\varepsilon \rightarrow 0} G_{\varepsilon}(u_{\varepsilon}) = C < \infty$, and suppose that $|u_{\varepsilon}| \rightarrow |u|$

in $L^1(\Omega)$. Suppose also for now that $|u_\varepsilon| \leq 1$, an assertion we will justify later by means of a truncation procedure. In the argument below, we will make use of the function $\Phi(t) := \int_0^t \sqrt{V(s)} ds$.

As $L_\varepsilon \geq 0$, we have

$$\begin{aligned} G_\varepsilon(u_\varepsilon) &= \frac{1}{2} \int_\Omega \left(\frac{1}{\varepsilon} W(u_\varepsilon) + \varepsilon |\nabla u_\varepsilon|^2 + L_\varepsilon (\operatorname{div} u_\varepsilon)^2 \right) dx \geq \int_\Omega \sqrt{V(|u_\varepsilon|)} |\nabla |u_\varepsilon|| dx \\ &\geq \int_\Omega |\nabla \Phi(|u_\varepsilon|)| dx. \end{aligned}$$

By the assumption that $\liminf G_\varepsilon(u_\varepsilon) = C < \infty$, we obtain a uniform bound on $\{\Phi(|u_\varepsilon|)\}_{\varepsilon>0}$ in $BV(\Omega)$, implying the existence of a subsequence converging in L^1 to $\Phi(|u|)$. Therefore, by lower semi-continuity in BV ,

$$\begin{aligned} \liminf_{\varepsilon \rightarrow 0} G_\varepsilon(u_\varepsilon) &\geq \liminf_{\varepsilon \rightarrow 0} \int_\Omega |\nabla \Phi(|u_\varepsilon|)| dx \\ &\geq \int_\Omega |\nabla \Phi(|u|)| dx \\ &= c_0 \operatorname{Per}_\Omega(\{|u|=1\}). \end{aligned}$$

This then completes the proof of (3.4) under the assumption that $|u_\varepsilon| \leq 1$.

If it does not hold that $|u_\varepsilon| \leq 1$ then we define

$$u_\varepsilon^*(x) := \begin{cases} u_\varepsilon(x) & \text{if } |u_\varepsilon(x)| \leq 1, \\ \frac{u_\varepsilon(x)}{|u_\varepsilon(x)|} & \text{if } |u_\varepsilon(x)| > 1. \end{cases}$$

We compute that

$$G_\varepsilon(u_\varepsilon) \geq \frac{1}{2} \int_\Omega \left(\frac{1}{\varepsilon} W(u_\varepsilon) + \varepsilon |\nabla u_\varepsilon|^2 \right) dx \geq \frac{1}{2} \int_\Omega \left(\frac{1}{\varepsilon} W(u_\varepsilon^*) + \varepsilon |\nabla u_\varepsilon^*|^2 \right) dx. \quad (3.6)$$

Finally, we have that

$$\| |u_\varepsilon^*| - |u| \|_{L^1(\Omega)} \leq \| |u_\varepsilon| - |u| \|_{L^1(\Omega)} \rightarrow 0,$$

so that we can combine the previous arguments with (3.6) to obtain lower semi-continuity for the original sequence $\{u_\varepsilon\}$. \square

Proof of the recovery sequence condition (3.5). Suppose we are given $u : \Omega \rightarrow \mathbb{S}^1 \cup \{0\}$ with $|u| \in BV(\Omega; \{0, 1\})$. We will construct a sequence $w_\varepsilon \subset H^1(\Omega; \mathbb{R}^2)$ with $w_\varepsilon \rightarrow u$ in $L^1(\Omega; \mathbb{R}^2)$ such that $\limsup_{\varepsilon \rightarrow 0} G_\varepsilon(w_\varepsilon) \leq G_0(u)$. We first briefly discuss the main idea, in order to motivate the construction that follows. Suppose that u is smooth on the set, say N , where it is \mathbb{S}^1 -valued, except for finitely many singular points a_i , and suppose u carries degree d_i around each “vortex” a_i . Suppose also that ∂N is smooth. We would like to define w_ε using a boundary layer near ∂N which bridges the values of $u|_N$ near ∂N to 0 outside. In order to recover the correct Γ -limit with constant $2c_0$, we must define w_ε on a neighborhoods \mathcal{N}_ε of N so that

$$\frac{1}{2} \int_{\mathcal{N}_\varepsilon} \left(\frac{1}{\varepsilon} W(w_\varepsilon) + \varepsilon |\nabla w_\varepsilon|^2 + L_\varepsilon (\operatorname{div} w_\varepsilon)^2 \right) dx \rightarrow c_0 \operatorname{Per}_\Omega(\{|u| = 1\}).$$

As this is the least upper bound we could achieve even if $L_\varepsilon = 0$, we must therefore construct w_ε on \mathcal{N}_ε so that

$$\int_{\mathcal{N}_\varepsilon} L_\varepsilon (\operatorname{div} w_\varepsilon)^2 dx \rightarrow 0$$

and so that the gradient squared and potential terms give the correct asymptotic limit. Since there is no assumption on how fast the sequence $\{L_\varepsilon\}$ approaches zero, a natural construction to try is to define w_ε on \mathcal{N}_ε so that it is divergence-free there. This can be done by setting

$$w_\varepsilon = f_\varepsilon(d(x))(\nabla^\perp d)(x), \tag{3.7}$$

where $d(x)$ is the distance function to ∂N and f_ε is a suitably defined scalar function bridging the values 0 and 1. Then

$$\operatorname{div} w_\varepsilon = f'_\varepsilon(d)(\nabla d) \cdot \nabla^\perp d + f_\varepsilon(d) \operatorname{div}(\nabla^\perp d) = 0. \tag{3.8}$$

It is easy to check that if w_ε is a smooth, non-zero vector field tangent to level sets of d , as above, then its degree restricted to such a level set is 1. If, however, $\sum_i d_i \neq 1$, then degree considerations imply that it is impossible to define smooth w_ε which are non-zero and tangent to ∂N but equal to u in the interior of N away from the boundary. In addition, even if $\sum d_i = 1$, defining w_ε inside

N by mollifying u could yield vortices which result in unbounded energy as $\varepsilon \rightarrow 0$; see Theorem 3.3.1.

To address these issues, it is instructive to consider the case in which Ω is the ball of radius 2 centered at the origin, $N := \{|u| = 1\}$ is the unit disk with $u \equiv \vec{e}_1$ there and u vanishes on the annulus $\{1 < |x| < 2\}$. As explained above, there is no smooth field tangent to the boundary of the disk and equal to u inside the disk. However, suppose we alter the boundary of the disk by adding two small cusps. Then we can define a continuous vector field tangent to the modified boundary, except at the cusps, which has degree zero. This tangent vector field allows for the construction of a boundary layer similar to (3.7) which contributes a perimeter term differing from $G_0(u)$ by a negligible amount, and a second, \mathbb{S}^1 -valued boundary layer inside the disk which bridges the degree zero tangent field to the constant \vec{e}_1 . The energetic contribution of this second layer vanishes in the limit.

Our general construction utilizes this basic idea. Given any component of the nematic region N , we first approximate u there by a map with degree zero around any closed curve lying in that component. This allows us to avoid the creation of vortices which are energetically too expensive for the divergence term. Then, we add two cusps to the boundary components of the nematic regions; and finally, we use two boundary layers to bridge 0 to the values in the nematic regions. We should emphasize that the approximations will be close to the original function u in L^1 but of course will not be close in a stronger topology as that would violate basic properties of degree.

We now fix any $u : \Omega \rightarrow \mathbb{S}^1 \cup \{0\}$ such that $|u| \in BV(\Omega; \{0, 1\})$ and begin our construction of the recovery sequence. We first approximate u by vector fields u_n , then construct a recovery sequence for any u_n . A standard diagonal procedure will then imply the existence of a recovery sequence for u . We begin by showing that there exists an intermediate sequence of vector fields $\{v_n\} : \mathbb{R}^2 \rightarrow \mathbb{S}^1 \cup \{0\}$ such that

$$(i) \quad \{|v_n| = 1\} =: \tilde{A}_n \text{ has } C^2 \text{ boundary,}$$

- (ii) v_n is smooth restricted to \tilde{A}_n ,
- (iii) for each n , there exists a non-empty arc $I_n \subset \mathbb{S}^1$ such that $v_n(x) \notin I_n$ for all $x \in \tilde{A}_n$,
- (iv) $\mathcal{H}^1(\partial\tilde{A}_n \cap \partial\Omega) = 0$ where \mathcal{H}^1 denotes one-dimensional Hausdorff measure,
- (v) $v_n \rightarrow u$ in L^1 , and
- (vi) $\text{Per}_\Omega(\tilde{A}_n \cap \Omega) \rightarrow \text{Per}_\Omega(|u|=1)$.

It is standard that there exist \tilde{A}_n such that (i), (iv), and (vi) hold and $\chi_{\tilde{A}_n} \rightarrow \chi_{\{|u|=1\}}$ in L^1 , see e.g. [44, Theorem 1.24]. Next, we define a sequence \tilde{v}_n by

$$\tilde{v}_n = \begin{cases} u(x) & \text{if } x \in \tilde{A}_n \cap \{|u|=1\}, \\ \vec{e}_1 & \text{if } x \in \tilde{A}_n \setminus \{|u|=1\}, \\ 0 & \text{if } x \notin \tilde{A}_n. \end{cases}$$

The choice of \vec{e}_1 is arbitrary, since any unit vector would suffice. From the convergence of $\chi_{\tilde{A}_n}$ to $\chi_{\{|u|=1\}}$ and the dominated convergence theorem, it follows that, up to a subsequence, $\tilde{v}_n \rightarrow u$ in $L^1(\Omega; \mathbb{R}^2)$. The sequence $\{\tilde{v}_n\}$ satisfies properties (i) and (iv)–(vi), so it remains to argue we can modify it so that (ii) and (iii) hold as well. For each n , we define for $1 \leq j \leq n$

$$C_j^n := \{x \in \Omega : \tilde{v}_n(x) \in (\cos([2\pi(j-1)/n, 2\pi j/n]), \sin([2\pi(j-1)/n, 2\pi j/n)))\},$$

and observe that for some j_n , $|C_{j_n}^n| \leq |\Omega|/n$, since $\sum_j |C_j^n| \leq |\Omega|$. Then for $x \in C_{j_n}^n$, we redefine $\tilde{v}_n(x)$ to be identically $(\cos(2\pi(j_n-1)/n), \sin(2\pi(j_n-1)/n))$, so that the \tilde{v}_n now avoids an arc $I_n \subset \mathbb{S}^1$ of length $2\pi/n$. Now we can mollify \tilde{v}_n to obtain smooth v_n which also avoid I_n and satisfy (i)–(vi). Indeed, this can be done by choosing an interval $[a_n, b_n]$ in which to define the values of the phase of v_n and mollifying the phase function itself. We also point out that inside \tilde{A}_n , the degree of v_n around any simple, closed curve is zero, since v_n cannot take values in I_n .

Next, for each n , we add small cusps to the sets \tilde{A}_n and modify v_n to obtain u_n . For each connected component of $\partial\tilde{A}_n$, we add two cusps pointing into the isotropic region, which change

the perimeter of \tilde{A}_n by at most $1/n$. We denote the resulting modification of \tilde{A}_n by A_n , and smoothly alter the values of the function v_n , yielding u_n . This procedure can be carried out in such a fashion so that properties (ii)–(vi) above still hold for the sequence $\{u_n\}$, and property (i), the smoothness of ∂A_n , holds except at the cusps. This completes the construction of the sequence $\{u_n\}$.

For each n , we now construct a recovery sequence $\{u_\varepsilon\}$, suppressing the dependence of $\{u_\varepsilon\}$ on n for ease of notation. Away from ∂A_n , u_ε will be identically equal to u_n . Near ∂A_n , we will use a boundary layer of the form $f_\varepsilon \vec{t}$, where \vec{t} is a unit vector field tangent to level sets of the signed distance function d to A_n and where f_ε solves a certain ODE. Away from the cusps, the level sets of the d are smooth, which will be enough for our purposes. For each connected component of ∂A_n , we define \vec{t} there by choosing a unit vector field tangent to that component and continuous on all of that component; see Fig. 3.1 below.

The fact that each component contains two cusps implies that for the field \vec{t} to be continuous, it must change the sense of tangency at every cusp. Thus on ∂A_n , \vec{t} is always equal to $\pm \nabla^\perp d$. From these observations it follows that the degree of \vec{t} around any connected component of ∂A_n is zero. We then extend \vec{t} to a continuous, unit vector field tangent to level sets of d for x such that $d(x)$ is small and positive and the nearest point projection x onto ∂A_n is not contained in any one of a union of rectangles near each cusp; see Fig. 3.2 below. To bridge the divergence free field $f_\varepsilon \vec{t}$ to the values of u_n inside A_n , there is a second boundary layer, which is defined via an \mathbb{S}^1 -valued homotopy between \vec{t} and the values of u_n inside A_n . This is only possible because \vec{t} has degree zero around ∂A_n , as does u_n around any simple, closed curve in A_n . The energy contribution from this layer in the limit will be zero, since $W(u_\varepsilon) = 0$ there.

We now specify u_ε in the first boundary layer, which contributes the perimeter term in the asymptotic limit. In the interior of A_n and in A_n^c at sufficient distances away from ∂A_n to be specified shortly, we set u_ε equal to u_n .

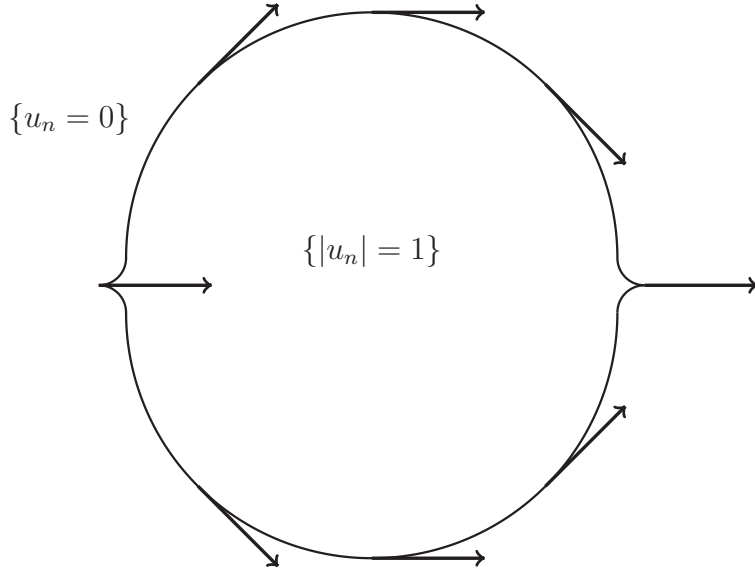


Figure 3.1: The Lipschitz vector field \vec{t} is tangent to this connected component of ∂A_n and has degree zero around it.

First, for some fixed $\delta > 0$, we consider the following ODE, similar to [14, Equation 3.2]:

$$\left(\frac{\partial}{\partial s} f_\varepsilon(s) \right)^2 = \frac{\delta + V(f_\varepsilon(s))}{\varepsilon^2 (f_\varepsilon(s))^2}.$$

As argued in [14], there exists a constant C , depending on δ , such that for every ε , there exist positive numbers C_ε and strictly decreasing solutions $f_\varepsilon : [0, C_\varepsilon] \rightarrow [0, 1]$ of this ODE such that

$$C_\varepsilon \leq C\varepsilon \tag{3.9}$$

and

$$f_\varepsilon(0) = 1 \text{ and } f_\varepsilon(C_\varepsilon) = 0.$$

Each f_ε in fact depends on δ , but we suppress this dependence. Next, we excise a small rectangle at each cusp. Let

$$m_\varepsilon := \max\{\varepsilon, L_\varepsilon\}. \tag{3.10}$$

For each cusp c_i , consider a rectangle R_i^ε with one side of length $2C_\varepsilon$, centered at c_i , and perpendicular to the one-sided tangents at c_i , such that R_i^ε protrudes $m_\varepsilon^{2/3}$ into the isotropic set $\{u = 0\}$

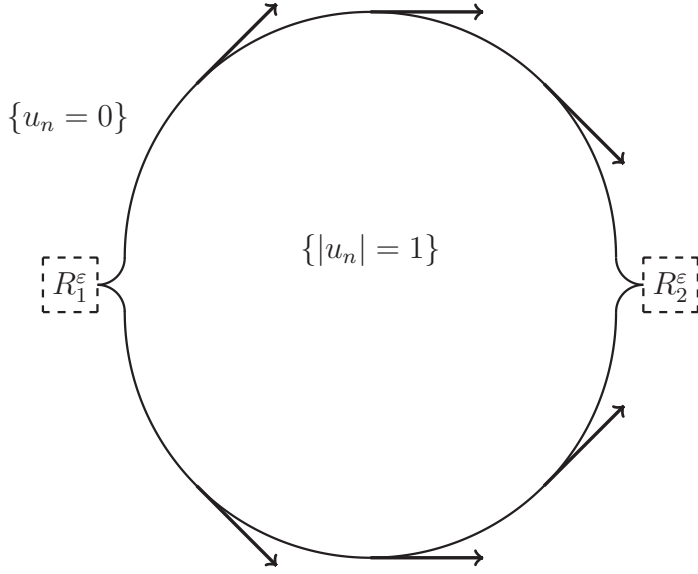


Figure 3.2: Each rectangle R_i^ε has length $m_\varepsilon^{2/3}$ and height $2C_\varepsilon$ and is perpendicular to the one-sided tangent vectors at the cusp c_i . For x near the interface and not in R_i^ε , we can extend the tangent field \vec{t} to be unit valued and tangent to level sets of the distance function to the interface.

in the other direction; see Fig. 3.2 below. We denote by \mathcal{R}_ε the union of all R_i^ε 's and then we define

$$u_\varepsilon(x) := \begin{cases} u_n(x) & \text{if } C_\varepsilon \leq d(x) \text{ or } d(x) \leq -m_\varepsilon^{2/3}, \\ f_\varepsilon(d(x))\vec{t}(x) & \text{if } 0 < d(x) < C_\varepsilon \text{ and } x \notin \mathcal{R}_\varepsilon. \end{cases}$$

In the definition above and in the remainder of the argument, we take d to denote the signed distance function to ∂A_n which is negative inside A_n . We will deal with u_ε on $\{x : -m_\varepsilon^{2/3} < d(x) \leq 0\}$ and on \mathcal{R}_ε at the end. It can be shown, by calculations similar to those preceding [84, Equation 3.33] that

$$\limsup_{\varepsilon \rightarrow 0} \frac{1}{2} \int_{\{0 \leq d(x) \leq C_\varepsilon\}} \left(\frac{1}{\varepsilon} W(u_\varepsilon) + \varepsilon |\nabla u_\varepsilon|^2 + L_\varepsilon(\operatorname{div} u_\varepsilon)^2 \right) dx \leq c_0 \operatorname{Per}_\Omega(A_n) + O(\sqrt{\delta}), \quad (3.11)$$

observing in the process the crucial fact that the divergence of u_ε on this set is zero, cf. (3.8).

Furthermore,

$$\begin{aligned} \frac{1}{2} \int_{\{C_\varepsilon \leq d(x) \text{ or } d(x) \leq -m_\varepsilon^{2/3}\}} & \left(\frac{1}{\varepsilon} W(u_\varepsilon) + \varepsilon |\nabla u_\varepsilon|^2 + L_\varepsilon (\operatorname{div} u_\varepsilon)^2 \right) dx \\ &= \frac{1}{2} \int_{\{C_\varepsilon \leq d(x) \text{ or } d(x) \leq -m_\varepsilon^{2/3}\}} \left(\frac{1}{\varepsilon} W(u_n) + \varepsilon |\nabla u_n|^2 + L_\varepsilon (\operatorname{div} u_n)^2 \right) dx \\ &\xrightarrow{\varepsilon \rightarrow 0} 0, \end{aligned}$$

since $W(u_n) = 0$ and $|\nabla u_n|^2$ and $(\operatorname{div} u_n)^2$ are bounded functions independent of ε away from ∂A_n .

It remains to define u_ε on the second boundary layer, $\{x : -m_\varepsilon^{2/3} < d(x) \leq 0\}$, and on \mathcal{R}_ε .

Let us first consider the second boundary layer. Because of the fact that u_ε defined thus far has degree zero around ∂A_n and $\{d(x) = -m_\varepsilon^{2/3}\}$, there exist Lipschitz phases $\psi_1 : \partial A_n \rightarrow \mathbb{R}$, $\psi_2 : \{d(x) = -m_\varepsilon^{2/3}\} \rightarrow \mathbb{R}$ such that $u_\varepsilon = (\cos(\psi_1), \sin(\psi_1))$ on ∂A_n and $u_\varepsilon = (\cos(\psi_2), \sin(\psi_2))$ on $\{d(x) = -m_\varepsilon^{2/3}\}$. Then we can interpolate on the intermediate region using convex combinations of ψ_1 and ψ_2 so that $|\nabla u_\varepsilon|^2$ and $(\operatorname{div} u_\varepsilon)^2$ are both $O(m_\varepsilon^{-4/3})$. Since u_ε is a unit vector field here, $W(u_\varepsilon)$ is 0. Hence we can calculate

$$\begin{aligned} \frac{1}{2} \int_{\{x : -m_\varepsilon^{2/3} < d(x) \leq 0\}} & \left(\frac{1}{\varepsilon} W(u_\varepsilon) + \varepsilon |\nabla u_\varepsilon|^2 + L_\varepsilon (\operatorname{div} u_\varepsilon)^2 \right) dx \\ &\lesssim |\{-m_\varepsilon^{2/3} < d(x) \leq 0\}|(\varepsilon m_\varepsilon^{-4/3} + L_\varepsilon m_\varepsilon^{-4/3}) \\ &\leq O(m_\varepsilon^{1/3}). \end{aligned} \tag{3.12}$$

So u_ε on the second boundary layer contributes nothing to the asymptotic limit.

Finally, we treat u_ε on the union \mathcal{R}_ε of rectangles R_i^ε . It suffices to demonstrate the construction on a single R_i^ε such that the cusp c_i contained on one of its sides is the origin and the isotropic phase is to the right of the x_2 -axis. Up to a translation, this is the situation depicted in Fig. 3.2 with R_2^ε . In these coordinates we may describe R_i^ε as the rectangle $[0, m_\varepsilon^{2/3}] \times [-C_\varepsilon, C_\varepsilon]$. We set

$$u_\varepsilon(x_1, x_2) = f_\varepsilon(|x_2|)(1 - m_\varepsilon^{-2/3} x_1) \vec{t}(0)$$

on R_i^ε , which ensures compatibility with u_ε as previously defined. We remark that $\vec{t}(0)$ is either plus or minus \vec{e}_1 . Then on R_i^ε , $(\operatorname{div} u_\varepsilon)^2 \sim O(m_\varepsilon^{-4/3})$, and $|\nabla u_\varepsilon|^2 \sim O(\varepsilon^{-2})$. Since the area of R_i^ε is $2C_\varepsilon m_\varepsilon^{2/3} \leq 2C\varepsilon m_\varepsilon^{2/3}$ by (3.9) and (3.10), we have for small ε

$$\frac{1}{2} \int_{R_i^\varepsilon} \left(\frac{1}{\varepsilon} W(u_\varepsilon) + \varepsilon |\nabla u_\varepsilon|^2 + L_\varepsilon (\operatorname{div} u_\varepsilon)^2 \right) dx \leq O(m_\varepsilon^{2/3}). \quad (3.13)$$

Combining (3.11)–(3.13), we obtain

$$G_\varepsilon(u_\varepsilon) \rightarrow G_0(u_n) + O\sqrt{\delta}.$$

In addition, the u_ε converge in L^1 to u_n by virtue of the dominated convergence theorem, since they are bounded and the set where they differ from u_n has measure going to zero. Therefore, recalling that $\{u_\varepsilon\}$ depends on δ as well, we diagonalize over ε and δ to obtain a recovery sequence for u_n . Since u_n converge in L^1 to u and $G_0(u_n) \rightarrow G_0(u)$, a second diagonalization argument over n and ε yields a recovery sequence for u . \square

3.2 A Model with Large Elastic Disparity and Singular Phase Boundaries

In the previous section we saw that disparity in the elastic energy density of the form

$$\varepsilon |\nabla u|^2 + L_\varepsilon (\operatorname{div} u)^2 \quad \text{with } \varepsilon \ll L_\varepsilon \rightarrow 0$$

is insufficient to induce a singular phase boundary between the isotropic state 0 and an \mathbb{S}^1 -valued nematic state in minimizers of the Γ -limit. We now introduce a model with still larger disparity, and it is this model we will work with for the remainder of the chapter.

To this end, for a positive constant L independent of ε we define

$$E_\varepsilon(u) := \frac{1}{2} \int_{\Omega} \left(\frac{1}{\varepsilon} W(u) + \varepsilon |\nabla u|^2 + L (\operatorname{div} u)^2 \right) dx, \quad (3.14)$$

where $W(u) = V(|u|)$ for some continuous $V : [0, \infty) \rightarrow [0, \infty)$ that vanishes only at 0 and 1. As always, our prototype is the potential given by $W_{CSH}(u) = |u|^2 (|u|^2 - 1)^2$, but in what follows

we can allow for more general potentials vanishing at 0 and 1, provided that for some constant $c > 0$ one has the condition

$$H(t) := \min(t^2, |1 - t^2|) \leq c\sqrt{V(t)} \quad (3.15)$$

for any $t \in [0, \infty)$.

In light of the divergence term in E_ε , it is clear that energy-bounded sequences $\{u_\varepsilon\}$ will have divergences that converge weakly in $L^2(\Omega)$. As we will discuss in Section 3.3, under the assumption (3.15), an adaptation of the compactness techniques of [32] allows us to also establish that a subsequence of $\{u_\varepsilon\}$ will converge strongly in $L^2(\Omega)$ to a limit taking values in $\mathbb{S}^1 \cup \{0\}$. We will write $u_\varepsilon \xrightarrow{\Delta} u$ when both $\operatorname{div} u_\varepsilon \rightharpoonup \operatorname{div} u$ weakly in $L^2(\Omega)$ and $u_\varepsilon \rightarrow u$ strongly in $L^2(\Omega; \mathbb{R}^2)$. See Theorem 3.2.4.

These compactness results naturally lead us to consider the Hilbert space $H_{\operatorname{div}}(\Omega; \mathbb{R}^2)$ of L^2 vector fields having L^2 divergence, and more specifically $H_{\operatorname{div}}(\Omega; \mathbb{S}^1 \cup \{0\})$, in light of the assumed zero set of the potential W .

A vector field $u \in H_{\operatorname{div}}(\Omega; \mathbb{S}^1 \cup \{0\})$ that additionally lies in the space $BV(\Omega; \mathbb{S}^1 \cup \{0\})$ is known to have a countably 1-rectifiable jump set J_u off of which u is approximately continuous. In our pursuit of a possible candidate for the limit of the sequence $\{E_\varepsilon\}$ we will focus on functions lying in the intersection of these two spaces.

Mappings in BV have well-defined traces, say u_+ and u_- on either side of J_u and an easy application of the Divergence Theorem reveals that when H_{div} vector fields have jump discontinuities across J_u then necessarily the normal component is continuous, i.e.

$$u_+ \cdot \nu = u_- \cdot \nu \quad \mathcal{H}^1 \text{ a.e. on } J_u \quad (3.16)$$

where ν is the (approximate) normal to J_u .

This brings us to a crucial distinction when attempting to identify a limiting energy for the sequence $\{E_\varepsilon\}$ – a mapping $u \in (H_{\operatorname{div}} \cap BV)(\Omega; \mathbb{S}^1 \cup \{0\})$ may undergo a jump between two \mathbb{S}^1 -valued

states, in which case (3.16) is supplemented by the additional requirement that

$$u_+ \cdot \tau = -(u_- \cdot \tau) \quad \text{along } J_u, \quad (3.17)$$

where τ is the approximate tangent to J_u . We will refer to any component of J_u bridging two \mathbb{S}^1 -valued states as a *wall*. On the other hand, u may jump between an \mathbb{S}^1 -valued state, say u_+ , and $u_- = 0$, in which case (3.16) implies that u_+ must coincide with $\pm\tau$. We will refer to any such component of J_u as an *interface*. It is this tangency requirement along an interface that can induce singularities in the isotropic-nematic phase boundary.

3.2.1 A Conjecture for the Γ -Limit of E_ε

Our goal in this section is to make the case for a proposed Γ -limit of the sequence $\{E_\varepsilon\}$ defined in (3.14). While we do not at present have matching upper and lower asymptotic bounds for this sequence, we do have a construction leading to an asymptotic upper bound which we strongly suspect is sharp. We will begin with a description of this construction and then discuss various strategies for lower bounds, why the analogue of what works for the Ginzburg-Landau potential, cf. [45], apparently fails here and what the evidence is to support our conjecture on the sharpness of the upper bound.

We should say at the outset that our pursuit of the Γ -limit $E_0(u)$ begins with the assumption that $u \in (BV \cap H_{\text{div}})(\Omega; \mathbb{S}^1 \cup \{0\})$. While this is not the natural space from the standpoint of compactness, the identification of the correct limiting space is non-trivial and we do not attempt to address it here. We refer the reader to [7, 29, 64] for more discussion of this issue. We make the BV assumption here in order to speak sensibly about the 1-rectifiability of the jump set J_u , though for that part of J_u corresponding to interfaces, i.e. to $\partial\{|u| = 1\}$, as we will note below, this rectifiability comes easily from the fact that limits u of energy-bounded sequences satisfy $|u| \in BV(\Omega)$.

As noted above, for such a vector-valued function u , the jump set naturally splits into two types:

walls and interfaces, though these two types of singular curves may well meet in junctions, see e.g. Theorem 3.2.12 and Fig. 3.3. An upper bound construction then rests on efficiently smoothing out these jump discontinuities, and in both cases, we rely on a one-dimensional type of resolution described formally below. The rigorous execution of these ideas follows the approach of [26] as adapted in [45].

To resolve an interface separating an isotropic region where $u = 0$ from a nematic region where $u \in \mathbb{S}^1$ we invoke a by-now standard Modica-Mortola type of heteroclinic connection in the *modulus*. More precisely, after mollifying the interface to smoothen it if necessary, we mollify u in the nematic region and make a boundary layer construction, say $\{w_\varepsilon\}$, of the form

$$w_\varepsilon(x) = h\left(\frac{\text{dist}(x, J_u)}{\varepsilon}\right) u(x) \quad (3.18)$$

where $\text{dist}(x, J_u)$ denotes the signed distance function to J_u and where $h : \mathbb{R} \rightarrow \mathbb{R}$ minimizes the 1D energy

$$\int_{-\infty}^{\infty} V(f) + |f'|^2 dt \quad \text{taken over } f \in H^1(\mathbb{R}) \text{ such that } f(-\infty) = 0, f(\infty) = 1. \quad (3.19)$$

This leads to the same ‘interfacial cost’ encountered in Section 2, namely

$$c_0 = \int_0^1 \sqrt{V(s)} ds,$$

multiplying the perimeter of the interface. Since

$$\text{div } w_\varepsilon(x) = h\left(\frac{\text{dist}(x, J_u)}{\varepsilon}\right) \text{div } u(x) + \frac{1}{\varepsilon} h'\left(\frac{\text{dist}(x, J_u)}{\varepsilon}\right) \nabla \text{dist}(x, J_u) \cdot u(x),$$

the term $L \int (\text{div } w_\varepsilon)^2$ in $E_\varepsilon(w_\varepsilon)$ will contribute nothing to such a boundary layer construction in the limit $\varepsilon \rightarrow 0$ since the first term is controlled by the fact that $u \in H_{\text{div}}$ and the second term is negligible due to the required tangency of u and J_u along an interface. We note that the ansatz (3.18) would fail for the sequence of functionals F_ε analyzed in Section 3.1 since there u is not required to lie in H_{div} and so the term $\nabla \text{dist}(x, J_u) \cdot u(x)$ will in general not vanish.

With appropriate care taken to treat issues of regularity, this can be made rigorous. What is more, this construction, based only on appropriate interpolation of the modulus between 0 and 1, gives a sharp upper bound on the interfacial energy, in light of the inequality

$$E_\varepsilon(u) \geq \left(\frac{1}{2} \int_{\Omega} \frac{1}{\varepsilon} V(|u|) + \varepsilon |\nabla |u||^2 \right) dx \quad \text{for any } u \in H^1(\Omega; \mathbb{R}^2). \quad (3.20)$$

Since this is the classical scalar Modica-Mortola functional in terms of the function $|u|$, when applied in a neighborhood of the interface it yields the matching lower bound of $c_0 \operatorname{Per}_\Omega(\{|u|=1\})$.

Our boundary layer construction in a neighborhood of a wall separating two \mathbb{S}^1 -valued states, say u_+ and u_- , is one-dimensional in a different sense. In light of the continuity of the normal component of u across a wall, cf. (3.16), a natural choice is to fix the value of $u \cdot \nu$ across the boundary layer and use a heteroclinic connection to bridge the value of $u_- \cdot \tau$ to $u_+ \cdot \tau$, that is, to bridge $-\sqrt{1 - (u \cdot \nu)^2}$ to $\sqrt{1 - (u \cdot \nu)^2}$ in light of (3.17).

At a point on the wall, such a choice leads to a cost per unit length given by the minimum of a heteroclinic connection problem that is a bit different from (3.19), namely

$$\inf_f \int_{-\infty}^{\infty} W(f\tau + (u \cdot \nu)\nu) + |f'|^2 dt = \inf_f \int_{-\infty}^{\infty} V\left(\sqrt{f^2 + (u \cdot \nu)^2}\right) + |f'|^2 dt,$$

taken over $f \in H^1(\mathbb{R})$ such that

$$f(-\infty) = (u_- \cdot \tau) = -\sqrt{1 - (u \cdot \nu)^2} \quad \text{and} \quad f(\infty) = (u_+ \cdot \tau) = \sqrt{1 - (u \cdot \nu)^2}.$$

One easily checks that this infimum is given by $K(u \cdot \nu)$ where we define

$$K(z) := \int_{-\sqrt{1-z^2}}^{\sqrt{1-z^2}} \sqrt{V}\left(\sqrt{z^2 + y^2}\right) dy, \quad (3.21)$$

which in the prototypical case of $W_{CSH}(u) := |u|^2 (|u|^2 - 1)^2$ takes the form

$$K(z) = \int_{-\sqrt{1-z^2}}^{\sqrt{1-z^2}} \sqrt{z^2 + y^2} (1 - z^2 - y^2) dy. \quad (3.22)$$

We point out that $c_0 = \frac{K(0)}{2}$ and also note that K is not a monotone function of z on $[0, 1]$, but rather increases to a unique maximum and then decreases down to zero at $z = 1$.

Such an upper bound construction leads us to our conjectured Γ -limit when $u \in (H_{\text{div}} \cap BV)(\Omega; \mathbb{S}^1 \cup \{0\})$, namely E_0 given by

$$E_0(u) = \frac{L}{2} \int_{\Omega} (\operatorname{div} u)^2 dx + \frac{K(0)}{2} \operatorname{Per}_{\Omega}(\{|u|=1\}) + \int_{J_u \cap \{|u|=1\}} K(u \cdot \nu) d\mathcal{H}^1. \quad (3.23)$$

One should also impose upon competitors in the minimization of E_0 a boundary condition of the form (1.21) if one imposes the Dirichlet condition $u|_{\partial\Omega} = g$ for E_ε or an area constraint on the measure of the isotropic or nematic region within Ω if an integral constraint has been imposed on E_ε .

In particular, we can rigorously assert:

Theorem 3.2.1. *For any $u \in (H_{\text{div}} \cap BV)(\Omega, \mathbb{S}^1 \cup \{0\})$, there exists a sequence $\{w_\varepsilon\} \in H^1(\Omega; \mathbb{R}^2)$ with $w_\varepsilon \overset{\Delta}{\rightharpoonup} u$ such that*

$$\limsup_{\varepsilon \rightarrow 0} E_\varepsilon(w_\varepsilon) = E_0(u). \quad (3.24)$$

Furthermore, we state a conjecture:

Conjecture : Suppose W satisfies (3.15). Then for any $u \in (H_{\text{div}} \cap BV)(\Omega, \mathbb{S}^1 \cup \{0\})$ and any sequence $u_\varepsilon \overset{\Delta}{\rightharpoonup} u$ we have

$$\liminf_{\varepsilon \rightarrow 0} E_\varepsilon(u_\varepsilon) \geq E_0(u). \quad (3.25)$$

Proof. The proof of (3.24) is similar to the proof of [45, Theorem 3.2(ii)], which itself is an adaptation of the techniques laid out in [26] for Aviles-Giga recovery sequences, so we omit the details. The only difference between the argument here and the argument in [45] is that, as discussed above, in addition to walls, there are also interfaces now in which u jumps from a tangent \mathbb{S}^1 -valued state to 0. However, this does not pose a serious obstacle to the construction, as the important technical components are the rectifiability of the jump set J_u and the condition (3.16) satisfied along J_u at either a wall or interface, which goes to guarantee that the boundary layer constructions do not contribute asymptotically to the L^2 -norm of the divergence. \square

Remark 3.2.2. We have not addressed in (3.23) or in Theorem 3.2.1 the issue of boundary conditions, so we describe now how to incorporate them. Suppose one were to fix Dirichlet data $g_\varepsilon \in H^{1/2}(\partial\Omega; \mathbb{R}^2)$ for admissible functions in E_ε . The functions g_ε could be \mathbb{S}^1 -valued, or could transition smoothly between \mathbb{S}^1 and $\{0\}$ if we are trying to induce a phase transition. Let us assume that $g_\varepsilon \rightarrow g$ in $L^2(\partial\Omega; \mathbb{R}^2)$ for some $g : \partial\Omega \rightarrow \mathbb{S}^1 \cap \{0\}$. We observe that for a sequence $\{u_\varepsilon\} \in H^1(\Omega; \mathbb{R}^2)$ satisfying $u_\varepsilon = g_\varepsilon$ on $\partial\Omega$ and so in particular $u_\varepsilon \cdot \nu_\Omega = g \cdot \nu_\Omega$, under the convergence $u_\varepsilon \xrightarrow{\Delta} u$ with $u \in (BV \cap H_{\text{div}}(\Omega; \mathbb{S}^1 \cap \{0\}))$, it follows from the divergence theorem and the convergence of g_ε to g that

$$u \cdot \nu_\Omega = g \cdot \nu_\Omega.$$

In this case, the limiting energy E_0 would also contain integrals around the portion of $\partial\Omega$ where $u \cdot \tau_\Omega \neq g \cdot \tau_\Omega$, and the cost along these portions would either be given by $K(0)/2$ or $K(u \cdot \nu_\Omega)$.

Remark 3.2.3. An a priori sharper upper bound for the wall cost K could be obtained for these energies using the techniques of [87]. There, the author obtains an upper bound without assuming that the optimal profile is one-dimensional. Instead, the cost is defined via a cell problem. As the class of admissible functions for the cell problem is strictly larger than the class of 1D competitors, the cell problem yields what could in theory be a sharper upper bound. However, since we conjecture that the one-dimensional profile is optimal and since at present we see no way to analyze the abstract cell problem to make this comparison, we do not pursue the strategy from [87].

Given the presence of arguments leading to matching lower bounds for one-dimensional constructions in the Aviles-Giga problem [12] and for the energy E_0 with the potential replaced by a Ginzburg-Landau potential $W_{GL}(v) := (1 - |v|^2)^2$, in [45], it behooves us to comment on why, at present, we have no such argument here. In [12] and in [45], the authors employ the celebrated Jin-Kohn entropy [55]. Defining

$$\Xi(v_1, v_2) = 2 \left(\frac{1}{3}v_2^3 + v_2 v_1^2 - v_2, \frac{1}{3}v_1^3 + v_1 v_2^2 - v_1 \right), \quad (3.26)$$

the version of these entropies well-suited to the situation where the jump set is parallel to one of the coordinate axes, one can then calculate

$$\operatorname{div} \Xi(v_1, v_2) = 2(|v|^2 - 1)(\partial_{x_1} v_2 + \partial_{x_2} v_1) + 4v_1 v_2 \operatorname{div} v. \quad (3.27)$$

In the divergence-free Aviles-Giga setting of [55], the last term drops out and an application of the inequality $a^2 + b^2 \geq 2ab$ allows one to bound the Aviles-Giga energy density from below by $\operatorname{div} \Xi(v_1, v_2)$. When the divergence is possibly non-zero, as in [45], a slight modification yields

$$\operatorname{div} \Xi(v_1, v_2) \leq \left(\varepsilon |\nabla v|^2 + \frac{1}{\varepsilon} (|v|^2 - 1)^2 + L(\operatorname{div} v)^2 \right) + \text{error terms},$$

which is the crux of the argument.

Unfortunately, for most radial potentials that are not the Ginzburg-Landau potential W_{GL} , this technique does not seem to work. First, we note that

$$\Xi(v_1, v_2) = \left(\int_{-v_2}^{v_2} (v_1^2 + s^2 - 1) ds, \int_{-v_1}^{v_1} (s^2 + v_2^2 - 1) ds \right),$$

where the integrands are, up to signs, given by $\sqrt{W_{GL}}$. Therefore, to obtain a version of (3.27) with W_{GL} replaced by \sqrt{W} , where W is our potential vanishing on $\mathbb{S}^1 \cup \{0\}$, the natural choice for the vector field to replace Ξ would be

$$\Xi_W(v_1, v_2) = \left(\int_{-v_2}^{v_2} \sqrt{W(v_1, s)} ds, \int_{-v_1}^{v_1} \sqrt{W(s, v_2)} ds \right).$$

When we calculate the divergence of $\Xi_W(v_1, v_2)$, we get

$$\begin{aligned} & \operatorname{div} \Xi(v_1, v_2) \\ &= 2\sqrt{W(v)}(\partial_{x_1} v_2 + \partial_{x_2} v_1) + \partial_{x_1} v_1 \int_{-v_2}^{v_2} (\partial_{v_1} \sqrt{W(v_1, s)}) ds + \partial_{x_2} v_2 \int_{-v_1}^{v_1} (\partial_{v_2} \sqrt{W(v_2, s)}) ds. \end{aligned}$$

The only way for $\operatorname{div} v$ to factor out of the last two terms is if

$$\int_{-v_2}^{v_2} \partial_{v_1} \sqrt{W(v_1, s)} ds = \int_{-v_1}^{v_1} \partial_{v_2} \sqrt{W(v_2, s)} ds,$$

which holds for radial W when \sqrt{W} is linear in $|v|^2$. This cannot hold for any W that vanishes only at \mathbb{S}^1 and $\{0\}$.

We point out that a related problem that has resisted resolution for several decades is the determination of a sharp lower bound for the sequence of energies

$$\int_{\Omega} \frac{1}{\varepsilon}(|u|^2 - 1)^p + \varepsilon |\nabla u|^2 \quad \text{with } 1 \leq p < 2 \quad (3.28)$$

where competitors $u : \Omega \rightarrow \mathbb{R}^2$ must be divergence-free. Here too it is conjectured that the optimal lower bound for the wall cost is based on a one-dimensional ansatz, [7], but a proof has not been found, and in particular, no version of the Jin-Kohn entropy is evident. An abstract lower bound involving a cell problem for functionals of this type has been derived in [88], but has not yet to our knowledge been matched by a corresponding upper bound. The strategy in this and other papers involving a lower bound phrased in terms of a cell problem is based on a blow up procedure introduced in [40]. Such a lower bound of the form $\int_{J_u} \tilde{K}(u \cdot \nu) d\mathcal{H}^1$ for some $\tilde{K} : [0, \infty) \rightarrow [0, \infty)$ defined as the solution to a cell problem could be derived for our wall energy as well, but we do not include the argument since it does not provide much insight here.

On the other hand, for $p > 2$ in (3.28), as shown in [7], the one-dimensional ansatz is *not* optimal, with an oscillatory construction, often referred to as ‘microstructure,’ whose modulus hews close to \mathbb{S}^1 , yielding a lower asymptotic energy.

So what is the rationale behind our conjecture (3.25)? One key point is that for W given by W_{CSH} or more generally by a potential satisfying (3.15), the level of degeneracy of the \mathbb{S}^1 potential well is no flatter than that of W_{GL} where again it is known that walls follow a one-dimensional profile asymptotically. Thus, it seems unlikely that microstructure of the type emerging, for example, in (3.28) for $p > 2$ would appear here since for our model it is no more beneficial energetically to abandon one-dimensionality in order to be nearer to \mathbb{S}^1 across a wall than it was in (1.17).

Other evidence for our conjecture is numerical. Repeated numerical experiments in the form of gradient flow for E_ε with ε small in a variety of domains, for a variety of boundary conditions and for a wide range of L values have not indicated any lack of one-dimensionality in the wall structure. Were the transition to be truly 2D, one might expect the wall to exhibit some oscillation or other

instability. For example, in [45] while we prove that for (1.17)-(1.18) the wall cost is based on a one-dimensional construction, we also find that when minimizing (1.17) in a rectangle with \mathbb{S}^1 -valued Dirichlet data given by $(\pm a, \sqrt{1-a^2})$ for $a \in [0, 1]$ on the top and bottom respectively and periodic boundary conditions on the sides, there exists a parameter regime in L and in the box dimensions where the minimizer is not one-dimensional, cf. [45], Thm. 6.6. Indeed this theorem is supported by numerics revealing the eventual instability of a horizontal wall and the emergence of so-called ‘cross-ties’ commonly arising in studies of micromagnetics such as [5]. On the other hand, as we discuss in Section 3.3.1, numerically we detect no such instability of a horizontal wall for E_ε under these boundary conditions. Then a numerical examination in Section 3.3.3 of wall structure for a version of our problem posed in a disk also indicates a one-dimensional heteroclinic connection for the wall structure. This gives us further confidence in the conjectured one-dimensionality of the wall cost.

3.2.2 Compactness

In this section we establish a compactness result for energy-bounded sequences. Recalling the assumption (3.15), we begin by observing that

$$E_\varepsilon(u) \geq \frac{1}{2} \int_{\Omega} \left(\frac{1}{\varepsilon c^2} H^2(|u|) + \varepsilon |\nabla u|^2 + L(\operatorname{div} u)^2 \right) dx. \quad (3.29)$$

Both the Ginzburg-Landau and the Chern-Simons-Higgs potentials satisfy this inequality and in [45] it is shown that for W given by the Ginzburg-Landau potential, the compactness result of [32] generalizes to E_ε . In this section, we show that this compactness approach generalizes to potentials also vanishing at the origin provided we assume (3.15).

Theorem 3.2.4. *Let $\{u_\varepsilon\}_{\varepsilon>0} \subset H^1(\Omega; \mathbb{R}^2)$ be a sequence such $E_\varepsilon(u_\varepsilon) \leq C$, with C independent of ε . Then there exists a subsequence (still denoted here by u_ε) and a function $u \in H_{\operatorname{div}}(\Omega; \mathbb{S}^1 \cup \{0\})$*

with $|u| \in BV(\Omega; \{0, 1\})$ such that

$$u_\varepsilon \rightharpoonup u \quad \text{in } H_{\text{div}}(\Omega; \mathbb{R}^2), \quad (3.30)$$

$$u_\varepsilon \rightarrow u \quad \text{in } L^2(\Omega; \mathbb{R}^2). \quad (3.31)$$

The fact that for a subsequence of $\{u_\varepsilon\}$, one has $|u_\varepsilon| \rightarrow |u|$ in $L^1(\Omega)$ where $|u| \in BV(\Omega; \{0, 1\})$ follows from inequality (3.20) via the standard Modica-Mortola approach, cf. [76] or [99]. The proof of (3.30) follows immediately from the uniform bound on the L^2 norm of the divergences, so we turn to the proof of (3.31). The proof follows closely the proof in [32, Proposition 1.2], with the details suitably modified to account for the fact that the potential may now possibly vanish at 0 in addition to \mathbb{S}^1 . Below we outline the procedure and indicate which portions require changes from [32].

The proof relies on compensated compactness and a careful analysis of the Young measure $\{\mu_x\}_{x \in \Omega}$ generated by the sequence $\{u_\varepsilon\}$. One of the key tools in this analysis is the concept of an entropy, defined here as a mapping $\Phi \in C_0^\infty(\mathbb{R}^2; \mathbb{R}^2)$ such that

$$\Phi(0) = 0, \quad D\Phi(0) = 0 \quad \text{and for all } z \in \mathbb{R}^2 \text{ one has } z \cdot D\Phi(z) z^\perp = 0,$$

where $z^\perp = (-z_2, z_1)$, cf. [32, Definition 2.1]. A crucial property of any such entropy is that Φ satisfies a certain equation relating $\nabla \cdot [\Phi(u)]$ and $\nabla(1 - |u|^2)$ for any $u \in H^1(\Omega; \mathbb{R}^2)$. We state this equation precisely in (3.40), and refer the reader to [32, Lemmas 2.2, 2.3] for the proof, which is a straightforward calculation. In Lemma 3.1, we prove that the class of entropies is large enough for our purposes. Next, in Proposition 3.2.6, we prove the requisite compactness for the sequence $\{u_\varepsilon\}$. We achieve this by first adapting the proof of [32, Proposition 1.2] using the aforementioned equation (3.40) to show that for any entropy Φ ,

$$\{\nabla \cdot [\Phi(u_\varepsilon)]\} \text{ is compact in } H^{-1}(\Omega).$$

This compactness then allows us to use the div-curl lemma of Murat and Tartar [80, 102] and the result of Lemma 3.1 to conclude that each μ_x is a Dirac measure. One can then quickly deduce,

in the same fashion as in [32, page 843], that the sequence $\{u_\varepsilon\}$ is precompact in L^2 . We begin the proof with

Lemma 3.1. (cf. [32, Lemma 2.2]) *Let μ be a probability measure on \mathbb{R}^2 supported on $\mathbb{S}^1 \cup \{0\}$.*

Suppose it has the property

$$\int \Phi \cdot \tilde{\Phi}^\perp d\mu = \int \Phi d\mu \cdot \int \tilde{\Phi}^\perp d\mu \text{ for all entropies } \Phi, \tilde{\Phi}. \quad (3.32)$$

Then μ is a Dirac measure.

Remark 3.2.5. *We point out that the proof of this lemma does not generalize to the case where the potential vanishes on a pair of circles that both have non-zero radius. As a consequence, this proof of Theorem 3.2.4 does not generalize to such situations.*

Proof. We begin by recalling the definition of “generalized entropy” from [32, Lemma 2.5]. These are functions Φ defined by

$$\Phi(z) = \begin{cases} |z|^2 e & \text{for } z \cdot e > 0 \\ 0 & \text{for } z \cdot e \leq 0 \end{cases}$$

for any fixed $e \in \mathbb{S}^1$. Any such Φ can be approximated closely enough by entropies Φ_n such that (3.32) holds for Φ as well. Using the fact that these generalized entropies vanish at the origin, we have

$$\int_{\mathbb{S}^1} \Phi \cdot \tilde{\Phi}^\perp d\mu = \int_{\mathbb{S}^1} \Phi d\mu \cdot \int_{\mathbb{S}^1} \tilde{\Phi}^\perp d\mu.$$

We rewrite this as

$$e \cdot \tilde{e}^\perp \mu(\{z \cdot e > 0\} \cap \{z \cdot \tilde{e} > 0\} \cap \mathbb{S}^1) = e \cdot \tilde{e}^\perp \mu(\{z \cdot e > 0\} \cap \mathbb{S}^1) \mu(\{z \cdot \tilde{e} > 0\} \cap \mathbb{S}^1) \text{ for all } e, \tilde{e} \in \mathbb{S}^1$$

or

$$\begin{aligned} \mu(\{z \cdot e > 0\} \cap \{z \cdot \tilde{e} > 0\} \cap \mathbb{S}^1) &= \mu(\{z \cdot e > 0\} \cap \mathbb{S}^1) \mu(\{z \cdot \tilde{e} > 0\} \cap \mathbb{S}^1) \\ &\quad \text{for all } \tilde{e} \in \mathbb{S}^1 \setminus \{e, -e\} \text{ and all } e \in \mathbb{S}^1. \end{aligned}$$

Letting \tilde{e} approach e , we obtain

$$\mu(\{z \cdot e > 0\} \cap \mathbb{S}^1) \leq \mu(\{z \cdot e > 0\} \cap \mathbb{S}^1) \mu(\{z \cdot e \geq 0\} \cap \mathbb{S}^1) \text{ for all } e \in \mathbb{S}^1$$

or

$$\mu(\{z \cdot e > 0\} \cap \mathbb{S}^1) = 0 \text{ or } \mu(\{z \cdot e \geq 0\} \cap \mathbb{S}^1) \geq 1 \text{ for all } e \in \mathbb{S}^1. \quad (3.33)$$

If $\mu(\{0\}) > 0$ then it cannot be that $\mu(\{z \cdot e \geq 0\} \cap \mathbb{S}^1) \geq 1$ for any $e \in \mathbb{S}^1$. In this case $\mu(\{z \cdot e > 0\} \cap \mathbb{S}^1) = 0$ for all \mathbb{S}^1 -valued e , and μ is clearly a Dirac measure concentrated at zero. So we may assume that $\mu(\{0\}) = 0$, implying that μ is a probability measure on \mathbb{S}^1 . In this case, we deduce from (3.33) that

$$\text{supp } \mu \subset \{z \cdot e \leq 0\} \cap \mathbb{S}^1 \text{ or } \text{supp } \mu \subset \{z \cdot e \geq 0\} \cap \mathbb{S}^1 \text{ for all } e \in \mathbb{S}^1.$$

As μ is a probability measure on \mathbb{S}^1 , this implies that μ is concentrated on a single point. \square

We can now prove the main result.

Proposition 3.2.6. (*cf. [32, Proposition 1.2]*) Let $\Omega \subset \mathbb{R}^2$ be open and bounded. Let $\{u_\varepsilon\} \subset H^1(\Omega; \mathbb{R}^2)$ be such that

$$\nabla \cdot u_\varepsilon \text{ are uniformly bounded in } L^2, \quad (3.34)$$

$$\|H(|u_\varepsilon|)\|_{L^2(\Omega)} \xrightarrow{\varepsilon \rightarrow 0} 0, \quad (3.35)$$

and

$$\|\nabla u_\varepsilon\|_{L^2} \|H(|u_\varepsilon|)\|_{L^2} \text{ are uniformly bounded.} \quad (3.36)$$

Then

$$\{u_\varepsilon\} \subset L^2(\Omega; \mathbb{R}^2) \text{ is relatively compact.} \quad (3.37)$$

Proof. First, we modify our sequence slightly for convenience. By choosing real numbers r_ε close enough to 1 and considering the sequence $\{r_\varepsilon u_\varepsilon\}$, we can without loss of generality assume that for each ε ,

$$\left| \left\{ x \in \Omega : |r_\varepsilon u_\varepsilon(x)| = \frac{1}{\sqrt{2}} \right\} \right| = 0. \quad (3.38)$$

In addition, we can choose r_ε so that $\{r_\varepsilon u_\varepsilon\}$ has uniformly bounded energies and is precompact in $L^2(\Omega; \mathbb{R}^2)$ if and only if $\{u_\varepsilon\}$ is as well. Henceforth we refer to the modified sequence as simply $\{u_\varepsilon\}$ and assume that these conditions hold for u_ε .

We aim to show for any entropy Φ that

$$\{\nabla \cdot [\Phi(u_\varepsilon)]\} \text{ is compact in } H^{-1}(\Omega). \quad (3.39)$$

Utilizing (3.34), (3.38) and [32, Lemmas 2.2, 2.3], we see that there exists $\Psi \in C_0^\infty(\mathbb{R}^2)^2$ and $\alpha \in C_0^\infty(\mathbb{R}^2)$ such that at a.e. point in Ω one has

$$\begin{aligned} -\alpha(u_\varepsilon) \operatorname{div} u_\varepsilon + \nabla \cdot [\Phi(u_\varepsilon)] &= \Psi(u_\varepsilon) \cdot \nabla(1 - |u_\varepsilon|^2) = -\Psi(u_\varepsilon) \cdot \nabla(|u_\varepsilon|^2) \\ &= \operatorname{sgn}\left(|u_\varepsilon| - 1/\sqrt{2}\right) \Psi(u_\varepsilon) \cdot \nabla H(|u_\varepsilon|). \end{aligned}$$

Before proceeding, we let $s : \mathbb{R} \rightarrow \mathbb{R}$ denote a smooth, increasing, bounded function with bounded derivative such that $s(z) \equiv -1$ for $z \leq \frac{1}{2\sqrt{2}}$ and $s(z) \equiv 1$ for $z \geq \frac{1}{2\sqrt{2}}$. We will utilize the sequence $s(|u_\varepsilon|)$, and we remark that $\frac{1}{2\sqrt{2}}$ could readily be replaced by any number less than $\frac{1}{\sqrt{2}}$. Replacing $\operatorname{sgn}(|u_\varepsilon| - 1/\sqrt{2})$ by $s(|u_\varepsilon|)$ as such allows us to maintain L^1 control on $\nabla s(|u_\varepsilon|)$ as opposed to having to analyze the distributional gradient of a sgn function, as will be necessary in a step at the end of the proof. Continuing from (3.40), we find that

$$-\alpha(u_\varepsilon) \operatorname{div} u_\varepsilon + \nabla \cdot [\Phi(u_\varepsilon)] = s(|u_\varepsilon|) \Psi(u_\varepsilon) \cdot \nabla H(|u_\varepsilon|) + R_\varepsilon, \quad (3.40)$$

$$R_\varepsilon := \left(\operatorname{sgn}\left(|u_\varepsilon| - 1/\sqrt{2}\right) - s(|u_\varepsilon|) \right) \Psi(u_\varepsilon) \cdot \nabla H(|u_\varepsilon|). \quad (3.41)$$

We claim the remainder terms R_ε are bounded uniformly in L^1 . Noticing that $s(|u_\varepsilon|) = \operatorname{sgn}(|u_\varepsilon| - 1/\sqrt{2})$

$1/\sqrt{2}|$) if $\left||u_\varepsilon| - 1/\sqrt{2}\right| \geq \frac{1}{2\sqrt{2}}$, we have

$$\int_{\Omega} |R_\varepsilon| \leq C \int_{\Omega} \left| \chi_{\left\{ \left| |u_\varepsilon| - \frac{1}{2\sqrt{2}} \right| < \frac{1}{2\sqrt{2}} \right\}} \right| |\nabla|u_\varepsilon|| dx.$$

Continuing now using Holder's inequality and the bound $\int_{\Omega} W(u_\varepsilon) \leq C\varepsilon$, we have

$$\begin{aligned} \int_{\Omega} |R_\varepsilon| &\leq C \|\nabla|u_\varepsilon|\|_{L^2} \cdot \text{meas} \left\{ \left| |u_\varepsilon| - \frac{1}{\sqrt{2}} \right| < \frac{1}{2\sqrt{2}} \right\}^{1/2} \\ &\leq C \frac{1}{\sqrt{\varepsilon}} \sqrt{\varepsilon} \\ &\leq C. \end{aligned}$$

To prove (3.39), we will prove that the sequence

$$\{\nabla \cdot [\Phi(u_\varepsilon) - s(|u_\varepsilon|)H(|u_\varepsilon|)\Psi(u_\varepsilon)]\} \text{ is compact in } H^{-1}(\Omega). \quad (3.42)$$

Since the energy bound implies that $s(|u_\varepsilon|)H(|u_\varepsilon|)\Psi(u_\varepsilon)$ converges to 0 in L^2 , the divergence of this sequence converges to 0 in H^{-1} . Thus (3.42) implies (3.39). Thanks to (3.40), we have that

$$\begin{aligned} \nabla \cdot [\Phi(u_\varepsilon) - sH(|u_\varepsilon|)\Psi(u_\varepsilon)] &= \nabla \cdot [\Phi(u_\varepsilon)] - \nabla \cdot [s\Psi(u_\varepsilon)]H(|u_\varepsilon|) - s\Psi(u_\varepsilon) \cdot \nabla[H(|u_\varepsilon|)] \\ &= R_\varepsilon + \alpha(u_\varepsilon) \operatorname{div} u_\varepsilon - \nabla \cdot [s\Psi(u_\varepsilon)]H(|u_\varepsilon|) \end{aligned}$$

We will show the desired compactness by appealing to a lemma of [81], cf. [32, Lemma 3.1].

This entails verifying the following two claims:

- (1) The sequence $\{\nabla \cdot [\Phi(u_\varepsilon) - sH(|u_\varepsilon|)\Psi(u_\varepsilon)]\}$ is uniformly bounded in $L^1(\Omega)$.
- (2) The sequence $\{|[\Phi(u_\varepsilon) - s(|u_\varepsilon|)H(|u_\varepsilon|)\Psi(u_\varepsilon)]|^2\}_{\varepsilon>0}$ is uniformly integrable.

Proof of (1): We have shown that the R_ε are uniformly bounded in L^1 , and the boundedness of the function α along with the L^2 bound on $\operatorname{div} u_\varepsilon$ yield that $\alpha(u_\varepsilon) \operatorname{div} u_\varepsilon$ is uniformly bounded in L^1 . It remains to show that the last term, namely $\nabla \cdot [s(|u_\varepsilon|)\Psi(u_\varepsilon)]H(|u_\varepsilon|)$, is bounded in L^1 . We have

$$H(|u_\varepsilon|)\nabla \cdot [s\Psi(u_\varepsilon)] = H(|u_\varepsilon|) (s'(|u_\varepsilon|) \nabla|u_\varepsilon| \cdot \Psi(u_\varepsilon) + s(|u_\varepsilon|) \operatorname{div} \Psi(u_\varepsilon)).$$

The desired L^1 bound follows from Cauchy-Schwarz along with the energy bound.

Proof of (2): This is clear from the fact that Φ , s , H , and Ψ are bounded functions.

We have now proved that $\{\nabla \cdot [\Phi(u_\varepsilon)]\}$ is compact in $H^{-1}(\Omega)$. The rest of the proof follows as in the second step of [32, Propositon 1.2]. \square

3.2.3 The Γ -Limit of E_ε Among 1D Competitors

In this section we analyze Γ -convergence of E_ε where competitors $u_\varepsilon = (u_\varepsilon^{(1)}, u_\varepsilon^{(2)})$ are defined on an interval $[-H, H]$ for some $H > 0$ and are required to satisfy \mathbb{S}^1 -valued boundary conditions of the form

$$u(\pm H) = (\pm \sqrt{1 - a^2}, a) \quad \text{for some } a \in [0, 1). \quad (3.43)$$

Under the one-dimensional assumption, E_ε takes the form

$$E_\varepsilon^{1D}(u) := \begin{cases} \frac{1}{2} \int_{-H}^H \left(\frac{1}{\varepsilon} W(u) + \varepsilon |u'|^2 + L(u^{(2)'}')^2 \right) dx_2 & \text{if } u \in H^1((-H, H); \mathbb{R}^2), \\ +\infty & \text{otherwise.} \end{cases} \quad (3.44)$$

In a manner similar to [45], Section 6, within this one-dimensional ansatz we can obtain a sharp compactness theorem for energy bounded sequences, a complete Γ -convergence result of the E_ε functionals and a complete characterization of minimizers of the Γ -limit. Since the proofs of the results in this section are completely analogous to those in [45, Section 6], we only sketch the arguments highlighting differences.

In Section 3.3.1, we present results of numerical simulations obtained via gradient flow for E_ε with $\varepsilon > 0$ for the two-dimensional problem in a rectangle $\Omega = (-1/2, 1/2) \times (-H, H)$, subject to the boundary conditions (3.43) on the top and bottom and periodic boundary conditions on the left and right sides. These computations suggest convergence in large time to configurations that resemble the one-dimensional minimizers of this section, lending further evidence to our conjecture (3.25). We emphasize that the initial data for these numerics were *not* restricted to be one-dimensional.

We continue making the assumption (3.15) on our potentials. Recall that we are writing $W(u) = V(|u|)$. We begin with a compactness result.

Theorem 3.2.7. *Let $u_\varepsilon = (u_\varepsilon^{(1)}, u_\varepsilon^{(2)}) \in H^1((-H, H); \mathbb{R}^2)$ with $E_\varepsilon^{\text{1D}}(u_\varepsilon) \leq C$. Then there exists $u = (u_1, u_2)$ with*

$$\Psi(u_1) := \int_{-u_1}^{u_1} \sqrt{V} \left(\sqrt{s^2 + 1 - u_1^2} \right) ds \in BV((-H, H); [0, 1])$$

such that up to a subsequence, $u_\varepsilon^{(1)} \rightarrow u_1$ in $L^2(-H, H)$. In addition, $u_2 \in H^1((-H, H); \mathbb{R})$, $u_\varepsilon^{(2)} \rightarrow u_2$ in $C^{0,\gamma}(-H, H)$ for all $\gamma < 1/2$, and $|(u_1, u_2)| = 1$ or 0 a.e.

Proof. Throughout the course of the proof, we repeatedly pass to further and further subsequences of ε converging to zero but suppress this from our notation. We notice that thanks to the uniform L^4 bound from (3.15), after passing to a subsequence,

$$u_\varepsilon \rightharpoonup u = (u_1, u_2) \text{ in } L^4. \quad (3.45)$$

Furthermore, this bound, along with the uniform L^2 bound on $(u_\varepsilon^{(2)})'$ yields after passing to a further subsequence that

$$u_\varepsilon^{(2)} \rightharpoonup u_2 \text{ in } H^1 \quad \text{and} \quad u_\varepsilon^{(2)} \rightarrow u_2 \text{ in } C^{0,\gamma}([-H, H]) \text{ for every } \gamma < 1/2. \quad (3.46)$$

Finally, from the bound on the potential, there exists $\rho \in L^2((-H, H); \{0, 1\})$ such that

$$|u_\varepsilon| \rightarrow \rho \text{ in } L^2. \quad (3.47)$$

It remains to upgrade the convergence of $u_\varepsilon^{(1)}$ from weak to strong convergence. An algebraic identity is used in the proof of [45, Theorem 6.1] to obtain strong convergence. Here, without an explicit expression for W , we proceed differently. As in [45], we utilize the “entropy” ψ defined by

$$\psi(u_\varepsilon) := \int_{-u_\varepsilon^{(1)}}^{u_\varepsilon^{(1)}} \sqrt{V} \left(|(s, u_\varepsilon^{(2)})| \right) ds = u_\varepsilon^{(1)} \int_{-1}^1 \sqrt{V} \left(|(u_\varepsilon^{(1)} t, u_\varepsilon^{(2)})| \right) dt. \quad (3.48)$$

We set $J_\varepsilon = \int_{-1}^1 \sqrt{V} \left(\left| (u_\varepsilon^{(1)} t, u_\varepsilon^{(2)}) \right| \right) dt$, so that

$$u_\varepsilon^{(1)} J_\varepsilon = \psi(u_\varepsilon). \quad (3.49)$$

On the one hand,

$$J_\varepsilon = \int_{-1}^1 \sqrt{V} \left(\sqrt{(|u_\varepsilon|^2 - (u_\varepsilon^{(2)})^2)t^2 + (u_\varepsilon^{(2)})^2} \right) dt;$$

thus (3.46)-(3.47) yield that

$$J_\varepsilon \rightarrow \int_{-1}^1 \sqrt{V} \left(\sqrt{(\rho^2 - (u^{(2)})^2)t^2 + (u^{(2)})^2} \right) dt =: J \quad \text{a.e. in } (-H, H). \quad (3.50)$$

On the other hand, using (3.15) and a Cauchy-Schwarz argument completely analogous to that found in [45], we note that $\psi(u_\varepsilon)$ is bounded in BV . Upon passing to a subsequence, we conclude that $\{\psi(u_\varepsilon)\}$ converges in L^1 , and upon passing to a further subsequence, $\{\psi(u_\varepsilon)\}$ converges almost everywhere. Consequently, using (3.49) and (3.50), we find that $u_\varepsilon^{(1)}$ converges almost everywhere as well.

Finally, since $|u_\varepsilon^{(1)}| \leq |u_\varepsilon|$ and $|u_\varepsilon| \rightarrow \rho$ strongly in L^2 , we can apply the Lebesgue dominated convergence theorem to conclude that $u_\varepsilon^{(1)}$ converges strongly in L^2 to some limit. From (3.45), this limit is u_1 , and it follows that $|(u_1, u_2)| = 0$ or 1 a.e. and that the limit of $\psi(u_\varepsilon)$ is $\psi(u_1, u_2) \in BV$. Since ψ is 0 when $u_1 = 0$, we see that $\Psi(u_1) = \psi(u)$, which concludes the proof. \square

We turn next to Γ -convergence in this one-dimensional setting. The analogue of E_0 from (3.23) is the energy

$$E_0^{1D}(u) := \frac{L}{2} \int_{-H}^H (u^{(2)'})^2 dx_2 + \sum_{x_2 \in J_{u^{(1)}} \cap \{|u|=1\}} K(u^{(2)}(x_2)) + c_0 \mathcal{H}_{(-H, H)}^0(\partial(\{|u|=1\})). \quad (3.51)$$

One can establish the Γ -convergence of E_ε^{1D} to E_0^{1D} in a completely analogous manner to the proof of Theorem 6.2 in [45], so we omit the details.

Finally, as in Theorem 6.4 of [45], and with identical proofs, one can characterize the minimizers of (3.51) explicitly. When the boundary conditions (3.43) are different from $(\pm 1, 0)$ the minimizer

is unique and consists of a single wall occurring at $y = 0$, no interfaces and bulk contribution in the regions $\{y > 0\} \cup \{y < 0\}$: the function $u^{(2)}$ is piecewise linear and $u^{(1)}$ jumps from $\sqrt{1 - (u^{(2)})^2}$ to $-\sqrt{1 - (u^{(2)})^2}$ across $y = 0$. The optimal jump value is easily determined by optimizing over the bulk and jump contributions. Finally when the Dirichlet boundary conditions on the top and the bottom are given by $(\pm 1, 0)$, we find two parameter regimes similar to the situation in [45]. When L/H is smaller than a certain threshold, the minimizer is unique and has both bulk divergence and jump contributions. However for larger L/H values, the minimizer only has perimeter contribution, along with two interfaces, one connecting $(-1, 0)$ to $(0, 0)$ and the other connecting $(0, 0)$ to $(1, 0)$. These interfaces divide the interval into subintervals in each of which the minimizer is a constant. See Section 3.3.1 for numerical simulations.

3.2.4 Criticality Conditions for E_0

In this section we will describe criticality conditions associated with critical points u of the conjectured Γ -limit E_0 given by (3.23). For $u \in (H_{\text{div}} \cap BV)(\Omega; \mathbb{S}^1 \cup \{0\})$, we recall the notation $K(u \cdot \nu)$, with K given by (3.21) or (3.22) in the case of the Chern-Simons-Higgs potential, for the cost per arclength of a jump from one \mathbb{S}^1 -valued state, say u_1 to another one, say u_2 across a jump set J_u , with ν denoting the unit normal pointing from the 1 side of a wall to the 2 side. We recall that for such a jump, an H_{div} vector field must satisfy the requirement

$$u_1 \cdot \nu = u_2 \cdot \nu \quad \text{along the jump set } J_u. \quad (3.52)$$

In light of (3.52), we will sometimes write just $u \cdot \nu$ when evaluating the normal component of u along J_u .

We also recall that for portions of J_u corresponding to a jump from the isotropic state 0 to an \mathbb{S}^1 -valued state u , the cost per unit arclength is given by $\frac{K(0)}{2}$ and condition (3.52) becomes simply $u \cdot \nu = 0$.

Parts of the argument follow the same lines as in the proof of Theorem 4.1 in [45] except that

the cost in that paper is the one associated with a Ginzburg-Landau potential, namely $K_{GL}(u \cdot \nu)$

where

$$K_{GL}(z) := \int_{-\sqrt{1-z^2}}^{\sqrt{1-z^2}} (1 - z^2 - y^2) dy,$$

which can also be written as $\frac{4}{3} (1 - (u \cdot \nu)^2)^{3/2}$ or equivalently $\frac{1}{6} |u_- - u_+|^3$.

However, in the present context, we will need to distinguish between variations of the ‘walls’ separating two \mathbb{S}^1 -valued states and ‘interfaces’ separating the isotropic state from an \mathbb{S}^1 -valued state. We will also examine criticality conditions at a junction corresponding to the intersection of these two kinds of curves. We begin with:

Theorem 3.2.8. (*Variations that fix the jump set*)

Consider any $u \in BV(\Omega, \mathbb{S}^1 \cup \{0\}) \cap H_{\text{div}}(\Omega, \mathbb{S}^1 \cup \{0\})$ such that $u_{\partial\Omega} \cdot \nu_{\partial\Omega} = g \cdot \nu_{\partial\Omega}$ on $\partial\Omega$. Denote by J_u its jump set. Then if the first variation of E_0 evaluated at u vanishes when taken with respect to perturbations compactly supported in $\Omega \setminus J_u$, one has the condition

$$u^\perp \cdot \nabla \operatorname{div} u = 0 \text{ holding weakly on } \Omega \setminus J_u, \quad (3.53)$$

where $u^\perp = (-u_2, u_1)$.

Now assume the first variation vanishes at u when taken with respect to perturbations that fix J_u and are supported within any ball $B(p, R)$ centered at a smooth point of $p \in J_u \cap \Omega$. If J_u separates the ball $B(p, R)$ into two regions where u is given by \mathbb{S}^1 -valued states u_1 and u_2 and if the traces $\operatorname{div} u_1$ and $\operatorname{div} u_2$ are sufficiently smooth, then one has the condition

$$K'(u \cdot \nu) = L[\operatorname{div} u] \text{ on } J_u \cap \Omega, \quad (3.54)$$

where $[\operatorname{div} u] = \operatorname{div} u_2 - \operatorname{div} u_1$ represents the jump in divergence across J_u and ν is the unit normal to J_u pointing from region 1 to region 2.

Remark 3.2.9. There is no natural boundary condition analogous to (3.54) for such variations taken about a point of J_u where J_u separates an isotropic state 0 from an \mathbb{S}^1 -valued state since

the requirement of tangency in such a configuration is too rigid to allow for a rich enough class of perturbations.

Proof. To derive conditions (3.53) and (3.54) we assume that for some point $p \in \Omega$ and for some $R > 0$, either $B(p, R) \cap J_u = \emptyset$ or else $p \in J_u$ and the following conditions hold $B(p, R)$:

- (i) The set $B(p, R) \cap J_u$ is a smooth curve, which we denote by Γ and which admits a smooth parametrization by arclength, which we denote by $r : [-s_0, s_0] \rightarrow \Omega$ for some $s_0 > 0$ with $r(0) = p$.
- (ii) On either side of Γ the critical point u and $\operatorname{div} u$ possess smooth traces on J_u . We will denote the two components of $B(p, R) \setminus \Gamma$ by Ω_1 and Ω_2 and we denote u on these two sets by $u_j : \Omega_j \rightarrow \mathbb{S}^1$, for $j = 1, 2$.

We will present the argument for case (ii), indicating how the easier case (i) follows from the same analysis.

To define an allowable perturbation u^t of the critical point u given by u_1 and u_2 , we must maintain the property of being \mathbb{S}^1 -valued, so to that end we introduce smooth functions $\phi_j : B(p, R) \times (-T, T) \rightarrow \mathbb{R}$ for some $T > 0$ such that the perturbations of u_1 and u_2 take the form

$$u_j^t(x) := u_j(x)e^{it\phi_j(x,t)}, \quad (3.55)$$

shifting just for the moment to complex notation. Introducing $\phi_j(x) := \phi_j(x, 0)$, expanding (3.55) and reverting back to an R^2 -valued description of u_j^t we find that for $x \in \Omega_j^t$ one has

$$u_j^t(x) \sim u_j(x) + t\phi_j(x)u_j(x)^\perp. \quad (3.56)$$

Along J_u , we must also be sure to preserve to $O(t)$ the H_{div} condition (3.52), namely

$$u_1^t \cdot \nu = u_2^t \cdot \nu \quad \text{along } \Gamma. \quad (3.57)$$

Invoking (3.52) for the unperturbed critical point, along with (3.56) we find that $u_1^t \cdot \nu = u_2^t \cdot \nu$ to $O(t)$ provided

$$\phi_1 u_1^\perp \cdot \nu = \phi_2 u_2^\perp \cdot \nu.$$

However, since

$$u_j^\perp \cdot \nu = u_j \cdot \tau \quad \text{and} \quad u_1 \cdot \tau = -u_2 \cdot \tau \neq 0 \quad (3.58)$$

along the jump set J_u bridging \mathbb{S}^1 -valued states, it follows that we must require

$$\phi_1(x) = \phi_2(x) \quad \text{for } x \in \Gamma. \quad (3.59)$$

For later use, we also record that from (3.56) and (3.58) one has along Γ the expansion

$$u^t \cdot \nu \sim u_1 \cdot \nu + t\phi_1(u_1 \cdot \tau) + o(t). \quad (3.60)$$

Now we calculate

$$\begin{aligned} \frac{d}{dt}_{|t=0} E_0(u^t) &= \frac{d}{dt}_{|t=0} \left\{ \frac{L}{2} \sum_{j=1}^2 \int_{\Omega_j} (\operatorname{div} u_j^t)^2 dx \right\} + \frac{d}{dt}_{|t=0} \int_{\Gamma} K(u^t \cdot \nu) ds \\ &= \frac{d}{dt}_{|t=0} \left\{ \sum_{j=1}^2 \frac{L}{2} \int_{\Omega_j} (\operatorname{div} (u_j(x) + t\phi_j(x)u_j(x)^\perp))^2 dx \right\} + \\ &\quad \frac{d}{dt}_{|t=0} \int_{\Gamma} K(u_1 \cdot \nu + t\phi_1(u_1 \cdot \tau)) ds \end{aligned}$$

Taking the t -derivatives and evaluating at $t = 0$ we obtain

$$\begin{aligned} \frac{d}{dt}_{|t=0} E_0(u^t) &= \left\{ L \sum_{j=1}^2 \int_{\Omega_j} (\operatorname{div} u_j)(\operatorname{div}(\phi_j u_j^\perp)) dx \right\} \\ &\quad \int_{\Gamma} K'(u \cdot \nu)(u_1 \cdot \tau) ds. \end{aligned}$$

Integrating by parts, a vanishing first variation of this type leads to the condition

$$\begin{aligned} &-L \sum_{j=1}^2 \int_{\Omega_j} \nabla(\operatorname{div} u_j) \cdot \phi_j u_j^\perp dx + L \int_{\Gamma} \{ (\operatorname{div} u_1)\phi_1 u_1^\perp \cdot \nu - (\operatorname{div} u_2)\phi_2 u_2^\perp \cdot \nu \} ds \\ &+ \int_{\Gamma} K'(u \cdot \nu)(u_1 \cdot \tau) ds = 0. \end{aligned} \quad (3.61)$$

Now by taking the functions ϕ_j to be supported off of J_u we arrive at condition (3.53). This also handles case (i) where $B(p, R) \cap J_u = \emptyset$. Then, in light of (3.53), along with (3.58) and (3.59) we find that

$$\int_{\Gamma} \{ K'(u \cdot \nu)(u_1 \cdot \tau) + L(\operatorname{div} u_1 - \operatorname{div} u_2) \} (u_1 \cdot \tau) \phi_1 ds = 0.$$

Since $u_1 \cdot \tau \neq 0$ along the jump set and ϕ_1 is arbitrary, we arrive at (3.54). \square

Corollary 3.2.10. (cf. [45], Cor. 4.2). Suppose u is smooth and critical for E_0 in the sense of (3.53). Then writing u locally in terms of a lifting as $u(x) = e^{i\theta(x)}$ and defining the scalar $v := \operatorname{div} u$ one has that (3.53) is equivalent to the following system for the two scalars θ and v :

$$-\sin \theta \theta_{x_1} + \cos \theta \theta_{x_2} = v \quad (3.62)$$

$$-\sin \theta v_{x_1} + \cos \theta v_{x_2} = 0. \quad (3.63)$$

Consequently, starting from any initial curve in Ω parametrized via $s \mapsto (x_1^0(s), x_2^0(s))$ along which θ and v take values $\theta_0(s)$ and $v_0(s)$ respectively, the characteristic curves, say $t \mapsto (x_1(s, t), x_2(s, t))$, are given by

$$x_1(s, t) = \frac{1}{v_0(s)} [\cos(v_0(s)t + \theta_0(s)) - \cos \theta_0(s)] + x_1^0(s), \quad (3.64)$$

$$x_2(s, t) = \frac{1}{v_0(s)} [\sin(v_0(s)t + \theta_0(s)) - \sin \theta_0(s)] + x_2^0(s), \quad (3.65)$$

whenever $v_0(s) \neq 0$. The corresponding solutions $\theta(s, t)$ and $v(s, t)$ are given by

$$\theta(s, t) = v_0(s)t + \theta_0(s), \quad v(s, t) = v_0(s), \quad (3.66)$$

so that the characteristics are circular arcs of curvature $v_0(s)$ and carry constant values of the divergence. In case the divergence vanishes somewhere along the initial curve, i.e. $v_0(s) = 0$, then the characteristic is a straight line.

We also consider the implications of criticality with respect to perturbations of the jump set itself.

Theorem 3.2.11. (Variations of the jump set)

Under the same assumptions on u as in the previous theorem, suppose in addition to the criticality with respect to perturbations that fix the location of J_u , one also assumes the vanishing of the first variation of E_0 , evaluated at u , allowing for local perturbations of the jump set $J_u \cap \Omega$ itself. Then along any points of J_u where u jumps between two \mathbb{S}^1 -valued maps u_1 and u_2 , a vanishing first

variation leads to the condition

$$\frac{L}{2} \left((\operatorname{div} u_1)^2 - (\operatorname{div} u_2)^2 \right) - L(\operatorname{div} u_1 + \operatorname{div} u_2)' (u_1 \cdot \tau) - L(\operatorname{div} u_1 + \operatorname{div} u_2) (u_1 \cdot \tau)' - K(u \cdot \nu) \kappa = 0, \quad (3.67)$$

at any point $p \in J_u$ such that J_u , u_1 and u_2 are sufficiently smooth in some ball centered at p .

Here κ denotes the curvature of J_u , τ denotes the unit tangent to J_u and ν is the unit normal to J_u pointing from the u_1 side of J_u to the u_2 side. The notation $(\cdot)'$ refers to the tangential derivative along the jump set.

For portions of J_u separating an \mathbb{S}^1 -valued state u^ from the isotropic state 0, criticality takes the form*

$$\frac{L}{2} (\operatorname{div} u^*)^2 - L (\operatorname{div} u^*)' (u^* \cdot \tau) + \frac{K(0)}{2} \kappa = \lambda, \quad (3.68)$$

where λ is a Lagrange multiplier that is present only if E_0 is considered subject to an area constraint on the measure of the isotropic phase 0. Also, since $u \in H_{\operatorname{div}}(\Omega)$ requires that $u^ \cdot \nu = 0$ along such a portion of J_u , we note that in (3.68) one either has $u^* \cdot \tau \equiv 1$ or $u^* \cdot \tau \equiv -1$.*

Proof. To derive condition (3.67) assume that for some point $p \in J_u$ the following conditions hold in a ball $B(p, R)$ for some radius R :

- (i) The set $B(p, R) \cap J_u$ is a smooth curve, which we denote by Γ and which admits a smooth parametrization by arclength, which we denote by $r : [-s_0, s_0] \rightarrow \Omega$ for some $s_0 > 0$ with $r(0) = p$.
- (ii) On either side of Γ the critical point u is C^2 with C^1 traces on J_u . We will denote the two components of $B(p, R) \setminus \Gamma$ by Ω_1 and Ω_2 and we denote u on these two sets by $u_j : \Omega_j \rightarrow \mathbb{S}^1$, for $j = 1, 2$. Again, our convention for the unit normal ν is that it points out of Ω_1 into Ω_2 .

For the calculation it will be convenient to assume that for $j = 1, 2$, u_j has been smoothly extended so as to be defined in an open neighborhood of Γ . We take this extension to be executed so that u_1 is constant along ν and so that u_2 is constant along $-\nu$.

In order to effect a smooth perturbation of Γ , u_1 and u_2 we now introduce a vector field

$X \in C_0^1(B(p, R); \mathbb{R}^2)$. For convenience we will assume that $X(x)$ is parallel to $\nu(x)$ for $x \in \Gamma$ and so we introduce the scalar function $h : [-s_0, s_0] \rightarrow \mathbb{R}$ such that

$$X(r(s)) = h(s)\nu(s) \quad \text{for } s \in [-s_0, s_0], \quad (3.69)$$

where $h(\pm s_0) = 0$. Here we have written $\nu(s)$ for the composition $\nu(r(s))$. Then let $\Psi : B(p, R) \times (-T, T) \rightarrow \Omega$ solve

$$\frac{\partial \Psi}{\partial t} = X(\Psi) \quad \Psi(x, 0) = x, \quad (3.70)$$

for some $T > 0$. Expanding in t we find that

$$D\Psi(\cdot, t) \sim I + t\nabla X + o(t), \quad (3.71)$$

so that in particular one has the identity

$$J\Psi(x, t) := \det D\Psi \sim 1 + t \operatorname{div} X(x) + o(1). \quad (3.72)$$

Throughout this proof, the symbol \sim refers to an equivalence up to terms that are $o(t)$.

Now we define the evolution of the curve Γ via the vector field X by $\Gamma^t := \Psi(\Gamma, t)$ with corresponding parametrization

$$r^t(s) := \Psi(r(s), t) \sim r(s) + X(r(s))t \sim r(s) + th(s)\nu(s), \quad (3.73)$$

in light of (3.69). A simple calculation goes to show that the normal ν^t to Γ^t takes the form

$$\nu^t(s) \sim \nu(s) - th'(s)\tau(s), \quad (3.74)$$

where we have introduce the notation τ for the unit tangent $r'(s)$ to Γ . We caution that the parameter s used to parametrize Γ^t is not an arclength parametrization on this deformed curve. Indeed one finds through an application of the Frenet equation that

$$r'^t(s) = r'(s) + th'(s)\nu(s) + th\nu'(s) = (1 - th(s)\kappa(s))\tau(s) + th'(s)\nu(s)$$

where κ denotes the curvature of Γ , so that

$$|r^t'(s)| \sim 1 - th(s)\kappa(s). \quad (3.75)$$

Similarly, we define the deformation of the two sets Ω_1 and Ω_2 via

$$\Omega_j^t := \Psi(\Omega_j, t) \quad \text{for } j = 1, 2. \quad (3.76)$$

To define the allowable evolution of the critical point u given by u_1 and u_2 requires a little more care. Firstly, we must maintain the property of being \mathbb{S}^1 -valued, so to that end we introduce smooth functions $\phi_j : B(p, R) \times (-\tau, \tau) \rightarrow \mathbb{R}$ such that the perturbations of u_1 and u_2 take the form

$$u_j^t(x) := u_j(x)e^{it\phi_j(x,t)}, \quad (3.77)$$

shifting just for the moment to complex notation. Introducing $\phi_j(x) := \phi_j(x, 0)$, expanding (3.77) and reverting back to an R^2 -valued description of u_j^t we find that for $x \in \Omega_j^t$ one has

$$u_j^t(x) \sim u_j(x) + t\phi_j(x)u_j(x)^\perp. \quad (3.78)$$

As before $(a, b)^\perp = (-b, a)$.

Secondly, we must preserve to $O(t)$ the H_{div} condition (3.52), namely

$$u_1^t \cdot \nu^t = u_2^t \cdot \nu^t \quad \text{along } \Gamma^t. \quad (3.79)$$

To this end, we observe that along Γ^t one has

$$\begin{aligned} u_j^t(r^t(s)) &\sim u_j^t(r(s) + th(s)\nu(s)) + t\phi_j(r(s) + th(s)\nu(s))u_j^\perp(r(s) + th(s)\nu(s)) \\ &\sim u_j(r(s)) + t\phi_j(r(s))u_j^\perp(r(s)). \end{aligned} \quad (3.80)$$

It is here that we require the slight extensions of the original functions u_j that are constant along the normal direction of ν to make (3.78) well-defined in $\Omega_j^t \setminus \Omega_j$ and to make (3.80) correct to $O(t)$.

Then once we apply (3.74) and (3.80) to (3.79) we arrive at the requirement that

$$(u_1 + t\phi_1 u_1^\perp) \cdot (\nu - th'\tau) \sim (u_2 + t\phi_2 u_2^\perp) \cdot (\nu - th'\tau) \quad \text{along } \Gamma. \quad (3.81)$$

Equating terms at $O(t)$ and using (3.58), we find that necessarily,

$$h'(s) = \frac{1}{2}(\phi_1(r(s)) + \phi_2(r(s))) \quad \text{for } s \in [-s_0, s_0]. \quad (3.82)$$

For later use we also record that fact, based on expanding the left hand side of (3.81), that

$$u_1^t(r^t(s)) \cdot \nu^t(s) \sim u(r(s)) \cdot \nu(s) + t(\phi_1(r(s)) - h'(s))(u_1 \cdot \tau) \quad \text{for } s \in [-s_0, s_0]. \quad (3.83)$$

With these preliminaries taken care of, we are now ready to proceed with the calculation of the first variation $\frac{d}{dt}|_{t=0} E_0(u^t)$. We begin with the variation of the divergence term in the energy taken over Ω_j^t for $j = 1, 2$. We observe that

$$\begin{aligned} \int_{\Omega_j^t} (\operatorname{div} u_j^t)^2 dx &\sim \int_{\Omega_j^t} (\operatorname{div} u_j + t \operatorname{div}(\phi_j u_j^\perp))^2 dx \\ &\sim \int_{\Omega_j} \left[\operatorname{div} u_j(\Psi(y, t)) + t \operatorname{div} \phi_j(\Psi(y, t)) u_j^\perp(\Psi(y, t)) \right]^2 (1 + t \operatorname{div} X(y)) dy, \end{aligned}$$

where we have utilized the change of variables $x = \Psi(y, t)$ and invoked (3.72) to obtain the leading order behavior of the Jacobian of the change of variables. Then, since $\Psi \sim y + tX(y)$ we find

$$\begin{aligned} \frac{d}{dt}|_{t=0} \int_{\Omega_j^t} (\operatorname{div} u_j^t)^2 dx \\ &= \int_{\Omega_j} \left[(\operatorname{div} u_j(y))^2 \operatorname{div} X + 2 \operatorname{div} u_j(y) \operatorname{div}(\phi_j(y) u_j^\perp(y)) + \frac{\partial}{\partial t}|_{t=0} (\operatorname{div} u_j(y + tX(y)))^2 \right] dy \\ &= \int_{\Omega_j} \left[(\operatorname{div} u_j(y))^2 \operatorname{div} X + 2 \operatorname{div} u_j(y) \operatorname{div}(\phi_j(y) u_j^\perp(y)) + 2 \operatorname{div} u_j(y) \nabla \operatorname{div} u_j(y) \cdot X(y) \right] dy \\ &= \int_{\Omega_j} \left[\operatorname{div}((\operatorname{div} u_j)^2 X) + 2 \operatorname{div} u_j(y) \operatorname{div}(\phi_j(y) u_j^\perp(y)) \right] dy \end{aligned} \quad (3.84)$$

Applying the divergence theorem, and invoking (3.53) along with the compact support of X within the ball $B(p, R)$, we conclude that

$$\begin{aligned} \frac{d}{dt}|_{t=0} \frac{L}{2} \left(\int_{\Omega_1^t} (\operatorname{div} u_1^t)^2 dx + \int_{\Omega_2^t} (\operatorname{div} u_2^t)^2 dx \right) \\ &= \frac{L}{2} \int_{\Gamma} \left\{ ((\operatorname{div} u_1)^2 - (\operatorname{div} u_2)^2) h + 2 (\operatorname{div} u_1) \phi_1 u_1^\perp \cdot \nu - 2 (\operatorname{div} u_2) \phi_2 u_2^\perp \cdot \nu \right\} ds \\ &= \frac{L}{2} \int_{\Gamma} \left\{ ((\operatorname{div} u_1)^2 - (\operatorname{div} u_2)^2) h + 2 (\phi_1 \operatorname{div} u_1 + \phi_2 \operatorname{div} u_2) (u_1 \cdot \tau) \right\} ds, \end{aligned} \quad (3.85)$$

where in the last line we used (3.58).

We turn now to the variation of the jump energy. By (3.83) we have

$$\begin{aligned} K(u^t(r^t(s)) \cdot \nu^t(s)) &\sim K(u(r(s)) \cdot \nu(s) + t(\phi_1(r(s)) - h'(s))(u_1(r(s)) \cdot \tau(s))) \\ &\sim K(u \cdot \nu) + tK'(u \cdot \nu)(\phi_1 - h')(u_1 \cdot \tau), \end{aligned}$$

where all terms in the last line are evaluated along Γ , that is, evaluated at $x = r(s)$. Then we can appeal to (3.75) to calculate that

$$\begin{aligned} \frac{d}{dt}_{|t=0} \int_{\Gamma^t} K(u^t \cdot \nu^t) ds &= \frac{d}{dt}_{|t=0} \int_{-s_0}^{s_0} \left\{ (K(u(r(s)) \cdot \nu(s)) + tK'(u(r(s)) \cdot \nu(s))(\phi_1(r(s)) - h'(s))(u_1(r(s)) \cdot \tau(s))) \right. \\ &\quad \left. - h'(s))(u_1(r(s)) \cdot \tau(s)) \right\} \left\{ 1 - th(s)\kappa(s) \right\} ds \\ &= \int_{\Gamma} K'(u \cdot \nu)(\phi_1 - h')(u_1 \cdot \tau) - K(u \cdot \nu)h\kappa ds \\ &= \int_{\Gamma} L(\operatorname{div} u_2 - \operatorname{div} u_1)(\phi_1 - h')(u_1 \cdot \tau) - K(u \cdot \nu)h\kappa ds, \end{aligned} \quad (3.86)$$

where in the last line we have used the criticality condition (3.54).

Combining (3.85) and (3.86) we obtain

$$\begin{aligned} \frac{d}{dt}_{|t=0} E_0(u^t) &= \int_{\Gamma} \left\{ \frac{L}{2} ((\operatorname{div} u_1)^2 - (\operatorname{div} u_2)^2) - K(u \cdot \nu)\kappa \right\} h ds \\ &\quad + L \int_{\Gamma} \{(\phi_1 + \phi_2)\operatorname{div} u_2 + (\operatorname{div} u_1 - \operatorname{div} u_2)h'\} (u_1 \cdot \tau) ds \\ &= \int_{\Gamma} \left\{ \frac{L}{2} ((\operatorname{div} u_1)^2 - (\operatorname{div} u_2)^2) - K(u \cdot \nu)\kappa \right\} h ds \\ &\quad + L \int_{\Gamma} (\operatorname{div} u_1 + \operatorname{div} u_2) (u_1 \cdot \tau)h' ds, \end{aligned}$$

in light of (3.82). Integrating by parts in the last integrals, and using that $h(-s_0) = h(s_0) = 0$ we finally obtain

$$\begin{aligned} \frac{d}{dt}_{|t=0} E_0(u^t) &= \int_{\Gamma} \left\{ \frac{L}{2} ((\operatorname{div} u_1)^2 - (\operatorname{div} u_2)^2) - L(\operatorname{div} u_1 + \operatorname{div} u_2)'(u_1 \cdot \tau) \right. \\ &\quad \left. - L(\operatorname{div} u_1 + \operatorname{div} u_2)(u_1 \cdot \tau)' - K(u \cdot \nu)\kappa \right\} h ds. \end{aligned}$$

Since criticality implies that this last integral must vanish for all h , we obtain (3.67).

The derivation of (3.68) follows along similar lines so we omit the details. One difference to note, however, is that in the presence of an area constraint on the measure of $\{u \equiv 0\}$, the normal component h of the vector field X along Γ must additionally satisfy the requirement

$$\int_{-s_0}^{s_0} h(s) ds = 0$$

so that the perturbed jump set preserves area to $O(t)$. This condition leads to the appearance of the Lagrange multiplier in (3.68). \square

Our last consequence of criticality for a vector field u with respect to the functional E_0 concerns the possible presence in Ω of a junction point P such that for some $R > 0$, the set $B(p, R) \cap J_u$ consists of four curves meeting at p . We wish to focus on the configuration where two of these curves, which we label as Γ_{01} and Γ_{03} , are interfaces separating an isotropic region, which we label as Ω_0 , from two disjoint regions, Ω_1 and Ω_3 , where u is given by $u_1 : \Omega_1 \rightarrow \mathbb{S}^1$ and $u_3 : \Omega_3 \rightarrow \mathbb{S}^1$, respectively. Wedged between Ω_1 and Ω_3 we assume there exists a set Ω_2 where u takes on another \mathbb{S}^1 -valued state u_2 . The dashed curve separating Ω_1 from Ω_2 , representing the wall across which u jumps from u_1 to u_2 we denote by Γ_{12} , and the dashed curve separating Ω_2 from Ω_3 , representing the wall across which u jumps from u_2 to u_3 we denote by Γ_{23} . We write τ_{ij} and ν_{ij} for the unit tangent and unit normal to the curve Γ_{ij} where each τ_{ij} points away from the junction P and ν_{ij} points from the region Ω_i into the region Ω_j . See Fig. 3.3.

Our reason for focusing on this particular configuration is predicated on the belief that it is somehow quite generic behavior in a neighborhood of a singular point on the isotropic-nematic phase boundary; see the discussion in Section 3.3.4. This belief is grounded in the findings of numerous numerical experiments we have conducted and examples we have constructed for this model, some of which appear in the penultimate section of this chapter. Our hope is that the condition derived in Theorem 3.2.12 below will be of use in constructing particular candidates for minimizers of E_0 as well as perhaps being of use in ruling out certain junction configurations that

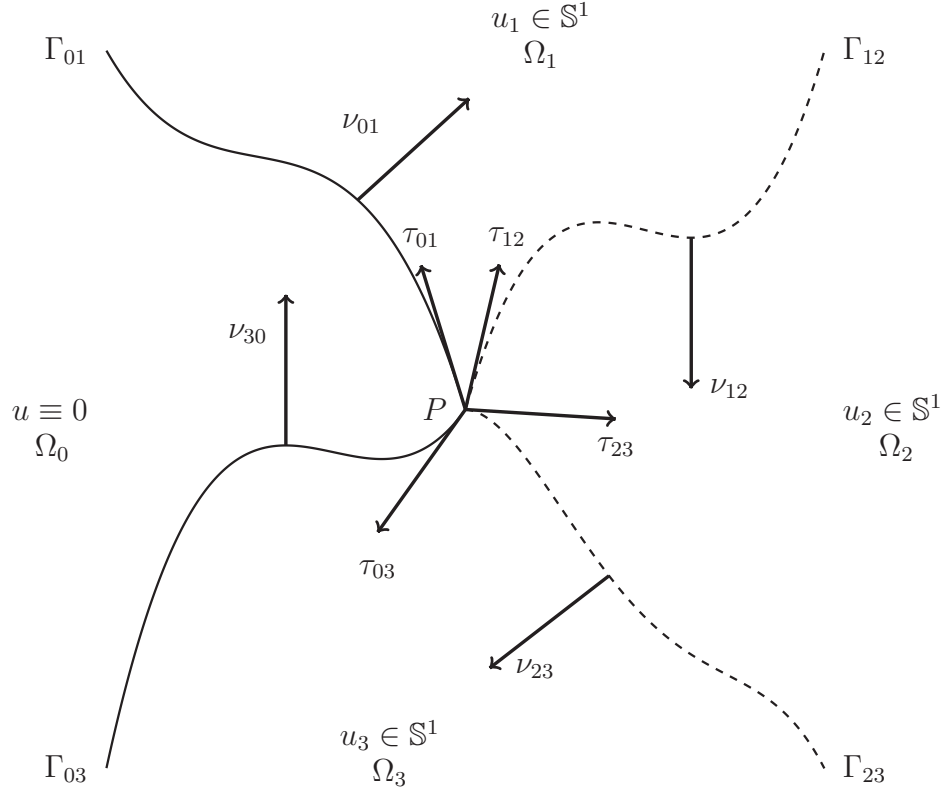


Figure 3.3: A configuration with a junction point P at which two components of the interface, Γ_{01} and Γ_{03} meet two components of the wall Γ_{12} and Γ_{23} .

are found to violate (3.152).

To state the next result we must introduce the notation τ_{ij} for the unit tangent on Γ_{ij} oriented so as to point away from P , and ν_{ij} for the unit normal to Γ_{ij} , pointing from region Ω_i into Ω_j .

Theorem 3.2.12. (*Criticality conditions at a junction*). *Assume a configuration in a neighborhood of a point $P \in \Omega$ as described above and as depicted in Fig. 3.3. Assume that in a neighborhood of P the functions u_j and their divergences $\operatorname{div} u_j$ for $j = 1, 2, 3$ are all smooth in the closure of Ω_j including at the junction point P . Assume further that the four curves $\Gamma_{01}, \Gamma_{12}, \Gamma_{23}$ and Γ_{03} are all smooth near P . Then criticality of E_0 with respect to variations of P , the four curves Γ_{ij} and*

the three functions u_j leads to the condition

$$\begin{aligned} & \frac{K(0)}{2}(\tau_{01} + \tau_{03}) + K(u_1 \cdot \nu_{12})\tau_{12} + K(u_2 \cdot \nu_{23})\tau_{23} \\ &= L \left\{ (\operatorname{div} u_1)(u_1 \cdot \tau_{01})\nu_{01} + (\operatorname{div} u_3)(u_3 \cdot \tau_{03})\nu_{03} \right\} \\ & \quad - L \left\{ (\operatorname{div} u_1 + \operatorname{div} u_2)(u_1 \cdot \tau_{12})\nu_{12} + (\operatorname{div} u_2 + \operatorname{div} u_3)(u_2 \cdot \tau_{23})\nu_{23} \right\} \end{aligned} \quad (3.87)$$

where all quantities above are evaluated at P .

The proof of Theorem 3.2.12 can be found in the appendix to Chapter 3.

3.3 Examples: Analytical Constructions for Large L and Some Numerics

We conclude with an exploration of possible morphologies for our limiting energy E_0 , which we recall is given by

$$E_0(u) = \frac{L}{2} \int_{\Omega} (\operatorname{div} u)^2 dx + \frac{K(0)}{2} \operatorname{Per}_{\Omega}(\{|u|=1\}) + \int_{J_u \cap \{|u|=1\}} K(u \cdot \nu) d\mathcal{H}^1,$$

with the cost K given by (3.21). After describing in Section 3.3.1 some numerics that complement our rigorous work in Section 3.2.3 for the case where Ω is a rectangle, we will focus on two main settings: (i) the case where Ω is a disk and competitors must satisfy a boundary condition in the sense of (1.21) where g has degree $k \in \mathbb{Z}$; and (ii) the case of an island of isotropic phase, generated by an area constraint, lying inside a nematic whose far field is given by \vec{e}_1 .

For both settings (i) and (ii) we will not work directly with E_0 but rather with a problem that at least formally can be viewed as the large L limit of E_0 , namely

$$E_0^\infty(u) := \frac{K(0)}{2} \operatorname{Per}_{\Omega}(\{|u|=1\}) + \int_{J_u \cap \{|u|=1\}} K(u \cdot \nu) d\mathcal{H}^1, \quad (3.88)$$

defined for $u \in (BV \cap H_{\operatorname{div}})(\Omega, \mathbb{S}^1 \cup \{0\})$ such that

$$\operatorname{div} u = 0 \quad \text{in } \Omega, \quad (3.89)$$

and perhaps supplemented by the condition $u_{\partial\Omega} \cdot \nu_{\partial\Omega} = g \cdot \nu_{\partial\Omega}$ on $\partial\Omega$ if one wishes to specify Dirichlet data $g : \partial\Omega \rightarrow \mathbb{S}^1 \cup \{0\}$, or such that $|\{u=0\}| = \text{const}$ or $|\{|u|=1\}| = \text{const}$ if one

wishes to specify an area constraint. We also note that the H_{div} requirement still enforces the condition that competitors have trace from the nematic side that is tangent to any interface, i.e. (3.17) where $u_- = 0$.

We will construct critical points for E_0^∞ that we expect to be local or even globally minimal and we observe that these divergence-free vector fields are competitors in the minimization of E_0 for finite L . Thus, we expect that they may well be close to critical points or *perhaps* even minimizers of E_0 when L is large. As we shall see, this expectation is supported by simulations on the gradient flow for E_ε where L is large but fixed and then ε is taken to be small.

Regarding all simulations in this section, we obtain critical points for the energy E_ε by simulating gradient flow for E_ε using the software package COMSOL [1]. Unless specified otherwise, we do not claim that solutions that we obtain are minimizers of E_ε or prove that these solutions converge to critical points of the limiting energy. We will infer such convergence in cases where we are able to show via an analytical construction that a similar looking critical point of E_0 does exist.

We consider E_0^∞ rather than E_0 here in part because, as we will describe below, the divergence-free condition (3.89) provides a rigidity that simplifies the search for critical points. We hasten to add, however, that to us minimization of E_0^∞ is a fascinating and nontrivial problem in its own right that one might view as a version of the Aviles-Giga limiting problem which allows for phase transitions, i.e. isotropic regions, as well as walls. Of course this entire project represents just an initial investigation of E_ε and E_0 that we hope will generate interest in future analysis of critical points and minimization of these functionals for L finite. In that vein, we hope the work in this section provides intuition and techniques that can be generalized, and that the criticality conditions derived in Section 3.2.4 provide some tools.

So what does criticality mean for E_0^∞ ? Within the nematic region where $|u| = 1$, but away from the jump set J_u , if we locally describe a competitor u via $u(x) = (\cos \theta(x), \sin \theta(x))$, then

(3.89) implies that

$$\nabla\theta \cdot (-\sin\theta, \cos\theta) = 0.$$

Defining the characteristic direction via $x'_1 = -\sin\theta$, $x'_2 = \cos\theta$ we see that θ and therefore u is constant along characteristics and further that u is orthogonal to characteristics and so one concludes in particular that:

Characteristics for E_0^∞ must be straight lines along which u is orthogonal and constant. (3.90)

This rigidity, familiar to those who work on Aviles-Giga, is what will allow us to carry out some of the analytical constructions in this section.

On the other hand, this amount of rigidity limits one's ability build a rich class of variations of E_0^∞ and so we will not attempt to directly compute $L = \infty$ analogues of the ODE's (3.67) or (3.68) or the junction condition (3.87).

3.3.1 Critical Points of E_0 in a Rectangle.

Here we take Ω to be the rectangle $(-0.2, 0.2) \times (-0.5, 0.5)$ and we seek critical points of the energy E_0 which satisfy the boundary conditions $u(\cdot, \pm 1/2) = \pm \vec{e}_1 = (\pm 1, 0)$ and satisfy periodic boundary conditions on the sides $x = \pm \frac{1}{2}$.

As discussed in Section 3.2.3, when restricting minimization of E_ε to one-dimensional competitors which in this case are functions of y , we obtain full Γ -convergence of the one-dimensional analog of E_ε to that of E_0 . Further, the behavior of minimizers of E_0 among one-dimensional competitors is determined by the value of L . When L exceeds a certain threshold, the bulk divergence contribution vanishes and the energy of a critical point is associated solely with a wall along the x -axis that separates the regions of zero divergence. When L falls below the threshold value, the bulk divergence contribution is present along with a cost of the wall associated with the jump set of the minimizer. When L tends to zero, the wall disappears and the energy minimizing vector field is essentially a linear interpolation of the boundary data.

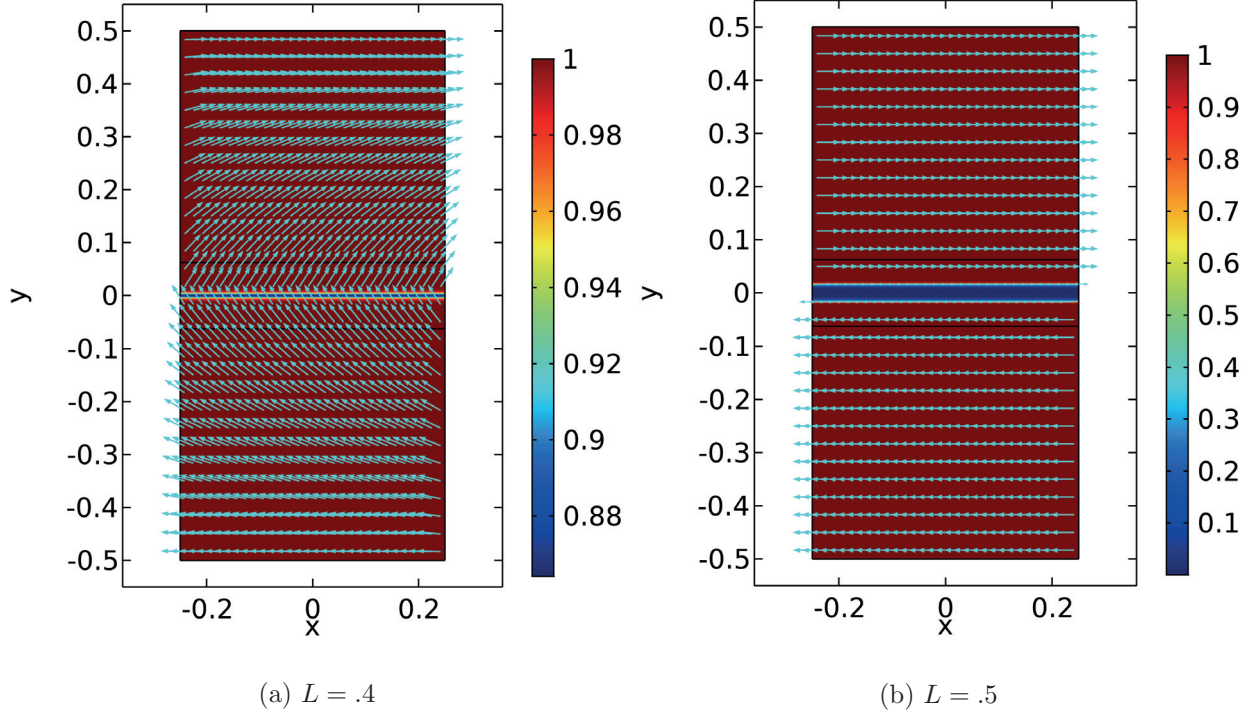


Figure 3.4: Critical points of E_ε in the rectangle. Here $\varepsilon = 0.001$.

Figs. 3.4-3.5 present the results of simulations for the gradient flow for E_ε in the rectangle. It is evident that, even though the simulations are fully two-dimensional, the critical points obtained in this way are one-dimensional and conform to the picture described in the previous paragraph. Two main observations follow from these figures. First, the results seem to indicate that the wall cost is indeed one-dimensional as we conjectured earlier in the chapter. Second, in all simulations done in the rectangle, the critical points we observe are always one-dimensional, even for large values of L . This is in contrast to the results in [45] for the version of the problem with the Ginzburg-Landau instead of the Chern-Simons-Higgs potential. In that work, one-dimensional critical points are found to be unstable with respect to formation of cross-tie configurations for large L —such instability does not seem to be present here, at least numerically.

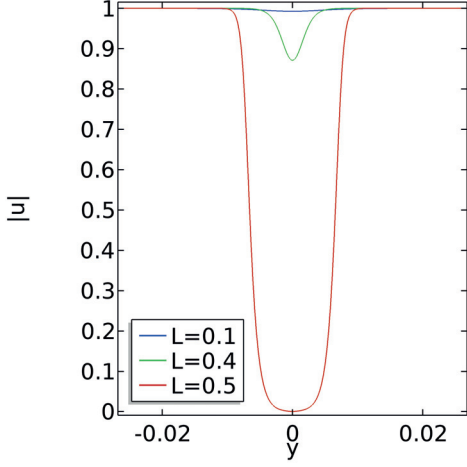


Figure 3.5: Cross-section of the wall for a critical point of E_ε in the rectangle. The y -axis is as shown in Fig. 3.4 and $\varepsilon = 0.001$. When $L \geq 0.5$, the profile is independent of L (not shown).

3.3.2 Degrees Other than 0 or 1 Are Too Costly

Before we begin the constructions and numerics pertaining to E_0^∞ , we first present a theorem which will elucidate the behavior of certain critical points for E_0 and provide an explanation for some of the morphology to come. The theorem yields a lower bound for the L^2 -norm of the divergence, in the spirit of analogous lower bound results of Jerrard [54] and Sandier [95] for the Ginzburg-Landau energy. The proofs of the Jerrard/Sandier results rely crucially on the fact that the square of the gradient of a function is a sum of squares of its components, a feature that is not shared by the square of the divergence of a vector field. We overcome this difficulty by working in Fourier space.

Theorem 3.3.1. *Fix $0 < \rho < \rho' \leq 1$, set $A := \{x \in \mathbb{R}^2 : \rho < |x| < \rho'\}$ and let C_t be a circle of radius t centered at the origin. Suppose that $u \in C^1(\bar{A}; \mathbb{R}^2)$ is such that $|u| \geq 1/2$ on A and $\deg(u, C_t) = d \neq 0, 1$ for any $t \in [\rho, \rho']$. Then*

$$\int_A (\operatorname{div} u)^2 dx \geq |\pi d \log(\rho'/\rho) + 4|, \quad d < 0, \quad (3.91)$$

$$\int_A (\operatorname{div} u)^2 dx \geq |\pi(d-1) \log(\rho'/\rho) - 4|, \quad d > 1. \quad (3.92)$$

Remark 3.3.2. By majorizing $\int_A (\operatorname{div} u)^2$ by $\int_A |\nabla u|^2$ in (3.91)-(3.92), it follows from results for $|\nabla u|^2$ that the scaling in ρ'/ρ is optimal. Note that there is no similar lower bound when $d = 1$ due to existence of the divergence-free vector field \vec{e}_θ .

Proof. The proof of this result proceeds using Fourier series.

1. Developing u in a Fourier series, given by

$$u \sim \sum_{n \in \mathbb{Z}} u_n(r) e^{in\theta},$$

we first derive a formula for the degree of u in terms of its Fourier coefficients. Denoting by u^t the restriction of u to C_t , and writing $u_n = f_n + ig_n$, we compute

$$\begin{aligned} d := \deg(u^t, C_t) &= \frac{1}{2\pi} \int_{C_t} u^t \times u_\tau^t d\mathcal{H}^1 \\ &= \frac{1}{2\pi} \int_{C_t} \sum_n n \begin{pmatrix} f_n \cos n\theta - g_n \sin n\theta \\ f_n \sin n\theta + g_n \cos n\theta \end{pmatrix} \times \begin{pmatrix} -f_n \sin n\theta - g_n \cos n\theta \\ f_n \cos n\theta - g_n \sin n\theta \end{pmatrix} \\ &= \sum_{n \in \mathbb{Z}} n (|f_n(t)|^2 + |g_n(t)|^2) \end{aligned} \tag{3.93}$$

$$= \sum_{n \in \mathbb{Z}} n |u_n(t)|^2, \tag{3.94}$$

where in the last line we have used orthogonality.

2. As in the proof of Thm. 5.1 in [45], we find

$$\operatorname{div} u = \sum_{n \in \mathbb{Z}} \operatorname{div} V_n,$$

in L^2 , where we have

$$\begin{aligned} \operatorname{div} V_1 &= \left(f'_1(r) + \frac{f_1(r)}{r} \right), \\ \operatorname{div} V_n &= \left(f'_n(r) + \frac{nf_n(r)}{r} \right) \cos(n-1)\theta - \left(g'_n(r) + \frac{ng_n(r)}{r} \right) \sin(n-1)\theta. \quad n \neq 1. \end{aligned}$$

It follows that

$$\begin{aligned}
\frac{1}{\pi} \int_A (\operatorname{div} u)^2 &= 2 \int_{\rho}^{\rho'} \left(f'_1 + \frac{f_1}{r} \right)^2 r dr + \sum_{n \neq 1} \int_{\rho}^{\rho'} \left(\left(f'_n + \frac{nf_n(r)}{r} \right)^2 + \left(g'_n + \frac{ng_n(r)}{r} \right)^2 \right) r dr \\
&\geq \int_{\rho}^{\rho'} \left[2 \frac{f_1^2}{r} + \sum_{n \neq 1} \frac{n^2(f_n(r)^2 + g_n(r)^2)}{r} \right] dr \\
&\quad + \int_{\rho}^{\rho'} \left[4f_1(r)f'_1(r) + \sum_{n \in \mathbb{Z}, n \neq 1} 2n(f_n(r)f'_n(r) + g_n(r)g'_n(r)) \right] dr \\
&:= I + II.
\end{aligned}$$

We estimate the integrals I and II separately as follows, beginning with II . From Eqn. (3.93) and the assumption that $\deg(u, C_t) = d$ for each $t \in [\rho, \rho']$, we obtain that for each r

$$\begin{aligned}
II &= \int_{\rho}^{\rho'} \frac{\partial}{\partial r} \left[2f_1^2 + \sum_{n \in \mathbb{Z}, n \neq 1} n(f_n^2 + g_n^2) \right] dr \\
&= \int_{\rho}^{\rho'} \frac{\partial}{\partial r} \left[f_1^2 - g_1^2 + \sum_{n \in \mathbb{Z}} n(f_n^2 + g_n^2) \right] dr \\
&= \int_{\rho}^{\rho'} \frac{\partial}{\partial r} [f_1^2 - g_1^2 + d] dr \\
&= f_1(\rho')^2 - f_1(\rho)^2 + g_1(\rho)^2 - g_1(\rho')^2. \tag{3.95}
\end{aligned}$$

Using now the definition of f_1, g_1 , and the fact that $|u| \leq 1$, we find that $\|f_1\|_{\infty}, \|g_1\|_{\infty} \leq 1$. It follows that

$$|II| \leq 4. \tag{3.96}$$

We next turn to estimating I . Let us first suppose $d > 1$. We have

$$\begin{aligned} I &\geq \int_{\rho}^{\rho'} \left(\frac{f_1(r)^2}{r} + \sum_{n \in \mathbb{Z}, n \neq 1} \frac{n^2(f_n(r)^2 + g_n(r)^2)}{r} \right) dr \\ &= \int_{\rho}^{\rho'} \left(\frac{f_1(r)^2}{r} + \sum_{n \in \mathbb{Z}, n \neq 1} \frac{(n^2 - n)(f_n(r)^2 + g_n(r)^2)}{r} + \frac{n(f_n(r)^2 + g_n(r)^2)}{r} \right) dr \\ &\geq \int_{\rho}^{\rho'} \left(\frac{f_1(r)^2}{r} + \sum_{n \in \mathbb{Z}, n \neq 1} \frac{n(f_n(r)^2 + g_n(r)^2)}{r} \right) dr \end{aligned} \tag{3.97}$$

$$= \int_{\rho}^{\rho'} \frac{d - g_1^2(r)}{r} dr \tag{3.98}$$

$$\geq \int_{\rho}^{\rho'} \frac{d - 1}{r} dr \tag{3.99}$$

$$= (d - 1) \log(\rho'/\rho). \tag{3.100}$$

In going from (3.97) to (3.98) we have used (3.100) while in going from (3.98) to (3.99) we have used that $g_1^2 \leq 1$. This completes the proof of the theorem when $d > 1$, so we turn our attention to when $d < 0$. In this case, we have

$$\begin{aligned} I &\geq \int_{\rho}^{\rho'} \left(\frac{f_1(r)^2}{r} + \sum_{n \in \mathbb{Z}, n \neq 1} \frac{n^2(f_n(r)^2 + g_n(r)^2)}{r} \right) dr \\ &= \int_{\rho}^{\rho'} \left(\frac{f_1(r)^2}{r} + \sum_{n \in \mathbb{Z}, n \neq 1} \frac{(n^2 + n)(f_n(r)^2 + g_n(r)^2)}{r} - \frac{n(f_n(r)^2 + g_n(r)^2)}{r} \right) dr \\ &\geq \int_{\rho}^{\rho'} \sum_{n \in \mathbb{Z}} -n \frac{f_n^2(r) + g_n^2(r)}{r} dr \\ &\geq -d \int_{\rho}^{\rho'} \frac{1}{r} dr \\ &= -d \log(\rho'/\rho) = |d| \log(\rho'/\rho). \end{aligned}$$

□

It also is worth mentioning that among degree 1 singularities, the L^2 -norm of the divergence can vary greatly and may or may not satisfy a lower bound of the type in the previous theorem. For example, for a Ginzburg-Landau vortex $\frac{x}{|x|}$, the L^2 -norm of the divergence taken over an annulus

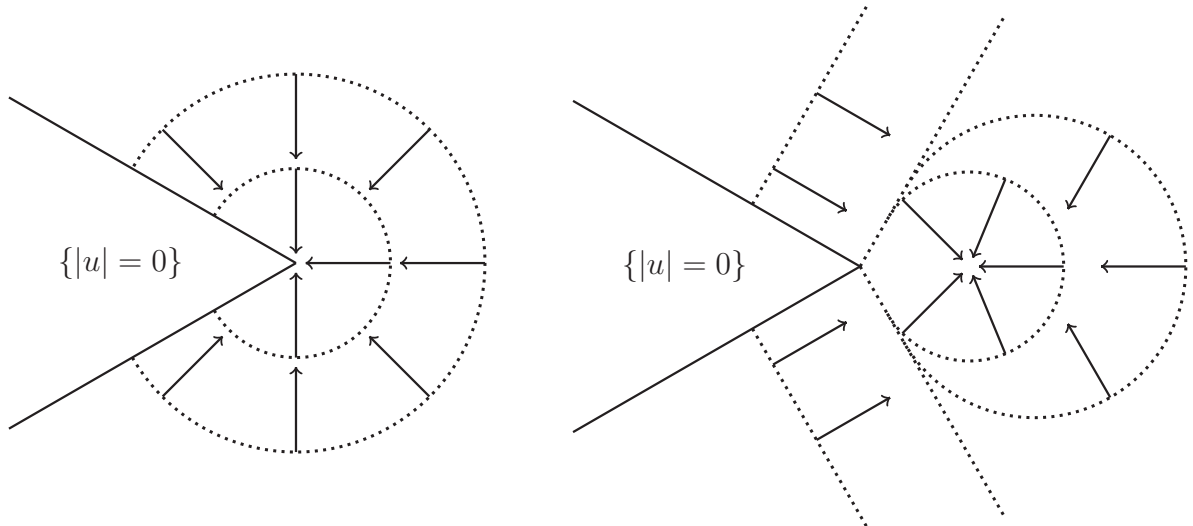


Figure 3.6: Corner on an interface at which u changes tangency: If there are no walls, a Ginzburg-Landau vortex forms in one of two ways, resulting in infinite E_0 energy. The dotted lines represent characteristics, and the arrows represent the \mathbb{S}^1 -valued director, which is perpendicular to the characteristics.

centered at the origin blows up logarithmically as the inner radius approaches 0. However, an \vec{e}_θ vortex, given by $\frac{x^\perp}{|x|}$, is divergence free. This observation is relevant to our model, especially at corner-type defects on the phase boundary. In many of our examples, the director u , which must be tangent to the phase boundary, switches the sense of tangency at a corner. If such a switch occurs at a corner of the phase boundary in the interior of the domain, then walls must intersect the defect in order to avoid infinite energy from the bulk divergence term; see Fig. 3.6. Conversely, if u does not change its sense of tangency at a corner on the interface, then the singularity can be locally resolved by the formation of a partial \vec{e}_θ vortex in which an infinite family of characteristics emanate from the defect.

3.3.3 Critical Points of E_0 and E_0^∞ in a Disk.

In this section we consider critical points of the energy E_0^∞ in the disk Ω of radius R among competitors satisfying the boundary condition

$$u\left(R \cos \frac{s}{R}, R \sin \frac{s}{R}\right) \cdot \nu_{\partial \Omega} = (\cos(ks + \alpha), \sin(ks + \alpha)) \cdot \nu_{\partial \Omega} \quad \text{for } s \in [0, 2\pi R], \quad (3.101)$$

where $k \in \mathbb{Z}$, $\alpha \in \mathbb{R}$, and the boundary is parametrized with respect to arc-length.

The simplest cases to consider are $(k, \alpha) = (1, \pi/2)$ and when $k = 0$ for which minimizers of E_0 are the divergence-free vortex

$$u_0 = \vec{e}_\theta = \left(\frac{-y}{\sqrt{x^2 + y^2}}, \frac{x}{\sqrt{x^2 + y^2}} \right),$$

and the constant state

$$u_0 = (\cos \alpha, \sin \alpha),$$

respectively. Indeed, trivially, in both cases $E_0(u_0) = \min E_0 = 0$. Hence our principal interest in this section will be to understand the behavior of critical points for other choices of (k, α) .

We begin by considering the case where k is a negative integer and $\alpha = \pi$. To gain some insight into how these boundary conditions influence the morphology of interfaces and walls, we present in Figure 3.7 the large-time asymptotics for gradient flow dynamics for the energy E_ε with boundary conditions $u|_{\partial \Omega} = -(\cos ks, \sin ks)$ for two values of L . Then in Figure 3.8 we present simulations for data with degrees -2 and -3 . Although we do *not* impose an area constraint in these simulations in order to induce a phase transition, these numerics nonetheless indicate a substantial presence of the isotropic phase in the form of an island with $2|k| + 2$ boundary singularities. Generally speaking, these islands appear to grow in size as $|k|$ grows, and for $k < -1$, both configurations with a single or multiple vortices are possible. Studies on vortices using the Ginzburg-Landau potential such as [19] or—more appropriately to this study—the Chern-Simons-Higgs potential with $L = 0$ in the elastic energy [63] tempt one to think of these islands for $\varepsilon > 0$ as “defects”

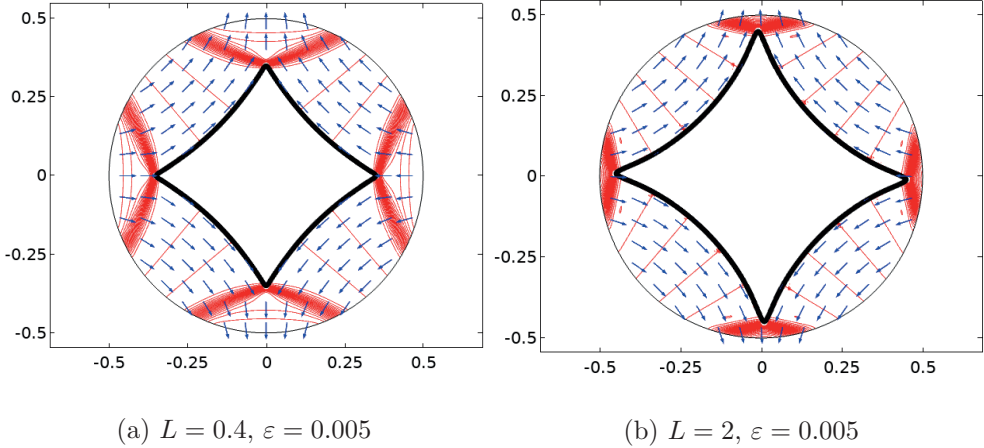


Figure 3.7: Critical points of E_ε for $(k, \alpha) = (-1, \pi)$. The red curves represent level sets of $\operatorname{div} u$ while $|u| = 0.5$ on the black curves that enclose the isotropic phase.

arising from the negative degree boundary condition. However, the numerics and Theorem 3.3.1 indicate that the cores of the defects do not shrink in the $\varepsilon \rightarrow 0$ limit. Indeed, from Theorem 3.3.1 it follows that a defect with a negative degree must either be inside an isotropic region or have walls originating from the defect. The latter situation was, in fact, observed in [45] for the degree -1 defects while the Ginzburg-Landau potential considered in [45] did not allow for presence of interfaces.

We now provide some analytical evidence that supports the observations in Figs. 3.7-3.8. Motivated by the gradient flow simulations, we construct critical points for E_0^∞ and so divergence-free competitors for E_0 . These constructions will have only interface, but no walls, with singular points of the interface always touching the boundary of the disk, though of course the numerics suggest that for L finite, there should exist walls branching off the phase boundary singularities and attaching to $\partial\Omega$.

Example 3.3.3. In this example, $\Omega = B(0, 1)$, and we are interested in competitors which exhibit the symmetry

$$u\left(e^{\pi i/(k+1)}x\right) = e^{-\pi ki/(k+1)}u(x) \quad \text{for } k \in \mathbb{N}. \quad (3.102)$$

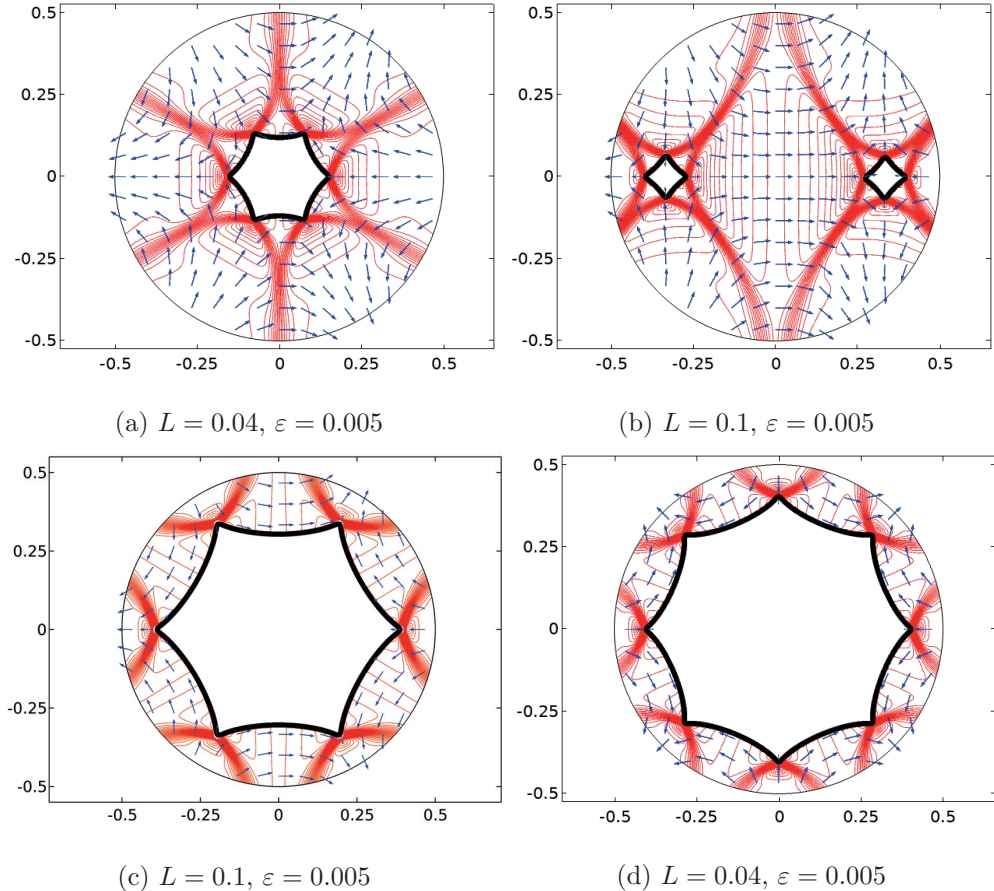


Figure 3.8: Critical points of E_ε for (a-c): $(k, \alpha) = (-2, \pi)$ and (d): $(k, \alpha) = (-3, \pi)$. The red curves represent level sets of $\operatorname{div} u$ while $|u| = 0.5$ on the black curves that enclose the isotropic phase. The configurations (b) and (c) are obtained starting from different initial conditions. Configuration (b) has slightly lower energy in E_ε .

This is the symmetry exhibited by the configurations in Figs. 3.7-3.8. The construction will proceed by issuing characteristics off $\partial\Omega$ and by adhering to the condition (3.90).

Owing to the condition (3.102), we construct a critical point of E_0^∞ in the sector S corresponding to $[0, \pi/(k+1)]$ and then extend the construction to the rest of the domain by symmetry. Shifting out of complex notation and parametrizing $\partial\Omega \cap \partial S$ by $(\cos s, \sin s)$ for $s \in [0, \pi/(k+1)]$, we will insist that $u|_{\partial\Omega} = (-\cos ks, \sin ks)$, rather than just having agreement between the normal component of u and that of the data.

Integrating the characteristic equations then yields

$$(x_1(s, t), x_2(s, t)) = (\cos s, \sin s) - t(\sin ks, \cos ks) \quad (3.103)$$

$$u(x_1(s, t), x_2(s, t)) = (-\cos ks, \sin ks), \quad (3.104)$$

with $s \in [0, \pi/(k+1)]$, $t \geq 0$. We represent the interface in the form

$$(p(s), q(s)) := (x_1(s, t(s)), x_2(s, t(s)))$$

for an appropriate arrival time $t(s) \geq 0$. Here, for each s , a characteristic arrives at the interface at the time $t(s)$ and we require that u at the point of arrival is tangent to the interface, that is

$$(p'(s), q'(s)) = \alpha(u(p(s)), u(q(s))) \text{ for some } \alpha \in \mathbb{R}.$$

Using this expression in (3.103), we find that

$$x'_1(s, t(s)) = -\sin s - t'(s) \sin ks - kt(s) \cos ks = -\alpha \cos ks,$$

$$x'_2(s, t(s)) = \cos s - t'(s) \cos ks + kt(s) \sin ks = \alpha \sin ks.$$

Upon rearrangement, we have

$$-\sin s + \alpha \cos ks - kt(s) \cos ks = t'(s) \sin ks,$$

$$\cos s - \alpha \sin ks + kt(s) \sin ks = t'(s) \cos ks.$$

Multiplying these equations by $\sin ks$ and $\cos ks$, respectively, and adding the results gives

$$t' = -\sin s \sin ks + \cos s \cos ks = \cos(k+1)s.$$

Integration then yields

$$t(s) = \frac{1}{k+1} \sin(k+1)s + c.$$

Motivated by numerics, we seek an interface that meets $\partial\Omega$ at $(1, 0)$, so that $t(0) = 0$. Then $c = 0$, so that $t(s) = \frac{1}{k+1} \sin(k+1)s$. The parametric equation of the interface in the sector S is now given by

$$p(s) = \cos s - \frac{1}{k+1} \sin(k+1)s \sin ks = \left(1 - \frac{1}{2(k+1)}\right) \cos s + \frac{1}{2(k+1)} \cos(2k+1)s, \quad (3.105)$$

$$q(s) = \sin s - \frac{1}{k+1} \sin(k+1)s \cos ks = \left(1 - \frac{1}{2(k+1)}\right) \sin s - \frac{1}{2(k+1)} \sin(2k+1)s. \quad (3.106)$$

Extending the interface to all of Ω via the symmetry condition (3.102), we obtain a closed curve with $2(k+1)$ evenly-spaced cusps. When $k = 1$ one checks that $p(s) = \cos^3 s$ and $q(s) = \sin^3 s$ and the interface satisfies the equation $x_1^{2/3} + x_2^{2/3} = 1$. In Fig. 3.9 we compare the graph of this curve with the contour line $|u| = 0.5$ for the critical point obtained numerically via gradient flow when $L = 2$. It is clear that the two curves are very close to each other, which is quite striking since one might only expect a strong connection between the critical points of E_ε and E_0^∞ for L large.

One can also check that for the construction obtained above, the area of the isotropic island increases with $|k|$. In fact, a calculation that we omit goes to show that in the $k \rightarrow \infty$ limit, the isotropic region fills the entire disk!

The preceding calculation can also be used in the case of $L < \infty$ in order to reconstruct parts of critical points of E_0 . Recall that, in this case, by Corollary 3.2.10, the characteristics are circular arcs of finite radii that may run directly from the interface to $\partial\Omega$. In Fig. 3.7, for example, red curves correspond to level sets of $\operatorname{div} u$ and thus the characteristics for u connect large portions of the interface to the boundary. In order to fully reproduce the critical point of E_0 completely,

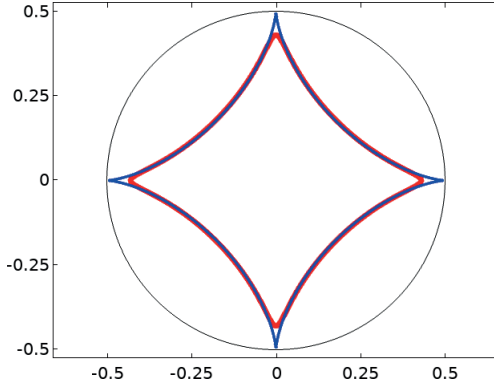


Figure 3.9: Contour line $|u| = 0.5$ for the critical point with $(k, \alpha) = (-1, \pi)$ obtained via gradient flow (red) and the plot of $x_1^{2/3} + x_2^{2/3} = 1$ (blue). Here $L = 2$ and $\varepsilon = 0.005$.

however, one needs to allow for the presence of walls, as evidenced by the gradient flow numerics in Fig. 3.7. Although a similar approach yielded critical points of (1.18) for degree -1 boundary data in [45], such a construction will be more elaborate here and we do not pursue this issue further in the present work.

We conclude this section by considering the boundary data in (3.101) corresponding to k positive and $\alpha = 0$. The results of the gradient flow simulations are shown in Fig. 3.10. Not surprisingly, when L is small for $k = 2$, the stable configuration consists of two degree one vortices looking locally like \vec{e}_θ , see Fig. 3.10a. As L increases, however, these vortices collapse onto and spread along $\partial\Omega$ while forming two walls along the upper and lower halves of the boundary, respectively, cf. Fig. 3.10b. Indeed this simulation suggests that for E_0 with L large, the preferred state is $u \equiv \vec{e}_1$. In fact, if one tries to construct a competitor u having a ‘boundary wall’ for this boundary data, that is, a unit vector field such that the normal component of the data is met but the tangential component switches sign, then one finds

$$u \cdot \nu_{\partial\Omega} = (\cos 2s, \sin 2s) \cdot (\cos s, \sin s) = \cos s = \vec{e}_1 \cdot (\cos s, \sin s)$$

and

$$u \cdot \tau_{\partial\Omega} = -(\cos 2s, \sin 2s) \cdot (-\sin s, \cos s) = -\sin s = \vec{e}_1 \cdot (-\sin s, \cos s).$$

Thus such a competitor u must have trace \vec{e}_1 along $\partial\Omega$ and there is no need then to accumulate divergence inside the disk by varying from constancy.

In the case of a degree 3 boundary data, cf. Figure 3.10c, the behavior is more complex—the degree 3 vortex appears to split into four degree 1 vortices and one degree -1 vortex. The four $+1$ vortices approach the boundary of the domain with an increasing L while the degree -1 vortex remains at the center of the disk.

We use the simulations in the case of $(k, \alpha) = (2, 0)$ to test Conjecture (3.25) on the one-dimensional character of the wall cost. The walls in this example turn out to be significantly deeper than in other cases that we considered and it is therefore easier to compare the numerically computed wall profiles with the corresponding heteroclinic connection. Consider the critical point for E_ε depicted in Fig. 3.10b. For a large value of L the defects present inside Ω for small ε spread along the boundary to form two boundary walls. Due to symmetry, it is sufficient to consider the wall in the first quadrant. Then along each ray emanating at angle θ from the origin, the wall connects the vector $\vec{e}_1 = (1, 0)$ to the vector $(\cos 2\theta, \sin 2\theta)$. Because the normal to the boundary/interface is $(\cos \theta, \sin \theta)$, the normal component of the vector field is continuous across the wall, while the tangential component reverses sign. The jump in the tangential component across the wall grows as θ changes from 0 to $\pi/2$. In Fig. 3.11a we plot cross-sections of $|u|$ for the critical point of E_ε shown in Fig. 3.10b, where the cross-sections are shown along several rays $\theta = \text{const}$. In Fig. 3.11b, the same scaled and translated profiles are shown together with the corresponding solutions of the ODE that describes a heteroclinic connection associated with E_ε , assuming one-dimensional cost. As Fig. 3.11b demonstrates, the graphs are close to each other for all respective values of θ —this is in agreement with our conjecture that the cost is one-dimensional.

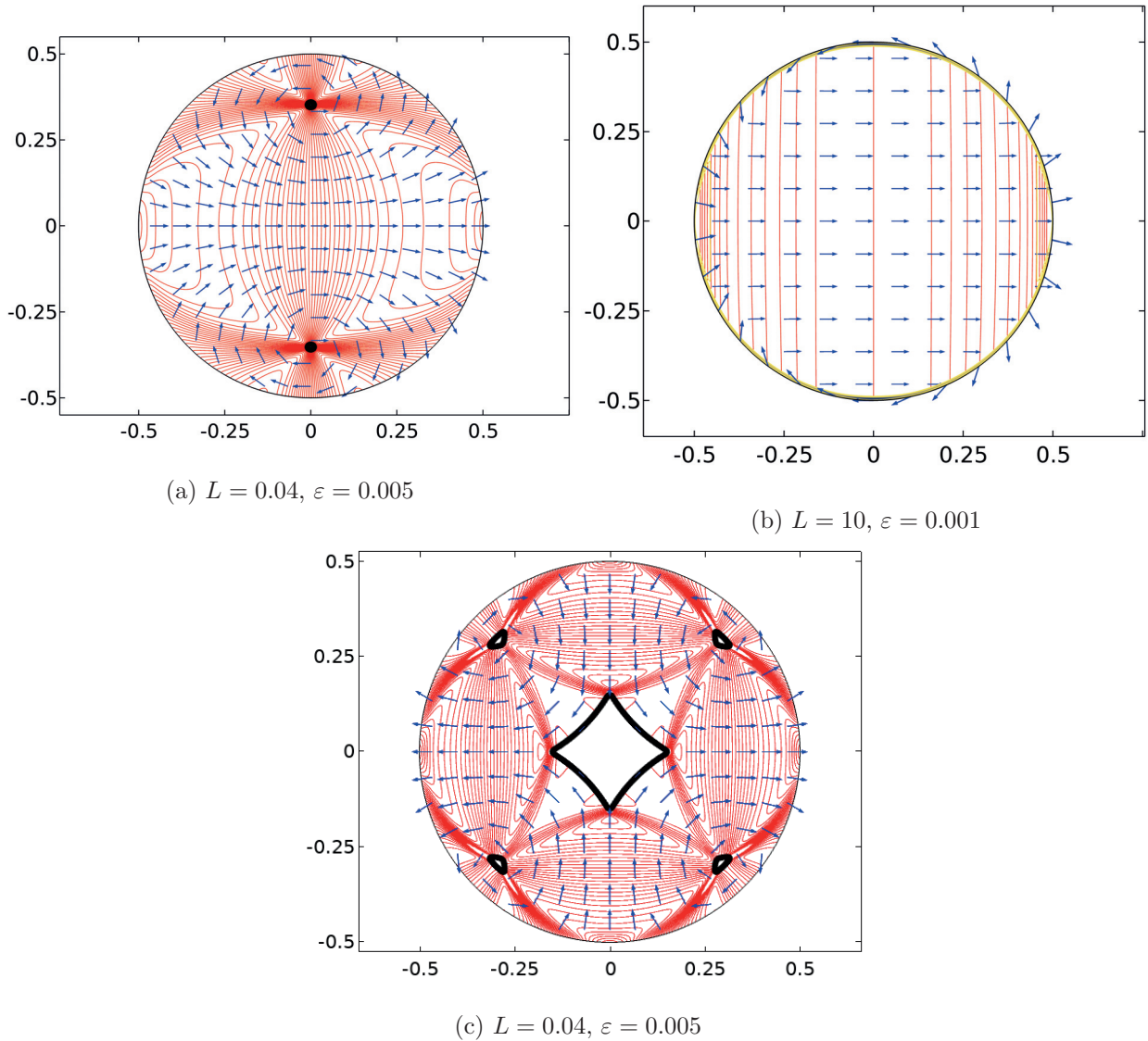


Figure 3.10: Critical points of E_ε for (a-b): $(k, \alpha) = (2, 0)$ and (c): $(k, \alpha) = (3, 0)$. The red curves represent level sets of $\text{div } u$ while $|u| = 0.5$ on the black curves that enclose the isotropic phase. The wall adjacent to the boundary in plot (b) is indicated in yellow.

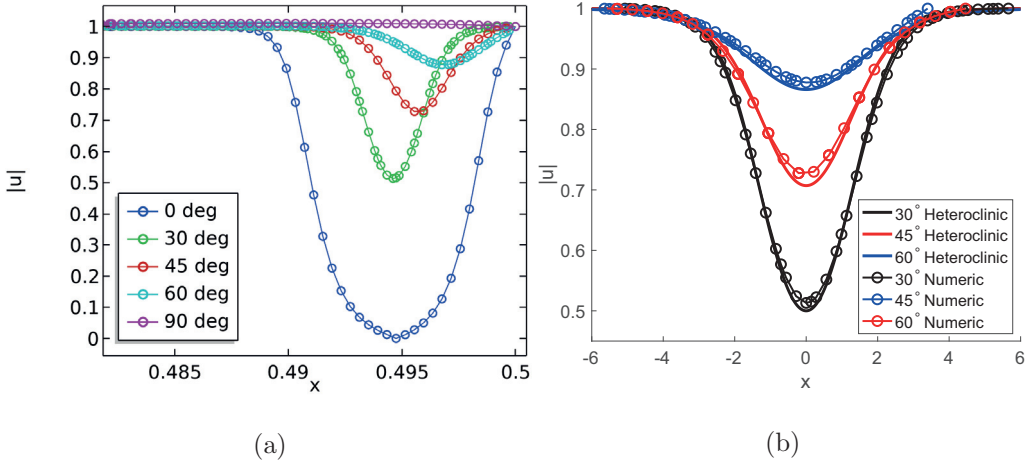


Figure 3.11: Wall cost is one-dimensional for the critical point shown in Fig. 3.10b. (a) Cross-sections of Fig. 3.10b in the direction of angle θ . Only parts of cross-sections closest to the boundary are shown; (b) Comparison between the numerical and analytical wall profiles.

3.3.4 Examples for Degree Zero Boundary Data

In this section, we analytically and numerically construct an example with an isotropic tactoid which exhibits two defects on the phase boundary. Let us describe a key feature of this example. Recall that at a nematic-isotropic interface for E_0 , the trace of a $BV \cap H_{\text{div}}$ competitor u from the nematic region is tangent to the interface, cf. (3.17). If, for example, u is smooth and does not change the sense of tangency along the interface, then the degree of u around any connected component of the interface is 1. If we specify a degree 0 boundary condition around $\partial\Omega$ or at infinity, this mismatch can be rectified by the presence of two defects along the interface, similar to the construction of the recovery sequence in Section 3.1. This is the effect we will see in the following example.

We begin with some numerics. Fig. 3.14a shows the result of gradient flow simulation in a large rectangular domain with constant boundary data \vec{e}_1 . We observe in Fig. 3.14a that (i) the interface surrounds a single isotropic island, (ii) there appear to be two walls which intersect the

two defects on the interface, and (iii) the solutions possess the symmetries

$$(u_1(x_1, x_2), u_2(x_1, x_2)) = (u_1(x_1, -x_2), -u_2(x_1, -x_2))$$

and

$$(u_1(x_1, x_2), u_2(x_1, x_2)) = (u_1(-x_1, x_2), -u_2(x_1, -x_2)).$$

Furthermore, in Fig. 3.14a we see that (iv) the walls divide the plane into three regions, with

$$u \equiv \vec{e}_1 \text{ in the two regions not containing the isotropic tactoid.} \quad (3.107)$$

This simulation, though depicting transient behavior, leads us to seek a critical point of E_0^∞ satisfying (i)-(iv) consisting of an isotropic tactoid in an infinite sea of nematic, where in the far field, $u \rightarrow \vec{e}_1$. To induce a static—and presumably stable—critical point having an isotropic phase, we will enforce an area constraint of the form $|\{u = 0\}| = const.$

The complication here—and it is a significant one—is that an interface and a wall are rigidly linked via the straight-line characteristics lying in between them, and the requirement of tangency of u along the interface and agreement of the normal component of u with that of \vec{e}_1 along the wall make the construction rather daunting.

Somewhat surprisingly, we are able to achieve this construction by deriving a formula of the form

$$E_0^\infty(u) = \int_{\partial\{|u|=1\}} f(\theta) d\mathcal{H}^1 \quad (3.108)$$

for an explicit f , for competitors u satisfying (i)–(iv), where θ is the angle the tangent vector to $\partial\{|u|=1\}$ makes with the horizontal. For such u , the energy E_0^∞ therefore only depends on the interface, a reflection of the afore-mentioned rigidity of this problem. We then consider variations of the interface to derive an ODE (3.132) for θ along with the junction condition (3.133) at the intersection of walls and interfaces. Numerically integrating this ODE yields a configuration which closely resembles the results of the simulations shown in Figure 3.14a, cf. Figure 3.14b.

The Role of Walls: Before embarking on this construction, let us comment on the role of walls in this example. A natural question is: given these conditions, namely an area constraint on the isotropic region and the requirement that $u \equiv \vec{e}_1$ in the far field, is it necessary for a critical point to have walls? While we do not as yet have a proof, we believe the answer is yes. Let us present some heuristic arguments to this effect. Working within the symmetry assumption (iii), consider the possibility of constructing a competitor without walls. Then one of the two configurations depicted in Fig. 3.12 are possible where the isotropic island either has two corners and no walls or it has two cusps and no walls. In the former case, one can show that partial vortices should form near the corners in the nematic phase, causing the divergence contribution to the energy to blow up; see Fig. 3.6 above. If there are two cusps and no walls, Fig. 3.12 demonstrates that this is not possible as the characteristics emanating from the interface would have to intersect non-tangentially. In light of these observations, junctions between interfaces and walls appear to be fairly generic, making in particular the junction condition (3.87) potentially important when analyzing candidates for possible critical points or minimizers when L is finite.

Example 3.3.4. For this calculation, by (iii), it suffices to consider the problem in the first quadrant Q_1 . Let us assume that $\partial\{|u| = 1\} \cap Q_1$ is smooth and can be parametrized by $r(\sigma)$ where $r : [0, L] \rightarrow Q_1$, with $r(0)$ on the x_1 -axis and $r(L)$ on the x_2 -axis; see Figure 3.13. We do not assume that the interface is parametrized by the arclength variable s in this derivation. Then

$$r'(\sigma)/|r'(\sigma)| = \tau(\sigma) = (\cos \theta(\sigma), \sin \theta(\sigma)) = -u(r(\sigma)). \quad (3.109)$$

Let us define

$$\rho(\sigma) = |r'(\sigma)|,$$

and the normal vector

$$\nu(\sigma) = (\sin \theta(\sigma), -\cos \theta(\sigma)).$$

We now deduce the location of the wall, which we will see is determined by the interface. Recall

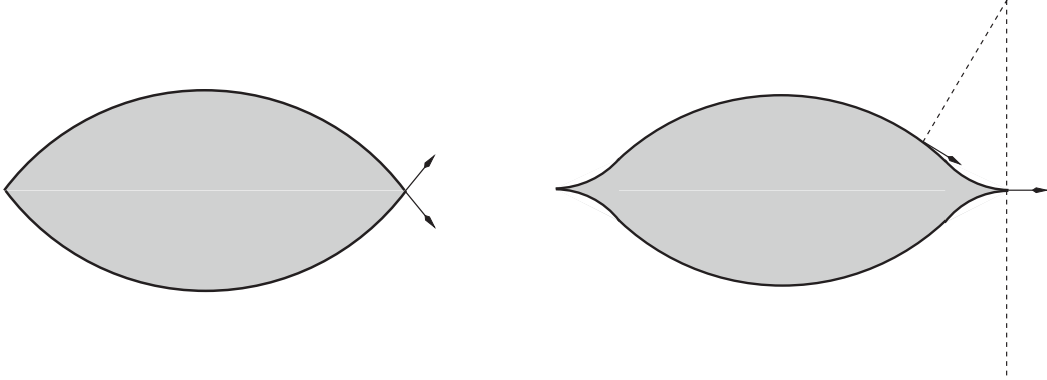


Figure 3.12: An isotropic island (marked in gray) surrounded by the nematic medium in \mathbb{R}^2 without wall singularities and satisfying $u = \vec{e}_1$ at infinity. The vector field is tangent to the boundary of the island and switches the sense of tangency at the boundary singularities. Left: the island has a corner and thus an infinite energy E_0 due to the bulk divergence term—cf. Fig. 3.6. Right: the island has a cusp—impossible without a wall since the characteristics will intersect. Characteristics are indicated by the dashed lines.

that in light of (3.90), u is perpendicular to the straight characteristics, which themselves intersect the interface perpendicularly, so we can parametrize the wall by shooting characteristics off of the interface until they hit the wall. We can write a parametrized path \tilde{r} for the wall then as

$$\tilde{r}(\sigma) := r(\sigma) + t(\sigma)\nu(\sigma). \quad (3.110)$$

Hence by (3.109) the trace of u on the wall from the left, denoted here by \tilde{u} , is given by

$$\tilde{u}(\sigma) = -(\cos \theta(\sigma), \sin \theta(\sigma)). \quad (3.111)$$

We define a function ψ by the equation

$$\tilde{r}'(\sigma) = |\tilde{r}'(\sigma)|(\cos \psi(\sigma), \sin \psi(\sigma)).$$

Then the tangent and normal vectors to the wall are given by

$$\tilde{\tau} = (\cos \psi, \sin \psi) \quad \text{and} \quad \tilde{\nu} = (\sin \psi, -\cos \psi). \quad (3.112)$$

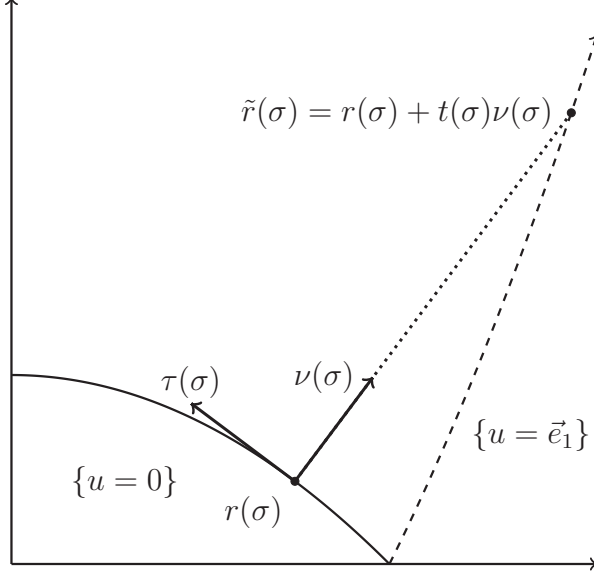


Figure 3.13: The isotropic island is surrounded by the nematic region. The dotted line represents a straight line characteristic, and the dashed line represents the wall.

Next, we collect some relations between several of the above quantities which will be useful in the following calculations. From the continuity of the normal traces across a wall, we have

$$\tilde{u} \cdot \tilde{\nu} = \vec{e}_1 \cdot \tilde{\nu},$$

which we rewrite using (3.111), (3.112), and the angle subtraction identity for sin as

$$\sin(\theta - \psi) = \sin \psi. \quad (3.113)$$

Similarly, the condition $\tilde{u} \cdot \tilde{\tau} = -\vec{e}_1 \cdot \tau$ for the tangential components across a wall, cf. (3.17), can be expressed as

$$\cos(\theta - \psi) = \cos \psi. \quad (3.114)$$

From (3.113), (3.114) it follows that $\psi = \theta/2 + k\pi$ for some integer k , and k is in fact 0 since at $\sigma = 0$, $\psi(0) \leq \theta(0) \leq \psi(0) + \pi/2$. Thus

$$\psi = \theta/2. \quad (3.115)$$

We can now write the energy $E_0(u, Q_1)$ in the first quadrant as

$$\begin{aligned} E_0(u, Q_1) &= \frac{K(0)}{2} \text{Per}_{Q_1}(\{|u|=1\}) + \int_{J_u \cap \{|u|=1\}} K(u \cdot \nu) d\mathcal{H}^1 \\ &= \int_0^L \left(\frac{K(0)}{2} |r'(\sigma)| + K(\vec{e}_1 \cdot \tilde{\nu}(\sigma)) |\tilde{r}'(\sigma)| \right) d\sigma. \end{aligned} \quad (3.116)$$

One can use (3.110) and the orthogonality of τ and ν to easily calculate

$$|\tilde{r}'| = ((\rho + t\theta')^2 + (t')^2)^{1/2}.$$

Substituting this and

$$\vec{e}_1 \cdot \nu = \sin \psi = \sin(\theta/2)$$

into (3.116) yields

$$\begin{aligned} E_0(u, Q_1) &= \int_0^L \left(\frac{K(0)}{2} |r'| + K(\sin(\theta/2)) ((\rho + t\theta')^2 + (t')^2)^{1/2} \right) d\sigma \\ &= \int_{\partial\{|u|=1\}} \frac{K(0)}{2} d\mathcal{H}^1 + \int_0^L \left(K(\sin(\theta/2)) ((\rho + t\theta')^2 + (t')^2)^{1/2} \right) d\sigma. \end{aligned} \quad (3.117)$$

In order to obtain a formula for E_0 depending only on the interface, it remains to simplify

$$((\rho + t\theta')^2 + (t')^2)^{1/2}. \quad (3.118)$$

We begin this simplification by finding an expression for t in terms of θ and ρ . Using the definitions (3.109), (3.110), and (3.112) for r , \tilde{r} , and $\tilde{\nu}$, respectively, along with (3.115), we calculate

$$\begin{aligned} 0 &= \tilde{r}' \cdot \tilde{\nu} \\ &= (r' + t'\nu + t\nu') \cdot \tilde{\nu} \\ &= [\rho(\cos \theta, \sin \theta) + t'(\sin \theta, -\cos \theta) + t\theta'(\cos \theta, \sin \theta)] \cdot (\sin(\theta/2), -\cos(\theta/2)). \end{aligned} \quad (3.119)$$

Expanding out (3.119) and using the angle subtraction formulae for sine and cosine eventually gives

$$t' \cos(\theta/2) - (\rho + t\theta') \sin(\theta/2) = 0. \quad (3.120)$$

Now we observe from our symmetry assumption on u that $u \equiv \vec{e}_1$ on the x_2 -axis, so that $\theta(L) = \pi$.

If we assume that $\theta(\sigma)$ does not reach π until $\theta(L) = \pi$, which in terms of the interface means that

$$\text{the tangent vector to the interface is not horizontal in the interior of } Q_1, \quad (3.121)$$

then we can divide (3.120) by $\cos(\theta/2)$. This results in the following ODE for t :

$$t' - \frac{\sin(\theta/2)}{\cos(\theta/2)} \theta' t = \rho \tan(\theta/2). \quad (3.122)$$

Multiplying both sides of (3.122) by the integrating factor

$$M = \exp \left(-2 \int \frac{\sin(\theta/2)}{\cos(\theta/2)} \frac{\theta'}{2} \right) = \exp(2 \ln(\cos(\theta/2))) = \cos^2(\theta/2)$$

results in

$$(t \cos^2(\theta/2))' = \rho \sin(\theta/2) \cos(\theta/2) = \frac{1}{2} \rho \sin \theta.$$

Integrating both sides, dividing by $\cos^2(\theta/2)$, and using the half angle formula for cosine, we obtain

$$t = \frac{1}{2 \cos^2(\theta/2)} \int_0^\sigma \rho(y) \sin \theta(y) dy = \frac{1}{1 + \cos \theta} \int_0^\sigma \rho \sin \theta dy. \quad (3.123)$$

Finally, let us record the identity

$$\rho + t\theta' = t' \frac{\cos(\theta/2)}{\sin(\theta/2)}, \quad (3.124)$$

which follows from rearranging (3.120).

We now use the formula (3.123) for t to calculate (3.118), the quantity we set out to simplify.

Let us assume that $t' > 0$, which means that

$$\text{the length of characteristics connecting the interface to the wall increases in } \sigma. \quad (3.125)$$

Then plugging in (3.124) for (3.118) and using the assumptions (3.121) and (3.125), namely $\theta/2 \leq \pi/2$ and $t' > 0$, we write

$$((\rho + t\theta')^2 + (t')^2)^{1/2} = \left((t')^2 \frac{\cos^2(\theta/2)}{\sin^2(\theta/2)} + (t')^2 \right)^{1/2} = \frac{t'}{\sin(\theta/2)}.$$

Utilizing the formula (3.123) to calculate t' and then a half angle formula for cosine and a double angle formula for sine, we arrive at

$$\begin{aligned}
((\rho + t\theta')^2 + (t')^2)^{1/2} &= \frac{1}{\sin(\theta/2)} \left[\frac{\rho \sin \theta}{1 + \cos \theta} + \frac{\theta' \sin \theta}{(1 + \cos \theta)^2} \int_0^\sigma \rho \sin \theta \, dy \right] \\
&= \frac{\sin \theta}{2 \sin(\theta/2)(1 + \cos \theta)} \left[\rho + \frac{\theta'}{1 + \cos \theta} \int_0^\sigma \rho \sin \theta \, dy \right] \\
&= \frac{2 \sin(\theta/2) \cos(\theta/2)}{2 \sin(\theta/2) \cos^2(\theta/2)} \left[\rho + \frac{\theta'}{1 + \cos \theta} \int_0^\sigma \rho \sin \theta \, dy \right] \\
&= \frac{1}{\cos(\theta/2)} \left[\rho + \frac{\theta'}{1 + \cos \theta} \int_0^\sigma \rho \sin \theta \, dy \right]. \tag{3.126}
\end{aligned}$$

Now we are ready to use the expression (3.126) for (3.118) in the E_0 energy (3.117). We have

$$\begin{aligned}
E_0(u, Q_1) &= E_0(\rho, \theta) \\
&= \int_{\partial\{|u|=1\}} \frac{K(0)}{2} d\mathcal{H}^1 + \int_0^L \left(\frac{K(\sin(\theta/2))}{\cos(\theta/2)} \left[\rho + \frac{\theta'}{1 + \cos \theta} \int_0^\sigma \rho \sin \theta \, dy \right] \right) d\sigma.
\end{aligned}$$

We focus on the term

$$\int_0^L \left(\frac{K(\sin(\theta/2))}{\cos(\theta/2)} \frac{\theta'}{1 + \cos \theta} \int_0^\sigma \rho \sin \theta \, dy \right) d\sigma. \tag{3.127}$$

Let us define the function $H(v)$ by the equations

$$H'(v) = \frac{K(v)}{(1 - v^2)^2}, \quad H(0) = 0.$$

It follows from (3.21) that H remains finite as v approaches 1 so long as $V(t)$ approaches 0 as $t \nearrow 1$ at least as fast as $c(1 - t^2)^p$ for some $p > 1$ and $c > 0$, an assumption which is satisfied by W_{CSH} . A straightforward calculation, which we omit, using the chain rule, the definition of H' , and some trigonometric identities yields

$$(H(\sin(\theta/2)))' = \frac{K(\sin(\theta/2))\theta'}{\cos(\theta/2)(1 + \cos \theta)}. \tag{3.128}$$

Inserting this expression into the last integral in (3.127), that term becomes

$$\int_0^L (H(\sin(\theta/2)))' \left(\int_0^\sigma \rho \sin \theta \, dy \right) d\sigma, \tag{3.129}$$

which we integrate by parts to obtain

$$\left[H(\sin(\theta/2)) \int_0^\sigma \rho \sin \theta \, dy \right]_0^L - \int_0^L H(\sin(\theta/2)) \rho \sin \theta \, d\sigma.$$

Note that by our symmetry assumptions, $\theta(L) = \pi$, so that

$$\begin{aligned} & \left[H(\sin(\theta/2)) \int_0^\sigma \rho \sin \theta \, dy \right]_0^L - \int_0^L H(\sin(\theta/2)) \rho \sin \theta \, d\sigma \\ &= H(1) \int_0^L \rho \sin \theta \, d\sigma - \int_0^L H(\sin(\theta/2)) \rho \sin \theta \, d\sigma. \end{aligned} \quad (3.130)$$

We combine (3.128)–(3.130) to rewrite (3.127):

$$\int_0^L \left(\frac{K(\sin(\theta/2))}{\cos(\theta/2)} \frac{\theta'}{1 + \cos \theta} \int_0^\sigma \rho \sin \theta \, dy \right) d\sigma = \int_0^L (H(1) - H(\sin(\theta/2))) \rho \sin \theta \, d\sigma. \quad (3.131)$$

Using the right hand side of (3.131) for (3.127), we finally have

$$\begin{aligned} E_0(u, Q_1) &= E_0(\rho, \theta) \\ &= \int_{\partial\{|u|=1\}} \frac{K(0)}{2} d\mathcal{H}^1 + \int_0^L \left(\frac{K(\sin(\theta/2))}{\cos(\theta/2)} \left[\rho + \frac{\theta'}{1 + \cos \theta} \int_0^\sigma \rho \sin \theta \, dy \right] \right) d\sigma \\ &= \int_{\partial\{|u|=1\}} \frac{K(0)}{2} d\mathcal{H}^1 + \int_0^L \left(\frac{K(\sin(\theta/2))}{\cos(\theta/2)} + (H(1) - H(\sin(\theta/2)) \sin \theta) \right) \rho \, d\sigma \\ &=: \int_{\partial\{|u|=1\}} f(\theta) \, d\mathcal{H}^1. \end{aligned}$$

Thus we arrive at (3.108).

We turn now to the criticality conditions for θ . For any u with smooth interface, we parametrize the interface of length l by arclength s . Then the standard derivation [11] gives the following condition on the interface

$$(f''(\theta) + f(\theta))\theta' + \lambda = 0. \quad (3.132)$$

along with the junction condition

$$f'(\theta) \sin \theta - f(\theta) \cos \theta = 0 \quad (3.133)$$

at $s = 0$, the intersection of $\partial\{|u|=1\}$ with the x_1 -axis.

The solution of (3.132)–(3.133) for $\lambda = 1$ is depicted in Fig. 3.14b and bears a strong resemblance to a configuration observed in gradient flow dynamics shown in Fig. 3.14a.

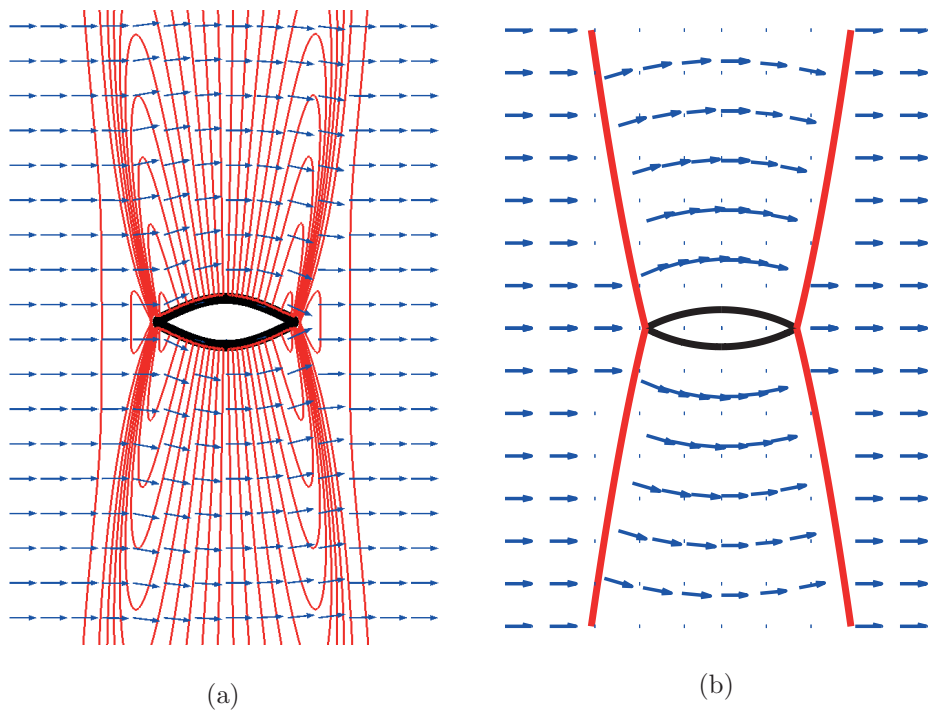


Figure 3.14: Isotropic island in \mathbb{R}^2 with $u = \vec{e}_1$ at infinity: (a) Gradient flow simulation in a large domain intended to represent \mathbb{R}^2 . The isotropic region is shrinking and the solution shown is a transient. Here $L = 10$, $\varepsilon = 0.02$; (b) Solution of (3.132)-(3.133) for $\lambda = 1$.

3.4 Appendix to Chapter 3: Proof of the Junction Condition

We present here the proof of Theorem 3.2.12. See Fig. 3.3 for a guide to the notation.

Proof. The derivation of (3.152) follows the same general lines as those appearing in the proof of Theorem 3.2.11. However, a major complicating consideration is that it is no longer possible to assume that the deforming vector field X is normal to all four curves Γ_{ij} since they all meet at p . Instead we will have to incorporate tangential components of X along these four curves as well.

To this end, we assume simply that $X \in C_0^1(B(p, R); \mathbb{R}^2)$ and again introduce the map Ψ via (3.70). We assume that each Γ_{ij} is smoothly parametrized by arclength through a map $r_{ij} : [0, s_0] \rightarrow \Gamma_{ij}$ for some $s_0 > 0$ with $r_{ij}(0) = p$. Then we replace (3.69) by

$$X(r_{ij}(s)) = h_{ij}^\tau(s)\tau_{ij}(s) + h_{ij}^\nu(s)\nu_{ij}(s) \quad \text{for } s \in [0, s_0], \quad (3.134)$$

where

$$h_{ij}^\tau := X(r_{ij}(s)) \cdot \tau_{ij}(s) \quad \text{and} \quad h_{ij}^\nu := X(r_{ij}(s)) \cdot \nu_{ij}(s).$$

As a consequence of the compact support of X , we have that

$$h_{ij}^\tau(s_0) = h_{ij}^\nu(s_0) = 0 \quad \text{for all functions } h_{ij}^\tau \text{ and } h_{ij}^\nu \quad (3.135)$$

but we stress that none of these functions is assumed to vanish at $s = 0$, namely at the location of the junction P .

We now deform each region Ω_j , for $j = 0, 1, 2, 3$ by the map Ψ to form four contiguous regions $\Omega_j^t := \Psi(\Omega_j, t)$ and we deform the four boundary curves Γ_{ij} to form four new boundary curves $\Gamma_{ij}^t := \Psi(\Gamma_{ij}, t)$. Of course the junction point P is also carried along by this flow.

The four curves Γ_{ij}^t are parametrized by $s \mapsto \Psi(r_{ij}(s), t)$ which we denote by $r_{ij}^t(s)$ though s no longer represents arclength. Indeed one calculates that

$$r_{ij}^t(x) \sim r_{ij}(s) + t(h_{ij}^\tau(s)\tau_{ij}(s) + h_{ij}^\nu(s)\nu_{ij}(s)) \quad (3.136)$$

from which it follows that

$$|r_{ij}^t'(s)| \sim 1 + t(h_{ij}^\tau'(s) - h_{ij}^\nu(s)\kappa_{ij}(s)), \quad (3.137)$$

where $\kappa_{ij}(s)$ denotes the curvature of Γ_{ij} at $r_{ij}(s)$ (compare with (3.75)) and we have invoked the Frenet relations $\tau'_{ij} = \kappa_{ij}\nu_{ij}$ and $\nu'_{ij} = -\kappa_{ij}\tau_{ij}$. A related calculation goes to show that the unit normal ν_{ij}^t to Γ_{ij}^t is given by

$$\nu_{ij}^t \sim \nu_{ij} - t(h_{ij}^\nu' + \kappa_{ij}h_{ij}^\tau)\tau_{ij}. \quad (3.138)$$

Now in the ball $B(p, R)$ the unperturbed critical point is given by

$$u(x) = \begin{cases} 0 & \text{for } x \in \Omega_0, \\ u_1(x) & \text{for } x \in \Omega_1, \\ u_2(x) & \text{for } x \in \Omega_2, \\ u_3(x) & \text{for } x \in \Omega_3 \end{cases}$$

and we wish to perturb it into a new function u^t given by

$$u^t(x) = \begin{cases} 0 & \text{if } x \in \Omega_0^t, \\ u_1^t(x) & \text{for } x \in \Omega_1^t, \\ u_2^t(x) & \text{for } x \in \Omega_2^t, \\ u_3^t(x) & \text{for } x \in \Omega_3^t \end{cases}.$$

To carry this out, as in the previous proof, we extend the domain of definition of u_j to a neighborhood of Ω_j in such a way that the extension is constant along the normals to the boundary of its original domain of definition. Then we introduce three functions ϕ_1, ϕ_2 and ϕ_3 such that

$$u_j^t(x) \sim u_j(x) + t\phi_j(x)u_j(x)^\perp \quad \text{for } x \in \Omega_j^t \text{ and for } j = 1, 2, 3 \quad (3.139)$$

so as to preserve the required \mathbb{S}^1 -valued nature of u_j^t .

We must also take care to preserve the property $u^t \in H_{\text{div}}$ in the sense of (3.52) and this requires that the following four conditions hold to $O(t)$ along $\Gamma_{01}, \Gamma_{12}, \Gamma_{23}$ and Γ_{03} respectively:

$$\begin{aligned} u_1^t(r_{01}^t(s)) \cdot \nu_{01}^t(s) &= 0, & u_1^t(r_{12}^t(s)) \cdot \nu_{12}^t(s) &= u_2^t(r_{12}^t(s)) \cdot \nu_{12}^t(s), \\ u_2^t(r_{23}^t(s)) \cdot \nu_{23}^t(s) &= u_3^t(r_{23}^t(s)) \cdot \nu_{23}^t(s), & \text{and} & & u_3^t(r_{03}^t(s)) \cdot \nu_{03}^t(s) &= 0 \text{ for } s \in [0, s_0]. \end{aligned} \quad (3.140)$$

We note that the first and last of these conditions implies at $t = 0$ that either $u_1 \equiv \tau_{01}$ or $\equiv -\tau_{01}$ along Γ_{01} and likewise either $u_3 \equiv \tau_{03}$ or $\equiv -\tau_{03}$ along Γ_{03} .

Substituting (3.136) and (3.138) into the four conditions of (3.140), and expanding to $O(t)$, a tedious but straight-forward calculation leads to the following requirements relating the traces of the ϕ_j to h_{ij}^ν :

$$\phi_1(r_{01}(s)) = h_{01}^\nu(s), \quad (3.141)$$

$$\frac{1}{2} \left(\phi_1(r_{12}(s)) + \phi_2(r_{12}(s)) \right) = h_{12}^\nu(s), \quad (3.142)$$

$$\frac{1}{2} \left(\phi_2(r_{23}(s)) + \phi_3(r_{23}(s)) \right) = h_{23}^\nu(s), \quad (3.143)$$

$$\phi_3(r_{03}(s)) = h_{03}^\nu(s), \quad (3.144)$$

for $s \in [0, s_0]$.

With the perturbations of the four curves Γ_{ij} and three functions u_j^t defined, we are ready to compute the variation of E_0 in a neighborhood of the junction point P . Carrying out the calculation (3.84) in Ω_j for $j = 1, 2, 3$ and then applying the divergence theorem we find with the aid of (3.53) that

$$\begin{aligned} \frac{d}{dt} \Big|_{t=0} \sum_{j=1}^3 \left(\int_{\Omega_j^t} (\operatorname{div} u_j^t)^2 dx \right) &= - \int_{\Gamma_{01}} \left((\operatorname{div} u_1)^2 h_{01}^\nu + 2(\operatorname{div} u_1)(u_1 \cdot \tau_{01})\phi_1 \right) ds \\ &\quad + \int_{\Gamma_{12}} \left((\operatorname{div} u_1)^2 h_{12}^\nu + 2(\operatorname{div} u_1)(u_1 \cdot \tau_{12})\phi_1 \right) ds \\ &\quad - \int_{\Gamma_{12}} \left((\operatorname{div} u_2)^2 h_{12}^\nu + 2(\operatorname{div} u_2)(u_2 \cdot \tau_{12})\phi_2 \right) ds \\ &\quad + \int_{\Gamma_{23}} \left((\operatorname{div} u_2)^2 h_{23}^\nu + 2(\operatorname{div} u_2)(u_2 \cdot \tau_{23})\phi_2 \right) ds \\ &\quad - \int_{\Gamma_{23}} \left((\operatorname{div} u_3)^2 h_{23}^\nu + 2(\operatorname{div} u_3)(u_3 \cdot \tau_{23})\phi_3 \right) ds \\ &\quad - \int_{\Gamma_{03}} \left((\operatorname{div} u_3)^2 h_{03}^\nu + 2(\operatorname{div} u_3)(u_3 \cdot \tau_{03})\phi_3 \right) ds, \end{aligned}$$

where we have used the fact that $u_1^\perp \cdot \nu_{01} = u_1 \cdot \tau_{01}$, $u_1^\perp \cdot \nu_{12} = u_1 \cdot \tau_{12}$, etc.

Now we appeal to the relations (3.141)–(3.144), along with the conditions $u_2 \cdot \tau_{12} = -u_1 \cdot \tau_{12}$

and $u_3 \cdot \tau_{23} = -u_2 \cdot \tau_{23}$ and perform an integration by parts to find

$$\begin{aligned}
\frac{d}{dt}_{|t=0} \sum_{j=1}^3 \left(\int_{\Omega_j^t} (\operatorname{div} u_j^t)^2 dx \right) &= \\
&\int_{\Gamma_{01}} \left\{ -(\operatorname{div} u_1)^2 + 2(\operatorname{div} u_1)'(u_1 \cdot \tau_{01}) \right\} h_{01}^\nu ds \\
&+ \int_{\Gamma_{12}} \left\{ \left((\operatorname{div} u_1)^2 - (\operatorname{div} u_2)^2 - 4[(\operatorname{div} u_2)'(u_1 \cdot \tau_{12}) + (\operatorname{div} u_2)(u_1 \cdot \tau_{12})'] \right) h_{12}^\nu \right. \\
&\quad \left. + 2(\operatorname{div} u_1 - \operatorname{div} u_2)(u_1 \cdot \tau_{12})\phi_1 \right\} ds \\
&+ \int_{\Gamma_{23}} \left\{ \left((\operatorname{div} u_2)^2 - (\operatorname{div} u_3)^2 - 4[(\operatorname{div} u_3)'(u_2 \cdot \tau_{23}) + (\operatorname{div} u_3)(u_2 \cdot \tau_{23})'] \right) h_{23}^\nu \right. \\
&\quad \left. + 2(\operatorname{div} u_2 - \operatorname{div} u_3)(u_2 \cdot \tau_{23})\phi_2 \right\} ds \\
&+ \int_{\Gamma_{03}} \left\{ -(\operatorname{div} u_3)^2 + 2(\operatorname{div} u_3)'(u_3 \cdot \tau_{03}) \right\} h_{03}^\nu ds \\
&+ 2(\operatorname{div} u_1(p))(u_1(p) \cdot \tau_{01}(0))h_{01}^\nu(0) - 4 \operatorname{div} u_2(p)(u_1(p) \cdot \tau_{12}(0))h_{12}^\nu(0) \\
&- 4 \operatorname{div} u_3(p)(u_2(p) \cdot \tau_{23}(0))h_{23}^\nu(0) + 2(\operatorname{div} u_3(p))(u_3(p) \cdot \tau_{03}(0))h_{03}^\nu(0). \tag{3.145}
\end{aligned}$$

We turn now to calculating the variations of the four jump energies. We begin by invoking (3.137) to compute

$$\begin{aligned}
&\frac{d}{dt}_{|t=0} \left(\int_{\Gamma_{01}^t} 1 ds + \int_{\Gamma_{03}^t} 1 ds \right) \\
&= \frac{d}{dt}_{|t=0} \left(\int_0^{s_0} |r_{01}'(s)| ds + \int_0^{s_0} |r_{03}'(s)| ds \right) \\
&= \frac{d}{dt}_{|t=0} \left(\int_0^{s_0} 1 + t(h_{01}^\tau)'(s) - h_{01}^\nu(s)\kappa_{01}(s) ds + \int_0^{s_0} 1 + t(h_{03}^\tau)'(s) - h_{03}^\nu(s)\kappa_{03}(s) ds \right) \\
&= \int_0^{s_0} (h_{01}^\tau)'(s) - h_{01}^\nu(s)\kappa_{01}(s) ds + \int_0^{s_0} (h_{03}^\tau)'(s) - h_{03}^\nu(s)\kappa_{03}(s) ds
\end{aligned}$$

Thus,

$$\begin{aligned}
&\frac{d}{dt}_{|t=0} \frac{K(0)}{2} \left(\mathcal{H}^1(\Gamma_{01}^t) + \mathcal{H}^1(\Gamma_{03}^t) \right) = \\
&- \frac{K(0)}{2} \left(\int_{\Gamma_{01}} h_{01}^\nu \kappa_{01} ds + \int_{\Gamma_{03}} h_{03}^\nu \kappa_{03} ds + h_{01}^\tau(0) + h_{03}^\tau(0) \right). \tag{3.146}
\end{aligned}$$

To compute the variation in the jump energies over Γ_{12}^t and Γ_{23}^t requires an expansion to $O(t)$ of the quantities $u^t \cdot \nu_{12}^t$ and $u^t \cdot \nu_{23}^t$. Substituting the expression for r_{12}^t from (3.136) into the formula

for u_1^t from (3.139) and Taylor expanding in t we find with the use of (3.138) that along Γ_{12}^t we have

$$u^t \cdot \nu_{12}^t \sim \left(u_1(r_{12}^t(s)) + t u_1^\perp(r_{12}(s)) \phi_1(r_{12}(s)) \right) \cdot \nu_{12}^t \sim \quad (3.147)$$

$$\begin{aligned} & \left(u_1(r_{12} + t [h_{12}^\tau \tau_{12} + h_{12}^\nu \nu_{12}]) + t \phi_1(r_{12}) u_1^\perp(r_{12}) \right) \cdot \left(\nu_{12} - t(h_{12}^\nu' + \kappa_{12} h_{12}^\tau) \tau_{12} \right) \\ & \sim u_1 \cdot \nu_{12} + t \left[(\phi_1 - h_{12}^\nu' - \kappa_{12} h_{12}^\tau) (u_1 \cdot \tau_{12}) + h_{12}^\tau (u_1' \cdot \nu_{12}) \right], \end{aligned} \quad (3.148)$$

where u_1 and ϕ_1 in the expression above are evaluated at $x = r_{12}(s)$ and $u_1' = \frac{d}{ds} u_1(r_{12}(s))$. In the last line we have also used that our extension of u_1 was constant along ν_{12} to eliminate the term $\nabla u_1 \cdot \nu_{12}$ that would other have been present upon Taylor expanding.

Similarly, we calculate that along Γ_{23} we have

$$u^t \cdot \nu_{23}^t \sim u_2 \cdot \nu_{23} + t \left[(\phi_2 - h_{23}^\nu' - \kappa_{23} h_{23}^\tau) (u_2 \cdot \tau_{23}) + h_{23}^\tau (u_2' \cdot \nu_{23}) \right]. \quad (3.149)$$

From (3.148) and (3.149), along with (3.137) we can compute that

$$\begin{aligned} & \frac{d}{dt} \Big|_{t=0} \left(\int_{\Gamma_{12}} K(u^t \cdot \nu_{12}^t) ds + \int_{\Gamma_{23}} K(u^t \cdot \nu_{23}^t) ds \right) \\ &= \frac{d}{dt} \Big|_{t=0} \left(\int_0^{s_0} K(u^t(r_{12}^t(s)) \cdot \nu_{12}^t(s)) |r_{12}^t'(s)| ds + \int_0^{s_0} K(u^t(r_{23}^t(s)) \cdot \nu_{23}^t(s)) |r_{23}^t'(s)| ds \right) \\ &= \int_{\Gamma_{12}} K(u_1 \cdot \nu_{12}) (h_{12}^\tau' - h_{12}^\nu \kappa_{12}) ds + \\ & \quad \int_{\Gamma_{12}} K'(u_1 \cdot \nu_{12}) \left((\phi_1 - h_{12}^\nu' - h_{12}^\tau \kappa_{12})(u_1 \cdot \tau_{12}) + h_{12}^\tau (u_1' \cdot \nu_{12}) \right) ds + \\ & \quad \int_{\Gamma_{23}} K(u_2 \cdot \nu_{23}) (h_{23}^\tau' - h_{23}^\nu \kappa_{23}) ds + \\ & \quad \int_{\Gamma_{23}} K'(u_2 \cdot \nu_{23}) \left((\phi_2 - h_{23}^\nu' - h_{23}^\tau \kappa_{23})(u_2 \cdot \tau_{23}) + h_{23}^\tau (u_2' \cdot \nu_{23}) \right) ds. \end{aligned}$$

Now since

$$\frac{d}{ds} [K(u_1 \cdot \nu_{12})] = (u_1' \cdot \nu_{12}) - \kappa_{12}(u_1 \cdot \tau_{12})$$

and

$$\frac{d}{ds} [K(u_2 \cdot \nu_{23})] = (u_2' \cdot \nu_{23}) - \kappa_{23}(u_2 \cdot \tau_{23}),$$

we have that

$$K(u_1 \cdot \nu_{12}) h_{12}^\tau' + K'(u_1 \cdot \nu_{12}) ((u_1' \cdot \nu_{12}) - \kappa_{12}(u_1 \cdot \tau_{12})) h_{12}^\tau = \frac{d}{ds} [K(u_1 \cdot \nu_{12}) h_{12}^\tau]$$

and

$$K(u_2 \cdot \nu_{23}) h_{23}^\tau' + K'(u_2 \cdot \nu_{23}) ((u_2' \cdot \nu_{23}) - \kappa_{23}(u_2 \cdot \tau_{23})) h_{23}^\tau = \frac{d}{ds} [K(u_2 \cdot \nu_{23}) h_{23}^\tau].$$

Using these last two identities in (3.150) and integrating by parts implies that

$$\begin{aligned} & \frac{d}{dt}_{|t=0} \left(\int_{\Gamma_{12}} K(u^t \cdot \nu_{12}^t) ds + \int_{\Gamma_{23}} K(u^t \cdot \nu_{23}^t) ds \right) \\ &= - \int_{\Gamma_{12}} K(u_1 \cdot \nu_{12}) h_{12}^\nu \kappa_{12} ds + \int_{\Gamma_{12}} K'(u_1 \cdot \nu_{12}) (\phi_1 - h_{12}^\nu') (u_1 \cdot \tau_{12}) ds \\ & \quad - \int_{\Gamma_{23}} K(u_2 \cdot \nu_{23}) h_{23}^\nu \kappa_{23} ds + \int_{\Gamma_{23}} K'(u_2 \cdot \nu_{23}) (\phi_2 - h_{23}^\nu') (u_2 \cdot \tau_{23}) ds \\ & \quad - K(u_1(p) \cdot \nu_{12}(0)) h_{12}^\tau(0) - K(u_2(p) \cdot \nu_{23}(0)) h_{23}^\tau(0). \end{aligned} \tag{3.150}$$

Then invoking the criticality condition (3.54) from Theorem 3.2.8 and integrating by parts we can rewrite this identity as

$$\begin{aligned} & \frac{d}{dt}_{|t=0} \left(\int_{\Gamma_{12}} K(u^t \cdot \nu_{12}^t) ds + \int_{\Gamma_{23}} K(u^t \cdot \nu_{23}^t) ds \right) \\ &= - \int_{\Gamma_{12}} K(u_1 \cdot \nu_{12}) h_{12}^\nu \kappa_{12} ds + L \int_{\Gamma_{12}} (\operatorname{div} u_2 - \operatorname{div} u_1) (\phi_1 - h_{12}^\nu') (u_1 \cdot \tau_{12}) ds \\ & \quad - \int_{\Gamma_{23}} K(u_2 \cdot \nu_{23}) h_{23}^\nu \kappa_{23} ds + L \int_{\Gamma_{23}} (\operatorname{div} u_3 - \operatorname{div} u_2) (\phi_2 - h_{23}^\nu') (u_2 \cdot \tau_{23}) ds \\ & \quad - K(u_1(p) \cdot \nu_{12}(0)) h_{12}^\tau(0) - K(u_2(p) \cdot \nu_{23}(0)) h_{23}^\tau(0) \\ &= \int_{\Gamma_{12}} \left\{ L(\operatorname{div} u_2 - \operatorname{div} u_1)' (u_1 \cdot \tau_{12}) + L(\operatorname{div} u_2 - \operatorname{div} u_1) (u_1 \cdot \tau_{12})' - K(u_1 \cdot \nu_{12}) \kappa_{12} \right\} h_{12}^\nu ds \\ & \quad + L \int_{\Gamma_{12}} (\operatorname{div} u_2 - \operatorname{div} u_1) (u_1 \cdot \tau_{12}) \phi_1 ds \\ & \quad + \int_{\Gamma_{23}} \left\{ L(\operatorname{div} u_3 - \operatorname{div} u_2)' (u_2 \cdot \tau_{23}) + L(\operatorname{div} u_3 - \operatorname{div} u_2) (u_2 \cdot \tau_{23})' - K(u_2 \cdot \nu_{23}) \kappa_{23} \right\} h_{23}^\nu ds \\ & \quad + L \int_{\Gamma_{23}} (\operatorname{div} u_3 - \operatorname{div} u_2) (u_2 \cdot \tau_{23}) \phi_2 ds \\ & \quad - K(u_1(p) \cdot \nu_{12}(0)) h_{12}^\tau(0) + L(\operatorname{div} u_2(p) - \operatorname{div} u_1(p)) (u_1(p) \cdot \tau_{12}(0)) h_{12}^\nu(0) \\ & \quad - K(u_2(p) \cdot \nu_{23}(0)) h_{23}^\tau(0) + L(\operatorname{div} u_3(p) - \operatorname{div} u_2(p)) (u_2(p) \cdot \tau_{23}(0)) h_{23}^\nu(0). \end{aligned} \tag{3.151}$$

Now we can combine (3.145), (3.146) and (3.151), and through a use of the criticality conditions (3.67) and (3.68) of Theorem 3.2.11 we find that all integrals over the four curves Γ_{ij} drop, leaving only

$$\begin{aligned} \frac{d}{dt}_{|t=0} E_0(u^t) = & \\ & -\frac{K(0)}{2}(h_{01}^\tau(0) + h_{03}^\tau(0)) - K(u_1(p) \cdot \nu_{12}(0))h_{12}^\tau - K(u_2(p) \cdot \nu_{23}(0))h_{23}^\tau \\ & + L \left\{ \operatorname{div} u_1(p)(u_1(p) \cdot \tau_{01}(0))h_{01}^\nu(0) + \operatorname{div} u_3(p)(u_3(p) \cdot \tau_{03}(0))h_{03}^\nu(0) \right\} \\ & - L \left\{ (\operatorname{div} u_1(p) + \operatorname{div} u_2(p))(u_1(p) \cdot \tau_{12}(0))h_{12}^\nu + (\operatorname{div} u_2(p) + \operatorname{div} u_3(p))(u_2(p) \cdot \tau_{23}(0))h_{23}^\nu \right\} \end{aligned}$$

Recall now that $h_{01}^\tau(0) = X(p) \cdot \tau_{01}(0)$, $h_{01}^\nu(0) = X(p) \cdot \nu_{01}(0)$, etc. Thus, the arbitrary value of the vector $X(p)$, implies that a vanishing first variation $\frac{d}{dt}_{|t=0} E_0(u^t) = 0$ leads to the necessary condition at a junction P of the form

$$\begin{aligned} & \frac{K(0)}{2}(\tau_{01} + \tau_{03}) + K(u_1 \cdot \nu_{12})\tau_{12} + K(u_2 \cdot \nu_{23})\tau_{23} \\ & = L \left\{ \operatorname{div} u_1(u_1 \cdot \tau_{01})\nu_{01} + \operatorname{div} u_3(u_3 \cdot \tau_{03})\nu_{03} \right\} \\ & - L \left\{ (\operatorname{div} u_1 + \operatorname{div} u_2)(u_1 \cdot \tau_{12})\nu_{12} + (\operatorname{div} u_2 + \operatorname{div} u_3)(u_2 \cdot \tau_{23})\nu_{23} \right\} \end{aligned} \tag{3.152}$$

where all quantities above are evaluated at the junction P .

□

Chapter 4

A Novel Landau-de Gennes Model with Higher Order Elastic Terms

4.1 A Well-Posed Landau-de Gennes Model that Converges to Oseen-Frank

In this section, we are interested in obtaining the Oseen-Frank model as a limit of well-posed Landau-de Gennes models. We begin our analysis with several calculations which establish equalities between the terms in the Oseen-Frank energy of an \mathbb{S}^2 -valued vector field n , cf. (1.1), and quartic terms in $n \otimes n$ and $\nabla(n \otimes n)$. These calculations are the basis for our choice of elastic terms for a Landau-de Gennes energy.

4.1.1 Alternative Forms for the Oseen-Frank Elastic Terms

Proposition 4.1. *Let n be a smooth vector field defined on an open subset $\Omega \subset \mathbb{R}^3$ and taking values in \mathbb{S}^2 . Then*

$$(\operatorname{div} n)^2 = |(n \otimes n)\operatorname{div}(n \otimes n)|^2. \quad (4.1)$$

Proof. Let us first note that

$$0 = \frac{1}{2}\nabla(|n|^2) = \nabla n^T n, \quad (4.2)$$

which follows from the fact that $|n| = 1$ everywhere. We now use (4.2) to write

$$\begin{aligned}
(\operatorname{div} n)n &= (\operatorname{div} n)n + \nabla n^T n \\
&= (\operatorname{div} n)n + (\nabla n^T n \cdot n)n \\
&= (\operatorname{div} n)n + (n \cdot \nabla n)n \\
&= (n \otimes n)(\operatorname{div} n)n + (n \otimes n)(\nabla n)n \\
&= (n \otimes n)\operatorname{div}(n \otimes n).
\end{aligned} \tag{4.3}$$

Taking $|\cdot|^2$ on both sides yields (4.1). \square

In order to calculate terms involving the curl of a symmetric tensor, we need the following lemma.

Lemma 4.1. (i) *For any smooth vector field m , we have*

$$\operatorname{curl}(m \otimes m) = ((\operatorname{curl} m_j m)_i) \in \mathbb{R}^{3 \times 3}.$$

That is, the j -th column of $\operatorname{curl}(m \otimes m)$ is $\operatorname{curl}(m_j m)$.

(ii) *For any tensor field Q taking values in the space of symmetric matrices, if we refer to the j -th row of Q as Q_j , we have the same result:*

$$\operatorname{curl} Q = ((\operatorname{curl} Q_j)_i) \in \mathbb{R}^{3 \times 3}. \tag{4.4}$$

Proof. We define the curl of a tensor field A by

$$(\operatorname{curl} A)v := \operatorname{curl}(A^T v) \quad \text{for all } v \in \mathbb{R}^3, \tag{4.5}$$

which is equivalent to defining $\operatorname{curl} A$ via

$$\operatorname{curl} A = \varepsilon_{ijk} A_{mj,i} e_k \otimes e_m.$$

Hence the j -th column of $\operatorname{curl} A$ is the curl of the j -th row of A . The result follows. \square

Proposition 4.2. *Let n be as in the previous proposition. Then*

$$((\operatorname{curl} n) \cdot n)^2 = |(n \otimes n)\operatorname{curl}(n \otimes n)|^2, \quad (4.6)$$

where for any matrix M , $|M|^2$ denotes the sum of the squares of the entries.

Proof. Let us first record

$$(n \otimes n)(\nabla n_j \times n) = (n \cdot (\nabla n_j \times n))n = (\nabla n_j \cdot (n \times n))n = 0. \quad (4.7)$$

In the following calculation, we will use the fact that $|n|^2 = 1$ in the first and third lines and use (4.7) once to add 0 in the fourth line. We write

$$\begin{aligned} ((\operatorname{curl} n) \cdot n)^2 &= |((\operatorname{curl} n) \cdot n)n|^2 \\ &= |(n \otimes n)(\operatorname{curl} n)|^2 \\ &= \sum_j |n_j(n \otimes n)(\operatorname{curl} n)|^2 \\ &= \sum_j |n_j(n \otimes n)(\operatorname{curl} n) + (n \otimes n)(\nabla n_j \times n)|^2 \\ &= \sum_j |(n \otimes n)(n_j \operatorname{curl} n + \nabla n_j \times n)|^2 \\ &= \sum_j |(n \otimes n)\operatorname{curl}(n_j n)|^2. \end{aligned} \quad (4.8)$$

But $\operatorname{curl}(n_j n)$ is precisely the j -th column of $\operatorname{curl}(n \otimes n)$, so that

$$\sum_j |(n \otimes n)\operatorname{curl}(n_j n)|^2 = |(n \otimes n)\operatorname{curl}(n \otimes n)|^2.$$

Combining this with (4.8) finishes the proof of (4.6). \square

Proposition 4.3. *Let n be as in the previous propositions. Then*

$$|(\operatorname{curl} n) \times n|^2 = |(\mathbf{I} - n \otimes n)\operatorname{div}(n \otimes n)|^2 \quad (4.9)$$

Proof. Using the calculation from (4.3) of $(n \otimes n)\operatorname{div}(n \otimes n)$, let us first write

$$\begin{aligned} (\mathbf{I} - n \otimes n)\operatorname{div}(n \otimes n) &= \operatorname{div}(n \otimes n) - (\operatorname{div} n)n \\ &= \nabla n \cdot n + (\operatorname{div} n)n - (\operatorname{div} n)n \\ &= \nabla n \cdot n. \end{aligned}$$

Now recalling (4.2), we may subtract $\nabla n^T n = 0$ from the right hand side of previous equation to obtain

$$\begin{aligned} (\mathbf{I} - n \otimes n)\operatorname{div}(n \otimes n) &= \nabla n \cdot n - \nabla n^T n \\ &= \begin{pmatrix} 0 & n_{1,y} - n_{2,x} & n_{1,z} - n_{3,x} \\ n_{2,x} - n_{1,y} & 0 & n_{2,z} - n_{3,y} \\ n_{3,x} - n_{1,z} & n_{3,y} - n_{2,z} & 0 \end{pmatrix} n \\ &= \begin{pmatrix} 0 & -(\operatorname{curl} n)_3 & (\operatorname{curl} n)_2 \\ (\operatorname{curl} n)_3 & 0 & -(\operatorname{curl} n)_1 \\ -(\operatorname{curl} n)_2 & (\operatorname{curl} n)_1 & 0 \end{pmatrix} n \\ &= \begin{pmatrix} (\operatorname{curl} n)_2 n_3 - (\operatorname{curl} n)_3 n_2 \\ (\operatorname{curl} n)_3 n_1 - (\operatorname{curl} n)_1 n_3 \\ (\operatorname{curl} n)_1 n_2 - (\operatorname{curl} n)_2 n_1 \end{pmatrix} \\ &= (\operatorname{curl} n) \times n. \end{aligned}$$

Taking $|\cdot|^2$ on both sides completes the proof. \square

Proposition 4.4. *Let n be as in the previous propositions. Then*

$$|\nabla n|^2 = |(\mathbf{I} - n \otimes n)\operatorname{curl}(n \otimes n)|^2. \quad (4.10)$$

Proof. Let us first calculate $|\operatorname{curl}(n \otimes n)|^2$, after which we can use Proposition 4.2 to find $|(\mathbf{I} - n \otimes n)\operatorname{curl}(n \otimes n)|^2$.

$n)\operatorname{curl}(n \otimes n)|^2$. Invoking Lemma 4.1 and then expanding, we write

$$\begin{aligned}
|\operatorname{curl}(n \otimes n)|^2 &= \sum_j |\operatorname{curl}(n_j n)|^2 \\
&= \sum_j |\nabla n_j \times n + n_j(\operatorname{curl} n)|^2 \\
&= \sum_j |\nabla n_j \times n|^2 + \sum_j n_j^2 |\operatorname{curl} n|^2 + \sum_j 2(\nabla n_j \times n) \cdot (n_j \operatorname{curl} n) \\
&=: I + II + III.
\end{aligned} \tag{4.11}$$

For I , we use Lagrange's identity and the identity $(\operatorname{curl} n) \times n = \nabla n \cdot n$ from the previous lemma to write

$$\begin{aligned}
I &= \sum_j (|\nabla n_j|^2 |n|^2 - (\nabla n_j \cdot n)^2) \\
&= \left(\sum_j |\nabla n_j|^2 \right) - |\nabla n \cdot n|^2 \\
&= |\nabla n|^2 - |(\operatorname{curl} n) \times n|^2.
\end{aligned} \tag{4.12}$$

Moving on to II , we immediately see that

$$II = |\operatorname{curl} n|^2. \tag{4.13}$$

Finally, III disappears since

$$III = \sum_j (\nabla(|n_j|^2) \times n) \cdot (\operatorname{curl} n) = (\nabla(|n|^2) \times n) \cdot (\operatorname{curl} n) = 0. \tag{4.14}$$

Substituting (4.12)-(4.14) into (4.11) yields

$$|\operatorname{curl}(n \otimes n)|^2 = |\nabla n|^2 - |(\operatorname{curl} n) \times n|^2 + |\operatorname{curl} n|^2 = |\nabla n|^2 + ((\operatorname{curl} n) \cdot n)^2. \tag{4.15}$$

But with the aid of Lemma 4.2, we can also calculate $|\operatorname{curl}(n \otimes n)|^2$ as

$$\begin{aligned}
&|(\mathbf{I} - n \otimes n)\operatorname{curl}(n \otimes n)|^2 + |(n \otimes n)\operatorname{curl}(n \otimes n)|^2 \\
&= |(\mathbf{I} - n \otimes n)\operatorname{curl}(n \otimes n)|^2 + ((\operatorname{curl} n) \cdot n)^2.
\end{aligned} \tag{4.16}$$

Setting (4.15) and (4.16) equal to each other and subtracting $((\operatorname{curl} n) \cdot n)^2$, we arrive at (4.10). \square

4.1.2 Landau-de Gennes Energy

Let us briefly summarize the relevant ideas for the Landau-de Gennes model we will propose. The bulk Landau-de Gennes energy density we will use in this chapter is

$$W(Q) := 3a \operatorname{tr}(Q^2) - 2b \operatorname{tr}(Q^3) + \frac{1}{4} (\operatorname{tr}(Q^2))^2, \quad (4.17)$$

cf. [79], which differs slightly from the version in the introduction. The form of W guarantees that the isotropic state $Q \equiv 0$ yields a global minimum at high temperatures while a uniaxial state of the form (1.8) gives the minimum when temperature (i.e. the parameter a) is reduced below a certain critical value, cf. [75, 79]. We remark for future use that W is bounded from below and can be made non-negative by adding an appropriate constant.

Let

$$\mathcal{S} := \{Q \in M^{3 \times 3} : Q^T = Q, \operatorname{tr} Q = 0\}.$$

As long as $Q \in \mathcal{S}$, one finds that this potential depends only on the eigenvalues of Q , say λ_1 and λ_2 with $\lambda_3 = -(\lambda_1 + \lambda_2)$, and with a slight abuse of notation we arrive at

$$W(\lambda_1, \lambda_2) = 6a(\lambda_1^2 + \lambda_2^2 + \lambda_1\lambda_2) + 6b\lambda_1\lambda_2(\lambda_1 + \lambda_2) + (\lambda_1^2 + \lambda_2^2 + \lambda_1\lambda_2)^2.$$

We are interested in describing the extrema of $W(\lambda_1, \lambda_2)$. Taking the derivatives of W gives

$$\begin{aligned} \frac{\partial W}{\partial \lambda_1} &= 2(2\lambda_1 + \lambda_2)(3a + 3b\lambda_2 + (\lambda_1^2 + \lambda_2^2 + \lambda_1\lambda_2)), \\ \frac{\partial W}{\partial \lambda_2} &= 2(\lambda_1 + 2\lambda_2)(3a + 3b\lambda_1 + (\lambda_1^2 + \lambda_2^2 + \lambda_1\lambda_2)), \\ \frac{\partial^2 W}{\partial \lambda_1^2} &= 12a + 12b\lambda_2 + 2(2\lambda_1 + \lambda_2)^2 + 4(\lambda_1^2 + \lambda_2^2 + \lambda_1\lambda_2), \\ \frac{\partial^2 W}{\partial \lambda_2^2} &= 12a + 12b\lambda_1 + 2(\lambda_1 + 2\lambda_2)^2 + 4(\lambda_1^2 + \lambda_2^2 + \lambda_1\lambda_2), \\ \frac{\partial^2 W}{\partial \lambda_1 \partial \lambda_2} &= 6a + 12b(\lambda_1 + \lambda_2) + 2(2\lambda_1 + \lambda_2)(\lambda_1 + 2\lambda_2) + 2(\lambda_1^2 + \lambda_2^2 + \lambda_1\lambda_2). \end{aligned}$$

It is easy to check that the critical points of W are $(\lambda_1, \lambda_2) = (0, 0)$ as well as $(\lambda_1, \lambda_2) = (\lambda, -2\lambda)$,

$(\lambda_1, \lambda_2) = (-2\lambda, \lambda)$, and $(\lambda_1, \lambda_2) = (\lambda, \lambda)$, where λ solves

$$a + b\lambda + \lambda^2 = 0. \quad (4.18)$$

The point $(\lambda_1, \lambda_2) = (0, 0)$ corresponds to a local minimum of W if $a > 0$ and to a local maximum of W if $a < 0$. The solutions of Eq. (4.18) are given by

$$\lambda = \frac{-b \pm \sqrt{b^2 - 4a}}{2},$$

hence there are no nematic critical points whenever $a > b^2/4$ and W has a single extremum corresponding to the global minimum at $(\lambda_1, \lambda_2) = (0, 0)$. By considering second derivatives of W , we also find that

$$\lambda_m = \frac{-b - \sqrt{b^2 - 4a}}{2} \quad (4.19)$$

is a point of a local minimum and

$$\lambda_s = \frac{-b + \sqrt{b^2 - 4a}}{2}$$

is a saddle point of W if $a < b^2/4$. We conclude that the nematic minima at $(\lambda_m, -2\lambda_m)$, $(-2\lambda_m, \lambda_m)$, and (λ_m, λ_m) coexist with the isotropic minimum at $(0, 0)$ as long as $0 < a < b^2/4$.

An easy computation shows that all of these minima have the same depth of 0 when

$$a = a_0 := 2b^2/9. \quad (4.20)$$

Because here we will be interested in the regime $0 \leq a \leq a_0$ when the energy value in the isotropic state is greater than or equal to the minimum energy in a nematic state, we subtract

$$W_m := W(\lambda_m, \lambda_m) = 9ab^2 - 9a^2 - \frac{3}{2}b^4 - \frac{3}{2}b(b^2 - 4a)^{\frac{3}{2}} \quad (4.21)$$

from W to ensure that the global minimum value of the Landau-de Gennes energy is 0. Hence, from now on

$$W(Q) \rightarrow W(Q) - W_m.$$

Note that decreasing a from a_0 to 0 corresponds to increased undercooling and a larger thermodynamic force driving the isotropic-to-nematic phase transition.

Next, we turn to the choice of elastic terms for our model. We want to derive elastic terms for Q -valued fields such that the elastic energy for Q formally reduces to the Oseen-Frank energy whenever Q is in a nematic state that minimizes the potential energy W . The minimum of W is achieved whenever Q has eigenvalues λ_m , λ_m , and $-2\lambda_m$ so that we can write

$$n \otimes n = \frac{1}{3}(\mathbf{I} - Q/\lambda_m), \quad (4.22)$$

where n is the unit eigenvector corresponding to the eigenvalue $-2\lambda_m$. We may now use the previous propositions to express the K_1 - K_3 terms from the Oseen-Frank energy in terms of Q as follows (when Q is uniaxial and $|n| = 1$):

$$K_1(\operatorname{div} n)^2 = \frac{K_1}{81}|(\mathbf{I} - Q/\lambda_m)\operatorname{div}(Q/\lambda_m)|^2, \quad (4.23)$$

$$K_2((\operatorname{curl} n) \cdot n)^2 = \frac{K_2}{81}|(\mathbf{I} - Q/\lambda_m)\operatorname{curl}(Q/\lambda_m)|^2, \quad (4.24)$$

and

$$K_3|(\operatorname{curl} n) \times n|^2 = \frac{K_3}{81}|(2\mathbf{I} + Q/\lambda_m)\operatorname{div}(Q/\lambda_m)|^2. \quad (4.25)$$

We also have

$$|\nabla n|^2 = \frac{1}{81}|(2I + Q/\lambda_m)\operatorname{curl}(Q/\lambda_m)|^2. \quad (4.26)$$

We will use these four elastic terms for Q as well as the Dirichlet energy $|\nabla Q|^2$.

Finally, we must specify the type of anchoring on the boundary of the sample. For simplicity we will assume throughout this chapter that admissible competitors are subject to the same Dirichlet boundary condition. This is known as strong anchoring in the literature.

4.1.3 Non-dimensionalization and Analysis of the 3D Model

Combining the elastic terms from (4.23)-(4.26) and the bulk potential W , our energy takes the form

$$F(Q) = \int_{\Omega} \left(\frac{L_1}{2} |\nabla(Q/\lambda_m)|^2 + \frac{L_2}{2} |(\mathbf{I} - Q/\lambda_m)\operatorname{div}(Q/\lambda_m)|^2 + \frac{L_3}{2} |(\mathbf{I} - Q/\lambda_m)\operatorname{curl}(Q/\lambda_m)|^2 + \frac{L_4}{2} |(2\mathbf{I} + Q/\lambda_m)\operatorname{div}(Q/\lambda_m)|^2 + \frac{L_5}{2} |(2\mathbf{I} + Q/\lambda_m)\operatorname{curl}(Q/\lambda_m)|^2 + w_0 W(Q) \right) dx,$$

where w_0 is a constant that has units of energy per unit volume. We assume that $L_i > 0$ for each i , which will ensure that our energy controls $\|\nabla Q\|_{L^2}^2$. In fact, it would be sufficient for this purpose to assume that

$$L_1 \geq 0 \text{ and } \min\{L_i : 2 \leq i \leq 5\} > 0,$$

as we shall see in Proposition 4.5.

Let $l > 0$ denote a characteristic length of the problem and set

$$\bar{L}_i := \frac{L_i}{L_2}, \quad \gamma := \frac{L_2}{4w_0 l^2 \lambda_m^4}.$$

We introduce the following rescalings:

$$\bar{x} = \frac{x}{l}, \quad \bar{Q} = \frac{Q}{\lambda_m}, \quad \bar{F} = \frac{Fl}{L_2}, \quad \bar{a} = \frac{a}{\lambda_m^2}, \quad \bar{b} = \frac{b}{\lambda_m}, \quad \bar{W}_m = \frac{W_m}{\lambda_m^4}. \quad (4.27)$$

Dropping the bar notation, we obtain

$$F_\gamma(Q) = \int_{\Omega} \left(\frac{L_1}{2} |\nabla Q|^2 + \frac{1}{2} |(\mathbf{I} - Q)\operatorname{div}(Q)|^2 + \frac{L_3}{2} |(\mathbf{I} - Q)\operatorname{curl}(Q)|^2 + \frac{L_4}{2} |(2\mathbf{I} + Q)\operatorname{div}(Q)|^2 + \frac{L_5}{2} |(2\mathbf{I} + Q)\operatorname{curl}(Q)|^2 + \frac{1}{4\gamma} W(Q) \right) dx$$

defined for $Q \in H^1(\Omega; \mathcal{S})$, where \mathcal{S} is the space of symmetric, traceless, 3×3 matrices. In this scaling, the potential W given by (4.50) is now minimized by any symmetric traceless matrix with eigenvalues 1, 1, -2, and the global minimum value of W is equal to zero, achieved by

$$Q = \mathbf{I} - 3n \otimes n \text{ for } n \in \mathbb{S}^2. \quad (4.28)$$

If Q is not sufficiently regular enough, $F_\gamma(Q)$ may be ∞ . We will refer to the elastic energy terms in F_γ as

$$\begin{aligned}\sigma(Q) := & \frac{L_1}{2} |\nabla Q|^2 + \frac{1}{2} |(\mathbf{I} - Q)\operatorname{div}(Q)|^2 + \frac{L_3}{2} |(\mathbf{I} - Q)\operatorname{curl}(Q)|^2 \\ & + \frac{L_4}{2} |(2\mathbf{I} + Q)\operatorname{div}(Q)|^2 + \frac{L_5}{2} |(2I + Q)\operatorname{curl}(Q)|^2.\end{aligned}\quad (4.29)$$

It is instructive at this point to comment on other considerations which motivated this choice of elastic terms. First, one can see from (4.23)-(4.26) that only the L_2 - L_4 (recall in our non-dimensionalization, $L_2 = 1$) terms are necessary for a formal calculation which yields the K_1 - K_3 from the Oseen-Frank energy. However, we are interested in a model which is well posed and yields Oseen-Frank in a more rigorous sense. The L_1 and L_5 terms are included to achieve this goal; they also give the null Lagrangian $K_2 + K_4$ term from the Oseen-Frank energy. Adding either term to the L_2 - L_4 terms yields a well-posed variational model which approximates Oseen-Frank and enjoys a crucial compactness property, cf. Propositions 4.5, 4.7. In some sense then the L_1 and L_5 terms are redundant in terms of the mathematical analysis. One can conceive of different choices regarding these terms as affecting only the core structure of defects in the liquid crystal, since in nematic region where $W(Q) \approx 0$, it is the L_2 - L_4 terms which describe the qualitative behavior of the liquid crystal.

Let us finally remark that one can split up the $|\nabla Q|^2$ term. Recalling our notation Q_j for the j -th row of Q , we write

$$\begin{aligned}|\nabla Q|^2 &= \sum_j |\nabla Q_j|^2 \\ &= \sum_j ((\operatorname{div} Q_j)^2 + |\operatorname{curl} Q_j|^2 + \operatorname{tr}(\nabla Q_j)^2 - (\operatorname{div} Q_j)^2).\end{aligned}\quad (4.30)$$

The last two terms are a null Lagrangian and can be rewritten as

$$\sum_j (\operatorname{tr}(\nabla Q_j)^2 - (\operatorname{div} Q_j)^2) = \sum_j \operatorname{div}((\nabla Q_j)Q_j - (\operatorname{div} Q_j)Q_j).\quad (4.31)$$

In fact, (4.31) only depends on $Q|_{\partial\Omega}$ and its tangential derivatives, cf. [51, Lemma 1.2].

Proposition 4.5. *For any $Q \in H^1(\Omega; \mathcal{S})$, we have (up to a null Lagrangian)*

$$\|Q\|_{H^1}^2 \lesssim F_\gamma(Q). \quad (4.32)$$

Proof. It is standard to bound $\|Q\|_{L^2}^2$ from above by the potential term in the energy F_γ , so we focus on σ . When $L_1 > 0$ it is clear that

$$\|\nabla Q\|_{L^2}^2 \leq \sigma(Q); \quad (4.33)$$

therefore, let us proceed assuming that $L_1 = 0$. We will find it convenient to represent the matrix Q as $\sum_{i=1}^3 \alpha_i v_i \otimes v_i$ for scalar fields α_i and vector fields v_i which form an orthogonal basis of \mathbb{R}^3 for any fixed $x \in \Omega$. Note that for any vector c , we have for every $x \in \Omega$

$$\begin{aligned} |(I - Q)c|^2 + |(2I + Q)c|^2 &= \left| \sum_i (1 - \alpha_i)(v_i \otimes v_i)c \right|^2 + \left| \sum_i (2 + \alpha_i)(v_i \otimes v_i)c \right|^2 \\ &= \sum_i (1 - \alpha_i)^2 (v_i \cdot c)^2 + \sum_i (2 + \alpha_i)^2 (v_i \cdot c)^2 \\ &\geq \sum_i \frac{9}{2} (v_i \cdot c)^2. \end{aligned}$$

The factor of $9/2$ arises as the minimum of the parabola $(1 - \alpha_i)^2 + (2 + \alpha_i)^2$. This estimate implies that

$$\sigma(Q) \gtrsim \left(|\operatorname{div} Q|^2 + |\operatorname{curl} Q|^2 \right). \quad (4.34)$$

Recalling from (4.30) that we can write

$$|\nabla Q|^2 = \sum_j ((\operatorname{div} Q_j)^2 + |\operatorname{curl} Q_j|^2 + \text{null Lagrangian}), \quad (4.35)$$

we can combine (4.34) and (4.35) to finish the proof. \square

To prove the existence of minimizers of F_γ subject to a Dirichlet condition and to prove a Γ -convergence result, we will need the following proposition.

Proposition 4.6. *For any sequence Q_n which converges weakly in $H^1(\Omega; \mathcal{S})$ to $Q \in H^1(\Omega; \mathcal{S})$, we have*

$$\int_\Omega \sigma(Q) dx \leq \liminf_{n \rightarrow \infty} \int_\Omega \sigma(Q_n) dx. \quad (4.36)$$

Proof. We focus on the term $|(\mathbf{I} - Q_n)\operatorname{div} Q_n|^2$; the argument for the other terms is the same, and in the case of $|\nabla Q|^2$, trivial. The essence of the subsequent proof is essentially the following real analysis fact:

$$\begin{aligned} f_n &\rightarrow f \text{ strongly in } L^2, g_n \rightarrow g \text{ weakly in } L^2, \|f_n g_n\|_{L^2} \leq C < \infty \\ &\implies f_n g_n \rightarrow f g \text{ weakly in } L^2. \end{aligned}$$

Without loss of generality, we can assume (by restricting to a subsequence) that $\liminf \int_{\Omega} |(\mathbf{I} - Q_n)\operatorname{div} Q_n|^2 dx$ is finite and the sequence of integrals converges to its limit inferior. Let us first recall that weak convergence in H^1 entails strong convergence in L^2 , so that

$$\mathbf{I} - Q_n \rightarrow \mathbf{I} - Q \text{ in } L^2. \quad (4.37)$$

Next, since $\operatorname{div} Q_n$ converges weakly in L^2 to $\operatorname{div} Q$ and $\mathbf{I} - Q_n$ converges strongly in L^2 to $\mathbf{I} - Q$, we have for any $\phi \in L^\infty(\Omega; \mathbb{R}^3)$:

$$\begin{aligned} \int_{\Omega} (\mathbf{I} - Q_n)\operatorname{div} Q_n \cdot \phi &= \int_{\Omega} [(\mathbf{I} - Q_n) - (\mathbf{I} - Q)] \operatorname{div} Q_n \cdot \phi + \int_{\Omega} (\mathbf{I} - Q)\operatorname{div} Q_n \cdot \phi \\ &\rightarrow \int_{\Omega} (\mathbf{I} - Q)\operatorname{div} Q \cdot \phi. \end{aligned}$$

Thus

$$(\mathbf{I} - Q_n)\operatorname{div} Q_n \rightarrow (\mathbf{I} - Q)\operatorname{div} Q \text{ weakly in } L^1.$$

Now from the uniform L^2 bound on $(\mathbf{I} - Q_n)\operatorname{div} Q_n$, we have that (up to a subsequence)

$$(\mathbf{I} - Q_n)\operatorname{div} Q_n \rightarrow h \text{ weakly in } L^2$$

for some $h \in L^2(\Omega; \mathbb{R}^3)$. But from the previous observation and the uniqueness of weak limits, we deduce that the weak L^2 -limit h must coincide with $(\mathbf{I} - Q)\operatorname{div} Q$, the weak L^1 -limit. The inequality

$$\int_{\Omega} |(\mathbf{I} - Q)\operatorname{div} Q|^2 dx \leq \liminf_{n \rightarrow \infty} \int_{\Omega} |(\mathbf{I} - Q_n)\operatorname{div} Q_n|^2 dx$$

now follows from the lower semicontinuity of the L^2 -norm under weak convergence. Repeating the same argument for the other terms in σ concludes the proof. \square

Next, we turn our attention to the existence of minimizers of F_γ among competitors subject to a Dirichlet condition. For the rest of this section, we will restrict our analysis to boundary conditions $g : \partial\Omega \rightarrow \mathcal{S}$ for which the infimum of F_γ is not infinity. Sufficient conditions in order to guarantee this include for example assuming that $g \in (H^{1/2} \cap L^\infty)(\partial\Omega; \mathcal{S})$.

Theorem 4.1. *For any $\gamma > 0$ and $g : \partial\Omega \rightarrow \mathcal{S}$ such that $\inf\{F_\gamma(Q) : Q \in H_g^1(\Omega; \mathcal{S})\} < \infty$, there exists Q_0 which minimizes F_γ within $H_g^1(\Omega; \mathcal{S})$.*

Proof. Fix $\gamma > 0$ and g as stated in the theorem. By virtue of the previous two propositions, the existence of a minimizer will follow without difficulty from the direct method in the calculus of variations.

Let $\{Q_n\}$ be a sequence such that

$$\lim_{n \rightarrow \infty} F_\gamma(Q_n) = \inf\{F_\gamma(Q) : Q \in H_g^1(\Omega; \mathcal{S})\}.$$

Then by Proposition 4.5, we have a uniform H^1 bound on $\{Q_n\}$ and a subsequence, which we still refer to as $\{Q_n\}$, converging weakly in H^1 to some $Q_0 \in H_g^1$. Proposition 4.6 then yields

$$\int_{\Omega} \sigma(Q_0) dx \leq \liminf_{n \rightarrow \infty} \int_{\Omega} \sigma(Q_n) dx. \quad (4.38)$$

By Rellich's theorem, we may assume as well that Q_n converge in L^4 to Q_0 , from which we deduce

$$\int_{\Omega} W(Q_0) dx = \lim_{n \rightarrow \infty} \int_{\Omega} W(Q_n) dx. \quad (4.39)$$

The minimality of Q_0 is now a consequence of (4.38) and (4.39). \square

We are now interested in the asymptotic behavior of minimizers of F_γ . Let us begin by identifying a limiting functional. Assume that the temperature is low enough so that the global minimum of W , the non-dimensionalized Landau-de Gennes potential, is achieved by a set of uniaxial states

$$N := \{I - 3n \otimes n : n \in \mathbb{S}^2\}; \quad (4.40)$$

cf. (4.28). We consider boundary data $g : \partial\Omega \rightarrow N$ such that $H_g^1(\Omega; N)$ is non-empty and $W(g) = 0$. The set of satisfactory boundary data includes, for example, g which are formed using a Lipschitz vector field $n : \partial\Omega \rightarrow \mathbb{S}^2$ and considering the tensor field

$$\mathbf{I} - 3n \otimes n : \partial\Omega \rightarrow N, \quad (4.41)$$

cf. [51, Lemma 1.1]. The limiting functional F_0 is then defined by

$$F_0(Q) = \begin{cases} \int_{\Omega} \sigma(Q) dx & \text{if } Q \in H_g^1(\Omega; N), \\ \infty & \text{otherwise.} \end{cases}$$

Let us point out a key feature of the limiting model: F_0 coincides with the Oseen-Frank model, in a sense we will make more precise. First, for any $n \in H^1(\Omega; \mathbb{S}^2)$, the Q -tensor field

$$\mathbf{I} - 3n \otimes n \quad (4.42)$$

is in $H^1(\Omega; N)$. Moreover, using (4.23)-(4.26) and

$$|\nabla Q|^2 = 18|\nabla n|^2, \quad (4.43)$$

we have

$$\begin{aligned} F_0(Q) &= \int_{\Omega} \sigma(Q) dx = \int_{\Omega} \left(\frac{\tilde{L}_2}{2} (\operatorname{div} n)^2 + \frac{\tilde{L}_3}{2} ((\operatorname{curl} n) \cdot n)^2 \right. \\ &\quad \left. + \frac{\tilde{L}_4}{2} |(\operatorname{curl} n) \times n|^2 + \frac{\tilde{L}_5}{2} |\nabla n|^2 \right) dx, \end{aligned}$$

where each $\tilde{L}_5 = 18L_1 + 81L_5$ and $\tilde{L}_i = 81L_i$ for $i = 2, 3, 4$. Breaking up the $|\nabla n|^2$ term, we obtain

$$\begin{aligned} &\int_{\Omega} \left(\frac{\tilde{L}_2}{2} (\operatorname{div} n)^2 + \frac{\tilde{L}_3}{2} ((\operatorname{curl} n) \cdot n)^2 + \frac{\tilde{L}_4}{2} |(\operatorname{curl} n) \times n|^2 + \frac{\tilde{L}_5}{2} |\nabla n|^2 \right) dx \\ &= \int_{\Omega} \left(\frac{\tilde{L}_2 + \tilde{L}_5}{2} (\operatorname{div} n)^2 + \frac{\tilde{L}_3 + \tilde{L}_5}{2} ((\operatorname{curl} n) \cdot n)^2 + \frac{\tilde{L}_4 + \tilde{L}_5}{2} |(\operatorname{curl} n) \times n|^2 \right. \\ &\quad \left. + \frac{\tilde{L}_5}{2} (\operatorname{tr}(\nabla n)^2 - (\operatorname{div} n)^2) \right) dx \end{aligned}$$

This is exactly the Oseen-Frank energy of n . Alternatively, one could split up the $|\nabla Q|^2$ term in F_γ as in (4.30), and it can be verified that the null Lagrangian (4.31) reduces to $\text{tr}(\nabla n)^2 - (\text{div } n)^2$ in the $\gamma \rightarrow 0$ limit.

The question of when minimizing F_0 among Q -tensor fields coincides with minimizing the version of the Oseen-Frank energy above is more delicate. There may well be strictly more competitors in the space of Q -tensors than in the space of \mathbb{S}^2 -valued fields n due to the possible ‘non-orientability’ of a Q -tensor field. It has been shown in [16] that when $\Omega \subset \mathbb{R}^k$ is simply connected and $k = 2, 3$, every $Q \in H^1(\Omega; N)$ has a lifting $\varphi^Q \in H^1(\Omega; \mathbb{S}^2)$ such that

$$Q = \mathbf{I} - 3n \otimes n.$$

If Ω is not simply connected or if $p < 2$, then there might exist tensor fields which cannot be ‘oriented’ to produce a vector field. We refer the reader to that paper for a more detailed treatment.

Let us now state our main theorem.

Theorem 4.2. *For any choice of boundary data g as above, the sequence $\{F_\gamma\}$ Γ -converges in the weak topology of $H_g^1(\Omega; \mathcal{S})$ to F_0 . That is,*

(i) *for any $Q \in H_g^1(\Omega; \mathcal{S})$ and for any sequence $\{Q_\gamma\}$ in $H_g^1(\Omega; \mathcal{S})$,*

$$Q_\gamma \rightharpoonup Q \text{ in } H_g^1(\Omega; \mathcal{S}) \text{ implies } \liminf_{\gamma \rightarrow 0} F_\gamma(Q_\gamma) \geq F_0(Q), \quad (4.44)$$

and

(ii) *for each $Q \in H_g^1(\Omega; \mathcal{S})$ there exists a recovery sequence $\{Q_\gamma\}$ in $H_g^1(\Omega; \mathcal{S})$ satisfying*

$$Q_\gamma \rightharpoonup Q_0 \text{ in } H_g^1(\Omega; \mathcal{S}), \quad (4.45)$$

$$\lim_{\gamma \rightarrow 0} F_\gamma(Q_\gamma) = F_0(Q_0). \quad (4.46)$$

Before we present the proof, we state the following compactness proposition, which follows immediately from Proposition 4.5.

Proposition 4.7. *Let $\{Q_\gamma\}$ be a sequence of maps from Ω to \mathcal{S} , and assume that the sequence of energies $F_\gamma(Q_\gamma)$ is uniformly bounded. Then there exists a subsequence $\{Q_{\gamma_j}\}$ and $Q \in H_g^1(\Omega; N)$ such that $Q_{\gamma_j} \rightharpoonup Q$ in $H^1(\Omega; \mathcal{S})$.*

Proof of Theorem 4.2. The lower-semicontinuity condition (4.44) has been proved in Proposition 4.6. For the construction of a recovery sequence given some Q_0 , we can simply take $Q_\gamma = Q_0$ for all γ . \square

4.2 A Landau-de Gennes Model for Thin Film Nematic-Isotropic Transitions with Highly Disparate Elastic Constants

In this section, we propose and analyze a Landau-de Gennes model for thin films. A key component of the model is elastic disparity similar to the previous chapter. The first subsection summarizes the experiments carried out by Y.-K. Kim and O. Lavrentovich. We then proceed with the introduction of our model and the analysis. The final subsection displays the results of numerical simulations, which qualitatively reproduce the experimental results.

4.2.1 Experimental Results

The sample configuration consisted of the ITO glass that was spin-coated with a polyimide layer, SE7511, in which the directors of disodium chromoglycate (DSCG) are aligned parallel to substrates. Subsequently, two substrates were assembled into a cell with the thickness of 2 μm . 16 wt% of DSCG solution was injected into the assembled cell.

The cell was cooled at the rate of $-0.4^\circ\text{C}/\text{min}$. As the temperature decreased from the isotropic phase, nematic domains appeared, grew, and coalesced. When many large nematic domains coalesced, they occasionally trapped isotropic islands, or tactoids, around which the director may have either zero or nonzero winding number. The snapshots of configurations with islands having different winding number of the director on their boundary are shown in Figs. 4.1-4.2. These

are Polscope textures with color representing optical retardance, bars giving the orientation of the director, and circles indicating the point where orientation was measured.

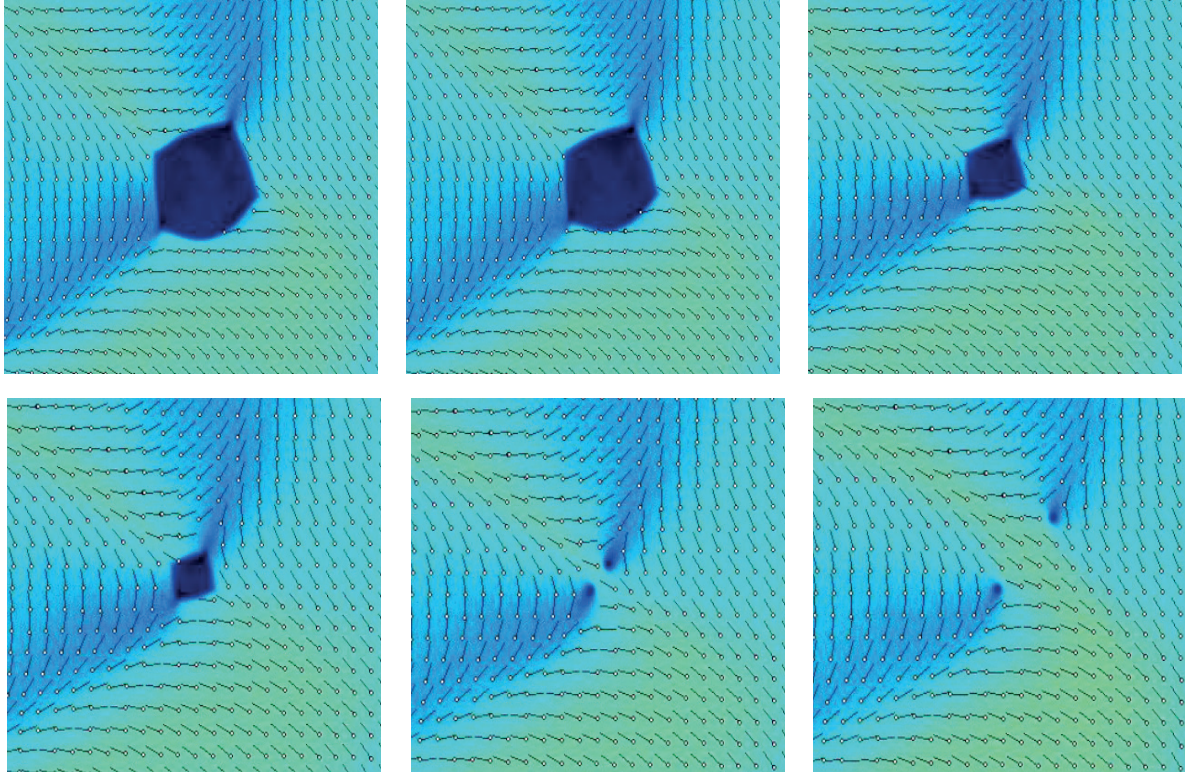


Figure 4.1: Experimentally observed evolution of an isotropic tactoid. The director field has the winding number -1 on the boundary of the tactoid. Once the tactoid disappears, it generates a vortex of degree -1 that subsequently splits into two degree $-1/2$ vortices.

4.2.2 Model Development

In this section we derive a version of the Landau-de Gennes model that is appropriate for the modeling of nematic systems with disparate elastic constants. In particular, we are interested in the case when the elastic constant corresponding to splay deformations is larger than those for bend and twist so that the splay of the director is relatively expensive. Note that this situation can be found in experimental systems, such as chromonic lyotropic liquid crystals [107] shown in Figures 4.1-4.2 and in thermotropic nematics of certain molecular shape, such as dimers [13].

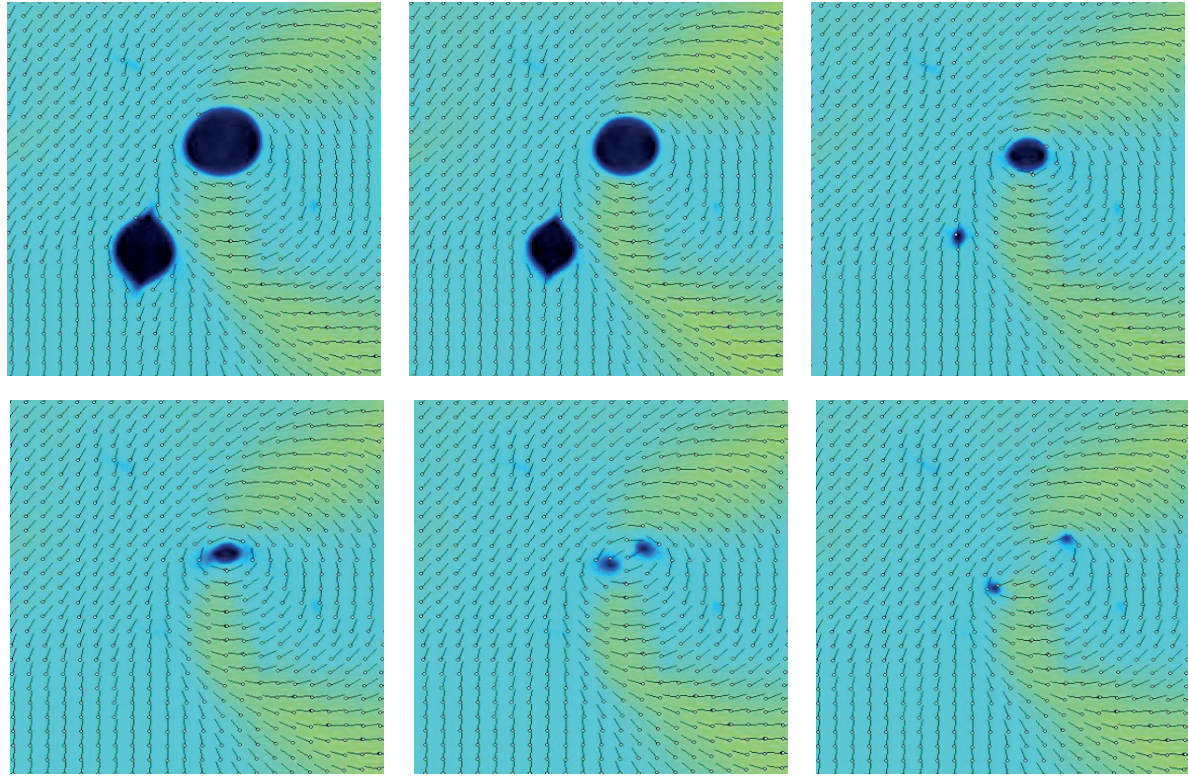


Figure 4.2: Experimentally observed evolution of isotropic tactoids. On each inset, the director field on the boundary of the right tactoid has the winding number 0 while it is equal to 1 on the boundary of the left tactoid. Once the right tactoid disappears, it generates a vortex of degree 1 that subsequently splits into two degree $1/2$ vortices. The disappearance of the left tactoid does not lead to the formation of topological singularities.

Let $\Omega \subset \mathbb{R}^3$ denote the region occupied by the liquid crystal sample. To derive an expression for the elastic energy, recall first that the Oseen-Frank energy defined over director fields $n \in H^1(\Omega, \mathbb{S}^2)$ is given by

$$E_{OF}[n] = \frac{1}{2} \int_{\Omega} \left\{ K_1 (\operatorname{div} n)^2 + K_2 (n \cdot \operatorname{curl} n)^2 + K_3 |n \times \operatorname{curl} n|^2 \right\} dx$$

where we assumed that the admissible competitors are subject to the same Dirichlet boundary data on $\partial\Omega$. Assuming in this section that $K_2 = K_3 < K_1$, the energy can be written (up to null Lagrangian terms) as

$$E_{OF}[n] = \frac{1}{2} \int_{\Omega} \left\{ \tilde{K}_1 (\operatorname{div} n)^2 + \tilde{K}_2 |\nabla n|^2 \right\} dx, \quad (4.47)$$

where $\tilde{K}_1 = K_1 - K_2$ and $\tilde{K}_2 = K_2$ are nonnegative elastic constants. Utilizing (4.23) and (4.43), we can write

$$\tilde{K}_1 (\operatorname{div} n)^2 + \tilde{K}_2 |\nabla n|^2 \sim \frac{L_1}{2} |\nabla(Q/\lambda_m)|^2 + \frac{L_2}{2} |(\mathbf{I} - Q/\lambda_m) \operatorname{div}(Q/\lambda_m)|^2$$

where $L_1 := \frac{\tilde{K}_2}{9}$ and $L_2 := \frac{2\tilde{K}_1}{81}$. Note that here we switched the indices of the elastic constants in order to conform with the standard notation.

The total energy of a nematic configuration as described within the Landau-de Gennes Q -tensor theory in the rest of this section will be given by

$$F[Q] := \int_{\Omega} \left(\frac{L_1}{2} |\nabla(Q/\lambda_m)|^2 + \frac{L_2}{2} |(\mathbf{I} - Q/\lambda_m) \operatorname{div}(Q/\lambda_m)|^2 + w_0 W(Q) \right) dx, \quad (4.48)$$

where w_0 is a constant that has units of energy per unit volume.

Remark 4.1. *Expanding the second elastic term in Eq. (4.48) we obtain*

$$|(\mathbf{I} - Q/\lambda_m) \operatorname{div}(Q/\lambda_m)|^2 = \frac{1}{\lambda_m^2} |\operatorname{div} Q|^2 - \frac{2}{\lambda_m^3} Q \operatorname{div} Q \cdot \operatorname{div} Q + \frac{1}{\lambda_m^4} |Q \operatorname{div} Q|^2.$$

Comparing the terms appearing in this expression with the elastic invariants of the generalized Landau-de Gennes theory in [68], we see that these terms correspond to $L_2^{(2)}$ -, $L_3^{(3)}$ - *and $L_6^{(4)}$ -invariants.*

If we set

$$\varepsilon := \frac{L_1}{L_2}, \bar{Q} = -Q/\lambda_m,$$

and rescale similarly to (4.27), we obtain (dropping the bar notation)

$$F[Q] = \int_{\Omega} \left(\frac{\varepsilon}{2} |\nabla Q|^2 + \frac{1}{2} |(\mathbf{I} + Q) \operatorname{div} Q|^2 + \frac{1}{4\gamma} W(Q) \right) dx, \quad (4.49)$$

where

$$W(Q) = 3a (\operatorname{tr} Q^2) - 2b (\operatorname{tr} Q^3) + \frac{1}{4} (\operatorname{tr} Q^2)^2 - W_m. \quad (4.50)$$

In our simulations we consider a simplified form of a Q -tensor that can be obtained via a dimension reduction procedure for thin nematic films [48]. In the corresponding ansatz, one eigenvector of admissible Q -tensors must be perpendicular to the plane of the film. Then in the system of coordinates in which the normal to the film is parallel to the z -axis, the Q -tensor is independent of z and can be written [18] as

$$Q(x, y) = \begin{pmatrix} \beta(x, y) + u_1(x, y) & u_2(x, y) & 0 \\ u_2(x, y) & \beta(x, y) - u_1(x, y) & 0 \\ 0 & 0 & -2\beta(x, y) \end{pmatrix}, \quad (4.51)$$

for a scalar-valued function β and vector-valued function $u = (u_1, u_2)$. Let

$$U = \begin{pmatrix} u_1 & u_2 \\ u_2 & -u_1 \end{pmatrix},$$

so that

$$\begin{pmatrix} \beta + u_1 & u_2 \\ u_2 & \beta - u_1 \end{pmatrix} = \beta \mathbf{I}_2 + U,$$

where \mathbf{I}_2 is the 2×2 identity matrix. In terms of β and u the contributions to the energy density are as follows

$$\begin{aligned} \frac{\varepsilon}{2} |\nabla Q|^2 &= \varepsilon \left(|\nabla u|^2 + 3|\nabla \beta|^2 \right), \\ \frac{1}{2} |(\mathbf{I} + Q) \operatorname{div} Q|^2 &= \frac{1}{2} |((\beta + 1)\mathbf{I}_2 + U) (\nabla \beta + \operatorname{div} U)|^2 \end{aligned}$$

and

$$\frac{1}{4\gamma} W(u, \beta) = \frac{1}{4\gamma} \left(\left(|u|^2 + 3\beta^2 \right)^2 - 12b\beta \left(|u|^2 - \beta^2 \right) + 6a \left(|u|^2 + 3\beta^2 \right) \right).$$

Suppose that the film occupies the region $\omega \in \mathbb{R}^2$. The system of Euler-Lagrange PDEs corresponding to the energy functional Eq. (4.49) then takes the form

$$\begin{aligned} & -\operatorname{div} \left\{ 2\varepsilon \nabla u_1 + \sigma_3 ((\beta + 1) \mathbf{I}_2 + U)^2 (\nabla \beta + \operatorname{div} U) \right\} \\ & + \sigma_3 ((\beta + 1) \mathbf{I}_2 + U) (\nabla \beta + \operatorname{div} U) \cdot (\nabla \beta + \operatorname{div} U) \\ & + \frac{1}{\gamma} \left(|u|^2 + 3\beta^2 - 6b\beta + 3a \right) u_1 = 0, \quad (4.52) \end{aligned}$$

$$\begin{aligned} & -\operatorname{div} \left\{ 2\varepsilon \nabla u_2 + \sigma_1 ((\beta + 1) \mathbf{I}_2 + U)^2 (\nabla \beta + \operatorname{div} U) \right\} \\ & + \sigma_1 ((\beta + 1) \mathbf{I}_2 + U) (\nabla \beta + \operatorname{div} U) \cdot (\nabla \beta + \operatorname{div} U) \\ & + \frac{1}{\gamma} \left(|u|^2 + 3\beta^2 - 6b\beta + 3a \right) u_2 = 0, \quad (4.53) \end{aligned}$$

$$\begin{aligned} & -\operatorname{div} \left\{ 6\varepsilon \nabla \beta + ((\beta + 1) \mathbf{I}_2 + U)^2 (\nabla \beta + \operatorname{div} U) \right\} \\ & + ((\beta + 1) \mathbf{I}_2 + U) (\nabla \beta + \operatorname{div} U) \cdot (\nabla \beta + \operatorname{div} U) \\ & + \frac{3}{\gamma} \left(|u|^2(\beta - b) + 3\beta(\beta^2 + b\beta + a) \right) = 0, \quad (4.54) \end{aligned}$$

where

$$\sigma_1 = \begin{pmatrix} 0 & 1 \\ 1 & 0 \end{pmatrix} \quad \text{and} \quad \sigma_3 = \begin{pmatrix} 1 & 0 \\ 0 & -1 \end{pmatrix}$$

are the Pauli matrices.

When the liquid crystal is in the energy minimizing nematic state while the director $n = (\cos \theta, \sin \theta, 0)$ lies in the plane of the film, we have

$$\begin{aligned} & \begin{pmatrix} \cos^2 \theta & \cos \theta \sin \theta & 0 \\ \cos \theta \sin \theta & \sin^2 \theta & 0 \\ 0 & 0 & 0 \end{pmatrix} = n \otimes n = \frac{1}{3}(I + Q) \\ & = \frac{1}{3} \begin{pmatrix} 1 + \beta + u_1 & u_2 & 0 \\ u_2 & 1 + \beta - u_1 & 0 \\ 0 & 0 & 1 - 2\beta \end{pmatrix}. \end{aligned}$$

It follows from this computation that

$$u = 3 \left(\cos^2 \theta - \frac{1}{2}, \cos \theta \sin \theta \right) = \frac{3}{2} (\cos 2\theta, \sin 2\theta), \quad \beta = 1/2, \quad (4.55)$$

hence the vector u winds twice as fast along a given curve in $\bar{\omega}$, compared to the director n when n is planar.

More generally, the ansatz Eq. (4.51) splits the nematic component of the minimal set of the bulk energy W into two disconnected components

$$C_1^N := \{(u, \beta) \in \mathbb{R}^2 \times \mathbb{R} : u = 0, \beta = -1\}$$

and

$$C_2^N := \{(u, \beta) \in \mathbb{R}^2 \times \mathbb{R} : |u| = 3/2, \beta = 1/2\}.$$

Here the first component corresponds to a constant nematic state with the director perpendicular to the surface of the film. The second component includes all configurations with the director lying in the plane of the film—these configurations can be nontrivial and, in particular, they include the director fields that carry a nonzero winding number.

Since we are interested in regimes when both nematic and isotropic phases coexist, we recall that whenever

$$0 \leq a \leq \frac{2b^2}{9},$$

the set

$$\{(u, \beta) \in \mathbb{R}^2 \times \mathbb{R} : u = 0, \beta = 0\}$$

yields a local minimum of W corresponding to the isotropic phase. The corresponding local minimum energy value is greater than or equal to the global minimum value of W . When $a = \frac{2b^2}{9}$, the set

$$C^I := \{(u, \beta) \in \mathbb{R}^2 \times \mathbb{R} : u = 0, \beta = 0\}$$

gives the third connected component of the minimal set of the bulk energy.

Given that W has a multi-component minimal set, the energy Eq. (4.49) is of Allen-Cahn-type as long as the factor in front of W is large. To this end, in what follows we assume that $\gamma = \varepsilon$ and $\varepsilon > 0$ is small. We will consider gradient flow dynamics associated with this model, but before we proceed further it is worth comparing our present situation to the more familiar one of gradient flow dynamics for a multi-well Allen-Cahn type potential with diffusion given simply by the Laplacian. In this scaling, when the diffusion is given by the Laplacian, formal asymptotics suggest that for Allen-Cahn dynamics one should expect an interface propagating by curvature flow that separates the different phases defined by components of the zero set of the potential. In the scalar setting of Allen-Cahn where a double well potential vanishes at two points, there are by now numerous rigorous proofs of this fact based on maximum principles, barriers and/or comparison principles, see e.g. [24, 30, 37, 53] as well as the energetic argument in the radial setting in [21]. For the vector setting of time-dependent Allen-Cahn, formal asymptotics based on multiple time-scale expansions again suggest that mean curvature flow emerges as the governing equation for the interface, [92, 93].

What distinguishes the dynamics in the present study, however, is the anisotropy of the diffusive terms indicated by the presence of the divergence terms in (4.52)–(4.54). While we again anticipate that in the regime $\varepsilon \ll 1$ an interface separating the different phases of the Q tensor will evolve by a law involving curvature, the process will be significantly affected by the interaction between the director associated with Q and the normal to the interface.

Our present model is closely related to the investigation in [49] of the $\varepsilon \rightarrow 0$ asymptotics for a director-like model based on an \mathbb{R}^2 -valued order parameter u . There the elastic energy is similarly anisotropic and is coupled to a Chern-Simons-Higgs-type potential $|u|^2(|u|^2 - 1)^2$. Thus, the structure of the energy functional in [49] is similar to the setup proposed here in that it involves a potential with minima at the isotropic and a nematic state as well as the elastic terms that are quadratic in the gradient of the order parameter field. The term penalizing splay deformations in [49] dominates other elastic terms so that the divergence of the director is very expensive. The

principal difference between the model considered in [49], which from now on we will refer to as the CSH-director model, and the present work is that here we consider non-orientable tensor fields, while the admissible fields in [49] are orientable.

Our numerical results indicate that similarity between the models leads to similar properties of critical points. In particular, one of the principal observations in [49] is that the director field is parallel to the interface in its immediate vicinity when the parameter ε is small. The same behavior is exhibited by the numerically obtained critical points of the Landau-de Gennes energy Eq. (4.48), as will be demonstrated in the next section.

We introduce dynamics into the problem by assuming that evolution of the isotropic-to-nematic transition proceeds via gradient flow

$$\mu_u u_t = -\frac{\delta F}{\delta u}, \quad \mu_\beta \beta_t = -\frac{\delta F}{\delta \beta},$$

where $\mu_u > 0$ and $\mu_\beta > 0$ are inverses of the scalar mobilities of u and β , respectively. This gives the following systems of PDEs

$$\begin{aligned} \mu_u u_{1t} = \operatorname{div} \left\{ 2\varepsilon \nabla u_1 + \sigma_3 ((\beta + 1) \mathbf{I}_2 + \mathbf{U})^2 (\nabla \beta + \operatorname{div} \mathbf{U}) \right\} \\ - \sigma_3 ((\beta + 1) \mathbf{I}_2 + \mathbf{U}) (\nabla \beta + \operatorname{div} \mathbf{U}) \cdot (\nabla \beta + \operatorname{div} \mathbf{U}) \\ - \frac{1}{\gamma} \left(|u|^2 + 3\beta^2 - 6b\beta + 3a \right) u_1, \end{aligned} \quad (4.56)$$

$$\begin{aligned} \mu_u u_{2t} = \operatorname{div} \left\{ 2\varepsilon \nabla u_2 + \sigma_1 ((\beta + 1) \mathbf{I}_2 + \mathbf{U})^2 (\nabla \beta + \operatorname{div} \mathbf{U}) \right\} \\ - \sigma_1 ((\beta + 1) \mathbf{I}_2 + \mathbf{U}) (\nabla \beta + \operatorname{div} \mathbf{U}) \cdot (\nabla \beta + \operatorname{div} \mathbf{U}) \\ - \frac{1}{\gamma} \left(|u|^2 + 3\beta^2 - 6b\beta + 3a \right) u_2, \end{aligned} \quad (4.57)$$

$$\begin{aligned} \mu_\beta \beta_t = \operatorname{div} \left\{ 6\varepsilon \nabla \beta + ((\beta + 1) \mathbf{I}_2 + \mathbf{U})^2 (\nabla \beta + \operatorname{div} \mathbf{U}) \right\} \\ - ((\beta + 1) \mathbf{I}_2 + \mathbf{U}) (\nabla \beta + \operatorname{div} \mathbf{U}) \cdot (\nabla \beta + \operatorname{div} \mathbf{U}) \\ - \frac{3}{\gamma} \left(|u|^2(\beta - b) + 3\beta (\beta^2 + b\beta + a) \right) = 0. \end{aligned} \quad (4.58)$$

In order to simulate experimentally available configurations, we will set the initial configuration of (u, β) to consist of an isotropic region ω_I embedded in a nematic phase corresponding to the component C_2^N of the minimal set of W . That is, we will assume that the initial condition is an appropriate mollification of (u, β) such that

$$(|u|, \beta) = (3/2, 1/2)\chi_{\omega \setminus \omega_I}. \quad (4.59)$$

Here $\chi_{\omega \setminus \omega_I}$ is the characteristic function of the region $\omega \setminus \omega_I$ occupied by the nematic phase. We also impose boundary conditions on $\partial\omega$ with values in C_2^N ; we will assume that the boundary data for u may have a nonzero winding number.

In the next section we present the result of simulations for the system Eq. (4.56)-Eq. (4.58) and compare the numerical outcomes to experimental observations. We remind the reader that our goal in the present chapter is to demonstrate numerically that behavior of interfaces and singularities observed in experiments with chromonic liquid crystals can be qualitatively recovered within the framework of the Landau-de Gennes model. We leave for future work both formal and rigorous analysis of our results, as well as any quantitative considerations and associated modifications of the model.

4.2.3 Simulations vs Experiment

The simulations in this section are performed using COMSOL Multiphysics® [1] with the domain ω taken to be a disk of nondimensional radius $1/4$, centered at the origin. In what follows, we set dimensional $b = 1$ and let $\gamma = \varepsilon = 0.06$. The initial data in all simulations is specified by choosing $\omega_I = \{(x, y) \in \omega : r(x, y) \leq \frac{1}{6}\}$ in Eq. (4.59). Both here and below $(r(x, y), \theta(x, y))$ are polar coordinates of the point $(x, y) \in \mathbb{R}^2$.

Recall that when a and b are related via Eq. (4.20) (either in dimensional or nondimensional setting), the energies of the nematic and isotropic states are the same. Then, if in dimensional

variables we set

$$a = \frac{2b^2}{9} - \alpha,$$

the parameter $\alpha \in (0, 2b^2/9)$ measures the degree of *undercooling* in the system. That is, when α increases, the bulk energy density of the isotropic state grows with respect to that of the nematic state and thermodynamic forces driving the isotropic-to-nematic transition become stronger. Setting $\bar{\alpha} = \alpha/\lambda^2$ and dropping the bar, the nondimensional a and b are given by

$$a = \frac{4(2 - 9\alpha)}{(3 + \sqrt{1 + 36\alpha})^2}, \quad b = \frac{6}{3 + \sqrt{1 + 36\alpha}}. \quad (4.60)$$

First, we verify the conjecture that the behavior of interfaces in our Landau-de Gennes system of PDEs with highly anisotropic elastic constants resembles that of interfaces in the related CSH-director system of [49]. To this end, we assume that a is given by Eq. (4.20) so that $\alpha = 0$ and both the nematic and the isotropic states are the global minimum of the Landau-de Gennes potential W . We simulate the system Eq. (4.56)-Eq. (4.58) subject to the boundary conditions

$$\beta|_{\partial\omega} = \frac{1}{2}, \quad u|_{\partial\omega} = \frac{3}{2}(-\cos 2\theta, \sin 2\theta).$$

Taking into account Eq. (4.55), the director field on the boundary can be chosen as

$$n|_{\partial\omega} = (-\cos \theta, \sin \theta),$$

where the topological degree of n is equal to -1 on $\partial\omega$.

The results of the gradient flow simulation for the degree -1 boundary data are shown in Fig. 4.3. An initially circular interface is seen to evolve into the shape given in the figure by a thick red curve that is also a contour line of $\beta = 1/4$. The system in Fig. 4.3 has reached a steady state that is very similar to what is observed for the CSH-director model in [49]. Indeed, for small ε , the energy of the isotropic/nematic configuration in both cases should include a penalty for divergence of the director in the nematic phase, as well as the cost for the perimeter of the interface. The anisotropy of the elastic constants also forces the director to align with the interface.

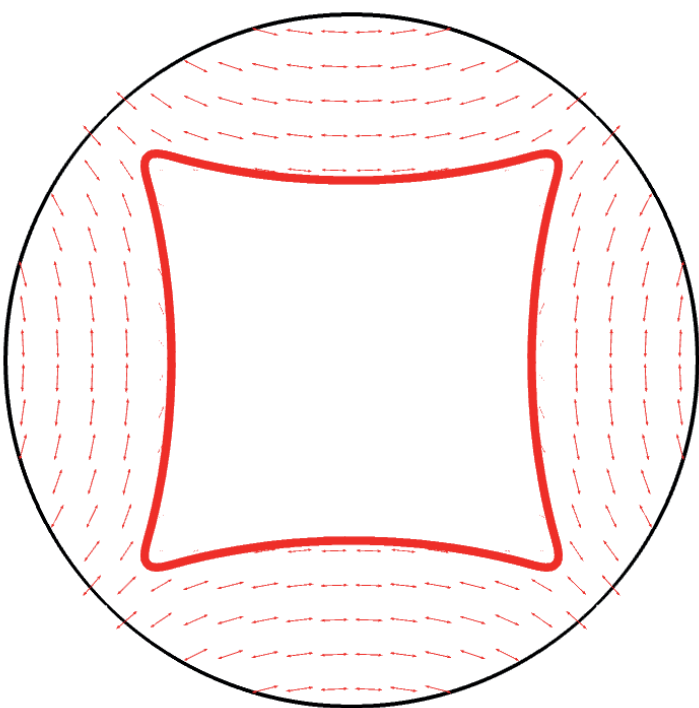


Figure 4.3: Simulated degree -1 tactoid. Here the director field n is set to be equal to $(-\cos \theta, \sin \theta)$ on the boundary of the disk and θ is a polar angle. The thick red line indicates the position of the interface.

The resulting director configuration and the shape of the interface are coupled; in particular, unlike the standard curvature flow, shrinking the perimeter and, thus, size of the isotropic region leads to unbounded growth of the elastic energy. The competition between the perimeter and elastic energy contributions enforces the equilibrium between the two phases observed in Fig. 4.3.

One is then tempted to ask whether there is any difference between the Landau-de Gennes and the CSH-director model [49] in terms of how the director field extracted from solutions of these two models should behave as $\varepsilon \rightarrow 0$. We expect that the difference would manifest itself when the size of an isotropic region is small enough so that this region can be thought of as a core of a topological vortex.

Suppose, for example, that the interface is a single smooth closed curve. Due to the director tangency condition on the interface and because the director field is orientable, the director has the winding number 1 around the interface. When the island shrinks to a small size and because the director is \mathbb{S}^1 -valued in the nematic phase, topological constraints would keep the isotropic island from disappearing completely in order to prevent the nematic configuration from having an infinite energy. The resulting degree 1 vortex is stable in the CSH-director setting and would persist for a finite time, perhaps until it annihilates with another vortex of the opposite sign or collides with the boundary of ω .

Now recall that within the Landau-de Gennes theory, a nematic state is described by a Q -tensor that is a translation and dilation of a projection matrix $n \otimes n$. The field $n \otimes n$ is *not* orientable and can be associated with an element of a projective plane \mathbb{RP}^2 . In other words, by working with $n \otimes n$ instead of n , we identify the opposite directions $-n$ and n as being the same. As the result, the smallest “quantum” of the winding number for a nematic tensor is $1/2$. Hence the degree 1 vortex in the director description contains two “quanta” of degree if we switch to the Landau-de Gennes framework. It is a well-established fact that a higher degree vortex is unstable with respect to splitting into several vortices of smaller degrees since the energetic cost of a degree d vortex

is proportional to d^2 , [19]. We expect that the degree 1 CSH vortex would split into two degree 1/2 vortices when considered in the sense of Landau-de Gennes. Our experimental observations conform to the latter picture; hence the description that disposes with orientability is necessary when considering an isotropic-to-nematic phase transition problem.

We now conduct numerical experiments to test whether evolution of tactoids observed in physical experiments can be captured within the Landau-de Gennes model.

4.2.3.1 Degree 1 Tactoid

Here we suppose that the director is parallel to the boundary of the disk ω , e.g.,

$$n|_{\partial\omega} = (-\sin \theta, \cos \theta),$$

so that the topological degree of the orientable director field n is equal 1 on $\partial\omega$. In the non-orientable, Q -tensor setting the corresponding condition can be expressed as

$$\beta|_{\partial\omega} = \frac{1}{2}, \quad u|_{\partial\omega} = -\frac{3}{2}(\cos 2\theta, \sin 2\theta).$$

If the simulations are conducted at zero undercooling, when a is given by Eq. (4.20), we observed both here and for the Ginzburg-Landau-type model [49] that, similar to Fig. 4.3, the isotropic domain evolving via gradient flow shrinks down to a certain size and then stabilizes. In order to drive this size down, we enforce larger undercooling by choosing $\alpha = 0.2$.

The evolution of the nematic/isotropic interface is shown in Fig. 4.4. While the isotropic tactoid is not too small, it maintains its circular shape and the director in the nematic region remains parallel to the boundary. Indeed, in this configuration the divergence contribution vanishes, the director is parallel to the interface, and the perimeter of the isotropic tactoid is minimal given its shape.

When the tactoid eventually shrinks to a vortex size seen in the right inset in the second row in Fig. 4.4, it loses stability and splits into two degree 1/2 vortices that drift away from each other with time. The overall behavior is qualitatively similar to that of the right tactoid in Fig. 4.2.

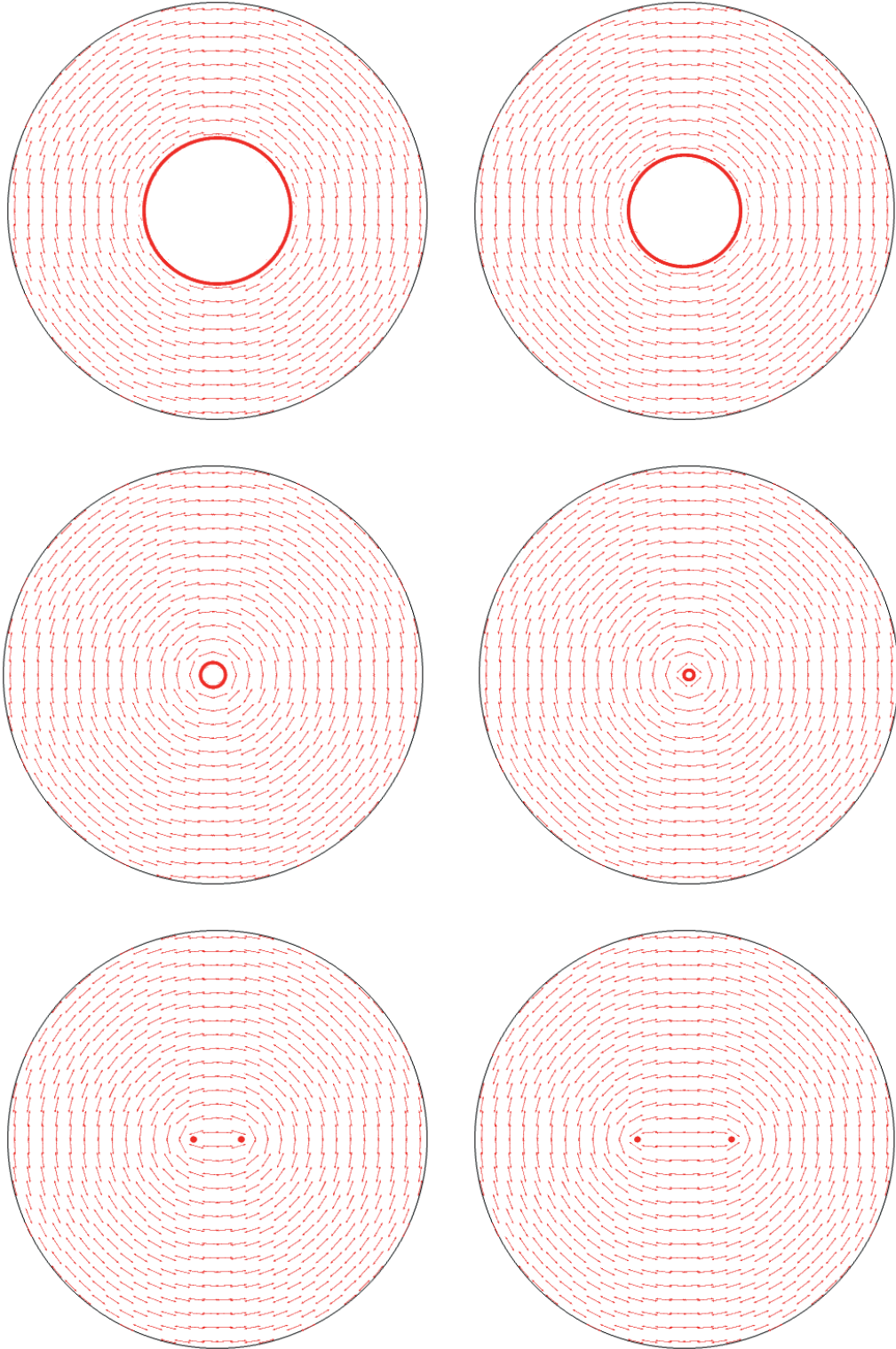


Figure 4.4: Simulated evolution of a degree 1 tactoid. Here the director field is set to be equal to $(-\sin \theta, \cos \theta)$ on the boundary of the disk and θ is a polar angle. (cf. Fig.4.2, right tactoid). The thick red line indicates the position of the interface.

4.2.3.2 Degree -1 Tactoid

We now return to the boundary conditions

$$\beta|_{\partial\omega} = \frac{1}{2}, \quad u|_{\partial\omega} = \frac{3}{2}(-\cos 2\theta, \sin 2\theta),$$

considered in the beginning of this section for zero undercooling. Here we assume instead that $\alpha = -0.1$ and look for the effects on evolution of the bias between the values of local minima of the potential energy corresponding to the nematic and isotropic state. This bias is associated with lowering the temperature below that of the nematic-to-isotropic transition. The corresponding numerical results are shown in Fig. 4.5. The first three figures essentially demonstrate the development of a configuration shown in Fig. 4.4. The larger thermodynamic forces driving the phase transition in the present case, however, push the size of the tactoid further down essentially to that of a vortex core. At this point, the isotropic region loses stability and splits into two vortices of degree $-1/2$, similar to what can be seen in Fig. 4.1.

4.2.3.3 Degree 0 Tactoid

Next, we impose the constant boundary conditions

$$\beta|_{\partial\omega} = \frac{1}{2}, \quad u|_{\partial\omega} = \frac{3}{2}(1, 0),$$

and suppose that $\alpha = 0$. The numerically computed evolution of a degree zero tactoid that results is shown in Fig. 4.6 and qualitatively resembles the behavior of a similar tactoid in the experiment as depicted in Fig. 4.2. A similar shape is also seen in evolution of degree zero interfaces in the CSH-director model in [49] and is explained by the fact that the director has to be parallel to the interface. In particular, the interface cannot be smooth, for if it were, then it would carry a nonzero topological degree different from the degree on the boundary of the domain. One interesting issue that we observed in the course of our simulations is illustrated in Fig. 4.7. When the undercooling is large ($\alpha = 0.2$), the director appears to be orthogonal to the moving interface rather than being

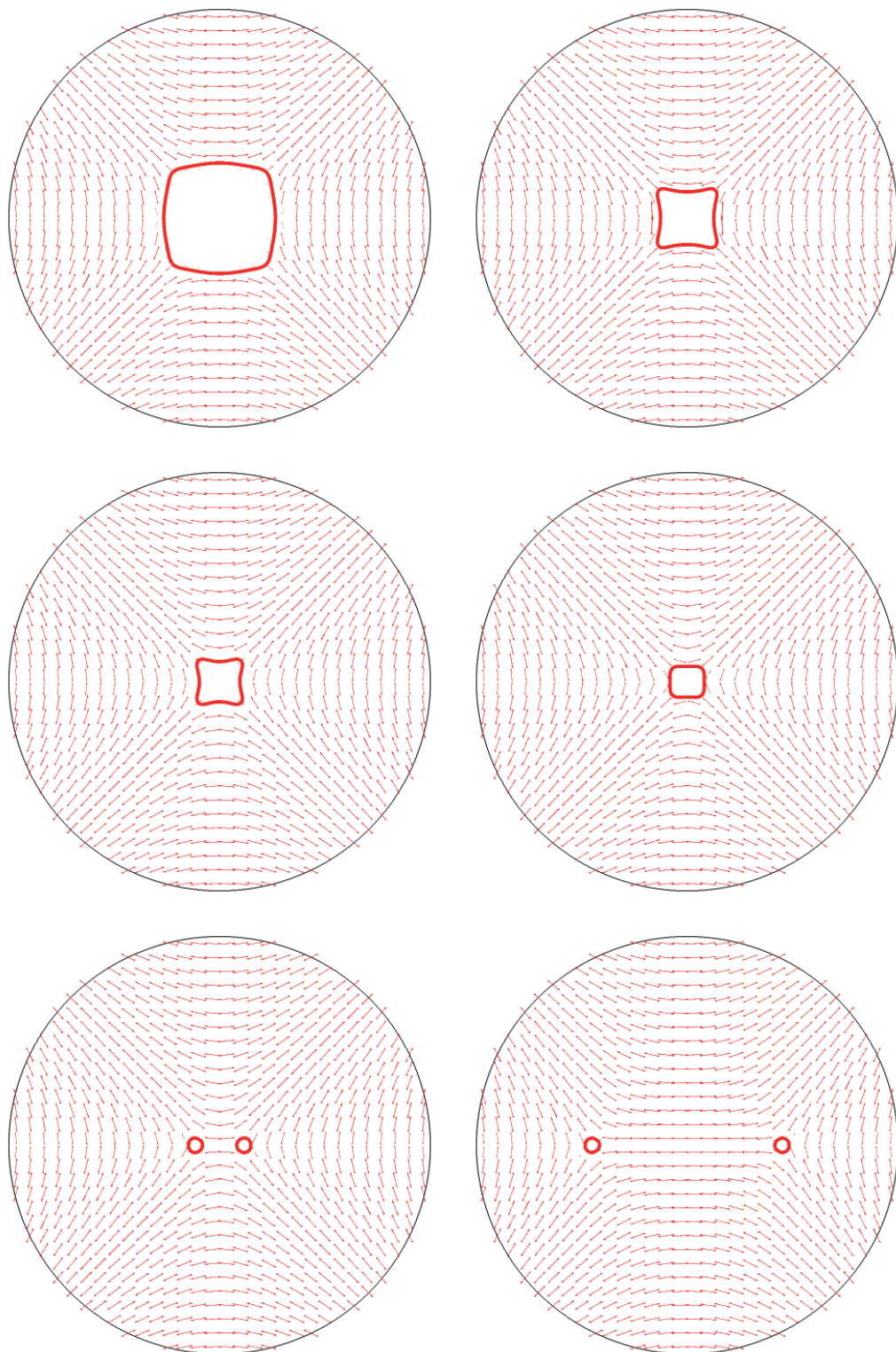


Figure 4.5: Simulated evolution of a degree -1 tactoid. Here the director field is set to be equal to $(-\cos \theta, \sin \theta)$ on the boundary of the disk and θ is a polar angle. (cf. Fig.4.1). The thick red line indicates the position of the interface.

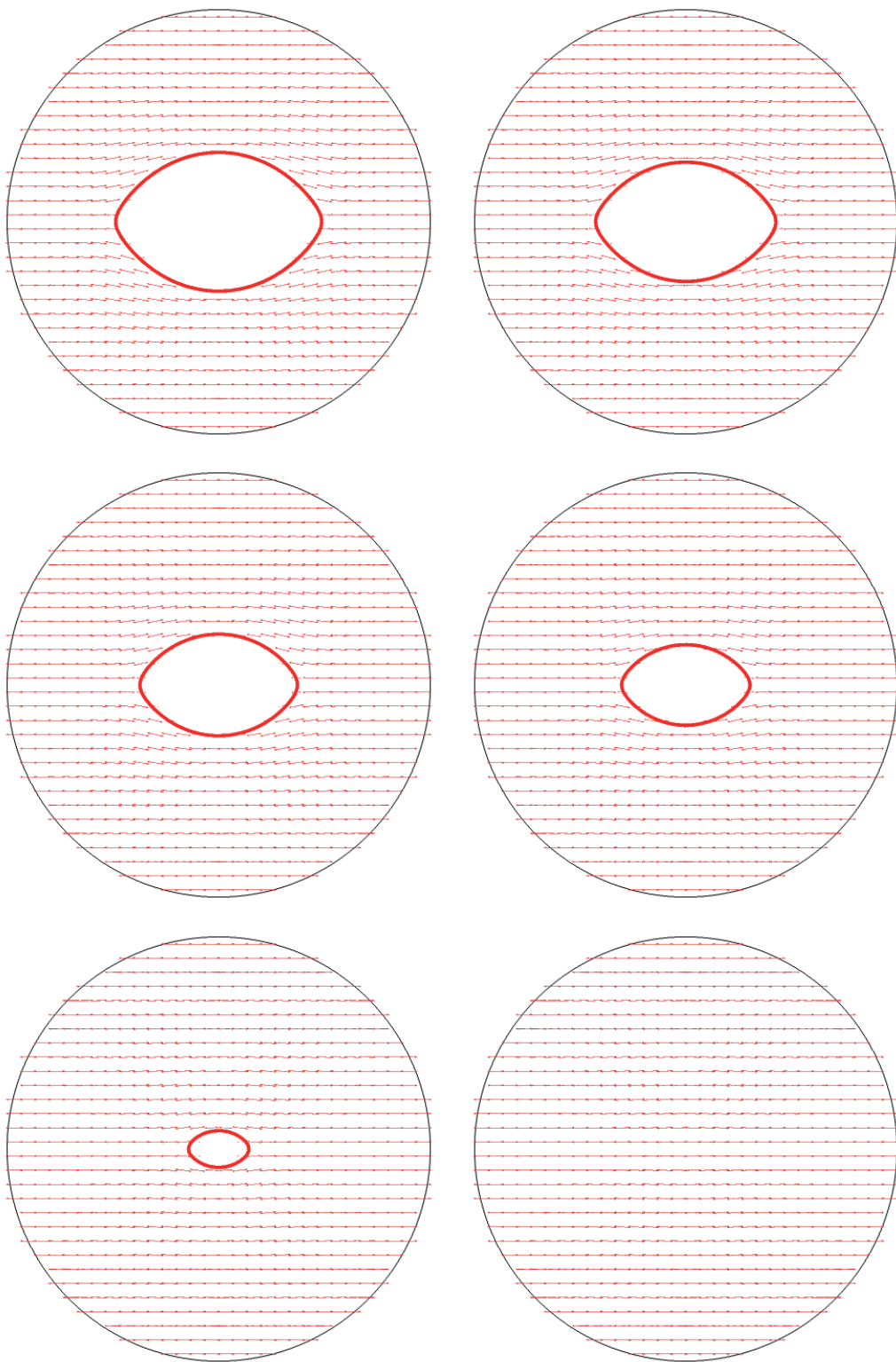


Figure 4.6: Simulated evolution of a degree 0 tactoid. Here the director field is set to be equal to $(1, 0)$ on the boundary of the disk. (cf. Fig.4.2, left tactoid). The thick red line indicates the position of the interface.

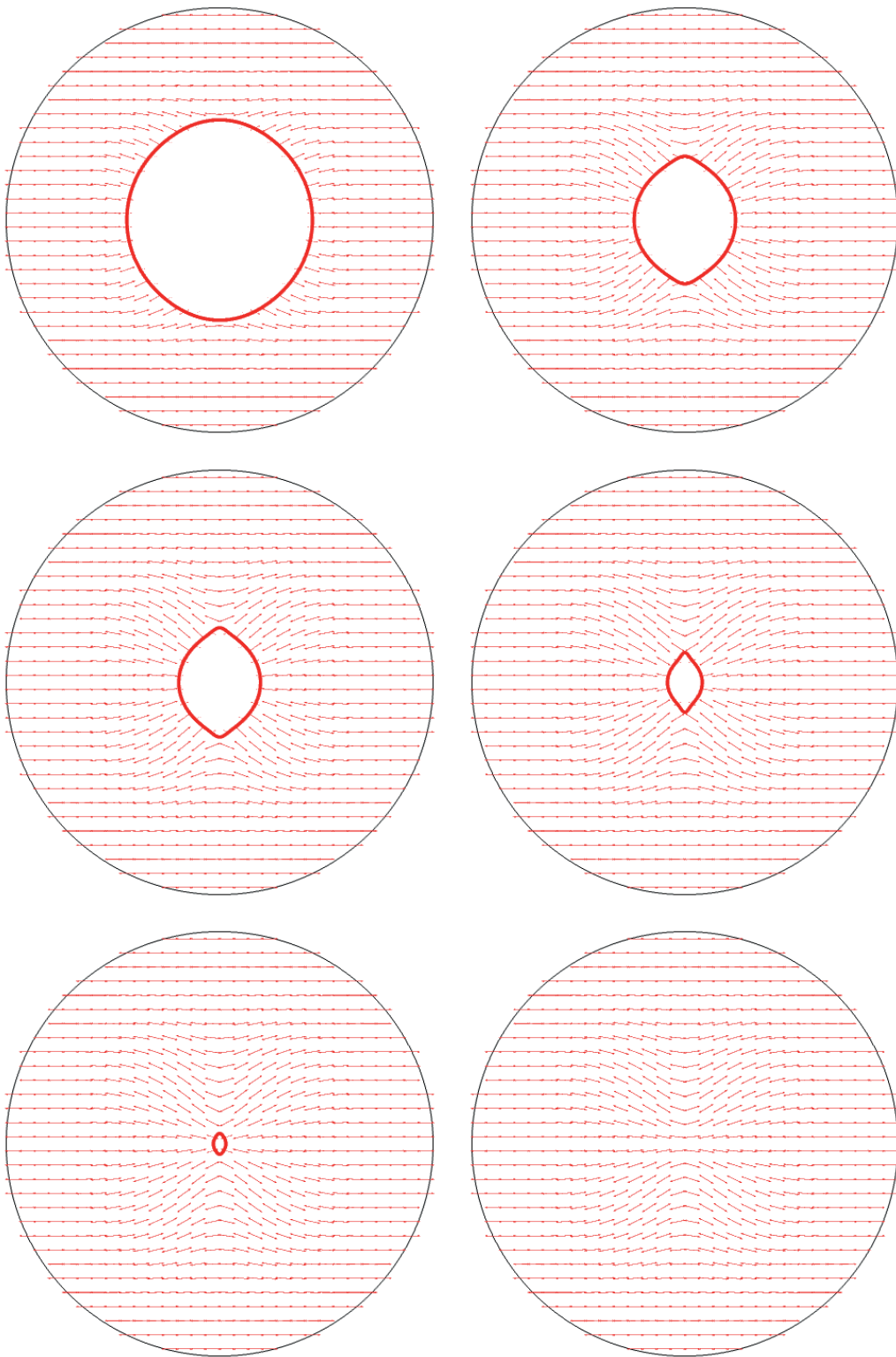


Figure 4.7: Simulated evolution of a degree 0 tactoid. Here the director field is set to be equal to $(1, 0)$ on the boundary of the disk and the undercooling is significantly larger than that in Fig.4.6. The thick red line indicates the position of the interface.

parallel to it as would be expected. A possible explanation for this effect is that the velocity of the interface is relatively large for larger undercoolings and the mobility of the director might not be sufficient for it to relax in a proper direction. We plan to investigate this behavior further in a future work.

4.2.3.4 Coalescence of Nematic Tactoids

Finally, the Landau - de Gennes model can also be used to simulate the reverse situation when positive nematic tactoids nucleate in the isotropic phase, then grow and coalesce to form the nematic phase with embedded topological defects (cf. [59]). In Fig. 4.8 the simulations were conducted subject to Neumann boundary data on $\partial\omega$ and assuming that ω has radius $1/2$, while $\alpha = 0.01$. Three circular tactoids of different orientations were assumed to be present at the time $t = 0$; in the course of the simulation, tactoids merged generating a single degree $-1/2$ defect. This situation closely resembles the original Kibble's model of strings formed in early universe through coalescence of domains with different "phase" [58].

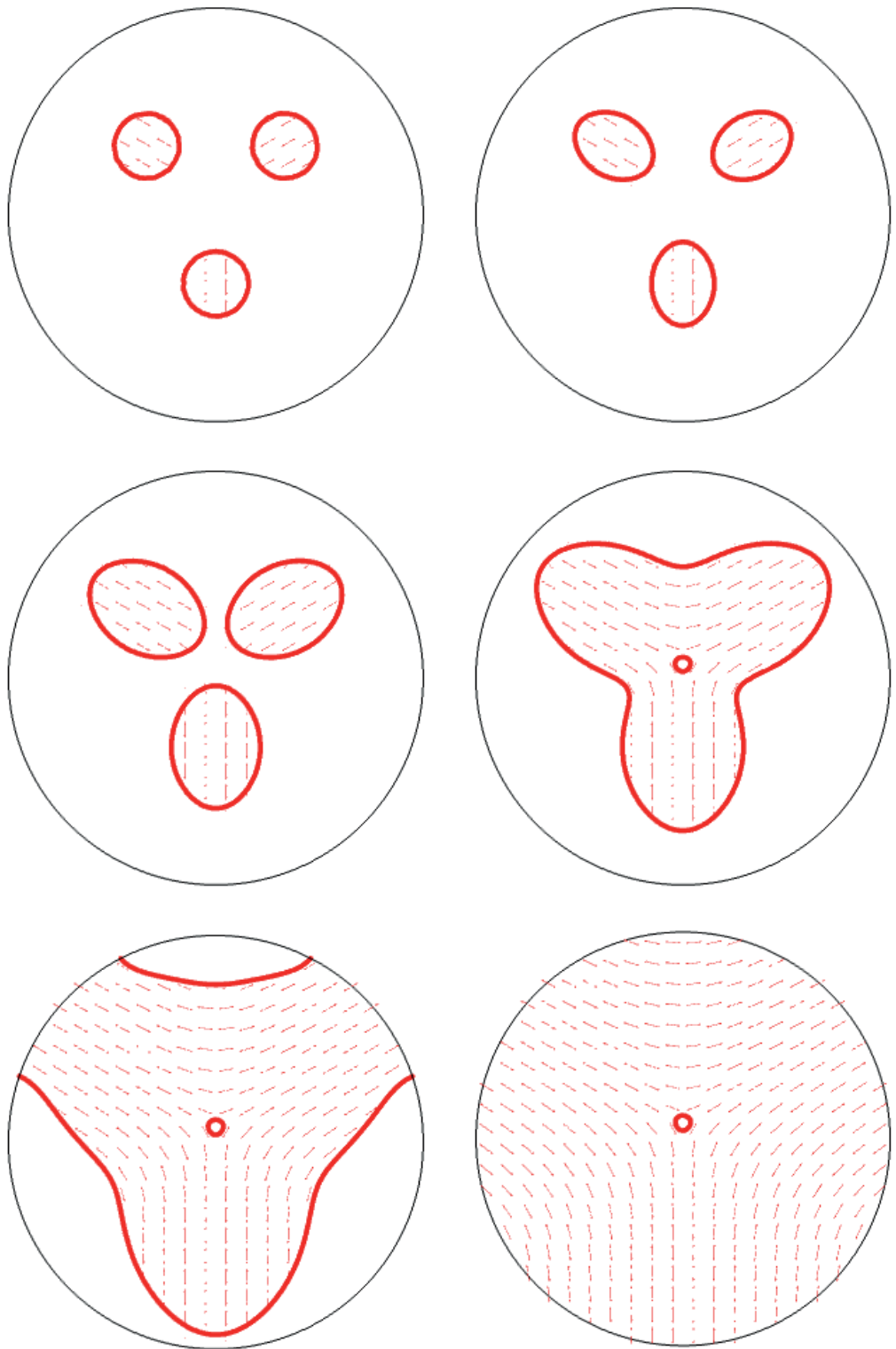


Figure 4.8: Simulated coalescence of three degree 0 nematic tactoids. The thick red lines indicate the position of the interface.

Bibliography

- [1] COMSOL Multiphysics® v. 5.3. <http://www.comsol.com/>. COMSOL AB, Stockholm, Sweden.
- [2] Bharat R. Acharya, Andrew Primak, and Satyendra Kumar. Biaxial nematic phase in bent-core thermotropic mesogens. *Phys. Rev. Lett.*, 92:145506, Apr 2004.
- [3] S. Alama, L. Bronsard, and X. Lamy. Spherical particle in a nematic liquid crystal under an external field: the Saturn ring regime. *ArXiv e-prints*, October 2017.
- [4] Stan Alama, Lia Bronsard, and Xavier Lamy. Minimizers of the Landau–de Gennes energy around a spherical colloid particle. *Arch. Ration. Mech. Anal.*, 222(1):427–450, 2016.
- [5] François Alouges, Tristan Rivière, and Sylvia Serfaty. Néel and cross-tie wall energies for planar micromagnetic configurations. *ESAIM Control Optim. Calc. Var.*, 8:31–68, 2002. A tribute to J. L. Lions.
- [6] Luigi Ambrosio. Metric space valued functions of bounded variation. *Ann. Scuola Norm. Sup. Pisa Cl. Sci. (4)*, 17(3):439–478, 1990.
- [7] Luigi Ambrosio, Camillo De Lellis, and Carlo Mantegazza. Line energies for gradient vector fields in the plane. *Calc. Var. Partial Differential Equations*, 9(4):327–255, 1999.
- [8] N. André and I. Shafrir. On a singular perturbation problem involving the distance to a curve. *J. Anal. Math.*, 90:337–396, 2003.

- [9] Nelly André and Itai Shafrir. Minimization of a Ginzburg-Landau type functional with nonvanishing Dirichlet boundary condition. *Calc. Var. Partial Differential Equations*, 7(3):191–217, 1998.
- [10] Nelly André and Itai Shafrir. On a singular perturbation problem involving a “circular-well” potential. *Trans. Amer. Math. Soc.*, 359(10):4729–4756, 2007.
- [11] Sigurd Angenent and Morton E. Gurtin. Multiphase thermomechanics with interfacial structure 2. Evolution of an isothermal interface. *Arch. Ration. Mech. Anal.*, 108(3):323–391, Nov 1989.
- [12] Patricio Aviles and Yoshikazu Giga. On lower semicontinuity of a defect energy obtained by a singular limit of the Ginzburg-Landau type energy for gradient fields. *Proc. Roy. Soc. Edinburgh Sect. A*, 129(1):1–17, 1999.
- [13] Greta Babakhanova, Zeinab Parsouzi, Sathyanarayana Paladugu, Hao Wang, Yu. A. Nas-tishin, Sergij V. Shiyanovskii, Samuel Sprunt, and Oleg D. Lavrentovich. Elastic and viscous properties of the nematic dimer CB7CB. *Phys. Rev. E*, 96:062704, Dec 2017.
- [14] Sisto Baldo. Minimal interface criterion for phase transitions in mixtures of Cahn-Hilliard fluids. *Ann. Inst. H. Poincaré Anal. Non Linéaire*, 7(2):67–90, 1990.
- [15] John M. Ball and Apala Majumdar. Nematic liquid crystals: From maier-saupe to a continuum theory. *Molecular Crystals and Liquid Crystals*, 525(1):1–11, 2010.
- [16] John M. Ball and Arghir Zarnescu. Orientability and energy minimization in liquid crystal models. *Arch. Ration. Mech. Anal.*, 202(2):493–535, 2011.
- [17] Ana Cristina Barroso and Irene Fonseca. Anisotropic singular perturbations—the vectorial case. *Proc. Roy. Soc. Edinburgh Sect. A*, 124(3):527–571, 1994.

- [18] Patricia Bauman, Jinhae Park, and Daniel Phillips. Analysis of nematic liquid crystals with disclination lines. *Arch. Ration. Mech. Anal.*, 205(3):795–826, 2012.
- [19] Fabrice Bethuel, Haïm Brezis, and Frédéric Hélein. *Ginzburg-Landau vortices*, volume 13 of *Progress in Nonlinear Differential Equations and their Applications*. Birkhäuser Boston, Inc., Boston, MA, 1994.
- [20] Haïm Brezis, Jean-Michel Coron, and Elliott H. Lieb. Harmonic maps with defects. *Comm. Math. Phys.*, 107(4):649–705, 1986.
- [21] Lia Bronsard and Robert V. Kohn. Motion by mean curvature as the singular limit of Ginzburg-Landau dynamics. *J. Differential Equations*, 90(2):211–237, 1991.
- [22] Giacomo Canevari. Biaxiality in the asymptotic analysis of a 2D Landau–de Gennes model for liquid crystals. *ESAIM Control Optim. Calc. Var.*, 21(1):101–137, 2015.
- [23] P. M. Chaikin and T. C. Lubensky. *Principles of Condensed Matter Physics*. Cambridge University Press, 1995.
- [24] Xinfu Chen. Generation and propagation of interfaces for reaction-diffusion equations. *J. Differential Equations*, 96(1):116–141, 1992.
- [25] C. Chiccoli, I. Feruli, O. D. Lavrentovich, P. Pasini, S. V. Shiyanovskii, and C. Zannoni. Topological defects in schlieren textures of biaxial and uniaxial nematics. *Phys. Rev. E*, 66:030701, Sep 2002.
- [26] Sergio Conti and Camillo De Lellis. Sharp upper bounds for a variational problem with singular perturbation. *Math. Ann.*, 338(1):119–146, 2007.
- [27] Gianni Dal Maso. *An introduction to Γ -convergence*, volume 8 of *Progress in Nonlinear Differential Equations and their Applications*. Birkhäuser Boston, Inc., Boston, MA, 1993.

- [28] Timothy A. Davis and Eugene C. Gartland, Jr. Finite element analysis of the Landau-de Gennes minimization problem for liquid crystals. *SIAM J. Numer. Anal.*, 35(1):336–362, 1998.
- [29] Camillo De Lellis and Felix Otto. Structure of entropy solutions to the eikonal equation. *J. Eur. Math. Soc. (JEMS)*, 5(2):107–145, 2003.
- [30] Piero de Mottoni and Michelle Schatzman. Geometrical evolution of developed interfaces. *Trans. Amer. Math. Soc.*, 347(5):1533–1589, 1995.
- [31] Andrew DeBenedictis and Timothy J. Atherton. Shape minimisation problems in liquid crystals. *Liquid Crystals*, 43(13-15):2352–2362, 2016.
- [32] Antonio DeSimone, Robert V. Kohn, Stefan Müller, and Felix Otto. A compactness result in the gradient theory of phase transitions. *Proc. Roy. Soc. Edinburgh Sect. A*, 131(4):833–844, 2001.
- [33] Stefan Dickmann. *Numerische Berechnung von Feld und Molekülausrichtung in Flüssigkristallanzeigen*. PhD thesis, 1995. Karlsruhe University.
- [34] J. L. Ericksen. Conservation laws for liquid crystals. *Trans. Soc. Rheology*, 5:23–34, 1961.
- [35] J. L. Ericksen. Hydrostatic theory of liquid crystals. *Arch. Rational Mech. Anal.*, 9:371–378, 1962.
- [36] J. L. Ericksen. Liquid crystals with variable degree of orientation. *Arch. Rational Mech. Anal.*, 113(2):97–120, 1990.
- [37] L. C. Evans, H. M. Soner, and P. E. Souganidis. Phase transitions and generalized motion by mean curvature. *Comm. Pure Appl. Math.*, 45(9):1097–1123, 1992.
- [38] Jiyu Fang, Ellis Teer, Charles M. Knobler, Kok-Kiong Loh, and Joseph Rudnick. Boojums and the shapes of domains in monolayer films. *Phys. Rev. E*, 56:1859–1868, Aug 1997.

- [39] Irene Fonseca. The wulff theorem revisited. *Proceedings: Mathematical and Physical Sciences*, 432(1884):125–145, 1991.
- [40] Irene Fonseca and Stefan Müller. Quasi-convex integrands and lower semicontinuity in L^1 . *SIAM J. Math. Anal.*, 23(5):1081–1098, 1992.
- [41] Irene Fonseca and Luc Tartar. The gradient theory of phase transitions for systems with two potential wells. *Proc. Roy. Soc. Edinburgh Sect. A*, 111(1-2):89–102, 1989.
- [42] F. C. Frank. I. liquid crystals. on the theory of liquid crystals. *Discuss. Faraday Soc.*, 25:19–28, 1958.
- [43] E. C. Gartland, Jr. Scalings and Limits of Landau-deGennes Models for Liquid Crystals: A Comment on Some Recent Analytical Papers. *ArXiv e-prints*, December 2015.
- [44] Enrico Giusti. *Minimal surfaces and functions of bounded variation*, volume 80 of *Monographs in Mathematics*. Birkhäuser Verlag, Basel, 1984.
- [45] D. Golovaty, P. Sternberg, and R. Venkatraman. A Ginzburg-Landau type problem for highly anisotropic nematic liquid crystals. *To appear in SIAM J. Math. Anal.*, 2018.
- [46] Dmitry Golovaty, Young-Ki Kim, Oleg D. Lavrentovich, Michael Novack, and Peter Sternberg. Phase Transitions in Nematics: Textures with Tactoids and Disclinations. *arXiv e-prints*, page arXiv:1902.06342, Feb 2019.
- [47] Dmitry Golovaty and José Alberto Montero. On minimizers of a Landau–de Gennes energy functional on planar domains. *Arch. Ration. Mech. Anal.*, 213(2):447–490, 2014.
- [48] Dmitry Golovaty, José Alberto Montero, and Peter Sternberg. Dimension reduction for the Landau–de Gennes model in planar nematic thin films. *J. Nonlinear Sci.*, 25(6):1431–1451, 2015.

- [49] Dmitry Golovaty, Michael Novack, Peter Sternberg, and Raghavendra Venkatraman. A Model Problem for Nematic-Isotropic Transitions with Highly Disparate Elastic Constants. *arXiv e-prints*, page arXiv:1811.12586, Nov 2018.
- [50] R. Hardt, D. Kinderlehrer, and Fang-Hua Lin. Stable defects of minimizers of constrained variational principles. *Ann. Inst. H. Poincaré Anal. Non Linéaire*, 5(4):297–322, 1988.
- [51] Robert Hardt, David Kinderlehrer, and Fang-Hua Lin. Existence and partial regularity of static liquid crystal configurations. *Comm. Math. Phys.*, 105(4):547–570, 1986.
- [52] Radu Ignat. Singularities of divergence-free vector fields with values into \mathbb{S}^1 or \mathbb{S}^2 . Applications to micromagnetics. *Confluentes Math.*, 4(3):1230001, 80, 2012.
- [53] Tom Ilmanen. Convergence of the Allen-Cahn equation to Brakke’s motion by mean curvature. *J. Differential Geom.*, 38(2):417–461, 1993.
- [54] Robert L. Jerrard. Lower bounds for generalized Ginzburg-Landau functionals. *SIAM J. Math. Anal.*, 30(4):721–746, 1999.
- [55] W. Jin and R. V. Kohn. Singular perturbation and the energy of folds. *J. Nonlinear Sci.*, 10(3):355–390, 2000.
- [56] AV Kaznacheev, MM Bogdanov, and AS Sonin. The influence of anchoring energy on the prolate shape of tactoids in lyotropic inorganic liquid crystals. *Journal of Experimental and Theoretical Physics*, 97(6):1159–1167, 2003.
- [57] AV Kaznacheev, MM Bogdanov, and SA Taraskin. The nature of prolate shape of tactoids in lyotropic inorganic liquid crystals. *Journal of Experimental and Theoretical Physics*, 95(1):57–63, 2002.
- [58] Thomas WB Kibble. Topology of cosmic domains and strings. *Journal of Physics A: Mathematical and General*, 9(8):1387, 1976.

- [59] Young-Ki Kim, Sergij V Shiyanovskii, and Oleg D Lavrentovich. Morphogenesis of defects and tactoids during isotropic–nematic phase transition in self-assembled lyotropic chromonic liquid crystals. *Journal of Physics: Condensed Matter*, 25(40):404202, 2013.
- [60] Maurice Kleman and Oleg D Laverntovich. *Soft matter physics: an introduction*. Springer Science & Business Media, 2007.
- [61] Robert V. Kohn and Peter Sternberg. Local minimisers and singular perturbations. *Proc. Roy. Soc. Edinburgh Sect. A*, 111(1-2):69–84, 1989.
- [62] Samo Kralj and Epifanio G. Virga. Universal fine structure of nematic hedgehogs. *J. Phys. A*, 34(4):829–838, 2001.
- [63] Matthias Kurzke and Daniel Spirn. Gamma limit of the nonself-dual Chern-Simons-Higgs energy. *J. Funct. Anal.*, 255(3):535–588, 2008.
- [64] Xavier Lamy and Felix Otto. On the regularity of weak solutions to Burgers’ equation with finite entropy production. *Calc. Var. PDE*, 57(4):Art. 94, 19, 2018.
- [65] F. M. Leslie. Some constitutive equations for liquid crystals. *Arch. Rational Mech. Anal.*, 28(4):265–283, 1968.
- [66] Fang-Hua Lin. A remark on the map $x/|x|$. *C. R. Acad. Sci. Paris Sér. I Math.*, 305(12):529–531, 1987.
- [67] Fanghua Lin, Xing-Bin Pan, and Changyou Wang. Phase transition for potentials of high-dimensional wells. *Comm. Pure Appl. Math.*, 65(6):833–888, 2012.
- [68] L. Longa, D. Monselesan, and H.-R. Trebin. An extension of the landau-ginzburg-de gennes theory for liquid crystals. *Liquid Crystals*, 2(6):769–796, 1987.
- [69] Andrew Lorent. A simple proof of the characterization of functions of low Aviles Giga energy on a ball *via* regularity. *ESAIM Control Optim. Calc. Var.*, 18(2):383–400, 2012.

- [70] Andrew Lorent. A quantitative characterisation of functions of low Aviles Giga energy in convex domains. *Ann. Sc. Norm. Super. Pisa Cl. Sci. (5)*, 13(1):1–66, 2014.
- [71] Geoffrey R. Luckhurst, Shohei Naemura, Timothy J. Sluckin, Kenneth S. Thomas, and Stefano S. Turzi. Molecular-field-theory approach to the landau theory of liquid crystals: Uniaxial and biaxial nematics. *Phys. Rev. E*, 85:031705, Mar 2012.
- [72] G.R. Luckhurst and C.A. Veracini, editors. *The Molecular Dynamics of Liquid Crystals*, volume 431 of *Nato Science Series C*. Birkhäuser Boston, Inc., Boston, MA, 1994.
- [73] L. A. Madsen, T. J. Dingemans, M. Nakata, and E. T. Samulski. Thermotropic biaxial nematic liquid crystals. *Phys. Rev. Lett.*, 92:145505, Apr 2004.
- [74] Apala Majumdar. Equilibrium order parameters of nematic liquid crystals in the Landau-de Gennes theory. *European J. Appl. Math.*, 21(2):181–203, 2010.
- [75] Apala Majumdar and Arghir Zarnescu. Landau-De Gennes theory of nematic liquid crystals: the Oseen-Frank limit and beyond. *Arch. Ration. Mech. Anal.*, 196(1):227–280, 2010.
- [76] Luciano Modica. The gradient theory of phase transitions and the minimal interface criterion. *Arch. Rational Mech. Anal.*, 98(2):123–142, 1987.
- [77] Luciano Modica and Stefano Mortola. Il limite nella Γ -convergenza di una famiglia di funzionali ellittici. *Boll. Un. Mat. Ital. A (5)*, 14(3):526–529, 1977.
- [78] Hiroyuki Mori, Eugene C. Gartland, Jack R. Kelly, and Philip J. Bos. Multidimensional director modeling using the q tensor representation in a liquid crystal cell and its application to the π cell with patterned electrodes. *Japanese Journal of Applied Physics*, 38(Part 1, No. 1A):135–146, jan 1999.
- [79] N. J. Mottram and C. J. P. Newton. Introduction to Q-tensor theory. *ArXiv e-prints*, September 2014.

- [80] François Murat. Compacité par compensation. *Ann. Scuola Norm. Sup. Pisa Cl. Sci. (4)*, 5(3):489–507, 1978.
- [81] François Murat. L’injection du cône positif de H^{-1} dans $W^{-1,q}$ est compacte pour tout $q < 2$. *J. Math. Pures Appl. (9)*, 60(3):309–322, 1981.
- [82] Yu. A. Nastishin, H. Liu, T. Schneider, V. Nazarenko, R. Vasyuta, S. V. Shiyanovskii, and O. D. Lavrentovich. Optical characterization of the nematic lyotropic chromonic liquid crystals: Light absorption, birefringence, and scalar order parameter. *Phys. Rev. E*, 72:041711, Oct 2005.
- [83] Luc Nguyen and Arghir Zarnescu. Refined approximation for minimizers of a Landau-de Gennes energy functional. *Calc. Var. Partial Differential Equations*, 47(1-2):383–432, 2013.
- [84] Michael R. Novack. Dimension reduction for the Landau–de Gennes model: the vanishing nematic correlation length limit. *SIAM J. Math. Anal.*, 50(6):6007–6048, 2018.
- [85] C. W. Oseen. The theory of liquid crystals. *Trans. Faraday Soc.*, 29:883–899, 1933.
- [86] N. C. Owen, J. Rubinstein, and P. Sternberg. Minimizers and gradient flows for singularly perturbed bi-stable potentials with a Dirichlet condition. *Proc. Roy. Soc. London Ser. A*, 429(1877):505–532, 1990.
- [87] Arkady Poliakovsky. On the Γ -limit of singular perturbation problems with optimal profiles which are not one-dimensional. Part I: The upper bound. *Differential Integral Equations*, 26(9-10):1179–1234, 2013.
- [88] Arkady Poliakovsky. On the Γ -limit of singular perturbation problems with optimal profiles which are not one-dimensional. Part II: The lower bound. *Israel J. Math.*, 210(1):359–398, 2015.

- [89] P Prinsen and PPAM van der Schoot. Continuous director-field transformation of nematic tactoids. *The European Physical Journal E*, 13(1):35–41, 2004.
- [90] P Prinsen and PPAM van der Schoot. Parity breaking in nematic tactoids. *Journal of Physics: Condensed Matter*, 16(49):8835, 2004.
- [91] Peter Prinsen and Paul van der Schoot. Shape and director-field transformation of tactoids. *Phys. Rev. E*, 68:021701, Aug 2003.
- [92] Jacob Rubinstein, Peter Sternberg, and Joseph B. Keller. Fast reaction, slow diffusion, and curve shortening. *SIAM J. Appl. Math.*, 49(1):116–133, 1989.
- [93] Jacob Rubinstein, Peter Sternberg, and Joseph B. Keller. Reaction-diffusion processes and evolution to harmonic maps. *SIAM J. Appl. Math.*, 49(6):1722–1733, 1989.
- [94] Joseph Rudnick and Robijn Bruinsma. Shape of domains in two-dimensional systems: Virtual singularities and a generalized wulff construction. *Phys. Rev. Lett.*, 74:2491–2494, Mar 1995.
- [95] Etienne Sandier. Lower bounds for the energy of unit vector fields and applications. *J. Funct. Anal.*, 152(2):379–403, 1998.
- [96] Richard Schoen and Karen Uhlenbeck. A regularity theory for harmonic maps. *J. Differential Geom.*, 17(2):307–335, 1982.
- [97] N. Schopohl and T. J. Sluckin. Defect core structure in nematic liquid crystals. *Phys. Rev. Lett.*, 59:2582–2584, Nov 1987.
- [98] Antonio Segatti, Michael Snarski, and Marco Veneroni. Analysis of a variational model for nematic shells. *Math. Models Methods Appl. Sci.*, 26(10):1865–1918, 2016.
- [99] Peter Sternberg. The effect of a singular perturbation on nonconvex variational problems. *Arch. Rational Mech. Anal.*, 101(3):209–260, 1988.

- [100] Peter Sternberg. Vector-valued local minimizers of nonconvex variational problems. *Rocky Mountain J. Math.*, 21(2):799–807, 1991. Current directions in nonlinear partial differential equations (Provo, UT, 1987).
- [101] Peter Sternberg and William P. Zeimer. Local minimisers of a three-phase partition problem with triple junctions. *Proc. Roy. Soc. Edinburgh Sect. A*, 124(6):1059–1073, 1994.
- [102] L. Tartar. Compensated compactness and applications to partial differential equations. In *Nonlinear analysis and mechanics: Heriot-Watt Symposium, Vol. IV*, volume 39 of *Res. Notes in Math.*, pages 136–212. Pitman, Boston, Mass.-London, 1979.
- [103] R. M. W. van Bijnen, R. H. J. Otten, and P. van der Schoot. Texture and shape of two-dimensional domains of nematic liquid crystals. *Phys. Rev. E*, 86:051703, Nov 2012.
- [104] Epifanio G. Virga. *Variational theories for liquid crystals*, volume 8 of *Applied Mathematics and Mathematical Computation*. Chapman & Hall, London, 1994.
- [105] Hassler Whitney. Elementary structure of real algebraic varieties. *Ann. of Math. (2)*, 66:545–556, 1957.
- [106] Chiqun Zhang, Amit Acharya, Noel J Walkington, and Oleg D Lavrentovich. Computational modelling of tactoid dynamics in chromonic liquid crystals. *Liquid Crystals*, 45(7):1084–1100, 2018.
- [107] Shuang Zhou, Adam J. Cervenka, and Oleg D. Lavrentovich. Ionic-content dependence of viscoelasticity of the lyotropic chromonic liquid crystal sunset yellow. *Phys. Rev. E*, 90:042505, Oct 2014.
- [108] H. Zocher. The effect of a magnetic field on the nematic state. *Trans. Faraday Soc.*, 29:945–957, 1933.

- [109] Andres Zuniga and Peter Sternberg. On the heteroclinic connection problem for multi-well gradient systems. *J. Differential Equations*, 261(7):3987–4007, 2016.

Michael R. Novack

mrnovack@indiana.edu

Nationality: United States Citizen

Research Interests

Partial Differential Equations, Calculus of Variations

Education

- Indiana University, Bloomington, Indiana, USA

Ph.D. in Mathematics, June 2019

◊ Advisors: Peter Sternberg and Dmitry Golovaty

◊ Dissertation Title: Variational Methods in the Mathematics of Liquid Crystals

- University of Illinois, Urbana-Champaign, Illinois, USA

B.S. Mathematics, May 2013

◊ Minor in Jazz Performance

Preprints

- Golovaty, D., Kim, Y.-K., Lavrentovich, O., Novack, M., Sternberg, P. *Phase transitions in nematics: textures with tactoids and disclinations.*

arXiv:1902.06342 [cond-mat.soft], 2019.

- Golovaty, D., Novack, M., Sternberg, P., Venkatraman, R. *A model problem for nematic-isotropic transitions with highly disparate elastic constants.*

arXiv:1811.12586 [math.AP], 2018.

Publications

- Novack, M. *Dimension reduction for the Landau–de Gennes model: the vanishing nematic correlation length limit.*

SIAM Journal on Mathematical Analysis **50** (2018), no. 6, 6007–6048.

Research Talks

- A Model Problem for Nematic-Isotropic Transitions with Highly Disparate Elastic Constants
 - ◊ Special Session on Modeling and Qualitative Study of PDEs from Materials Science and Geometry, AMS Spring Eastern Sectional Meeting. Hartford, CT (April 2019)
 - ◊ Purdue University PDE Seminar. West Lafayette, IN (February 2019)
 - ◊ Calculus of Variations and Probability Winter School, Centre International de Mathématiques et d’Informatique de Toulouse. Toulouse, France (February 2019)
- Dimension Reduction for Landau–de Gennes: The Vanishing Nematic Correlation Length Limit
 - ◊ Indiana University PDE Seminar. Bloomington, IN (August 2018)
 - ◊ Variational Problems from Materials Science Mini-symposium. SIAM MS18, Portland, OR (July 2018)
 - ◊ Working Group on Singularities in Nematic Liquid Crystals and Related Problems. IMA, Minneapolis, MN (June 2018)

Expository Talks

- On nematic–isotropic interfaces. Mathematics Seminar, Rose–Hulman Institute of Technology (September 2018)
- Functions of bounded variation and minimal surfaces. Indiana University Graduate Student PDE Seminar (October 2016)

- The method of moving planes and Alexandrov's theorem. Indiana University Graduate PDE Seminar (October 2015)

Service

- Co-organizer of Indiana University Graduate Student PDE Seminar (Fall 2016, Spring 2017)
- Volunteer for Indiana University Science Fest Outreach Events (October 2013)

Awards and Honors

- Glen Schober Memorial Travel Award (Summer 2018, Fall 2018, Spring 2019)
- Mathematics Departmental Fellowship (Spring 2018)
- Hazel King Thompson Fellowship (Summer 2017)
- Rothrock Teaching Award (2015)
- College of Arts and Sciences Top Up Fellowship (2013)
- University of Illinois Provost Scholarship (4-year full tuition merit scholarship) (2009–2013)

Teaching Experience

◊ Department of Mathematics, Indiana University

Course Instructor for:

- | | |
|---|---|
| • T103 (Math for Elementary Teachers III)
Spring 2019 | • T103 (Math for Elementary Teachers III)
Fall 2017 |
| • T103 (Math for Elementary Teachers III)
Fall 2018 | • J112 (Introduction to College Mathematics II) Summer 2016 |
| • M365 (Introduction to Probability and Statistics) Summer 2018 | • T103 (Math for Elementary Teachers III)
Spring 2016 |

- T103 (Math for Elementary Teachers III)
Fall 2016
- M027 (Precalculus with Trigonometry)
Fall 2014
- J113 (Introduction to Calculus with Applications) Fall 2015
- J112 (Introduction to College Mathematics II) Spring 2014
- M027 (Precalculus with Trigonometry)
Spring 2015
- M014 (Basic Algebra) Fall 2013

Course Assistant for:

- D116 (Introduction to Finite Mathematics) Spring 2014

Course Grader for:

- Analysis Head to Toes (Spring 2016)
- M513 Complex Variables I (Fall 2015)

Conferences & Summer Schools Attended

- Materials Research Society Spring Meeting and Exhibit. Phoenix, AZ (April 2019)
- AMS Spring Eastern Sectional Meeting. Hartford, CT (April 2019)
- Calculus of Variations and Probability Winter School. Centre International de Mathématiques et d'Informatique de Toulouse, Toulouse, France (February 2019)
- SIAM Conference on Mathematical Aspects of Materials Science. Portland, OR (July 2018)
- Working Group on Singularities in Nematic Liquid Crystals and Related Problems. IMA, Minneapolis, MN (June 2018)
- Conference on Multiscale Problems in Materials and Biology. The Fields Institute, Toronto, Canada (June 2018)
- Liquid Crystals, Soft-Matter Packing, and Active Systems. IMA, Minneapolis, MN (January 2018)

- Rivière–Fabes Symposium. University of Minnesota, Minneapolis, MN (April 2017)
- Calculus of Variations and Nonlinear PDE. Columbia University, New York, NY (May 2016)
- 77th Midwest PDE Seminar. University of Cincinnati, Cincinnati, OH (May 2016)
- Calculus of Variations and Nonlinear PDE. University of Texas, Austin, TX (May 2015)

Reproduced with permission of copyright owner. Further reproduction prohibited without permission.

Reproduced with permission of copyright owner. Further reproduction prohibited without permission.